UNIVERSITY OF OKLAHOMA

GRADUATE COLLEGE

OXO-RHENIUM CATALYZED TRANSFORMATIONS OF ALCOHOLS: DEOXYDEHYDRATION AND REDUCTIVE COUPLING

A DISSERTATION

SUBMITTED TO THE GRADUATE FACULTY

in partial fulfillment of the requirements for the

Degree of

DOCTOR OF PHILOSOPHY

By

CAMILLE BERNADINE CARINE BOUCHER JACOBS
Norman, Oklahoma
2016

Downloaded from SHAREOK. Persistent Handle URL: https://hdl.handle.net/11244/44915

OXO-RHENIUM CATALYZED TRANSFORMATIONS OF ALCOHOLS:
DEOXYDEHYDRATION AND REDUCTIVE COUPLING

A DISSERTATION APPROVED FOR THE
DEPARTMENT OF CHEMISTRY AND BIOCHEMISTRY

BY

_____
Dr. Kenneth M. Nicholas, Chair

_____
Dr. Daniel T. Glatzhofer

_____
Dr. Ronald L. Halterman

_____
Dr. Robert K. Thomson

_____
Dr. Steven P. Crossley

© Copyright by CAMILLE BERNADINE CARINE BOUCHER JACOBS 2016
All Rights Reserved.

To my parents,

Acknowledgements

In 2011, Dr. Nicholas welcomed me in his laboratory for a master exchange program. Five years later I am completing my Ph.D. with him. I would like to thank him for the opportunity he gave me to work for him and also for his mentorship and guidance over the years. I also would like to acknowledge my committee members for their support and their time, Dr. Glatzhofer, Dr. Halterman, Dr. Thomson and Dr. Crossley.

I would like to thank all members of Dr. Nicholas's laboratory that I have seen coming and leaving over the years. I have a special thank though to Mike, Alex, Garry and Dan who had a large input in my work and life of the lab. They were always ready to help and to share knowledge.

Leaving my family, my friends and my country to study in the United States was not easy but I found a home in Oklahoma not only in the department of Chemistry but also in my host family. Breck and Theresa thank you so much for your friendship and your time.

Five year ago I did not arrive in Norman alone. Julien came along with me and I would like to thank him for his presence, his support and his help.

Finally I would like to thank my parents for giving me the freedom to study what I liked and still like the most, chemistry and for supporting my choices to their accomplishment.

Table of Contents

Chapter I. Introduction to and Background of the Deoxydehydration Reaction 1

1. Introduction 1
2. Uncatalyzed Didehydroxylation of Glycols 2
3. Oxo-Metal Promoted and Catalyzed Deoxydehydration 4
   a. ReOx-based catalysts 4
   b. Non-precious metal catalyzed DODH 26
4. Applications of DODH Systems 30
5. Conclusions and Future Prospects 32

Chapter II. Hydroaromatics as DODH Reducing Agents 35

1. Introduction 35
2. Hydroaromatics as Reductants for DODH and Tandem DODH/Diels Alder Reactions 36
3. Indoline as Reducing Agent 39
4. Mechanistic Study of Indoline- $MeReO_3$ Interactions 43
5. Conclusions 48
6. Experimental 49
   a. General information: reagents and instruments. 49
   b. Representative procedure for DODH reactions. 50
   c. DODH/Diels Alder tandem reaction with diethyl tartrate and 1,3-cyclohexadiene. 50
   d. DODH reaction of glyceric acid with indoline. 51
   e. Reducing agent competition between 3-pentanol vs indoline. 51

f. Preparation of the $MeReO_3(\eta^1$-indoline) (**4**). 52

g. X-ray crystal structure determination of **4**..... 53

h. $MeReO_3$:indoline reactivity study. 56

i. MDO trapping. 57

j. Competition between indoline and ethylene glycol for $MeReO_3$..... 57

7. Acknowledgment..... 57

Chapter III. DODH/C-C Bond Forming Tandem Reactions 58

1. DODH / Hetero Diels Alder Coupling 58

a. Introduction 58

b. DODH using α-hydroxy carbonyls as reducing agent..... 60

c. Study of the Hetero Diels Alder step..... 66

d. Conclusions 69

e. Experimental..... 69

2. DODH / Metathesis Tandem Reaction..... 75

a. Introduction and Background..... 75

b. Study of metathesis reaction under DODH reaction conditions using $CoOMoO_3Al_2O_3$ as catalyst..... 77

c. Deoxygenation/Metathesis tandem reaction of styrene oxide..... 81

d. Conclusion..... 82

e. Experimental..... 83

3. DODH / Allylation tandem reaction..... 90

a. Introduction 90

b. DODH/Krische's Allylation..... 94

c. DODH/Masuyama's Allylation 101
d. Conclusions 108
e. Experimental 109
4. DODH / "Base-free catalytic" Wittig Tandem Reaction 122
a. Introduction 122
b. Study of the tandem system 124
c. Conclusions 127
d. Experimental 129
5. DODH/Heck Tandem Reactions 132
a. Introduction and Background 132
b. Study of the DODH step 134
c. Study of the Heck step 136
d. Conclusion 138
e. Experimental 138
6. DODH/Hydroacylation Tandem Reaction 142
a. Introduction 142
b. Intermolecular DODH/Hydroacylation 145
c. Intramolecular DODH/Hydroacylation 147
d. Conclusions and future prospects 151
e. Experimental 153
7. DODH/Hydroformylation Tandem Reaction 160
a. Introduction and Background 160
b. Hydrogen and Carbon monoxide as DODH reducing agents 163

c. Hydroformylation of 1-hexene 167
d. Tandem DODH/Hydroformylation 170
e. Conclusion 174
f. Experimental 175
Chapter IV. Mechanistic Study of $IReO_2TPP_2$-Promoted Reaction of Alcohols with Triphenylphosphine 186
1. Introduction and Background 186
2. Results 193
a. Study of the catalyst in solution; ligand dissociation 193
b. Stoichiometric reaction NMR study: $IReO_2(PPh_3)_2$ and benzhydrol ... 196
c. Kinetic study 206
d. Computational results summary of $(PPh_3)_2ReO_2I$ + MeOH (by K.Nicholas) 214
3. Discussion and Conclusions 216
4. Experimental 226
a. General information: reagents and instruments. 226
b. Catalyst synthesis 226
c. Study of the catalyst in solution; ligand dissociation 227
d. NMR Stoichiometric Experiments 227
e. Kinetic experiments 231
f. IR sampling 234
g. MS sampling 234

List of Tables

Table II. 2.1 Screening hydroaromatic reductants for DODH 38

Table II. 3.1 DODH with indoline as reductant 41

Table III. 1.1 DEF yield using α-hydroxy carbonyls (1, Figure III. 1.4) as reducing agent 61

Table III. 1.2 Alkene yield using ethyl lactate as reducing agent (Figure III. 1.5) 63

Table III. 1.3 Alkene (3) yield using α-hydroxy carbonyl (2) as reducing agents (Figure III. 1.6)..... 64

Table III. 3.1 DODH Study of the BOC Derivative of Glycerol 100

Table III. 3.2 TON of the DODH in glycerol : benzene solvent mixture..... 105

Table III. 3.3 Summary of reaction conditions for attempted allylation and tandem reaction 107

Table III. 6.1 Reported and Attempted Hydroacylations 146

Table III. 6.2 Reaction conditions tested on the DODH of 1c 150

Table III. 7.1 Results of the DODH of 1,2-hexane diol (Figure III. 7.5) with hydrogen and carbon monoxide under various reaction conditions..... 164

Table III. 7.2 Results of the hydroformylation of 1-hexene..... 168

Table IV.1 Deoxygenation and reductive coupling of alcohols by $PPh_3/IReO_2(PPh_3)_2$ (1)[a] 189

Table IV.2 New NMR signals in ^{1}H and ^{31}P NMR of $ROH/IReO_2(PPh_3)_2$ samples ... 203

Table IV.3 Integration ratios of new CH_2 signals in ethanol/catalyst samples 205

List of Figures

Figure I. 1.1 Biomass transformation process 1

Figure I. 2.1 Two steps uncatalyzed didehydroxylation of glycols 2

Figure I. 2.2 General reaction equation of one step uncatalyzed didehydroxylation 3

Figure I. 2.3 Substrate scope of one step uncatalyzed didehydroxylation diols 3

Figure I.3.a.1 Summary of DODH systems using PPh_3 as reducing agent 5

Figure I.3.a.2 Proposed mechanistic cycle for phosphine driven DODH reaction 5

Figure I.3.a.3 Erythritol and threitol products distribution 6

Figure I.3.a.4 Stereoselectivity of DODH reaction system 7

Figure I.3.a.5 Cp'ReO_3 reduction pathway 7

Figure I.3.a.6 Mechanistic probes of alkene extrusion from LReO(glycolate) 8

Figure I.3.a.7 General deoxygenation of epoxides using phosphite and rhenium oxide 10

Figure I.3.a.8 Summary of DODH systems using hydrogen as reducing agent 10

Figure I.3.a.9 Calculated lowest energy profile for hydrogen, $MeReO_3$- catalyzed DODH 11

Figure I.3.a.10 Summary of DODH systems using sulfite as reducing agent 13

Figure I.3.a.11 General reaction equation of DODH using sulfite as reducing agent 13

Figure I.3.a.12 Proposed mechanism of $MeReO_3$ catalytic cycle in DODH using sulfite reductant 14

Figure I.3.a.13 Calculated lowest energy profile for sulfite, CH_3ReO_3- catalyzed DODH 15

Figure I.3.a.14 Summary of DODH systems using sulfite as reducing agent 16

Figure I.3.a.15 First reported DODH reaction using alcohol as reducing agent 16

Figure I.3.a.16 $MeReO_3$-catalyzed disproportionation of glycerol in constant distillation system 18

Figure I.3.a.17 Alcohols as reducing agent in DODH system 19

Figure I.3.a.18 Purification and catalyst recycling in NH_4ReO_4 / benzyl alcohol DODH system 21

Figure I.3.a.19 Proposed mechanistic cycle for alcohol-driven, CH_3ReO_3-catalyzed DODH by Abu-Omar 22

Figure I.3.a.20 Calculated lowest energy profile for alcohol-driven, CH_3ReO_3-catalyzed DODH..... 23

Figure I.3.a.21 Proposed mechanistic cycle for alcohol-driven, CH_3ReO_3-catalyzed DODH by Fristrup 24

Figure I.3.a.22 Summary of DODH system using elemental reductant 25

Figure I.3.a.23 Summary of DODH system using heterogeneous rhenium catalyst..... 26

Figure I.3.b.1 Summary of DODH system using non precious metal catalyst 27

Figure I.3.b.2 Calculated lowest energy profile for diol-driven (left) and for isopropanol-driven (right), MoO_3-catalyzed DODH..... 28

Figure I.3.b.3 Vanadium catalyzed DODH and DO 30

Figure I. 4.1 Synthesis of adipic acid from mucic acid via DODH and Hydrogenation two steps process 31

Figure I. 4.2 Simultaneous DODH and hydrogenation of diols by ReO_x-Pd/CeO_2 heterogeneous catalyst..... 31

Figure I. 4.3 Benzannulation reaction to form substituted naphthalene..... 32

Figure I. 5.1 Summary of DODH systems 32

Figure II. 2.1 Tandem DODH/DA with DET and 1,3-cyclohexadiene..... 37

Figure II. 2.2 Tandem DODH/DA with DET and 9,10-dihydroanthracene..... 37

Figure II. 2.3 Activity of HA on DODH of DET and 1,2-octanediol 37

Figure II. 2.4 Hydrogen donors tested that gave limited alkene yield or ambiguous products 39

Figure II. 3.1 Reactivity of indoline as reducing agent on a variety of diols 40

Figure II. 3.2 DODH of glyceric acid using indoline as reducing agent..... 42

Figure II. 3.3 Reducing agent competition: (A)indoline vs. 2-butanol; (B): indoline vs. 3-pentanol..... 43

Figure II. 4.1 ^{1}H NMR and IR of 4..... 44

Figure II. 4.2 X-ray ORTEP diagram of $MeReO_3$(indoline) (4) 44

Figure II. 4.3 MDO-trapping experiment..... 45

Figure II. 4.4 ^{1}H and ^{13}C NMR spectra of 5..... 46

Figure II. 4.5 ^{1}H NMR experiment $MeReO_3$:indoline vs. $MeReO_3$:Glycolate formation 47

Figure II. 4.6 Possible mechanism of $MeReO_3$-indoline H-transfer redox reaction 47

Figure II. 4.7 Potential $MeReO_3$ catalytic cycle with indoline as reductant 48

Figure III. 1.1 Diels-Alder general reaction 58

Figure III. 1.2 DODH/DA reaction system 59

Figure III. 1.3 DODH/Hetero Diels Alder tandem concept 60

Figure III. 1.4 Activity of α-carbonyl alcohol as reducing agent for DODH of DET.... 61

Figure III. 1.5 Activity of ethyl lactate as reducing agent for DODH of diols (1)..... 62

Figure III. 1.6 Activity of other α-hydroxy carbonyl (2) as reducing agent for DODH of glycols (1) 63
Figure III. 1.7 Trapping experiment of methyl glyoxal (2) by cycloaddition with isoprene 65
Figure III. 1.8 Study of Hetero-Diel Alder step 66
Figure III. 1.9 Hetero-Diel Alder reaction of butadiene and benzaldehyde 68
Figure III. 2.1 General metathesis equation 75
Figure III. 2.2 Metathesis mechanistic cycle 76
Figure III. 2.3 DODH/ Olefin Metathesis tandem concept 77
Figure III. 2.4 Study of the metathesis reaction 79
Figure III. 2.5 Tests of compatibility of the metathesis with DODH reagents 80
Figure III. 2.6 $CoOMoO_3Al_2O_3$ as DODH catalyst 81
Figure III. 2.7 Deoxygenation/Metathesis tandem reaction 82
Figure III. 3.1 General allylation reaction equation 90
Figure III. 3.2 General carbonyl allylation 91
Figure III. 3.3 DODH/Carbonyl-Allylation (CA) tandem concept 91
Figure III. 3.4 DODH/Krische Allylation 92
Figure III. 3.5 DODH/Masuyama Allylation 94
Figure III. 3.6 (S)-I Catalyst preparation 95
Figure III. 3.7 Study of allylation step 95
Figure III. 3.8 DODH of Glycerol Monostearate 96
Figure III. 3.9 DODH reaction with added bases 97

Figure III. 3.10 DODH reaction with trans-[$ReO_2(py)_4$]PF_6 as catalyst and added pyridine 98
Figure III. 3.11 Carbonyl Allylation Step with added [$ReO_2(py)_4$]PF_6 or pyridine 98
Figure III. 3.12 *In situ* Formation of a Base with BOC Derivative of Glycerol 99
Figure III. 3.13 Synthesis of BOC derivative of glycerol 99
Figure III. 3.14 DODH of the BOC Derivative of Glycerol 100
Figure III. 3.15 Allylation reaction in benzene as solvent and at 150^oC 103
Figure III. 3.16 DODH of DET using $SnCl_2$ as reducing agent 103
Figure III. 3.17 DODH of glycerol in biphasic media 105
Figure III. 3.18 Allylation reaction in benzene : glycerol biphasic system 105
Figure III. 3.19 Allylation step in 3-octanol 106
Figure III. 3.20 Tandem DODH/Allylation reaction 106
Figure III. 3.21 Tandem DODH/Allylation in PEG or DME solvent 107
Figure III. 4.1 Formation of the phosphorus ylide and Wittig general scheme 122
Figure III. 4.2 Werner's base-free catalytic Wittig reaction 122
Figure III. 4.3 Proposed mechanism for reaction 123
Figure III. 4.4 DODH/ "base free catalytic" Wittig tandem reaction concept 123
Figure III. 4.5 Compatibility test of Bu_3P with DODH mixture 124
Figure III. 4.6 Tandem reaction using Bu_3P as stoichiometric reagent 125
Figure III. 4.7 Tandem DODH/ catalytic Wittig 126
Figure III. 4.8 Tandem DODH/Werner-Wittig and Werner-Wittig reaction using catalytic phosphine 127
Figure III. 4.9 Potential intramolecular DODH / "base free" Wittig 128

Figure III. 4.10 Variations in the diol and/or alcohol reducing agent 129

Figure III. 5.1 General Heck reaction..... 132

Figure III. 5.2 Heck catalytic cycle 133

Figure III. 5.3 DODH/Heck tandem concept 133

Figure III. 5.4 DODH/Heck tandem reaction with the reducing agent and aryl halide provided by one reagent 134

Figure III. 5.5 DODH reaction system using $ReO_2(Py)_4^{+}$-X as catalyst..... 135

Figure III. 5.6 Test of stoichiometric on Heck coupling 137

Figure III. 5.7 Test of the heck reaction using pyridine as additive..... 137

Figure III. 6.1 General Hydroacylation equation 142

Figure III. 6.2 Rhodium catalyst mechanism; Hydroacylcation and Decarbonylation 143

Figure III. 6.3 DODH/Hydroacylation tandem concept..... 144

Figure III. 6.4 Intramolecular DODH/Hydroacylation tandem concept 145

Figure III. 6.5 General Hydroacylation of cyclohexene and benzaldehyde 146

Figure III. 6.6 Hydroacylation catalyst..... 147

Figure III. 6.7 Intramolecular DODH/Hydroacylation study plan 147

Figure III. 6.8 General synthesis of compound 1 147

Figure III. 6.9 DODH of 1b..... 148

Figure III. 6.10 DODH of 1c..... 150

Figure III. 6.11 Reaction of 2 with 1-butanol to form acetal 6 150

Figure III. 6.12 Reported hydroacylation by Glorius and co-worker..... 151

Figure III. 6.13 Potential scope study for intramolecular DODH/hydroacylation 153

Figure III. 7.1 General Hydroformylation reaction..... 160

Figure III. 7.2 Rhodium catalyzed hydrofomylation mechanistic cycle 161

Figure III. 7.3 DODH/Hydroformylation tandem concept..... 162

Figure III. 7.4 Abu-Omar DODH of 1,2-hexanediol with H_2 as reducing agent 163

Figure III. 7.5 DODH of 1,2-hexanediol using H_2/CO as reducing agent 164

Figure III. 7.6 Shvo's Ruthenium catalyst dissociation equilibrium..... 165

Figure III. 7.7 Shvo's catalyst cycle for hydrogen activation in aldehyde reduction... 165

Figure III. 7.8 Synthesis of iron analogues to Shvo's catalyst 166

Figure III. 7.9 DODH of 1,2-hexanediol using 1 as hydrogen activating catalyst..... 166

Figure III. 7.10 Hydroformylation of 1-hexene..... 167

Figure III. 7.11 Pakkanen Hydroformylation of 1-hexene [167] 169

Figure III. 7.12 DODH of 1,2-hexanediol with PPh_3 as reducing agent 170

Figure III. 7.13 DODH/Hydroformylation tandem reaction of 1,2-hexane diol 171

Figure III. 7.14 DODH/Hydroformylation tandem reaction of phenyl-1,2-ethanediol 172

Figure III. 7.15 DODH/Hydroformylation tandem reaction of cis-1,2-cyclooctane diol 173

Figure IV.1 Hydrodeoxygenation (HDO) and Deoxydehydration (DODH) of alcohols 187

Figure IV.2 Deoxygenation (DO) and reductive coupling (RC) of alcohols 187

Figure IV.3 Other alcohols tested 2, 3 and 4..... 189

Figure IV.4 Possible catalytic cycle for deoxygenation and reductive coupling 191

Figure IV.5 (Non)Effect of H-Donors on reductive coupling..... 192

Figure IV.6 Calculated energetics of $MeReO_2$-promoted alcohol deoxygenation..... 193

Figure IV.7 Pre-catalyst $IReO_2(PPh_3)_2$..... 194

Figure IV.8 Color changes of the pre-catalyst $IReO_2(PPh_3)_2$ in solution..... 194

Figure IV.9 Pre-catalyst ligand dissociation equilibrium in solution 195

Figure IV.10 ^{1}H (left) and ^{31}P (right) NMR spectra of sample B over a month 198

Figure IV.11 ^{1}H (left) and ^{31}P (right) NMR spectra of sample D room temperature to $50^{o}C$ 200

Figure IV.12 Formation of phosphine oxide-rhenium complex 201

Figure IV.13 List of the alcohols studied 202

Figure IV.14 ^{1}H NMR spectra of sample [$PhCHCHCH_2OH$ + 1] (top) and [CH_3CH_2OH + 1] (bottom) with 5:1 ratio of alcohol to rhenium complex 203

Figure IV.15 Potential complexes formed with alcohols 204

Figure IV.16 Reductive coupling of benzhydrol in chlorobenzene 206

Figure IV.17 Kinetic plot 1 207

Figure IV.18 Kinetic plot 2 208

Figure IV.19 Kinetic plot 3 209

Figure IV.20 Kinetic plot 4 210

Figure IV.21 Kinetic plot 5 212

Figure IV.22 Kinetic plot 6 214

Figure IV.23 DFT study of the $IReO_2(PPh_3)_2$ catalyzed reductive coupling *(by Dr. Nicholas)* 216

Figure IV.24 List of reactive alcohol in reductive coupling reaction 217

Figure IV.25 Pre-catalyst A to active catalyst A' equilibrium 218

Figure IV.26 Alcohol coordination forming to species B_1 and B_2 218

Figure IV.27 Possible equilibrium between a mono (B_2) and bis (C) alkoxy rhenium complex. 219

Figure IV.29 Possible formation of Re-alkyl complexes F and F'..... 220

Figure IV.30 Possible formation of rhenium hydride intermediate E 221

Figure IV.31 Formation of PPh_3-Re-$OPPh_3$ D rhenium complex..... 222

Figure IV.32 Possible mechanistic pathway 224

Figure IV.33 Reductive coupling of (R)-1-phenylethanol 225

Abstract

One of the challenges for the future is to find alternative energy and chemical resources to petrol. Biomass-derived feedstocks offer a renewable source of highly oxygenated molecules. Recent chemical processes for the efficient and selective deoxygenation and refunctionalization of these renewable chemical resources are being developed such as: dehydration, deoxygenation and deoxydehydration (DODH). The latter is the removal of vicinal OH groups and the formation of C-C unsaturation producing value-added unsaturated products that find uses as laboratory and industrial intermediates and end-products.

Chapter II reports the study of a new class of reducing agent for the DODH reaction: hydroaromatics. In this study we tested the activity as DODH reducing agent with a range of hydroaromatics. We found several to be reactive and providing good yields. Two of them were found to not only be good DODH reducing agents but also to involve the alkene product in a cycloaddition. Indoline was found to be the most reactive of all and could be applied to a larger survey of diols. This superior reactivity of indoline was explained by the formation of indoline-rhenium complex which was isolated and its structure was solved with an X-ray crystal structure.

Chapter III covers the efforts we made in the development of DODH/C-C bond formation tandem reactions. The concept of these tandem reactions was to have the DODH reaction directly followed by a C-C bond reactions such as: Hetero Diels Alder, Allylation, Hydroacylation, Heck, Hydroformylation, Alkene metathesis and Wittig reactions. The compatibility of reagents and reaction conditions was the most challenging part of these tandem reactions. From all these we found some compromises between each

of the sides of the tandem reactions and could observe DODH/C-C bond forming tandem reactions.

The last chapter covers the mechanistic study of $IReO_2(PPh_3)_2$ catalyzed reductive coupling of activated alcohols. In this reaction activated alcohols form alkane dimers. Stoichiometric, kinetic and computational (*by K. Nicholas*) studies were conducted to find and support potential catalyst intermediates. Combining the information from each of these studies we could propose a potential catalytic cycle.

Chapter I. Introduction to and Background of the Deoxydehydration Reaction

1. Introduction

The highly oxygenated nature of biomass-derived feedstocks has stimulated the discovery and development of new chemical processes for the efficient and selective deoxygenation and refunctionalization of these renewable chemical resources.[1–4] Cellulose, carbohydrates and hydrolyzed plant oils are polyhydroxylated materials (polyols) and methods for their partial deoxygenation have largely focused on their dehydration reactions (Figure I. 1.1).[5–9] More recently, reductive processes for oxygen removal have garnered increasing attention. These approaches include catalytic hydrodeoxygenation, which replaces C-O bonds with C-H bonds[10–13], and deoxydehydration (DODH), which effects vicinal OH removal with the formation of C-C unsaturation. It produces value-added unsaturated products that have widespread use as laboratory and industrial intermediates and end-products. The development of the DODH reaction is thoroughly reviewed in this chapter.[14–18]

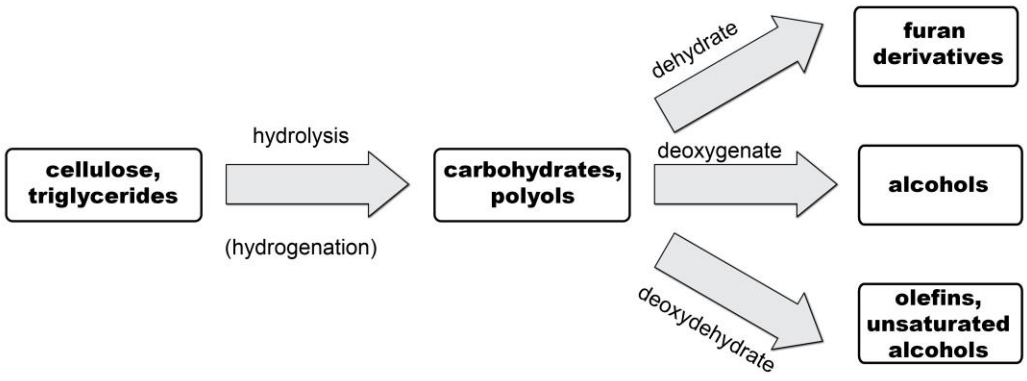


Figure I. 1.1 Biomass transformation process

2. Uncatalyzed Didehydroxylation of Glycols

The earliest reported methods for vicinal dehydroxylation of glycols involved a two-stage process beginning with their acid-catalyzed condensation with ortho-esters (Figure I. 2.1) to form dioxolanes that are subsequently thermolyzed (180-200^{o}C)[19] or heated with acetic anhydride (140^{o}C)[20] to produce olefins. These reactions provide moderate to good yields of olefins (40-95%) for a variety of glycols. The reactions are highly regioselective, locating the C-C unsaturation between the hydroxyl-bearing carbons (i.e. no double bond isomerization) and stereospecific, resulting from a syn-elimination process. Co-products of these processes include carbon dioxide, alcohols and, in the latter case, acetic acid; hence the process is neither atom-economical nor carbon-neutral.

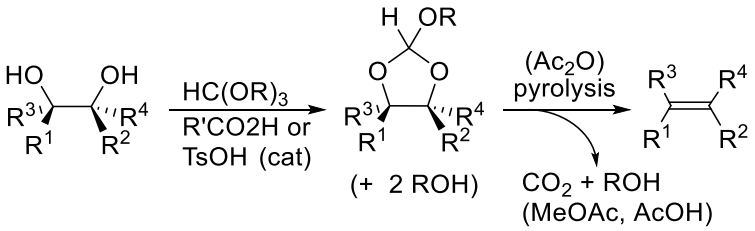


Figure I. 2.1 Two steps uncatalyzed didehydroxylation of glycols

A renewed interest in the glycol-to-olefin conversion was highlighted by the Bergman-Ellman team who reported a single-stage process involving high temperature reactions between glycols and polyols with formic acid as a reductant (Figure I. 2.2).[21,22] Water and carbon dioxide are the co-products of these transformations, hence the process is not carbon-neutral. When heated at 230-240^{o}C under a stream of nitrogen, unsaturated products were produced in high yields if distilled as they are formed; 80-90% yields were obtained with simple glycols and glycerol. Erythritol was converted to 2,5-dihydrofuran

in moderate yield, presumably via dehydration to 3,4-dihydroxyfuran followed by didehydroxylation (Figure I. 2.3). In their patent several other natural polyols were claimed as substrates; the cyclohexane derivatives, quinic and shikimic acids, were both largely converted to benzoic acid, the result of exhaustive dehydration/dehydroxylation. Reactivity studies with diastereomeric decane-3,4-diols demonstrated a stereospecific syn-elimination process. This feature, together with isotopic labeling experiments, supports a proposed mechanism involving an intermediate orthoester-carbocation.

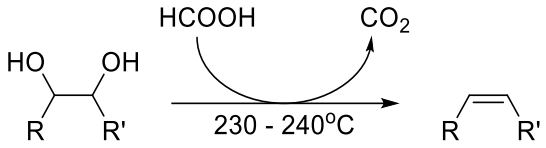


Figure I. 2.2 General reaction equation of one step uncatalyzed didehydroxylation

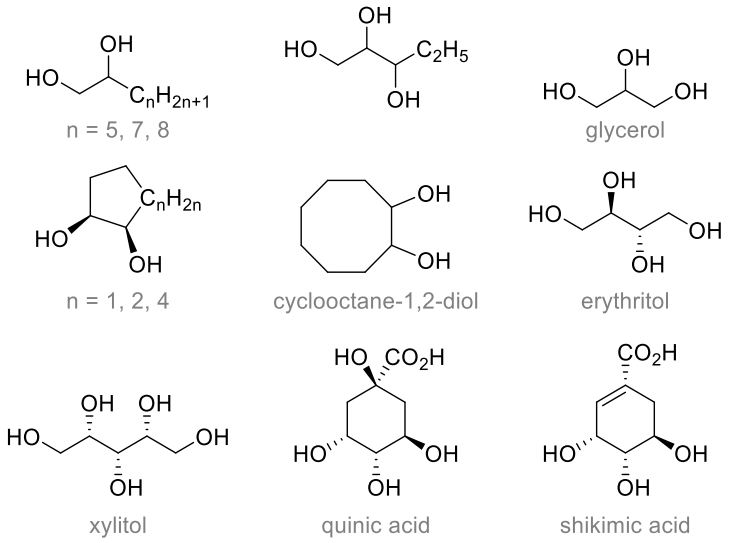


Figure I. 2.3 Substrate scope of one step uncatalyzed didehydroxylation diols

3. Oxo-Metal Promoted and Catalyzed Deoxydehydration

a. ReOx-based catalysts

i. Phosphine Reductants

The first transition metal-catalyzed deoxydehydration (DODH) reaction was reported by Cook and Andrews[23] employing Cp*ReO_3 (**1**, Cp*=pentamethyl-cyclopentadienyl) as the catalyst with PPh_3 as the stoichiometric reductant (Figure I.3.a.1). Typically, reactions were conducted with 2 mol% **1** at 90-100^oC in chlorobenzene as solvent for 1-2 days. Among the substrates evaluated were 1-phenyl-1,2-ethanediol (styrene diol), a 1,2:5,6-diketal of mannitol, glycerol and erythritol. The first two provided the corresponding alkenes in 80-95% yield, while the latter largely produced butadiene (ca. 80%) with smaller amounts of the butene-1,4- and 1,2-diols (6:1). Coordinating solvents were found to inhibit the reaction, while TsOH was found to be a promoter. Catalyst deactivation, ascribed to over-reduction to Re^{iii} was noted. A three stage catalytic cycle (Figure I.3.a.2) was proposed involving: a) reduction of **1** to Cp*ReO_2 (**2**); b) condensation with the diol with **2** to form the Re-glycolate **3**; and extrusion (retrocyclization) of the alkene from **3**. The rate of styrene formation from its glycol (**1**/TsOH co-catalyzed) was independent of the concentrations of both reactants and comparable to its rate of formation from the isolated Cp*ReO(glycolate) (vide infra), consistent with the Re-glycolate retrocyclization being rate-limiting.

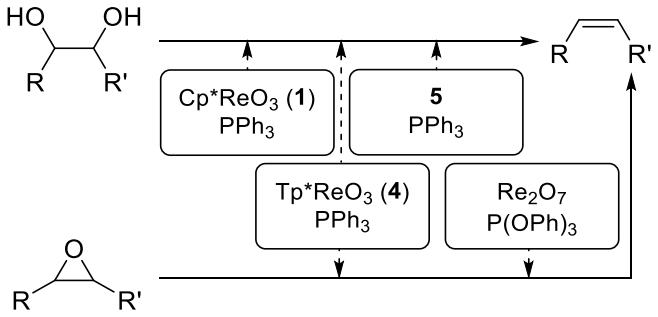


Figure I.3.a.1 Summary of DODH systems using PPh_3 as reducing agent

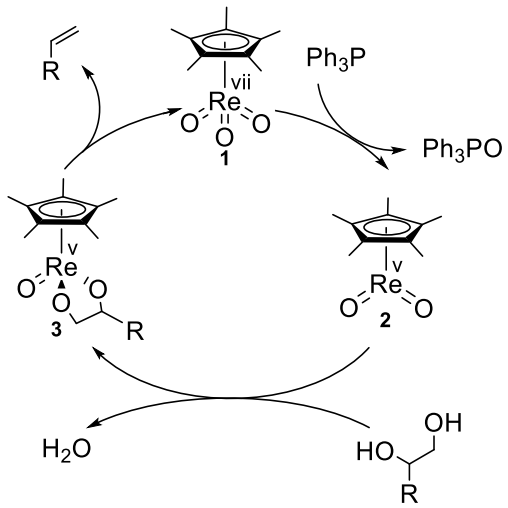


Figure I.3.a.2 Proposed mechanistic cycle for phosphine driven DODH reaction

Several years after the initial catalytic DODH report by Andrews, the Gable group reported that phosphine-driven glycol DODH and epoxide deoxygenation is catalyzed by (tris-dimethylpyrazolylborate)ReO_3 (Tp^*ReO_3) (4) (Figure I.3.a.3).[24] The sterically hindered and stronger donor TPB ligand provides a more robust, but somewhat less active catalyst. With the substrates styrene diol, glycerol, erythritol and threitol, reactions catalyzed by **4** (5 mol%) proceed at 120°C over 1-5 days in toluene. Yields were not reported for the diol or triol, but the tetrols were converted in 20-40% yields to unsaturated products. For erythritol, with one equivalent of PPh_3 moderate selectivity for

the terminal ene-diol (7.2:1 vs. internal) was observed at 40% conversion, whereas threitol produced the terminal ene-diol more selectively along with relatively more butadiene. These selectivities were explained in terms of the distribution of intermediate Re-diolates produced from each polyol. Kinetic studies again indicated that alkene extrusion is turnover-limiting in this system.

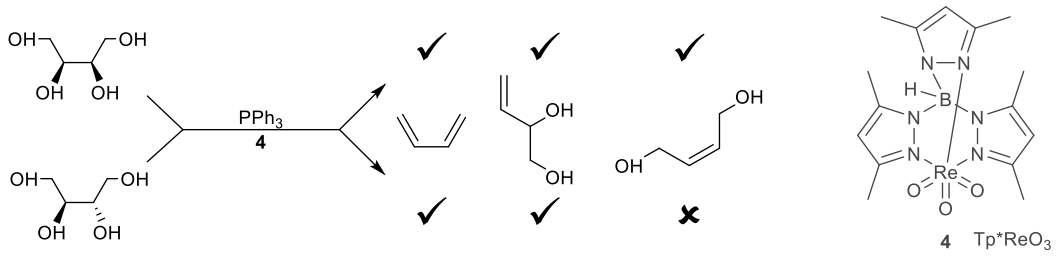


Figure I.3.a.3 Erythritol and threitol products distribution

Gebbink and co-worker revisited the Cp^*ReO_3/PPh_3 DODH system focusing on the use of the sterically bulky (1,2,4-tri-t-butyl-cyclopentadienyl)ReO_3 ($Cp'ReO_3$) complex **5** as catalyst with a range of glycols and polyols (Figure I.3.a.4).[25] The DODH reactions with **5** (0.05-2 mol%) are effective at 135-180^{o}C (chlorobenzene), producing alkenes from acyclic glycols in generally good yields (80-95%), albeit with small amounts (2-8%) of isomerized olefins being detected. The high turnover number achieved at low catalyst loading (ca. 1600) indicates a more robust catalyst than the original Cp^*ReO_3. Cis-cyclic diols gave relatively poor yields (10-50%), perhaps a result of limited access to the sterically hindered Cp'-catalyst. DODH reactions with meso- and d,l-dihydrobenzoin were stereospecific, providing the cis- and trans-stilbenes, respectively, indicative of a syn-elimination process via a stereoselective alkene extrusion from a Re-glycolate intermediate. Glycerol was efficiently converted to allyl alcohol (91%) but the

reaction with erythritol gave a mixture of butadiene and butene-diols in modest yield. Although reactions with alternative reductants (other phosphines, H_2, sec-alcohols, Na_2SO_3) were generally much less efficient than with PPh_3, with 3-octanol as solvent erythritol gave butadiene selectively in 67% yield. In a very recent report the Gebbink group provided a follow up mechanistic study of their Cp'ReO_3 catalytic system[26]. With a combination of experimental results, spectroscopic data and DFT computational study they demonstrated the effect of the bulky 1,2,4-tri-t-butyl-cyclopentadienyl ligand to prevent the formation of polynuclear Re^{v} complexes into which the catalyst is thought to decompose (Figure I.3.a.5).

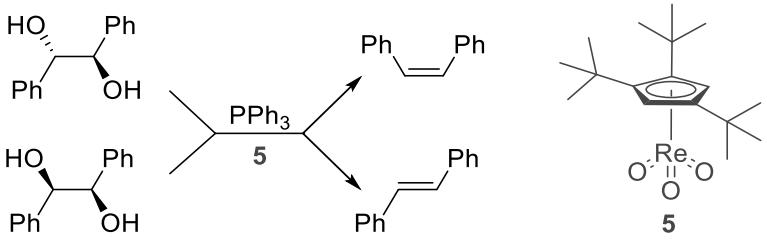


Figure I.3.a.4 Stereoselectivity of DODH reaction system

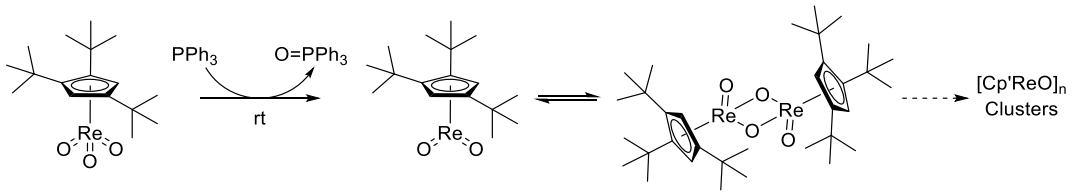


Figure I.3.a.5 Cp'ReO_3 reduction pathway

Gable and co-workers have made valuable contributions to elucidating the mechanism of oxo-Re-promoted DODH reactions, particularly regarding features of the alkene extrusion from LRe^{v}(O)-glycolate species. It is interesting from a historical perspective that their work on the Cp*Re^{v}(O)(glycolate) (**6a**) reactions actually preceded

the report by Andrews and Cook of the Re-catalyzed DODH reaction. Producing **6a** by glycol condensation/PPh_3-reduction of Cp^*ReO_3 (Figure I.3.a.6), the Gable group established that: 1) the addition/extrusion equilibrium is dependent on the strain present in the alkene; 2) the rate dependence for alkene extrusion is first order in [**6a**] with a small ΔS_{act} (+ 5 e.u.); 3) there is a significant normal secondary kinetic isotope effect (1.3) with C-H(D)-labeled glycols; and 4) the reaction rate for a series of Re-glycolates derived from 4-Z-ArCH(OH)CH_2OH correlated with σ^- and gave a reaction parameter ρ= 0.42.[27–29] When taken together with extended Huckel MO calculations, these results were interpreted in favor of an early (reactant-like), slightly polar transition state with asynchronous character with respect to the degree of C-O bond-breaking, favoring rate-limiting formation of a metallaoxetane intermediate (**7**) over a concerted [3+2] transition state (**8**).

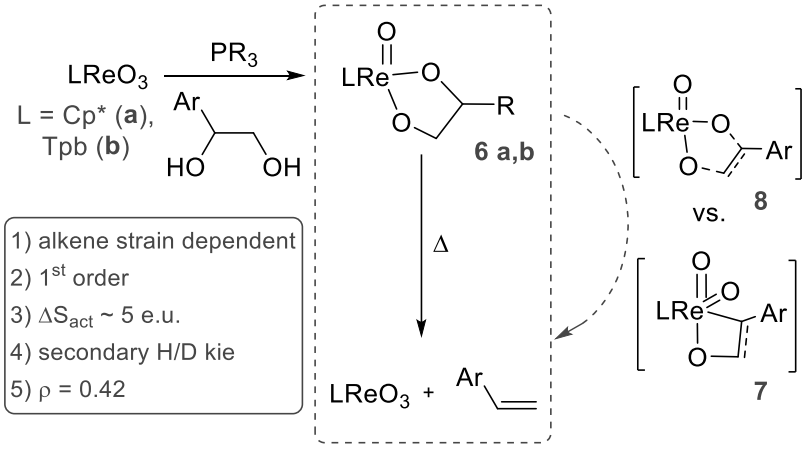


Figure I.3.a.6 Mechanistic probes of alkene extrusion from LReO(glycolate)

Subsequently, the Gable group investigated the alkene extrusion process from (tris-pyrazolylborate)Re(O)(glycolate) derivatives **6b**. The probes and findings from these

studies were generally quite similar to those from their investigation of the Cp*Re-derivatives. The Tpb-derivatives react with a slightly higher ΔH_{act} (2-4 kcal/mol) and lower rate (Figure I.3.a.6).[30,31] A later study focused on the kinetic isotope effects for derivatives separately labeled on the glycolate carbons, substituent effects for a series of Z-ArCHOHCH$_2$OH-derived glycolate complexes, and DFT computational analysis, including transition state modeling. The differences in the measured kinetic isotope effects were small, but significant, the Hammett substituent effect study showed dichotomous behavior, and the DFT-calculated transition state showed significantly different C-O bond lengths, consistent with an asynchronous extrusion process. On this issue we note that fragmentation of M-glycolates derived from symmetrical or aliphatic glycols may be more prone to concerted [3+2] cycloreversions (vide infra). This mechanistic subtlety notwithstanding, the examples of stereospecific syn-eliminations observed to date are indicative of a net syn-metalloglycolate cycloreversion, whether concerted or step-wise.

Although most of the DODH reactions described above used triphenyl phosphine a reductant, Nakagiri, Murai and Takai reported the use of triphenyl phosphite as reducing agent for related epoxide deoxygenation.[32] In combination with rhenium oxide (Re_2O_7) as catalyst they found phosphite to be highly efficient for the deoxygenation (DO) of unactivated aliphatic epoxides (Figure I.3.a.7). It is worth noticing that their system provides high yields (74-93%) with 2.5 mol% catalyst loading at 100^{o}C after only 2-8 hours.

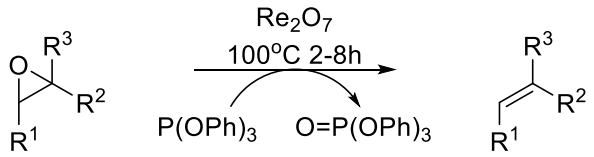


Figure I.3.a.7 General deoxygenation of epoxides using phosphite and rhenium oxide

ii. Hydrogen Reductant

The discovery of more practical, non-phosphine reductants for Re-catalyzed DODH began with a report by the Abu-Omar group employing hydrogen with the commercially available $MeReO_3$ as catalyst (Figure I.3.a.8).[33] Reactions were conducted with epoxides and glycols at 150°C in THF at 5-20 atm H_2 and 5-10 mol% $MeReO_3$ over 1-16 hr. Representative epoxides and glycols are converted moderately efficiently to olefins with high selectivity at lower pressures and shorter reaction times; alkanes, from over-reduction, were favored at higher pressures and longer times. The deoxygenation of cis- and trans-stilbene oxides, exhibit good, but not complete stereoretentive selectivity; cis-cyclic glycols eliminate much more effectively than the trans-glycols, consistent with the intervention and concerted fragmentation of $MeRe^{V}O$(glycolate). A catalytic process for deoxygenation and DODH was proposed involving initial hydrogenative reduction of $MeReO_3$ to $MeReO_2L$ (L=THF or H_2O), condensation of the latter with the glycol to form the Rev-glycolate, and subsequent alkene extrusion.

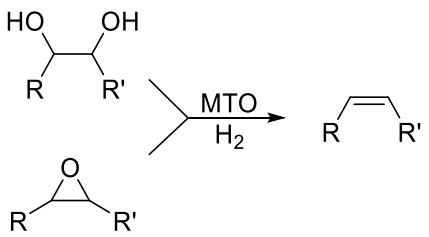


Figure I.3.a.8 Summary of DODH systems using hydrogen as reducing agent

Lin and coworkers reported a DFT-level computational study of the hydrogen-driven epoxide deoxygenation and glycol DODH catalyzed by $MeReO_3$.[34] Very high enthalpic barriers were found for both the [2+3] and the [2+2] addition of hydrogen to $MeReO_3$ (ΔH_{act} 61, 43 kcal respectively), and was judged not to be viable as a step in the catalytic process. Instead, reaction of $MeReO_3$ with the epoxide or the glycol (not shown) to produce $MeRe^{vii}O_2$(glycolate) (**9**) is more favorable (Figure I.3.a.9), followed by [2+3] addition of H_2 to **9** to give the Rev-glycol derivative **10** (ΔH_{act} 33 kcal). Extrusion of alkene from Re^{v}-glycolate **11** was calculated to proceed via a concerted [2+3] process with a barrier of 21 kcal. Thus, in the H_2-driven $MeReO_3$ reactions it appears that reduction of the glycolate **9** is likely turnover-limiting.

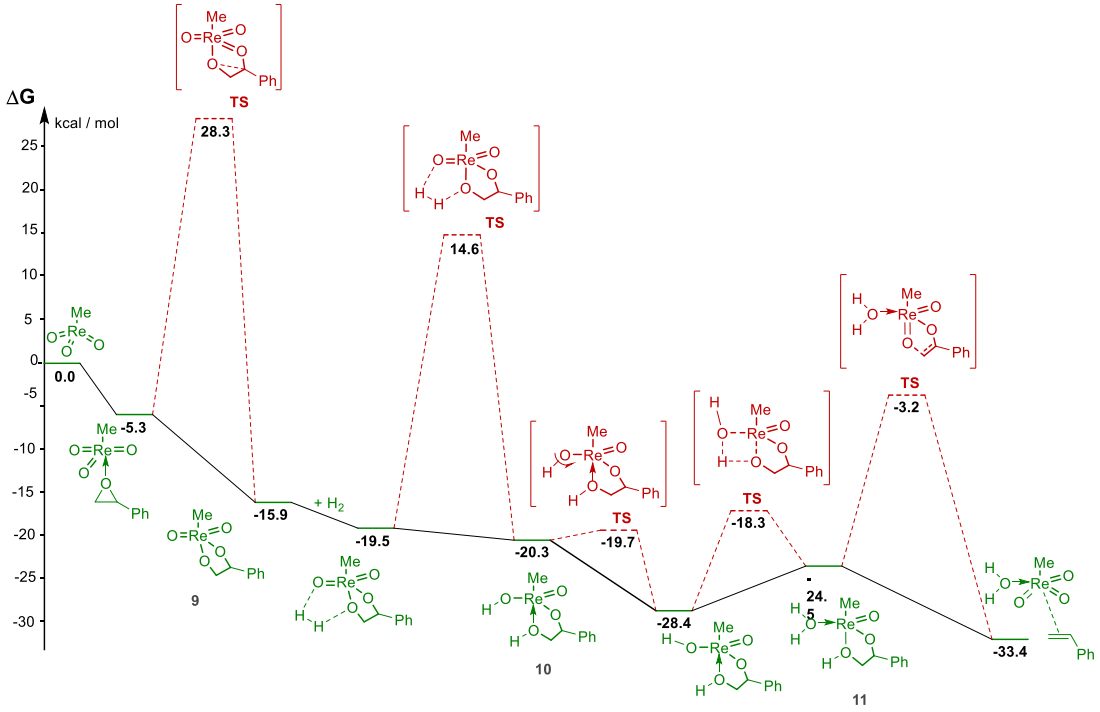


Figure I.3.a.9 Calculated lowest energy profile for hydrogen, $MeReO_3$- catalyzed DODH

iii. Sulfite Reductant

Soon thereafter the Nicholas group reported DODH and epoxide deoxygenation reactions driven by sulfite salts and catalyzed by $LReO_{3,4}$ derivatives (Figure I.3.a.10). Sulfite is an inexpensive and thermodynamically strong reductant, comparable to H_2 and CO.[35,36] A variety of glycol substrates are efficiently transformed into olefins (50-80% yields) with this system operating most effectively with $MeReO_3$ or $Bu_4N^+ReO_4^-$ (2-10 mol%) in aromatic solvents at 150ºC; yields and reaction rates are improved by the inclusion of 15-crown-5, presumably by increasing the solubility of the sulfite salt. Selective syn-elimination of the glycol was demonstrated by the preferential DODH of cis-1,2-cyclohexanediol and the stereoselective conversion of l-diethyl tartrate to (trans)-diethyl fumarate (Figure I.3.a.11). In a limited study erythritol was converted by Bu_4NReO_4/Na_2SO_3 largely to 1,3-butadiene along with 2,5-dihydrofuran and 2-butene-1,4-diol (5:1:0.5). Representative epoxides were deoxygenated by $MeReO_3/Na_2SO_3$ in moderate yields. Lewis base additives (e.g. amines) and potentially coordinating solvents (e.g. ethers, nitriles) were found to inhibit the $MeReO_3$-based reactions, but had little effect on the yields/conversions of those catalyzed by $Bu_4N^+ReO_4^-$. This may be the result of the high Lewis acidity of $MeReO_3$,[37–39] by which coordination of donor ligands can inhibit both glycol association and alkene extrusion from the metalloglycolate (vide infra).

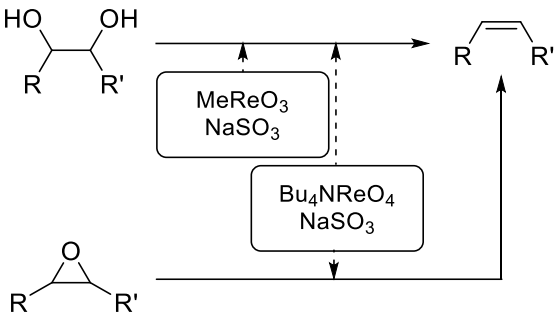
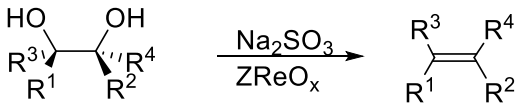


Figure I.3.a.10 Summary of DODH systems using sulfite as reducing agent



R^1 = alkyl, aryl, $R^{2,3,4}$ = H
$R^{1,2}$ = carbocycle, $R^{3,4}$= H
$R^{1,4}$ = CO_2R, $R^{2,3}$ = H

Figure I.3.a.11 General reaction equation of DODH using sulfite as reducing agent

A stoichiometric reactivity study with styrene-1,2-diol/$MeReO_3$ demonstrated the viability of a condensation/reduction/alkene extrusion pathway (Figure I.3.a.12) by spectroscopically detecting:[35] 1) that $MeReO_3$ reversibly forms $MeRe^{vii}(O)$(glycolate) (**9**) from the glycol (K_{eq} ca. 0.2) or more favorably from styrene oxide at 20°C; 2) the Re^{vii}-glycolate **9** is reduced at 20°C by PPh_3 or $(Bu_4N)_2SO_3$ to a mixture of Re^{v}-glycolates **12/12a**; and 3) the reduced Re-glycolates cleanly produce styrene and $MeReO_3$ upon heating at 60-100°C. These observations indicate that the latter step is likely turnover-limiting.

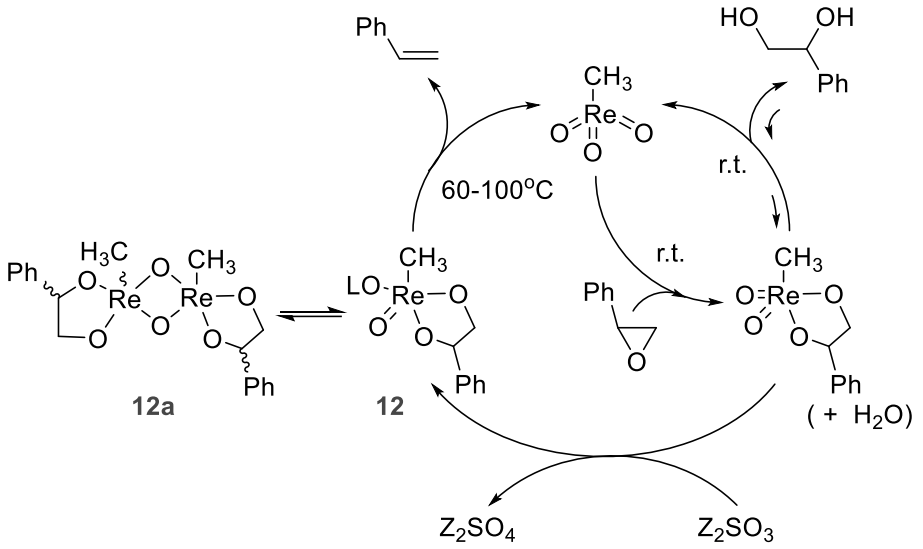


Figure I.3.a.12 Proposed mechanism of $MeReO_3$ catalytic cycle in DODH using sulfite reductant

The mechanism of the $MeReO_3$-catalyzed deoxydehydration of glycols to olefins by sulfite salts has been probed with Density Functional Theory (DFT) calculations.[40] Potential intermediates and transition states were evaluated for the three stages of reaction: a) dehydration of the glycol by an oxo-rhenium complex to form a Re-(O,O-glycolate); b) sulfite-induced O-transfer (to sulfate and a reduced oxo-Re); and c) fragmentation of the Re^{v}-glycolate to give the olefin and to regenerate $MeReO_3$. Various sulfite, sulfate, and Na-sulfite/sulfate species were evaluated as reactants/products and as ligands and solvation was taken into account. Transition states and activation energies were calculated for several of the key transformations, including the H-transfer glycol dehydration, the $LMeRe^{v}O$(glycolate) fragmentations (L=H_2O, $NaSO_3^-$, $NaSO_4^-$), and $NaSO_3^-$ attack on oxo-Re^{vii} species. The lowest energy catalytic pathway identified involves (Figure I.3.a.13): $NaSO_3^-$ attack on an oxo-oxygen of $MeReO_3$ to produce $MeRe^{v}O_2(OSO_3Na)^-$ (**13**); glycol coordination by **13**, followed by a series of H-transfer steps to LRe=O and/or LRe-OSO_3Na- to give $MeRe^{v}O$(glycolate)$(OSO_3Na)(H_2O)^-$ (**14**);

concerted extrusion of olefin from the Re^{V}-glycolate **14**; and dissociation of $NaSO_4^-$ from $MeReO_3(OSO_3Na)$ (**15**) to regenerate $MeReO_3$. Fragmentation of the Re-glycolate **14** is turnover-limiting with a calculated activation free energy of 35 kcal, a value consistent with the typical operating temperatures of these reactions. Coordination by H_2O, the reductant or its oxidized form to the Re^{V}-glycolate is calculated to greatly affect the facility of the olefin extrusion. The nature of the reductant, e.g. an O-transfer agent like PPh_3 or SO_3^- vs. the H-transfer agents, H_2 or sec-alcohols, thus likely affects both the thermodynamics and the kinetics of the reduction step.

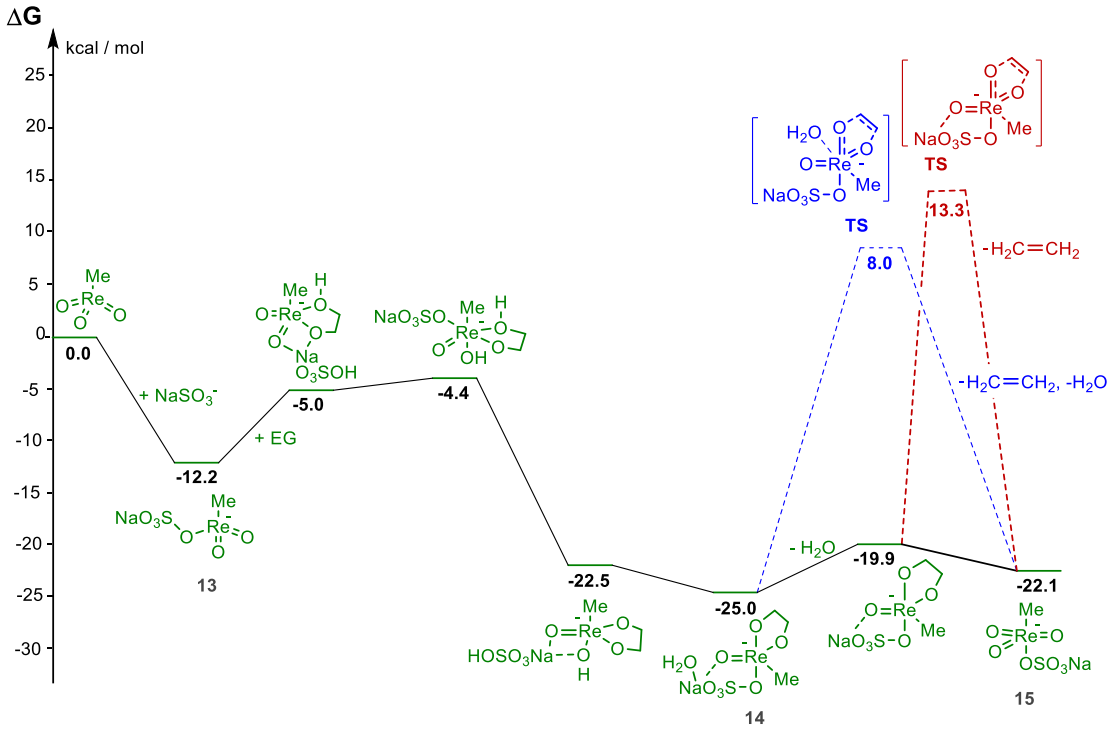


Figure I.3.a.13 Calculated lowest energy profile for sulfite, CH_3ReO_3- catalyzed DODH

iv. Alcohol Reductants

The use of secondary alcohols as reductants for DODH was first reported by Ellman, Bergman, and coworkers, who employed Re-carbonyl compounds, e.g. $Re_2(CO)_{10}$ as pre-catalysts under aerobic conditions (Figure I.3.a.14).[41] Optimized conditions used the glycol substrate with the mono-alcohol as the solvent, e.g. 3-octanol, at 150-175°C, with 1-2.5 mol% $Re_2(CO)_{10}$ and TsOH as a co-catalyst (2-5 mol%). Good yields of the olefin (50-84%) were obtained with representative glycols. The syn-3,4-decanediol was converted highly selectively to trans-3-decene, implicating a syn-elimination process in the diol to olefin conversion (Figure I.3.a.15). Erythritol was converted moderately efficiently to 2,5-dihydrofuran (62% yield), presumably the result of initial 1,4-diol dehydration followed by DODH of the THF-diol intermediate. The nature of the active catalyst was unknown at the time, but speculated to be an oxidized Re species.

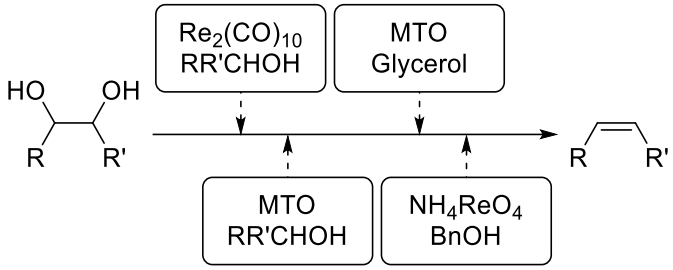


Figure I.3.a.14 Summary of DODH systems using sulfite as reducing agent

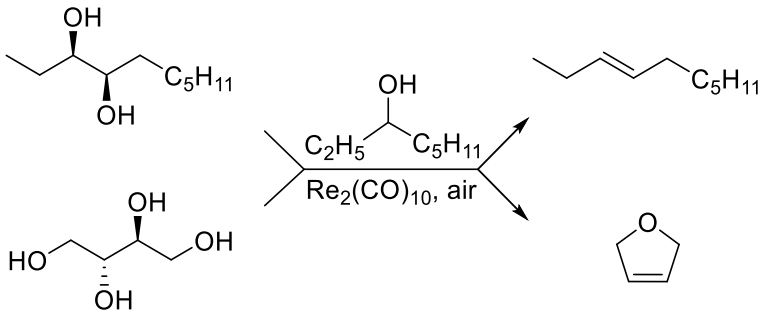


Figure I.3.a.15 First reported DODH reaction using alcohol as reducing agent

The Abu-Omar group demonstrated that in the absence of an added reductant $MeReO_3$ catalyzes redox disproportionation of glycols. Glycerol was shown to serve as both substrate and reductant (165^oC, 2 mol% $MeReO_3$) in a reactive distillation process, producing moderate yields of volatile allyl alcohol, acrolein and propanal (1.0: 0.22: 0.15) and non-volatile, reactive 1,3-dihydroxyacetone (Figure I.3.a.16). Redox disproportionation of cis-cyclohexanediol catalyzed by $MeReO_3$ was also efficient producing cyclohexene and 1,2-cyclohexanedione.[42] The rate of the glycerol reaction was determined to be first order in the diol and first order in $MeReO_3$ and a kinetic isotope effect of 2.4 was measured for d^5-glycerol$(OH)_3$, indicating turnover-limiting C-H(D) bond breaking. This was interpreted in terms of a catalytic cycle in which the Re^{vii}-glycolate intermediate undergoes rate-limiting H(D)-transfer redox reaction by glycerol. Following Abu-Omar's continuous distillation system d'Alessandro and co-worker reported a more extensive study of the deoxydehydration of glycerol by various rhenium oxo complexes without an added reducing agent and under hydrogen (sat atmospheric pressure).[43]

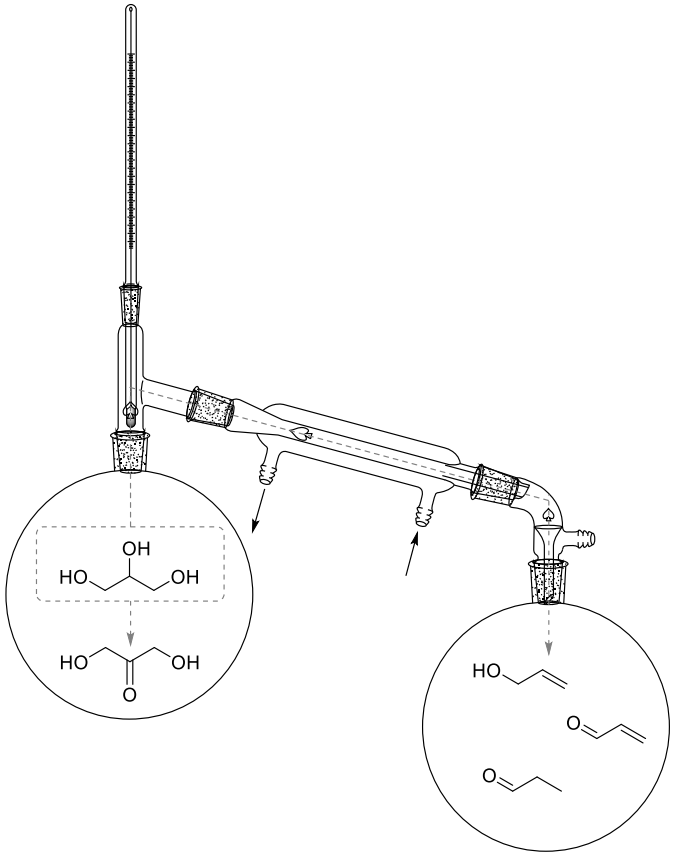


Figure I.3.a.16 $MeReO_3$-catalyzed disproportionation of glycerol in constant distillation system

Other researchers have expanded the scope of alcohol-driven DODH reactions. Shiramizu and Toste demonstrated that $MeReO_3$ was an effective catalyst for the DODH using sec-alcohol reductants and they extended the substrate scope to more complex polyols.[44] The alcohol reductant, preferably 3-octanol, was generally used as the solvent with 2.5 mol% of $MeReO_3$ at 155-200^{o}C in air; at the higher temperatures the DODH reactions of glycols and polyols were complete in 1-3 hr. The polyols glycerol, erythritol, and threitol were converted in high yields (80-90%) to allyl alcohol and 1,3-butadiene respectively, with 11-13 % of dihydrofuran derivatives as minor products from the tetraols. The C_5-sugar alcohols xylitol, arabinatol and ribitol were converted in moderate

(33-61%) yields to the same E-2,4-pentadienyl 3-pentyl ether derived from reaction with 3-pentanol as solvent. Similarly, the C_6-sugar alcohols sorbitol and mannitol were completely deoxygenated to the same E-hexatriene (54% yield). A series of stereoisomeric inositols were converted in low to moderate yields to mixtures of benzene (from exhaustive DODH) and phenol (from DODH and dehydration), with the former generally predominating (ca. 1:1 to 3:1). Application of the alcohol/ $MeReO_3$ protocol on sugars provided moderate yields of furan (47-60 %) from erythrose and threose, while pentoses gave low yields of 2-alkoxymethyl furan, resulting from a combination of dehydration and DODH steps. Regarding the mechanism of the catalytic process, it was found that reactions run in the presence of 3-hexyne, resulted in formation of isolable $MeRe^{v}O_2$(alkyne), which reacted at room temperature with glycol to form $MeRe^{v}O$(glycolate), and had comparable catalytic activity to $MeReO_3$, supporting $MeRe^{v}O_2$ as the catalytically relevant species.

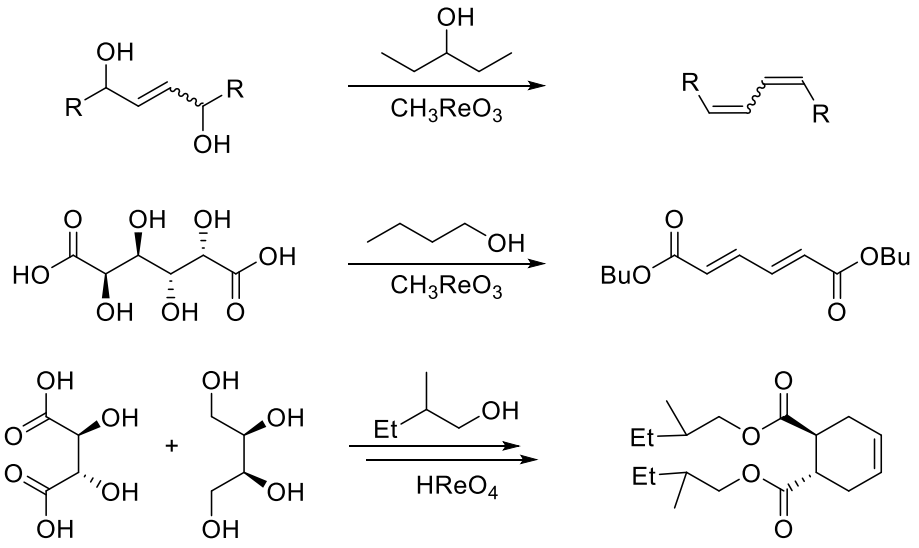


Figure I.3.a.17 Alcohols as reducing agent in DODH system

Shiramizu and Toste expanded the scope and utility of alcohol-driven, $MeReO_3$-catalyzed DODH by: 1) using $MeReO_3$'s ability to promote allylic alcohol 1,3-transposition to enable the conversion of 1,4-unsaturated alcohols to 1,3-dienes; 2) including new polyfunctional natural substrates in DODH; and 3) carrying out a one pot tandem DODH-Diels-Alder reaction sequence (Figure I.3.a.17).[45] Representative acyclic and cyclic ene-1,4-diols were converted in moderate to good yields to 1,3-dienes (18-70 %) with α,β-unsaturated ketones as minor side-products. The C_6 sugar acid, mucic acid and its ester, could be efficiently converted to the dienic muconic ester 16 (71%) with the primary alcohol 1-butanol as solvent/reductant and acidic $HReO_4$ as the catalyst. Similarly the C_6 gluconic acid was efficiently converted to the E,E-dienic ester 16 (47%). The tandem DODH/Diels-Alder process was demonstrated with tartaric acid and erythritol as the dienophile and diene precursors, respectively. These were first heated with $HReO_4$/2-methyl-1-butanol (170^{o}C, 4h) to generate butadiene and the fumarate ester; continued heating at 120^{o}C (42h) provided the Diels-Alder adduct in 70 % yield from tartaric acid.

Although secondary alcohols have generally been found to be more effective reductants in DODH reactions, Boucher-Jacobs and Nicholas showed that the reactive primary alcohol, benzyl alcohol was also an efficient reaction partner for DODH of representative glycols and polyols with less expensive NH_4ReO_4 (APR) as the catalyst (Figure I.3.a.18).[46] This system has practical advantages for facilitating separation of the alkene and aldehyde co-products via the insoluble bisulfite adduct of the aldehyde (not effective with ketones) and also enabling efficient recovery/re-use of the insoluble

catalyst. Operating at 150°C in aromatic solvents with 2.5 mol% APR several glycols were converted to corresponding alkenes in moderate to excellent yields (50-95%).

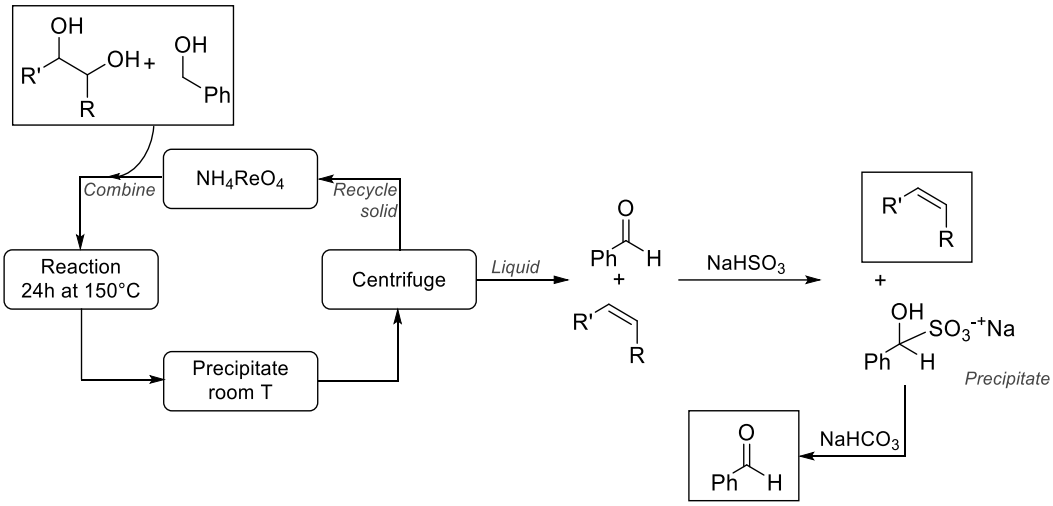


Figure I.3.a.18 Purification and catalyst recycling in NH_4ReO_4 / benzyl alcohol DODH system

An experimental mechanistic study of the $MeReO_3$-catalyzed, alcohol driven DODH of hydrobenzoin to trans-stilbene was recently reported by Abu-Omar and coworkers (Figure I.3.a.19; R=Ph).[47] Kinetic studies of the catalytic reaction in excess 3-octanol (solvent) at 140°C revealed an induction period, a zeroth order dependence on the glycol and half order behavior in $MeReO_3$; the rate dependence on the alcohol reductant was not determined. The half order catalyst dependence suggests the involvement of a monomer-dimer equilibrium of Re-complexes. Stoichiometric reactivity experiments with NMR monitoring showed that the $MeRe^{v}O$(glycolate) intermediate could be detected throughout the reaction and hence its conversion to product is probably rate-limiting. The authors claim that this conversion requires further reaction with the octanol to produce alkene and suggested that reduction to a Re^{iii}-diolate precedes alkene extrusion. A small

primary kinetic isotope effect (1.4) with 3-D-octanol and a large negative activation entropy (-37 eu) was taken as support for H(D)-transfer from the alcohol to the Re(diolate) as the rate-limiting step.

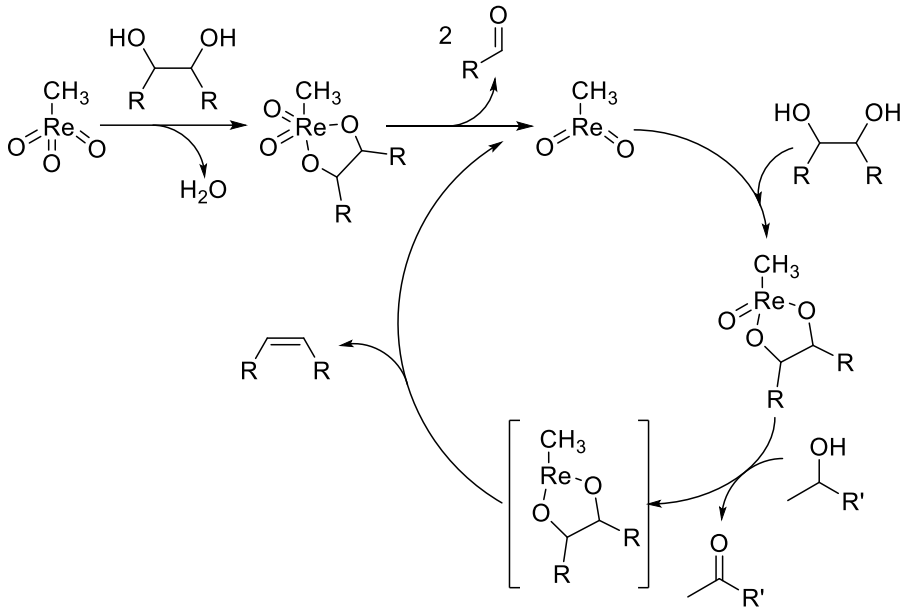


Figure I.3.a.19 Proposed mechanistic cycle for alcohol-driven, CH_3ReO_3-catalyzed DODH by Abu-Omar

A recent computational study by Wang and coworkers analyzed the energetics for various pathways in the alcohol-mediated DODH of glycols catalyzed by $MeReO_3$.[48] Free energies and enthalpies were calculated using DFT methods with the MO6 functional and corrected for temperature and solvent. Three pathways A, B, C were compared, differing in the timing of the $Re^{vii/v}$ reduction and the glycol condensation stage and in the condensation intermediates. In pathway A the $MeReO_3$ reduction precedes the condensation and the highest barrier (45/33 kcal for $\Delta G_{act}/\Delta H_{act}$) was found for intramolecular H-transfer reduction of a Re^{vii}-alkoxide-OH species. Pathway B, involving initial condensation followed by reduction, was found to have as its highest barrier (53/38

kcal) in the H-transfer reduction of a Re^{vii}-H-glycolate by the alcohol. The lowest energy pathway, C (Figure I.3.a.20), like A, involves initial $MeReO_3$ reduction followed by condensation, but differed from A in finding a somewhat lower barrier H-transfer step (39/27 kcal) for the Re^{vii}-alkoxide to form $MeReO(OH)_2$. The possibility that these reactions proceed through a Re^{iii}-glycolate, as proposed by Abu-Omar, was not considered.

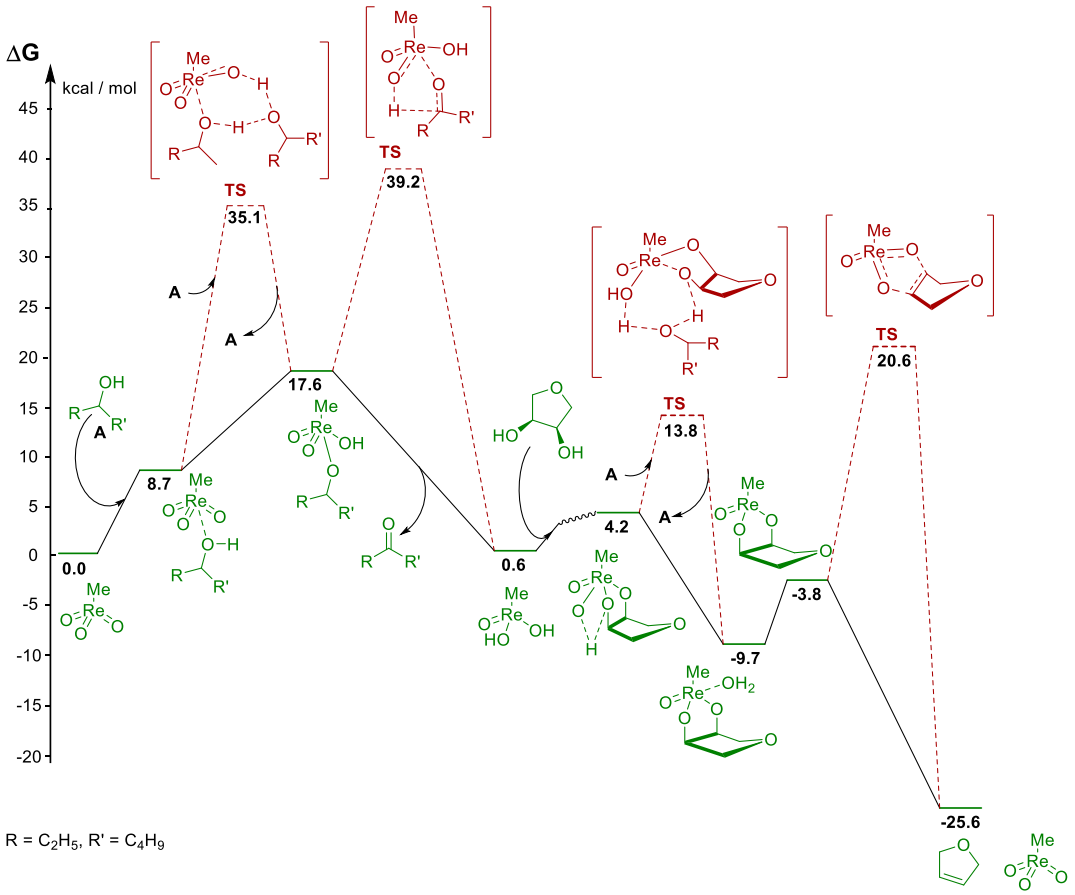


Figure I.3.a.20 Calculated lowest energy profile for alcohol-driven, CH_3ReO_3-catalyzed DODH

Complementing the computational study above, Dethlefsen and Fristrup conducted an experimental mechanistic study[49]. They observed the reaction over time by spectroscopy, studied the rate of the reaction by varying the concentration in the reagents

and observed the KIE by a D-labeling of the alcohol. They found that: 1) the rate limiting step was the oxidation of the alcohol reductant; 2) the reduction of the rhenium center occurs before the formation of the glycolate complex; and 3) a Re^{vii}-glycolate specie **16** is formed reversibly with the starting rhenium catalyst (CH_3ReO_3). (Figure I.3.a.21)

The DODH of 1,4-butendiol described by Shiramazu and Toste was recently investigated in a computational study by Wu, Zhang and Su.[50] Two pathways for the mechanism were considered: A) the isomerization of the allylic alcohol by $MeReO_3$ followed by the DODH reaction; and B) the direct DODH of the 1,4-butendiol. The kinetic comparison of both pathways showed path B to be more favored than path A. Like Fristrup in the case of vicinal diol Su and co-workers found the first step of the mechanism to be the reduction of rhenium center. In the case of the direct DODH of 1,4-butendiol the rate-limiting step appears to be extrusion of the olefin.

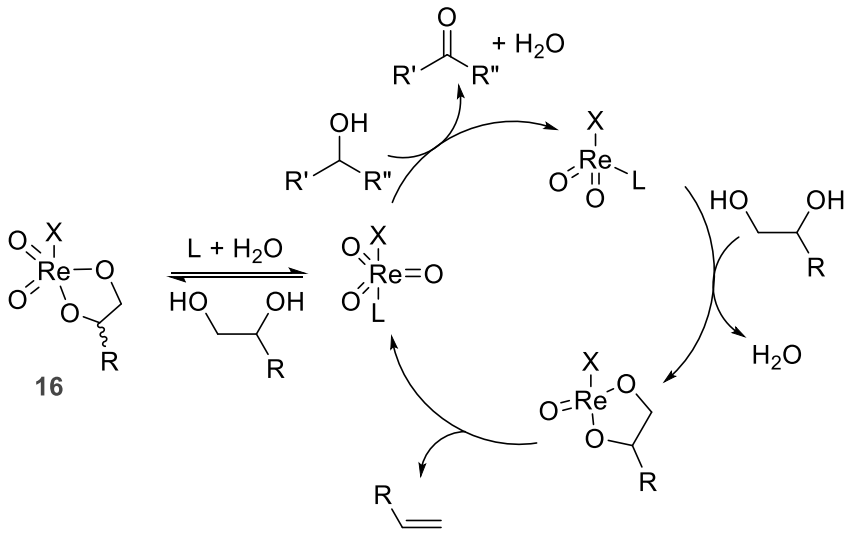


Figure I.3.a.21 Proposed mechanistic cycle for alcohol-driven, CH_3ReO_3-catalyzed DODH by Fristrup

v. Elemental reductants

A new class of DODH reducing agent, elements, was reported by McClain and Nicholas[51]. They described the efficiency of elements Zn, Fe, Mn and C as reducing agents on diols (48-85% Yield) using ammonium perrhenate as catalyst. (Figure I.3.a.22) The elemental reducing agents provide a cheap and easy to remove alternative to soluble reducing agents.

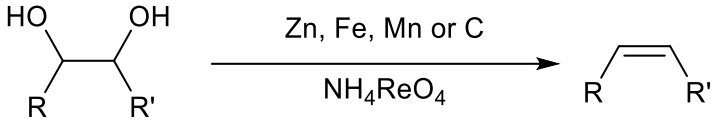


Figure I.3.a.22 Summary of DODH system using elemental reductant

vi. Heterogeneous ReO_x DODH catalyst

In an initial effort to develop heterogeneous (supported) DODH catalysts potentially suitable for industrial scale processes Nicholas, Jentoft and co-workers reported on the catalytic properties of a material prepared by treatment of activated carbon with ammonium perrhenate.[52] This material was found to be active for the hydrogenative DODH of representative glycols at 150-175^{o}C in aromatic solvents under 6-12 atm H_2 (Figure I.3.a.23). Under these conditions alkenes were produced selectively in moderate to excellent yields (40-90%) with no over-reduction to alkanes; l-diethyl tartrate was converted stereoselectively to diethyl fumarate. From a preparative scale experiment corresponding ketones, dimeric ethers and acetals were identified as minor by-products, apparently from acid-promoted dehydration processes. Catalyst recovery and filtrate activity tests show partial loss of activity by the recovered catalyst and suggest catalysis by both homogeneous and heterogeneous components. Partial leaching of a catalytically

active species apparently occurs under operating conditions that is re-adsorbed at room temperature. The ReO_x/C material also catalyzes moderately efficient DODH reactions (40-52 %) with hydrogen transfer reductants, including 3-hexanol, benzyl alcohol and tetralin.

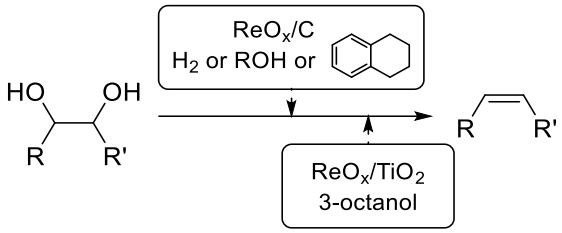


Figure I.3.a.23 Summary of DODH system using heterogeneous rhenium catalyst

With similar yields Palkovits and co-worker reported a titania supported ReO_x catalyst using 3-octanol as reducing agent[53]. They first did a screening of various catalyst support and found TiO_2 to be the most suitable along with a characterization of the heterogeneous catalyst before and after reaction. They were able to reuse this supported rhenium catalyst six times without loss of activity.

b. Non-precious metal catalyzed DODH

Until recently, all of the reported metal-catalyzed DODH systems have utilized oxo-rhenium catalysts. The low natural abundance and high cost of rhenium and its derivatives[54] provides an incentive for the discovery of non-precious metal catalysts for deoxydehydration that could be practically applied to large-scale biomass conversion processes.

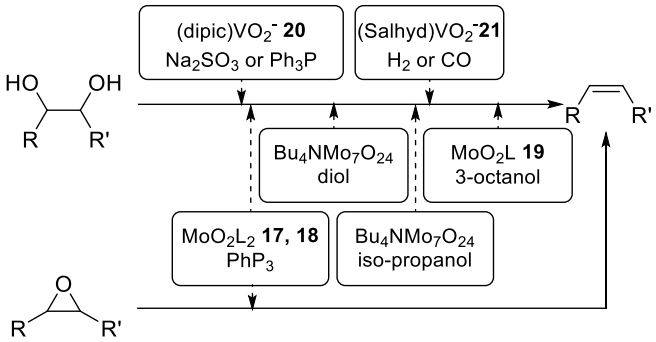


Figure I.3.b.1 Summary of DODH system using non precious metal catalyst

i. Molybdenum

Molybdenum's relative abundance[55] and lower cost stimulated investigations to evaluate the scope and efficacy of Mo-catalyzed DODH reactions. Three brief notes of modest Mo-based DODH activity have appeared (Figure I.3.b.1), the first with styrene oxide and styrene diol promoted by (dithiocarbamate)$_2$MoO$_2$/Na$_2$SO$_3$ (**17**, 10-30 % yield);[56] two examples employed (acylpyrazonolate)MoO$_2$/PPh$_3$ (**18**; 10, 55% yields);[56] and a survey from Fristrup group of several oxo-Mo-complexes with no reductant gave 35-45% olefin yields from tetradecanediol, with (NH$_4$)$_6$Mo$_7$O$_{24}$ [57] and MoO$_2$(DMF)$_2$Cl$_2$ [58] being the best. In a follow up publication Fristrup and co-worker conducted a computational study of the molybdenum ((NH$_4$)$_6$Mo$_7$O$_{24}$) catalyzed DODH system(Figure I.3.b.2).[59] They suggested the plausible formation of a molybdenum diglycolate forming acetaldehyde and formaldehyde (20.8 kcal/mol barrier) before the extrusion of the alkene (19.1 kcal/mol barrier). More recently the Fristrup group reported the use of (NH$_4$)$_6$Mo$_7$O$_{24}$ (AHM) to catalyze efficient DODH reactions with isopropanol as reducing agent and solvent.[60] Under these conditions they reached the high yield of 77% in alkene with tetrabutyl ammonium hydroxide as a 3 equivalent additive at 240^{o}C

for 12-18h. The Fristrup group conducted a computational study of this system as well, demonstrating that similar to the computational study of molybdenum catalyzed, alcohol driven DODH reaction, the oxidation of the alcohol and the extrusion of the alkene have the highest energy barriers at 24.1 and 13.8 kcal/mol respectively.

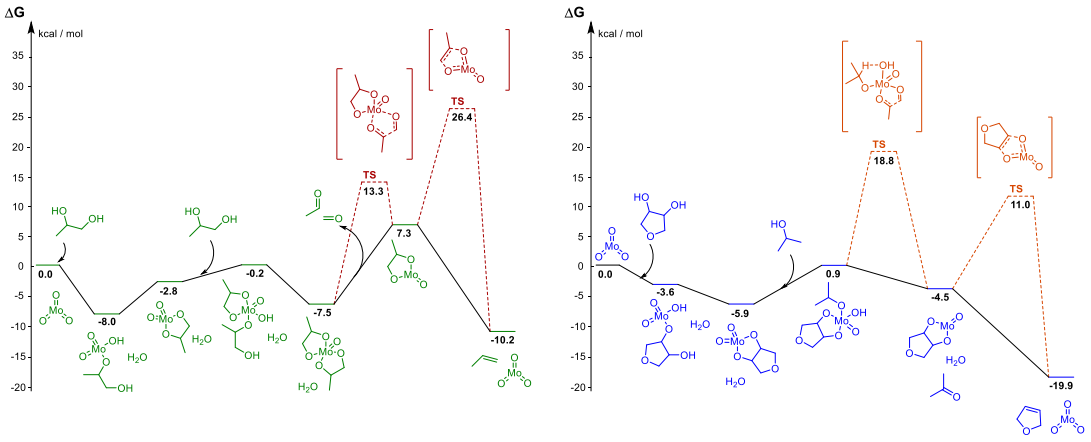


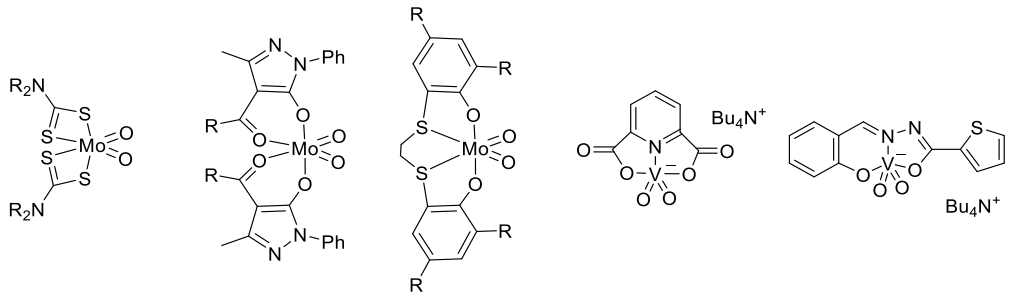
Figure I.3.b.2 Calculated lowest energy profile for diol-driven (left) and for isopropanol-driven (right), MoO_3-catalyzed DODH

Following the advances in molybdenum catalyzed DODH reaction, Okuda and co-worker have reported a new bis(phenolato)molybdenum complex **19** that catalyzes DODH in moderate to good yield using 3-octanol as reducing agent (200°C, 18h).[61]

ii. Vanadium

Recently, a more thorough study of DODH reactions catalyzed by non-precious vanadium complexes[62] was reported by Nicholas and coworkers. Several inexpensive and readily available oxo-vanadium compounds, including metavandate salts ($Z^+VO_3^-$) and dioxo-vanadium complexes, were evaluated for their catalytic activity with representative glycols (Figure I.3.b.3).[63] Among these, Bu_4N[(2,6-pyridinecarboxylate)VO_2] (**20**) was

found to be the most effective with either PPh_3 or Na_2SO_3 serving as the reductant. Under optimized conditions (150-170^oC, aromatic solvent, 10 mol % **20**, 24-48 h) high conversions and good yields of alkene were achieved. Highly selective syn-elimination was observed in the conversion of l-diethyl tartrate to diethyl fumarate catalyzed by PPh_3/**20** (Figure I.3.b.3(c)). This result supports a proposed catalytic cycle involving a reduction/condensation sequence (in either order) followed by stereoselective olefin extrusion from a V^{iii}-glycolate intermediate, (dipic)V^{V}(glycolate)$^-$. The Na_2SO_3/**20** combination is also highly efficient for the deoxygenation of epoxides to olefins (Figure I.3.b.3).[64] Following this report Galindo published computational studies of **20** (Bu_4N[(2,6-pyridinecarboxylate)VO_2])-catalyzed DODH using triphenylphosphine reductant[65]. The pathway of reduction of the metal center from V^v to V^{iii} by triphenylphosphine happening first was shown to be favored over activation of the diol.



17 **18** **19** **20** **21**

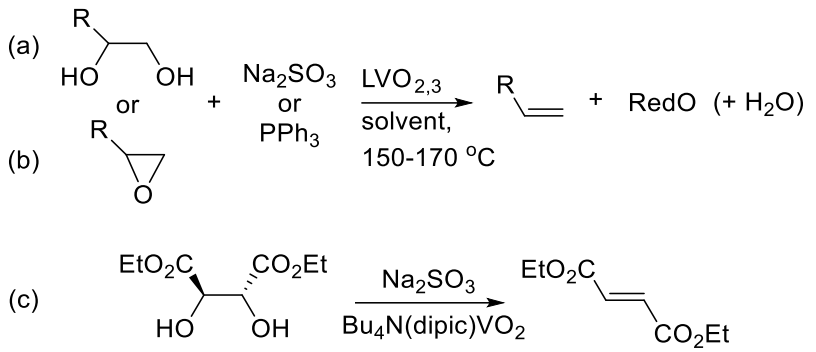


Figure I.3.b.3 Vanadium catalyzed DODH and DO

The recent advances toward non precious transition metal catalyzed DODH reactions are providing good alternatives to rhenium catalysts, inexpensive reducing agents such as hydrogen and carbon monoxide, and greener solvents such as isopropanol. The **21**/H_2 or CO combination is the most economical report providing potential for the DODH reaction to be done on an industrial scale.

4. Applications of DODH Systems

Even though the DODH reaction has been developed in order to directly transform biomass-derived polyols to olefins, we have seen the use of the DODH reaction as a step in a synthetic sequence. Shiramazu and Toste were the first to report the synthesis of adipic acid from mucic acid as a two steps process (Figure I. 4.1), DODH followed by hydrogenation, with 99% overall yield.[45] The Zhang group provided a more extensive study of this two step process.[67–69]

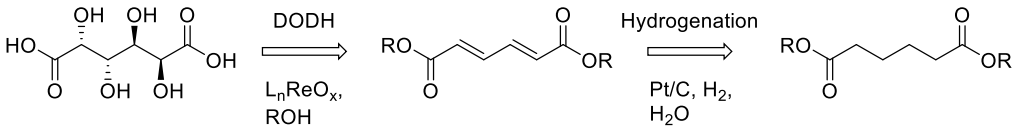


Figure I. 4.1 Synthesis of adipic acid from mucic acid via DODH and Hydrogenation two steps process

Tomishige and co-workers applied the concept of DODH followed by hydrogenation to a wider range of polyols.[70,71] Using heterogeneous catalyst ReO_x-Pd/CeO_2 they obtained 85 to 98 % yields of saturated alcohols and diols from glycerol, erythritol, xylitol and sorbitol (Figure I. 4.2). The overall transformation, vicinal hydrodeoxygenation, is done in a single reactor.

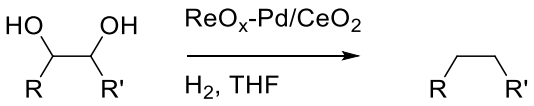


Figure I. 4.2 Simultaneous DODH and hydrogenation of diols by ReO_x-Pd/CeO_2 heterogeneous catalyst

In a different process Krische and co-workers utilized a vanadium catalyzed DODH in their benzannulation reaction to form fluoranthenes and acenes (Figure I. 4.3).[72] In the first step they used a ruthenium catalyzed [4+2] cycloaddition of cyclohexendiols. In the second step they effected DODH using the vanadium catalyst **20** along with sodium sulfite as reducing agent and finally treated the DODH product with charcoal to aromatize it into naphthalene derivatives.

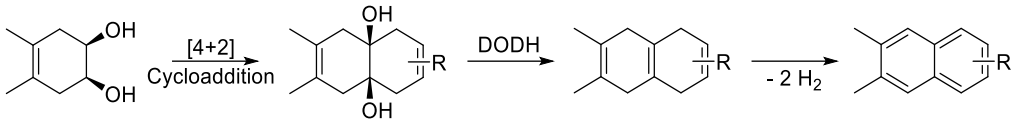


Figure I. 4.3 Benzannulation reaction to form substituted naphthalene

5. Conclusions and Future Prospects

A graphical summary of the catalytic glycol deoxydehydration and epoxide deoxygenation reactions reported to date is given in Figure I. 5.1.

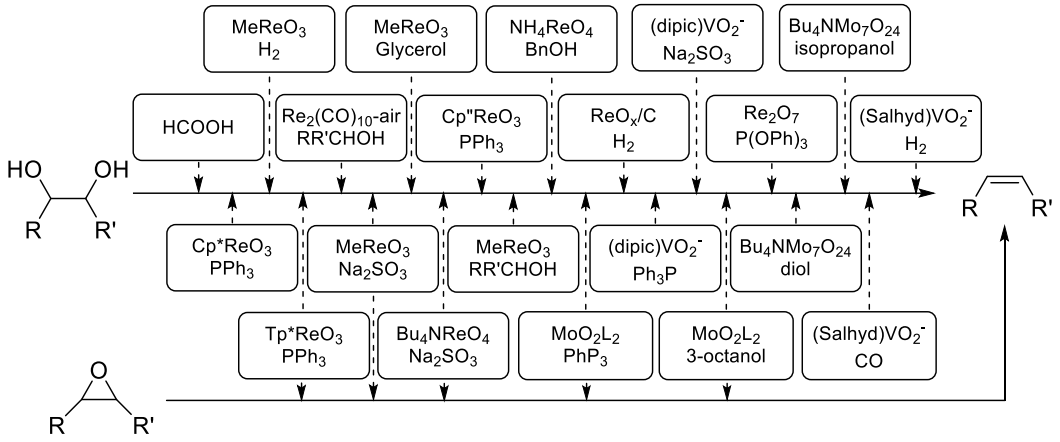


Figure I. 5.1 Summary of DODH systems

Since its discovery, the catalytic deoxydehydration reaction has seen rapid development. A variety of oxo-metal catalysts (mostly of rhenium) and reductants, including phosphines, hydrogen, sulfite and alcohols, have been shown to be effective. Numerous glycols and a growing set of biomass-derived polyol substrates undergo the reaction with good efficiency. The reactions are typically regiospecific and highly stereoselective. Results from experimental and computational mechanistic studies suggest the general operation of a catalytic process involving three basic stages: glycol condensation to a M-glycolate, reduction of the oxo-metal; and alkene extrusion from the

reduced metal-glycolate. The preferred sequence of the condensation and reduction steps and which step of the catalytic pathway is turnover-limiting depends on the catalyst and the reductant. Recent practical DODH developments include the discovery of non-precious V- and Mo-oxo DODH catalytic systems and supported oxo-rhenium catalysts.

There remain important needs for new more active, economical deoxygenation catalysts, reductants and practical reaction media, to improve the efficiency and extend the substrate scope to higher polyols. Reacting further the alkene to increase its carbon backbone is of importance as it could allow the small biomass derived polyols to be converted in highly valuable chemicals. In addition the involvement of the reducing agent in this C-C bond forming secondary reaction would make it an atom economical process.

Therefore we explore a new class of reducing agent, hydroaromatics. We started this study by screening the activity of various hydroaromatics. In the screening we found several of these compounds to be highly active. Two of them, cyclohexadiene and dihydroanthracene, provided C-C bond forming tandem reactions: DODH/Diels-Alder. Indoline was found to be the most active hydrogen donor species and was applied to a larger survey of diols. In competition with other reported reducing agent such as alcohols, indoline was found to be the most consumed as reducing agent. This superior activity was in part explained by a unique bonding affinity of indoline with the rhenium catalyst which was studied in more detail.

Additionally the development of processes utilizing DODH as a key step in synthesis of more valuable chemicals has been very limited so far. In an effort to increase the synthetic value of the DODH reaction we are examining the development of tandem reaction systems coupling the DODH reaction with C-C bond forming reactions. The

development of tandem reactions based on the DODH process is challenging due to the required compatibility of reagents and catalysts needed for each of the steps. We explore several reactions for coupling with the DODH reaction including crotylation, hetero Diels-Alder, base free Wittig, hydroformylation, hydroacylation, allylation and Heck type reactions.

Recently in our laboratory we, G. Kasner, M. McClain, Dr. Nicholas and I, discovered and developed a new catalytic reductive coupling reaction. In this reaction activated alcohols form alkane dimers. This novel and rare C-C bond formation attracted our attention. Dr. Nicholas and I studied the mechanism of this $IReO_2(PPh_3)_2$ catalyzed reductive coupling reaction by running stoichiometric, kinetic and computational experiments.

Chapter II. Hydroaromatics as DODH Reducing Agents

1. Introduction

The use of alcohols as H-transfer reductants in DODH reactions has also received attention.[41,44–46] Typically, secondary alcohols have been used, often as the reaction solvent.[41,44] The activated primary alcohol, benzyl alcohol, has been employed stoichiometrically together with $MeReO_3$ or NH_4ReO_4 for the DODH of organic soluble glycols.[46] Shiramizu and Toste found 1-butanol to be effective as a reducing agent and solvent in combination with perrhenic acid as catalyst.[45] The mechanistic details of the alcohol-driven DODH have been the subject of some debate regarding which Re-intermediates react with the reductant and how the hydrogens are transferred.[48,73,74]

Hydroaromatics (HA), several of which are abundant in fossil-resources, have been employed as liquid organic hydrogen carriers for hydrogenation reactions and for hydrogen storage.[75] The catalytic activity of redox-active solid metal oxides, e.g. V_2O_5, Fe_xO_y, for the dehydrogenation of alkyl aromatics, used for the production of styrene from ethyl benzene,[76–80] suggested to us the potential use of these reductants in homogeneous oxometal-catalyzed reactions. However, rather little is known about their reactivity with soluble oxo-metal species.[81,82] In the first report of ostensibly heterogeneous catalytic DODH reactions using perrhenate supported on carbon,[52] the primary reductant employed was hydrogen, but a few examples of H-transfer reductants, e.g. benzyl alcohol and tetrahydronaphthalene, were also noted. Here we report the development of efficient homogeneous catalytic DODH reactions with hydroaromatic hydrogen donors and provide insights into the nature of the reactive intermediates involved. Hydroaromatics can be seen as hydrogen carriers and could carry hydrogen

safely to the reaction mixture. Some hydrogen donors are able to provide two equivalents of hydrogen which could lower the loading in reducing agent. Finally some other hydroaromatic species could lead us to tandem DODH/C-C bond forming reactions.

Most results from this chapter have been published in 2015.[83]

2. Hydroaromatics as Reductants for DODH and Tandem DODH/Diels Alder Reactions

A set of six potential hydrogen donors were tested for efficacy under typical DODH conditions with diethyl tartrate (DET) and 1,2-octanediol as representative glycols. In these reactions (Table II. 2.1) we obtained moderate to very good yields of the alkene, from 70 to 99% with diethyl tartrate (DET) and 40 to 70% with octane diol (yields determined by NMR). In the cases of entries 2.1.5a and 2.1.6a, the DODH product, diethyl fumarate (DEF), underwent a tandem Diels-Alder (DA) reaction[45] (Figure II. 2.1 and Figure II. 2.2). In the first case (entry II.2.1.5.a) 1,3-cyclohexadiene serves both as the reducing agent for the DODH reaction and as the diene for the Diels-Alder reaction, providing the trans-cycloadduct **1**[84] in 78 to 90% yield depending on the solvent used. In the second case (entry II.2.1.6.a), 9,10-dihydroanthracene was employed as the reductant for DET, expecting to generate anthracene and fumarate, which would engage in cycloaddition. Indeed, the trans-adduct **2**[85] was formed, albeit in a modest 40% yield, with about 25% of fumarate remaining.

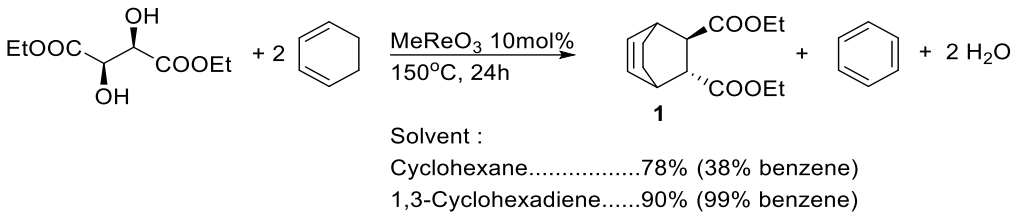


Figure II. 2.1 Tandem DODH/DA with DET and 1,3-cyclohexadiene

Tetrahydronaphthalene (THN) from coal has been studied as a hydrogen donor.[86–88] An attractive feature of this abundant hydroaromatic is that it could provide two equivalents of hydrogen. We further investigated its efficacy using a half or one equivalent on diethyl tartrate and 1,2-octanediol (entries II.2.1.2.a-d). After only 17h the yields were moderate using half an equivalent of THN, improving somewhat after 48h; use of one equivalent of THN increased the yield further.

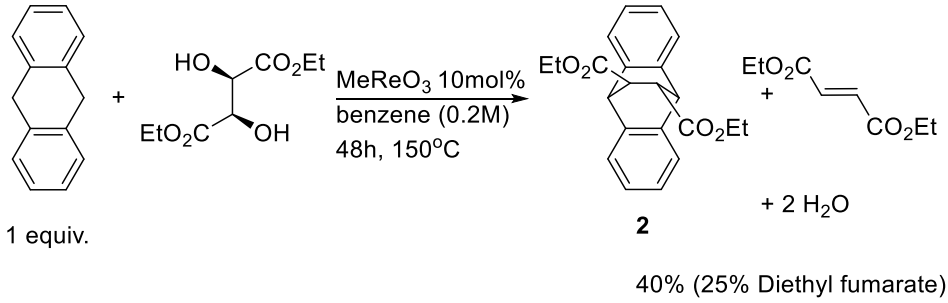


Figure II. 2.2 Tandem DODH/DA with DET and 9,10-dihydroanthracene

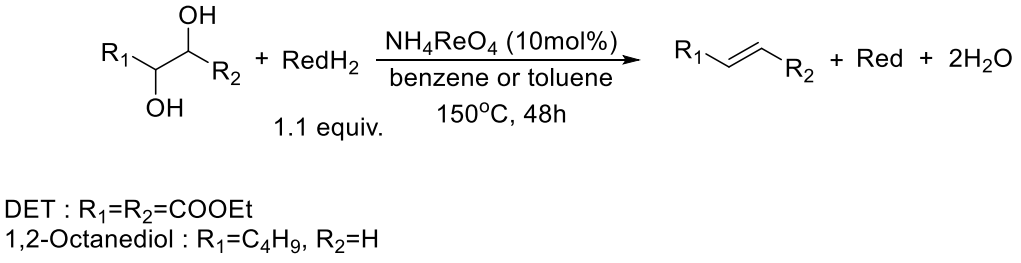
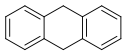
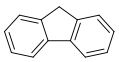


Figure II. 2.3 Activity of HA on DODH of DET and 1,2-octanediol

Table II. 2.1 Screening hydroaromatic reductants for DODH

Entry	Reducing agent	Glycol	Yield (%)[a]
II.2.1.1		DET	90
II.2.1.2.a		DET	92
II.2.1.2.b			73[b]
II.2.1.2.c		1,2-octanediol	60
II.2.1.2.d			48[b]
II.2.1.3.a		DET	99 (99% indole)
II.2.1.3.b		1,2-octanediol	70
II.2.1.4		DET	70
II.2.1.5.a		DET	78-90 in **1** (Figure II.2.1)
II.2.1.5.b		1,2-octanediol	52[c]
II.2.1.6.a		DET	40 in **2** (Figure II.2.2)
II.2.1.6.b		1,2-octanediol	64
II.2.1.7[d]		DET	82

a) yield determined by ^{1}H-NMR with internal standard
b) 17 h reaction time with 0.55 equiv. of reducing agent
c) $MeReO_3$ used as catalyst and the reductant as solvent
d) The oxidized product of fluorine not characterized.

Potential hydrogen donors other than the ones represented in Table II. 2.1 were also tested (Figure II. 2.4). With DET and octane diol most of them gave a reasonable yield around 50% (from 40% to 70%). These yields were judged to be insufficient, however, to demonstrate their hydrogen donor ability under the DODH reaction conditions for two reasons: 1) their oxidized products were not detected; 2) control experiments in which the reducing agent was left out demonstrated the ability of the diol to be its own reducing

agent forming up to 50% of alkene product. In addition, for a number of these two equivalents of reductant relative to the diol was required, making for poor atom economy.

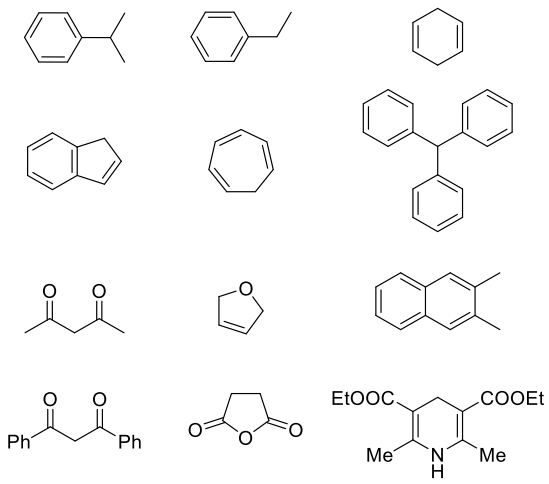


Figure II. 2.4 Hydrogen donors tested that gave limited alkene yield or ambiguous products

3. Indoline as Reducing Agent

The results in Table II. 2.1 demonstrated that indoline is the most effective hydroaromatic hydrogen donor for DODH of the model substrates. Not only did it provide the highest yields of olefin, but its co-product, indole, is easily detected and formed with high efficiency; typically the ratio of alkene to indole is close to 1:1. Accordingly, indoline was utilized in DODH reactions with a broader range of polyols (Table II. 3.1). While the DODH reactions of diols are efficient employing NH_4ReO_4 (APR) or $MeReO_3$ ($MeReO_3$) /indoline in aromatic solvents (entries II.2.1.3.a-b), to effectively convert poorly soluble higher polyols we turned to 1-butanol as a solvent.[45] The reaction utilizing indoline in combination with APR or $MeReO_3$ as catalysts in 1-butanol solvent proved to be effective for the DODH of several polar glycols and polyols (entries II.3.1.2-10). We

were pleased to obtain a quantitative yield (99%; 90% isolated) of N-allyl purine **3**[89] from diprophylline (entry II.3.1.2). By comparison, a 70% yield of **3** was obtained from this substrate using the benzyl alcohol/NH_4ReO_4 system.[46] N-allyl heterocycles such as **3** have diverse biological activity, including as modulators of drug-induced sleep and spontaneous activity,[90] as selective binders to the A2 adenosine receptor[91], and as anti-cancer and anti-viral agents.[92] Glycerol and its ester and ether derivatives (entries II.3.1.3-5) gave similarly high yields. Erythritol and xylitol (entries II.3.1.6 and II.3.1.7) afforded moderate yields of the corresponding diene products. The three polyhydroxy carboxylic acids- glyceric acid, tartaric acid and mucic acid (entries II.3.1.8, II.3.1.9 and II.3.1.10) each provided an esterified alkene product; tartaric acid yielded 78% dibutyl fumarate (60% isolated), while mucic acid gave 57% of the corresponding trans,trans-diene ester. Glyceric acid gave a fairly low yield of butyl acrylate, which may be the result of competing reactions. The same reaction as entry II.3.1.8 using APR as catalyst showed no acrylate product and GC-MS analysis revealed indoline- and indole/acrylate-coupled products (Figure II. 3.2).[93,94] Each of these products had a specific GC signals with matching mass spectrum (molecular ion and fragmentation pics).

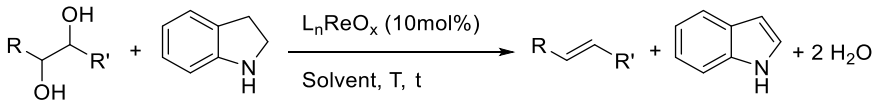
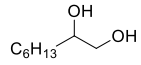
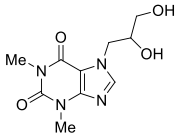
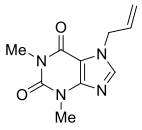
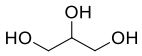
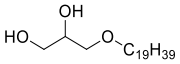
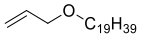
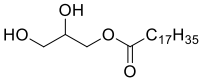
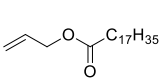
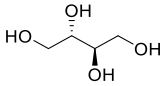
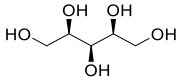
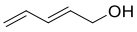
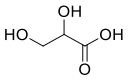
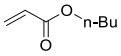
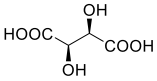
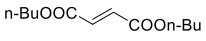
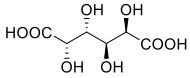
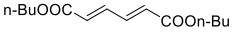


Figure II. 3.1 Reactivity of indoline as reducing agent on a variety of diols

Table II. 3.1 DODH with indoline as reductant

Entry	Substrate	Product	Conditions	Yield (%)[a] olefin/indole
II.3.1.1			A	70/90[b]
II.3.1.2		 **3**	B E	99/50 (90)[c,b] 62/54[d]
II.3.1.3			B D	80/75 66/67
II.3.1.4			C	78/80
II.3.1.5			C	80/56
II.3.1.6			C	43/61
II.3.1.7			B	56/55
II.3.1.8			C	35/64
II.3.1.9			D	78/65 (60%)[c]
II.3.1.10			D	57/88

Conditions: A) NH_4ReO_4, benzene (0.2M), 48 h, 150 ^oC; B) $MeReO_3$, 1-butanol (0.3M), 24 h, 150 ^oC; C) $MeReO_3$, 1-butanol (0.3M), 4 h, 170 ^oC (entry 7, 4.5 h); D) NH_4ReO_4, 1-butanol (0.3M), 24 h, 150 ^oC; E) $MeReO_3$ 2.5 mol%, 1-butanol (0.3M), 24 h, 150 ^oC;

[a] Yield determined by ^{1}H-NMR; [b] 100% conversion; [c] isolated yield, [d] 65%

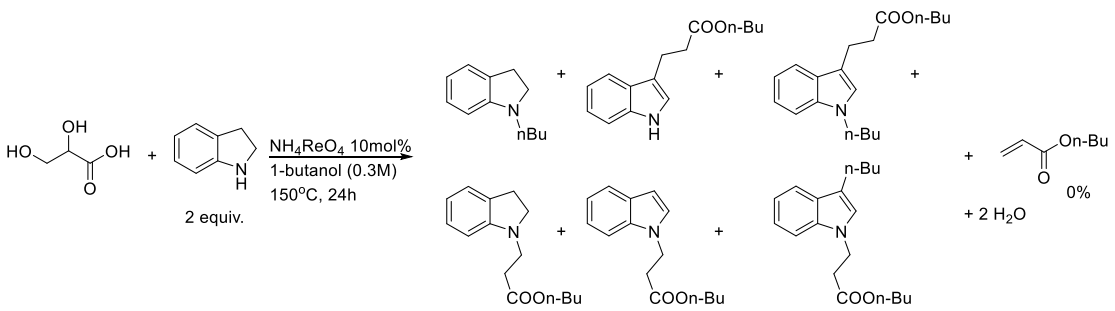


Figure II. 3.2 DODH of glyceric acid using indoline as reducing agent

Several observations indicate that indoline is a superior H-transfer agent relative to primary and secondary alcohols. In the indoline-driven reactions with 1-butanol as solvent, neither butanal and nor the butanal/1-butanol acetal were detected in appreciable amounts. Two competition experiments were conducted to determine the relative H-transfer reactivity of indoline vs. sec-alcohol reductants (Figure II. 3.3). Conducting the same reaction as entry II.3.1.3 with 2-butanol as solvent provided a lower yield of allyl alcohol, 46%, but a 1:1 ratio of allyl alcohol to indole and no detectable amount of butanone. In a fairer competition using conditions of entry II.2.1.3a the reaction of DET and 1.1 equiv each of indoline and of 3-pentanol provided an 82% yield of diethyl fumarate with an appreciable amount of 3-pentanol remaining.

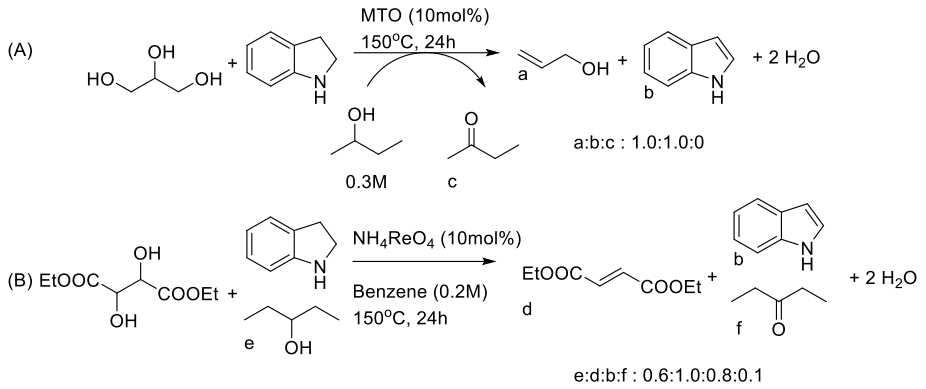


Figure II. 3.3 Reducing agent competition: (A)indoline vs. 2-butanol; (B): indoline vs. 3-pentanol

Several of the hydroaromatics in Table II. 2.1 have been used in H-transfer reactions, including heterogeneous hydrogenation,[95,96] hydrogenolysis of aralkyl- and aryl-oxygen and -nitrogen bonds[97] and light-driven alkane dehydrogenation.[98] In most of these studies indoline also showed high activity as a hydrogen donor. Computational and thermodynamic studies indicate an energetic driving force for the indoline/indole conversion ascribed to the gain of heteroaromatic stabilization, but little is known about the mechanism of H-transfer.[75,97]

4. Mechanistic Study of Indoline- $MeReO_3$ Interactions

The high efficiency of indoline-driven DODH reaction and the established affinity of amines for $MeReO_3$[99], prompted us to investigate the interaction of $MeReO_3$ with indoline. The addition of a stoichiometric amount of indoline to a $MeReO_3$ solution at room temperature results in a rapid color change from colorless to yellow or green (λ 656 nm) depending on the concentration. The ^1H NMR spectrum of the mixture shows significant shifting of the indoline and Me-Re resonances and the Re=O IR absorption is also shifted lower by 33 cm^{-1} (Figure II. 4.1). The $MeReO_3$-indoline adduct **4** was isolated

as crystals by slow evaporation of the solvent (benzene) and structurally characterized by X-ray diffraction (Figure II. 4.2) by Dr. Powell. The structure of **4** features a distorted trigonal bipyramidal Re center with the N-coordinated indoline unit occupying an apical position and the Me-Re is an equatorial position.

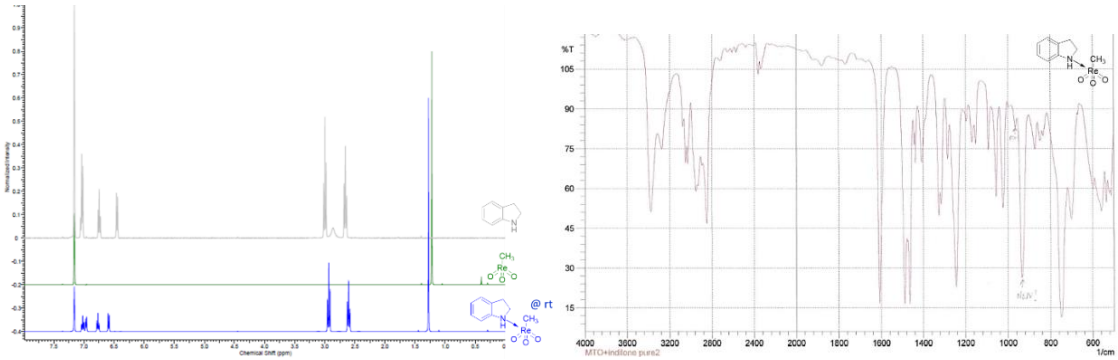


Figure II. 4.1 ^{1}H NMR and IR of 4

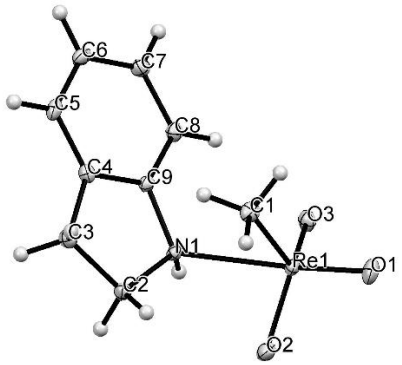


Figure II. 4.2 X-ray ORTEP diagram of $MeReO_3$(indoline) (4)
Selected bond lengths (Å) and angles (o). Re-O2 1.719(2), Re-O1 1.719(2), Re-O3 1.724(2), Re-C1 2.102(3), Re-N1 2.395(2), N-H 0.85(4); O2-Re-O1 105.01(10), O2-Re-O3 117.32(10), O1-Re-O3 106.26(10), O2-Re-C1 116.28(10), O1-Re-C1 90.03(11), O3-Re-C1 116.53(11), O2-Re-N1 78.62(9), O1-Re-N1 168.12(9).

In order to determine if this $MeReO_3$:indoline complex could be involved in the DODH catalytic cycle and if indoline is oxidized by $MeReO_3$; we heated a solution of **4** for an hour at 150^{o}C. The ^{1}H-NMR spectrum of the heated solution showed the formation of indole (ratio indoline : indole, 1.0:0.4); the indoline was entirely consumed after 4.5 h.

From these observations it is clear that indoline coordinates to $MeReO_3$ at room temperature and that, upon heating, is oxidized to indole. The less basic indole does not appreciably associate with $MeReO_3$ since after 20h at room temperature there was no change in the ^1H NMR spectrum of an equimolar mixture of the two.

Since the corresponding reduced Re-species, $MeReO_2$ (MDO), would be highly reactive and potentially undetectable under the reaction conditions[100], to test for its intermediacy we conducted a trapping reaction with 3-hexyne (Figure II. 4.3).[44] Heating a mixture of indoline, 3-hexyne and $MeReO_3$ (5:2:1) at 100°C for 19h fully consumed the $MeReO_3$ (disappearance of CH_3 at 2ppm [#] signal in the ^1H NMR, Figure II.4.3); the ^1H and ^{13}C NMR spectra of the resulting mixture showed the formation of $MeReO_2$(3-hexyne) (**5**) (formation of CH_3 signal at 2.5ppm [+] in the ^1H NMR, Figure II. 4.4). These changes in the ^1H NMR spectrum matched some changes we observed in the ^{13}C NMR spectrum (Figure II. 4.4). After standing overnight at room temperature no changes were observed in the NMR spectrum. Traces of indole (7.7, 7.4 and 6.5ppm [x] in the ^1H NMR, Figure II. 4.4) and the MDO-hexyne complex were detected by NMR after just an hour at 100°C.

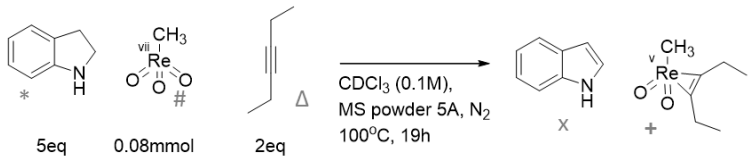


Figure II. 4.3 MDO-trapping experiment

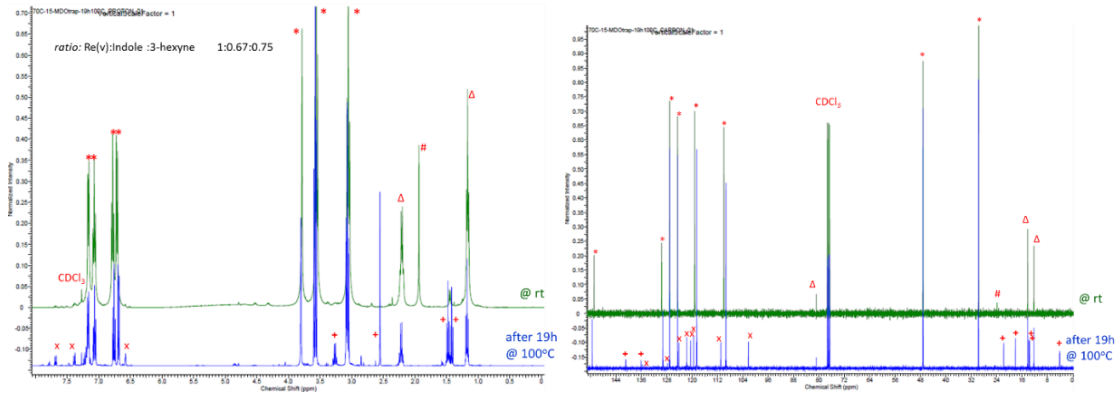


Figure II. 4.4 ^{1}H and ^{13}C NMR spectra of 5

In the DODH catalytic system two pathways (A,B Figure II. 4.7) have been considered viable, differing in the sequence of the reduction/condensation steps. In sequence A the rhenium^{vii} species is first reduced, followed by condensation with glycol to form the Re^{v}-glycolate and fragmentation, while in path B the rhenium^{vii} species first forms the glycolate, which is then reduced and fragments to the alkene. The affinity of $MeReO_3$ for indoline and the subsequent H-transfer redox reaction that proceeds at moderate temperatures indicates that path A (Figure II. 4.7), involving initial reduction of $MeReO_3$ by indoline, is viable. To assess the relative affinity of indoline vs. the diol substrate for $MeReO_3$, we prepared an equimolar mixture of these reactants to which was added an equivalent of $MeReO_3$ at room temperature. The resulting NMR spectrum showed a 1.0:0.1 ratio of $MeReO_3$-(indoline) (**4**) to Re-glycolate (**6**)[35,36] (Figure II. 4.5, R=H) that remained unchanged after 20 h, showing that indoline has a greater binding affinity than the glycol for $MeReO_3$ (Figure II. 4.5). This result also suggests a preference for pathway A, but does not exclude the operation of path B. By comparison with previously reported experimental and computational studies on alcohols reductants, the

idea of the reduction of the rhenium center first releasing the oxidized reducing agent and a Re^{v} complex is reasonable.[48]

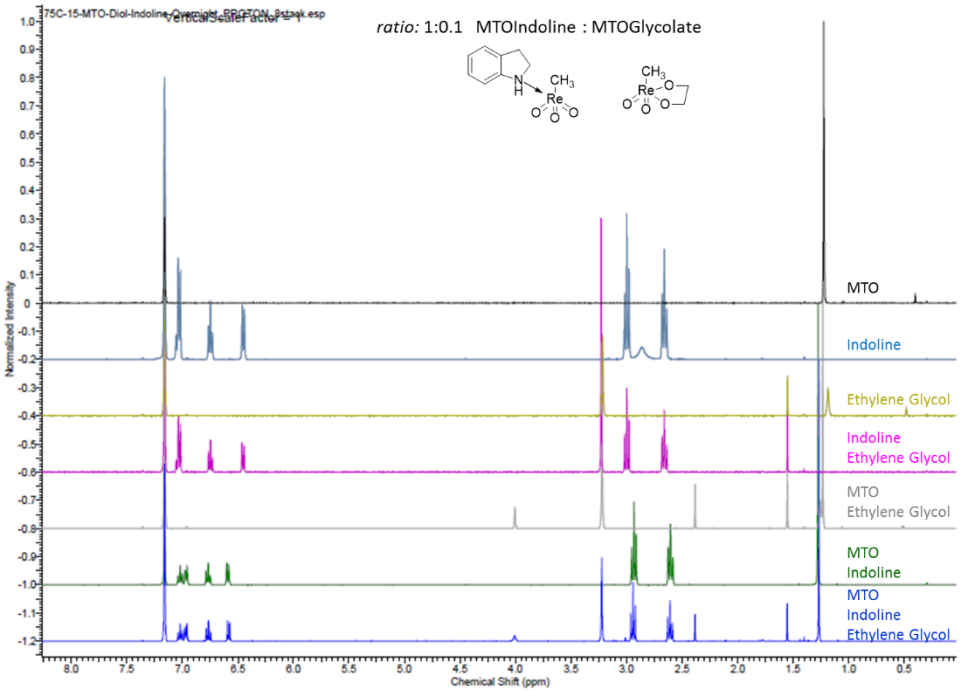


Figure II. 4.5 ^{1}H NMR experiment $MeReO_3$:indoline vs. $MeReO_3$:Glycolate formation

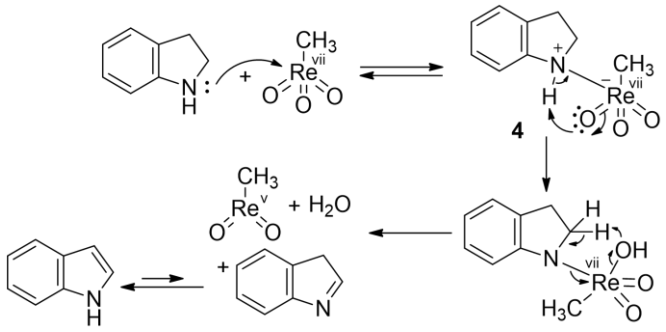


Figure II. 4.6 Possible mechanism of $MeReO_3$-indoline H-transfer redox reaction

In Figure II. 4.6 we suggest a possible mechanism for the formation of MDO and indole involving complexation, proton transfer of the acidified N-H to a Re=O unit, α-C-H transfer with H_2O-loss and iso-indoline tautomerization.[101]

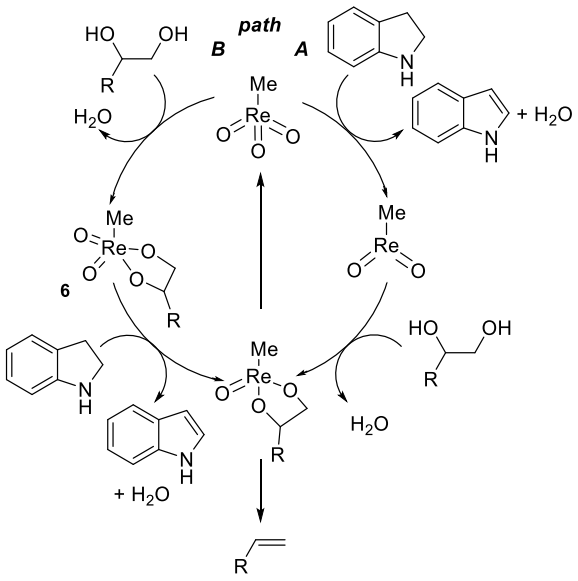


Figure II. 4.7 Potential $MeReO_3$ catalytic cycle with indoline as reductant

5. Conclusions

In conclusion we have demonstrated the ability of hydroaromatic compounds to serve as reductants in oxo-metal catalyzed deoxydehydration of polyols. From a practical perspective the value of this transformation will depend on the cost/availability of the particular polyol and hydroarene co-reactants and the respective olefinic and aromatic co-products. Indoline is particularly efficient for these reactions, being more reactive than representative primary and secondary alcohols. The combination of n-butanol and indoline can be seen as a more economical combination than the reported secondary alcohols used as solvent and reducing agent. Also we can envision even cheaper alcohol solvent than butanol in combination with indoline for ever more economic system. The effectiveness of indoline may be ascribed to its ability to coordinate to an electrophilic oxo-metal species, to then effect entropically-favored intramolecular H-transfer, and to form the stable, weakly coordinating aromatic, indole. Atom-economical tandem DODH/Diels-Alder reactions were also illustrated. The use of 1-butanol as solvent allows

expansion of the range of polyols that are effectively converted to unsaturated products. The efficacy and availability of the hydroaromatic reductants could lead to their use in other oxo-metal catalyzed reductions.

Further studies could be conducted with substituted indoline in order to probe the effect of electron withdrawing or donating groups as well as to guide the selectivity of the nucleophilic addition of indole on acrylic acid (Figure II.3.2). This last reaction, once it would be optimized, could lead to a new atom economical and biomass based synthesis of substituted indole as these type of compounds are interesting building blocks in drug synthesis.

In survey of hydroaromatics studied some were more reactive than hydrogen as reducing agents in the DODH reaction. Also these hydrogen carriers could be regenerated by hydrogen with a catalyst after the reaction and re-use. This system could then be optimized for industrial application.

6. Experimental

a. General information: reagents and instruments.

All reactants and catalysts were obtained commercially and used without further purification. All solvents were ACS grade and were used directly (unless otherwise described in the procedures). ^{1}H, ^{2}H and ^{13}C NMR spectra were collected on Varian VX300 MHz or VNMRS 400 MHz instruments. The NMR data were processed using SpinWorks[102] and ACD[103] software. GC-MS-EI analyses were performed on a Thermo-Finnigan instrument using a Stabil-wax capillary column.

b. Representative procedure for DODH reactions.

Diethyl tartrate (1.00 mmol, 0.17 mL), NH_4ReO_4 (0.10 mmol, 26.8 mg), indoline (1.10 mmol, 0.12 mL), and benzene (5 mL) were added to a thick-walled Ace glass reactor tube. A N_2 flow was bubbled into the mixture for at least 60 sec before the Teflon seal was closed. The purge was made to avoid any oxidation of the hydrogen donors by O_2. The reactor was placed in an oil bath at 150^{o}C for 48 h while stirring magnetically. After cooling to room temperature, a 100 µL aliquot of the reaction mixture was removed and added to 0.6 mL of $CDCl_3$ and 2.0 µL DMSO as internal standard for NMR analysis. This product and the others listed were characterized and quantified using ^{1}H NMR spectroscopy. Some of them were isolated and analyzed by NMR. The isolation of selected products was accomplished by column or preparative TL chromatography. The eluents varied according to different polarity of the alkene product; hexane/ethyl acetate or chloroform/ethyl acetate mixtures were used. All olefinic products from the DODH reactions have been previously reported and were identified by comparison of their NMR spectra with authentic samples or published data.

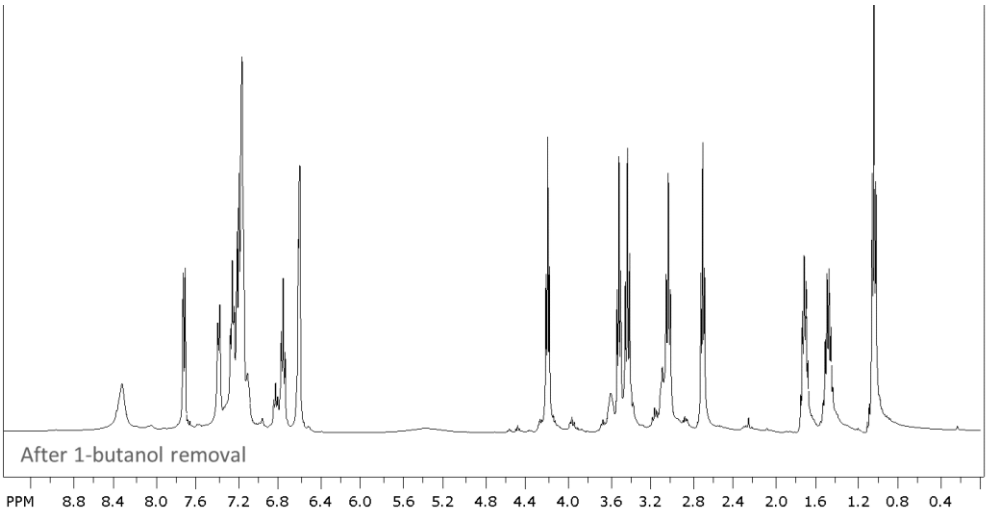
c. DODH/Diels Alder tandem reaction with diethyl tartrate and 1,3-cyclohexadiene.

Diethyl tartrate (0.33 mmol, 0.06 mL), NH_4ReO_4 (0.03 mmol, 9 mg) and 1,3-cyclohexadiene (1.1 mL) were added to a thick-walled Ace glass reactor tube. The Teflon seal was closed and the reactor was placed in an oil bath at 150^{o}C for 24 h while stirring magnetically. After cooling to room temperature, a 100 µL aliquot of the reaction mixture was removed and added to $CDCl_3$ and 2.0 µL DMSO as internal standard for NMR

analysis. The product was identified and quantified by ^{1}H NMR spectroscopy and by comparison with an authentic sample of the separately prepared D-A adduct from the corresponding diene and diethyl tartrate.

d. DODH reaction of glyceric acid with indoline.

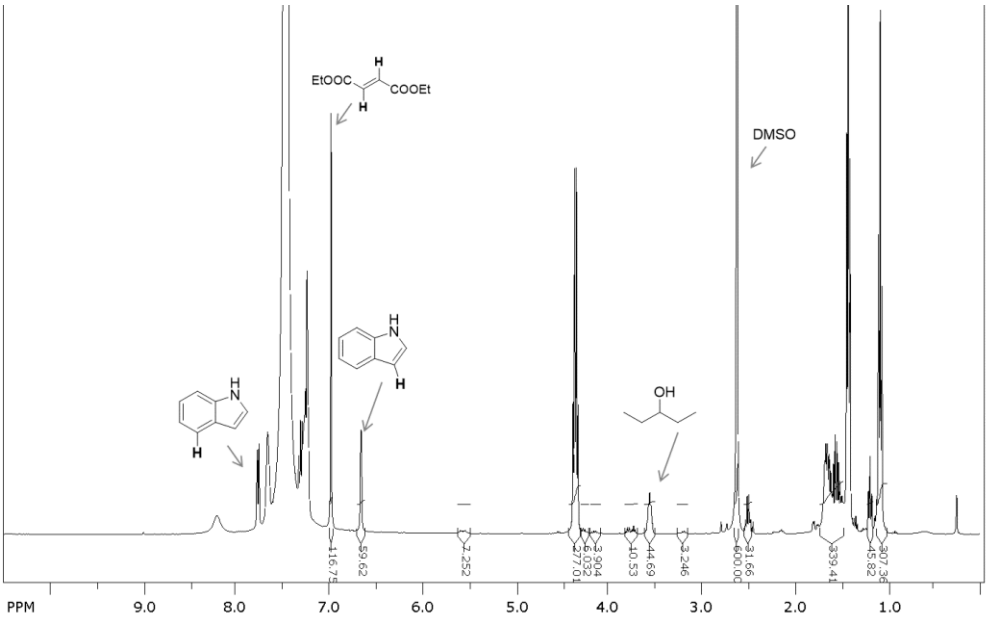
This reaction was conducted in the same way as the other DODH reactions. The NMR and GC-MS spectra of the crude product mixture after solvent evaporation indicated the presence of indole- and indoline-acrylate adducts.



e. Reducing agent competition between 3-pentanol vs indoline.

Diethyl tartrate (1.00 mmol, 0.17 mL), NH_4ReO_4 (0.10 mmol, 27 mg), 3-pentanol (1.10 mmol, 0.12 mL), indoline (1.10 mmol, 0.12 mL) and benzene (5 mL) were added to a thick-walled Ace glass reactor tube. A nitrogen flow was bubbled into the mixture for at least 60 seconds before the Teflon seal was closed and the reactor was placed in an oil bath at 150^{o}C for 24 h while stirring. After cooling to room temperature, a 100 µL aliquot of the reaction mixture was removed and added to $CDCl_3$ and 2.0 µL DMSO as

internal standard for NMR analysis. The product composition was determined and quantified using ^{1}H and ^{13}C NMR spectroscopy.



f. Preparation of the $MeReO_3(\eta^1$-indoline) (**4**).

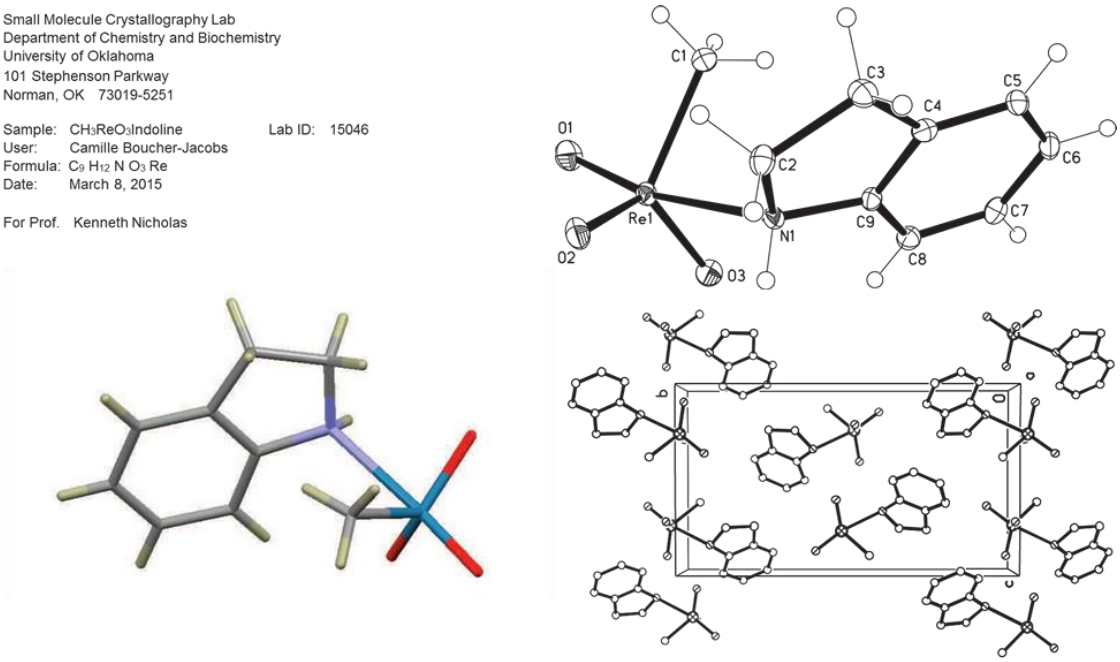
$MeReO_3$ (0.04 mmol, 10 mg) was added to 3 mL of a 0.05 M solution of indoline in hexanes; the color change to yellow-green occurred instantaneously. The mixture was warmed to 40 ^{o}C in order to dissolve all the material. At 3^{o}C, a yellow precipitate formed in 10 min. Crystals for X-ray analysis were obtained by slow evaporation of the solvent at room temperature. Color = yellow; IR: ν(Re=O) 933 cm^{-1}, ^{1}H NMR (C_6D_6, 400 MHz): 1.3 (s, 3 H), 2.6 (t, 2 H, J=8.2 Hz), 2.9 (t, 2 H, J=8.2 Hz), 6.6 (d, 1 H, J=7.8 Hz), 6.8 (t, 1 H, J=7.4 Hz), 6.9 (d, 1 H, J=7.2 Hz), 7.0 (t, 1 H, J=7.8 Hz). ^{13}C NMR (C_6D_6, 100 MHz): 151, 131, 128, 125, 121, 112, 48, 30, 19.

g. X-ray crystal structure determination of **4**

A yellow, plate-shaped crystal of dimensions 0.460 x 0.240 x 0.050 mm was selected for structural analysis. Intensity data for this compound were collected using a diffractometer with a Bruker APEX ccd area detector (1) and graphite-monochromated Mo Kα radiation (Z = 0.71073 Å). The sample was cooled to 100 K. Cell parameters were determined from a non-linear least squares fit of 6810 peaks in the range 2.32 < 0 < 28.32°. A total of 21419 data were measured in the range 2.318 < 0 < 28.333° using Ǝ and σ oscillation frames. The data were corrected for absorption by the empirical method (2) giving minimum and maximum transmission factors of 0.069 and 0.575. The data were merged to form a set of 2432 independent data with R(int) = 0.0395 and a coverage of 100.0 %.

The monoclinic space group P21/c was determined by systematic absences and statistical tests and verified by subsequent refinement. The structure was solved by direct methods and refined by full-matrix least-squares methods on F2. (3) The positions of hydrogens bonded to carbons were initially determined by geometry and were refined using a riding model. The hydrogen bonded to the nitrogen was located on a difference map, and its position was refined independently. Non-hydrogen atoms were refined with anisotropic dis-placement parameters. Hydrogen atom displacement parameters were set to 1.2 (1.5 for methyl) times the isotropic equivalent displacement parameters of the bonded atoms. A total of 131 parameters were refined against 2432 data to give wR(F2) = 0.0476 and S = 1.012 for weights of w = 1/[σ2 (F2) + (0.0280 P)2 + 1.4600 P], where P = [Fo2 + 2Fc2] / 3. The final R(F) was 0.0162 for the 2340 observed, [F > 4σ(F)], data.

The largest shift/s.u. was 0.003 in the final refinement cycle. The final difference map had maxima and minima of 0.840 and -0.873 e/Å3, respectively.



X-ray References

(1) (a) Data Collection: APEX2 (2007) Bruker AXS Inc., Madison, Wisconsin, USA. (b) Data Reduction: SAINT (2007) Bruker AXS Inc., Madison, Wisconsin, USA.

(2) SADABS (2002) Bruker AXS Inc., Madison, Wisconsin, USA.

(3) (a) G. M. Sheldrick (2015). *Acta Cryst., A71*, 3-8. (b) G. M. Sheldrick (2015). *Acta Cryst., C71*, 3-8.

Table 1. Crystal data and structure refinement for CH3ReO3Indoline.

Empirical formula	$C_9 H_{12} N O_3 Re$
Formula weight	368.40
Crystal system	monoclinic
Space group	$P2_1/c$
Unit cell dimensions	a = 5.6756(7) Å, α = 90°
	b = 17.576(2) Å, β = 92.0789(19)°
	c = 9.7832(12) Å, γ = 90°
Volume	975.3(2) Å^3
Z, Z'	4, 1
Density (calculated)	2.509 Mg/m^3
Wavelength	0.71073 Å
Temperature	100(2) K
F(000)	688
Absorption coefficient	12.439 mm^{-1}
Absorption correction	semi-empirical from equivalents
Max. and min. transmission	0.575 and 0.069
Theta range for data collection	2.318 to 28.333°
Reflections collected	21419
Independent reflections	2432 [R(int) = 0.0395]
Data / restraints / parameters	2432 / 0 / 131
$wR(F^2$ all data)	$wR2$ = 0.0476
$R(F$ obsd data)	$R1$ = 0.0162
Goodness-of-fit on F^2	1.012
Observed data [I > 2σ(I)]	2340
Extinction coefficient Largest	0.00166(16)
and mean shift / s.u. Largest	0.003 and 0.000
diff. peak and hole	0.840 and -0.873 e/Å^3

$wR2 = \{ \sum [w(F_o^2 - F_c^2)^2] / \sum [w(F_o^2)^2] \}^{1/2}$

$R1 = \sum ||F_o| - |F_c|| / \sum |F_o|$

Table 2. Atomic coordinates and equivalent isotropic displacement parameters for CH3ReO3Indoline. U(eq) is defined as one third of the trace of the orthogonalized U_{ij} tensor.

	x	y	z	U(eq)
Re(1)	0.11235(2)	0.51763(2)	0.76303(2)	0.01083(6)
O(1)	0.2237(4)	0.59071(13)	0.8626(2)	0.0197(4)
O(2)	-0.1867(4)	0.51963(11)	0.7848(2)	0.0161(4)
O(3)	0.2087(4)	0.53349(12)	0.6004(2)	0.0151(4)
N(1)	-0.0075(4)	0.39938(13)	0.6607(2)	0.0098(4)
C(1)	0.3060(5)	0.43885(17)	0.8834(3)	0.0144(5)
C(2)	-0.1485(5)	0.34919(17)	0.7538(3)	0.0131(5)
C(3)	-0.0265(5)	0.27107(16)	0.7602(3)	0.0140(5)
C(4)	0.1641(5)	0.27757(16)	0.6574(3)	0.0113(5)
C(5)	0.3241(5)	0.22350(16)	0.6156(3)	0.0134(5)
C(6)	0.4843(5)	0.24315(16)	0.5163(3)	0.0144(5)
C(7)	0.4823(5)	0.31587(17)	0.4598(3)	0.0141(5)
C(8)	0.3232(5)	0.37104(17)	0.5020(3)	0.0127(5)
C(9)	0.1668(4)	0.35040(15)	0.6015(3)	0.0103(5)

Table 3. Bond lengths [Å] and angles [°] for CH3ReO3Indoline.

Re(1)-O(2)	1.719(2)	C(3)-C(4)	1.508(4)
Re(1)-O(1)	1.719(2)	C(3)-H(3A)	0.9900
Re(1)-O(3)	1.724(2)	C(3)-H(3B)	0.9900
Re(1)-C(1)	2.102(3)	C(4)-C(5)	1.386(4)
Re(1)-N(1)	2.395(2)	C(4)-C(9)	1.392(4)
N(1)-C(9)	1.448(3)	C(5)-C(6)	1.398(4)
N(1)-C(2)	1.517(4)	C(5)-H(5)	0.9500
N(1)-H(1N)	0.85(4)	C(6)-C(7)	1.392(4)
C(1)-H(1A)	0.9800	C(6)-H(6)	0.9500
C(1)-H(1B)	0.9800	C(7)-C(8)	1.398(4)
C(1)-H(1C)	0.9800	C(7)-H(7)	0.9500
C(2)-C(3)	1.538(4)	C(8)-C(9)	1.389(4)
C(2)-H(2A)	0.9900	C(8)-H(8)	0.9500
C(2)-H(2B)	0.9900		
O(2)-Re(1)-O(1)	105.01(10)	C(3)-C(2)-H(2B)	110.3
O(2)-Re(1)-O(3)	117.32(10)	H(2A)-C(2)-H(2B)	108.5
O(1)-Re(1)-O(3)	106.26(10)	C(4)-C(3)-C(2)	103.8(2)
O(2)-Re(1)-C(1)	116.28(10)	C(4)-C(3)-H(3A)	111.0
O(1)-Re(1)-C(1)	90.03(11)	C(2)-C(3)-H(3A)	111.0
O(3)-Re(1)-C(1)	116.53(11)	C(4)-C(3)-H(3B)	111.0
O(2)-Re(1)-N(1)	78.62(9)	C(2)-C(3)-H(3B)	111.0
O(1)-Re(1)-N(1)	168.12(9)	H(3A)-C(3)-H(3B)	109.0
O(3)-Re(1)-N(1)	81.34(9)	C(5)-C(4)-C(9)	119.9(2)
C(1)-Re(1)-N(1)	78.30(9)	C(5)-C(4)-C(3)	129.7(3)
C(9)-N(1)-C(2)	106.1(2)	C(9)-C(4)-C(3)	110.5(2)
C(9)-N(1)-Re(1)	119.71(16)	C(4)-C(5)-C(6)	119.0(3)
C(2)-N(1)-Re(1)	113.68(16)	C(4)-C(5)-H(5)	120.5
C(9)-N(1)-H(1N)	109(2)	C(6)-C(5)-H(5)	120.5
C(2)-N(1)-H(1N)	111(2)	C(7)-C(6)-C(5)	120.4(3)
Re(1)-N(1)-H(1N)	97(2)	C(7)-C(6)-H(6)	119.8
Re(1)-C(1)-H(1A)	109.5	C(5)-C(6)-H(6)	119.8
Re(1)-C(1)-H(1B)	109.5	C(6)-C(7)-C(8)	121.1(3)
H(1A)-C(1)-H(1B)	109.5	C(6)-C(7)-H(7)	119.5
Re(1)-C(1)-H(1C)	109.5	C(8)-C(7)-H(7)	119.5
H(1A)-C(1)-H(1C)	109.5	C(9)-C(8)-C(7)	117.5(3)
H(1B)-C(1)-H(1C)	109.5	C(9)-C(8)-H(8)	121.2
N(1)-C(2)-C(3)	107.2(2)	C(7)-C(8)-H(8)	121.2
N(1)-C(2)-H(2A)	110.3	C(8)-C(9)-C(4)	122.1(2)
C(3)-C(2)-H(2A)	110.3	C(8)-C(9)-N(1)	126.0(2)
N(1)-C(2)-H(2B)	110.3	C(4)-C(9)-N(1)	111.8(2)

Table 3. Bond lengths [Å] and angles [°] for CH3ReO3Indoline.

Re(1)-O(2)	1.719(2)	C(3)-C(4)	1.508(4)
Re(1)-O(1)	1.719(2)	C(3)-H(3A)	0.9900
Re(1)-O(3)	1.724(2)	C(3)-H(3B)	0.9900
Re(1)-C(1)	2.102(3)	C(4)-C(5)	1.386(4)
Re(1)-N(1)	2.395(2)	C(4)-C(9)	1.392(4)
N(1)-C(9)	1.448(3)	C(5)-C(6)	1.398(4)
N(1)-C(2)	1.517(4)	C(5)-H(5)	0.9500
N(1)-H(1N)	0.85(4)	C(6)-C(7)	1.392(4)
C(1)-H(1A)	0.9800	C(6)-H(6)	0.9500
C(1)-H(1B)	0.9800	C(7)-C(8)	1.398(4)
C(1)-H(1C)	0.9800	C(7)-H(7)	0.9500
C(2)-C(3)	1.538(4)	C(8)-C(9)	1.389(4)
C(2)-H(2A)	0.9900	C(8)-H(8)	0.9500
C(2)-H(2B)	0.9900		

Table 4. Anisotropic displacement parameters (Å^{2}x 10^3) for CH3ReO3Indoline. The anisotropic displacement factor exponent takes the form:

$-2\pi^2[h^2 a^{*2} U_{11} + ... + 2 h k a^* b^* U_{12}]$

	U_{11}	U_{22}	U_{33}	U_{23}	U_{13}	U_{12}
Re(1)	13(1)	8(1)	11(1)	0(1)	1(1)	0(1)
O(1)	26(1)	10(1)	23(1)	-2(1)	-1(1)	-1(1)
O(2)	17(1)	13(1)	19(1)	0(1)	4(1)	3(1)
O(3)	18(1)	12(1)	15(1)	2(1)	3(1)	-2(1)
N(1)	12(1)	8(1)	9(1)	1(1)	2(1)	2(1)
C(1)	16(1)	15(1)	12(1)	-1(1)	-2(1)	1(1)
C(2)	14(1)	12(1)	14(1)	-1(1)	4(1)	-1(1)
C(3)	14(1)	14(1)	14(1)	2(1)	2(1)	0(1)
C(4)	12(1)	11(1)	10(1)	1(1)	-1(1)	-2(1)
C(5)	18(1)	9(1)	14(1)	-1(1)	-3(1)	0(1)
C(6)	15(1)	13(1)	16(1)	-4(1)	0(1)	3(1)
C(7)	15(1)	16(1)	12(1)	-2(1)	3(1)	-1(1)
C(8)	14(1)	12(1)	12(1)	1(1)	1(1)	-1(1)
C(9)	11(1)	9(1)	10(1)	-2(1)	0(1)	0(1)

Table 5. Hydrogen coordinates and isotropic displacement parameters for CH3ReO3Indoline.

	x	y	z	U(eq)
H(1N)	-0.095(6)	0.418(2)	0.597(4)	0.012
H(1A)	0.4712	0.4550	0.8915	0.022
H(1B)	0.2966	0.3886	0.8403	0.022
H(1C)	0.2405	0.4362	0.9746	0.022
H(2A)	-0.3125	0.3439	0.7171	0.016
H(2B)	-0.1525	0.3718	0.8464	0.016
H(3A)	0.0419	0.2609	0.8529	0.017
H(3B)	-0.1386	0.2299	0.7348	0.017
H(5)	0.3249	0.1738	0.6539	0.016
H(6)	0.5953	0.2067	0.4872	0.017
H(7)	0.5908	0.3282	0.3915	0.017
H(8)	0.3221	0.4208	0.4641	0.015

Table 6. Torsion angles [°] for CH3ReO3Indoline.

C(9)-N(1)-C(2)-C(3)	7.3(3)
Re(1)-N(1)-C(2)-C(3)	-126.33(18)
N(1)-C(2)-C(3)-C(4)	-6.1(3)
C(2)-C(3)-C(4)-C(5)	-177.2(3)
C(2)-C(3)-C(4)-C(9)	2.8(3)
C(9)-C(4)-C(5)-C(6)	-0.7(4)
C(3)-C(4)-C(5)-C(6)	179.3(3)
C(4)-C(5)-C(6)-C(7)	-0.3(4)
C(5)-C(6)-C(7)-C(8)	0.9(4)
C(6)-C(7)-C(8)-C(9)	-0.4(4)
C(7)-C(8)-C(9)-C(4)	-0.6(4)
C(7)-C(8)-C(9)-N(1)	178.6(2)
C(5)-C(4)-C(9)-C(8)	1.2(4)
C(3)-C(4)-C(9)-C(8)	-178.8(2)
C(5)-C(4)-C(9)-N(1)	-178.1(2)
C(3)-C(4)-C(9)-N(1)	1.9(3)
C(2)-N(1)-C(9)-C(8)	174.9(2)
Re(1)-N(1)-C(9)-C(8)	-54.8(3)
C(2)-N(1)-C(9)-C(4)	-5.8(3)
Re(1)-N(1)-C(9)-C(4)	124.5(2)

Table 7. Hydrogen bonds for CH3ReO3Indoline[Å and °].

D-H...A	d(D-H)	d(H...A)	d(D...A)	<(DHA)
N(1)-H(1N)...O(3)#1	0.85(4)	2.18(4)	3.002(3)	161(3)
C(8)-H(8)...O(3)	0.95	2.49	3.090(4)	121.5

Symmetry transformations used to generate equivalent atoms:
#1 -x, -y+1, -z+1

h. $MeReO_3$:indoline reactivity study.

$MeReO_3$ (0.04 mmol, 10 mg) was dissolved in 800 µL of *d_6*-benzene in a high pressure NMR tube. Indoline (0.04 mmol, 4.5 µL) was added and the tube was flushed with N_2. ^{1}H NMR spectra were collected before and after placing the tube in an oil bath at 150^{o}C for 1h. The reduction of $MeReO_3$ by indoline was set up similarly at a 0.20 mmol scale with benzene in a thick-walled Ace glass reactor tube. A N_2 flow was bubbled into the mixture for 60 sec and after sealing the reactor was placed in an oil bath at 150^{o}C for 4.5 h while stirring. After cooling at room temperature, the mixture was transferred to an NMR tube for analysis by no-D solvent NMR. The two CH_2 group absorptions from indoline (3.1 ppm and 3.6 ppm) were absent after the reaction, being replaced by the peaks for indole (with no overlap; 6.5 ppm and 7.8 ppm). The mixture changed from colorless to yellow upon the addition of indoline at room temperature, then turned green. At 150^{o}C the solution turned blue then brown/black.

i. MDO trapping.

In a high pressure NMR tube, 63 mg of MS 5Å powder and 20 mg of $MeReO_3$ (0.08 mmol) was added to 800 µL of solution of 3-hexyne (2 eq, 0.16 mmol, 18 µL) in d-chloroform (dried over 4Å molecular sieves). The tube was flushed with N_2. ^1H and ^{13}C NMR spectra were collected at room temperature and after placing the tube in an oil bath at 100°C. The reaction was completed after a total of 19h.

j. Competition between indoline and ethylene glycol for $MeReO_3$.

$MeReO_3$ (0.02 mmol, 5 mg) was added to 800 µL of a 0.03 M equimolar solution of indoline and ethylene glycol in d^6-benzene. ^1H NMR spectra were collected directly and con-firmed after standing overnight at room temperature.

7. Acknowledgment

We thank Dr. Douglas Powell for determination of the X-ray structure of **4**.

Chapter III. DODH/C-C Bond Forming Tandem Reactions

1. DODH / Hetero Diels Alder Coupling

a. Introduction

iii. The Diels-Alder and Hetero Diels-Alder reactions

The Diels-Alder (DA) reaction is a [4+2] cycloaddition between a diene and a dienophile (Figure III. 1.1). Developed in 1928 by O. Diels and K. Alder, the first report of the reaction involved only carbon atoms in the cycloaddition[104]. Later the concept of this cycloaddition was applied to systems containing heteroatoms and was called the Hetero Diels-Alder reaction (HDA).[105,106] The DA reaction is believed to proceed by a concerted mechanism via a cyclic transition state guided by orbital symmetry. In the most common case the π electrons in the HOMO of the diene interact with the LUMO (π* orbital) of the dienophile. The reaction can then be favored if the diene contains an electron donation group and the dienophile contains an electron withdrawing group. In addition a Lewis acid catalyst can coordinate to the dienophile making it more electrophilic and subsequently more reactive toward the diene.

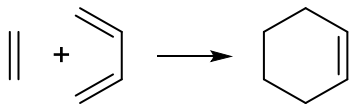


Figure III. 1.1 Diels-Alder general reaction

iv. Tandem reaction concept

The idea of a tandem DODH / DA reaction sounds the most straightforward. In this case both the diene and the dienophile could be formed in a DODH reaction from a polyol

and a glycol. We started by exploring such a tandem system. We studied DODH / DA tandem reaction of erythreitol and diethyl tartrate using $MeReO_3$ as catalyst and 3-octanol as reducing agent and solvent(Figure III. 1.2). We obtained the cyclo-added product with 60% yield starting with diethyl fumarate instead of diethyl tartrate. Early in our preliminary study a similar tandem system was reported by Shiramizu and Toste.[45] Subsequently we changed our focus for another system that we had in mind- a Hetero-Diels Alder (H-DA) transformation in which the dienophile would be an aldehyde produced from an alcohol reducing agent in the DODH step

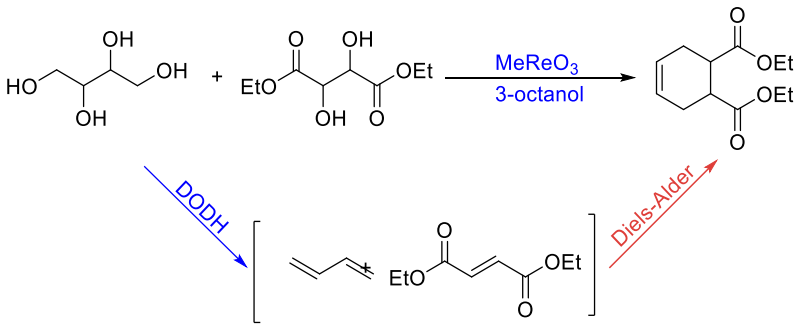


Figure III. 1.2 DODH/DA reaction system

In the DODH/Hetero-Diels Alder tandem system the DODH reaction produces from the polyol a diene and from the alcohol reductant (**1**) a dienophile (**2**) (Figure III. 1.3). Together the diene and dienophile can undergo subsequent Diels-Alder cycloaddition. Our goal was to focus on utilizing both of the DODH co-products for the Hetero Diels-Alder (H-DA) cycloaddition, producing O-heterocycles (**3**, Figure III. 1.3). By using the product of both the diol and the reducing agent this system will be atom economical. The products formed, pyrans, could have large application in organic synthesis and could be further transformed to valuable building blocks. In fact pyran's derivatives have

interesting biological activities and potential medical applications, more specifically in the area of cancer and HIV drugs development.[107–113]

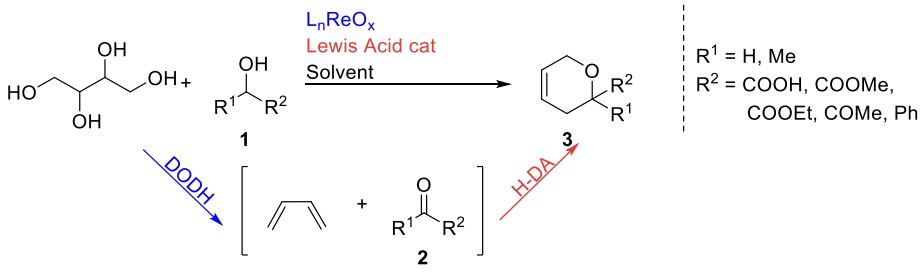


Figure III. 1.3 DODH/Hetero Diels Alder tandem concept

We first concentrated on the DODH side of this tandem system, since the alcohol (**1**, Figure III. 1.3) has never been reported as reducing agent for the DODH reaction. The most abundant four carbon polyol is erythritol and its conversion to butadiene has been reported with high yield in only one set of reaction conditions: $MeReO_3$ (2.5 mol%) with 3-octanol (170°C, 1.5h, N_2).[44] We determined the efficiency of the HDA reaction before attempting to further optimize the DODH reaction. We will consider also to potential need of Lewis acid catalyst on the H-DA step.

We will then consider using a less common dienophile for the HDA step: benzaldehyde. We have previously developed a DODH system using benzyl alcohol as a reducing agent which provide benzaldehyde as the co-product.[46] The HDA reaction of butadiene and benzaldehyde was first studied.

b. DODH using α-hydroxy carbonyls as reducing agent

From our previous DODH studies we knew that erythritol can be a challenging polyol to convert to olefin so we decided to test the α-hydroxy carbonyl (**1**, Figure III. 1.4) as reducing agent on a less problematic diol: diethyl tartrate. The best set of reaction

conditions for the conversion of tartrate to fumarate used one equivalent of the reducing agent, 10 mol% of NH_4ReO_4 as catalyst, 0.2M diol in benzene as solvent at 150°C for 24 hours (Figure III. 1.4).

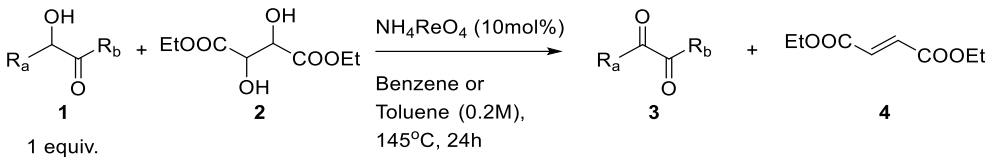


Figure III. 1.4 Activity of α-carbonyl alcohol as reducing agent for DODH of DET

Table III. 1.1 DEF yield using α-hydroxy carbonyls (1, Figure III. 1.4) as reducing agent

ROH 1 / entry	R_a	R_b	Yield of **4** (Figure III. 1.4)
III.1.1.1	H	OMe	72%
III.1.1.2	H	OEt	88%
III.1.1.3	Me	OEt	96% (55% with $MeReO_3$)
III.1.1.4	Me	OH	81%
III.1.1.5	H	Me	80%

We analyzed these reactions by ^{1}H-NMR. The formation of diethyl fumarate was simple to follow since it exhibits a strong singlet at 6.8 ppm in the proton NMR spectrum. This allowed us to determine an NMR yield for each alkene with the α-hydroxy carbonyl as reducing agent. Methyl glycolate (entry III.1.1.1) provided the lowest yield with 72%.

With ethyl glycolate (entry III.1.1.2) the yield was improved up to 88%. We were able to use lactic acid (entry III.1.1.4); an abundant and renewable chemical; as reducing agent with 81% yield. Lactic acid was used directly as an 81% solution in water exhibiting the tolerance of the DODH system to some amount of water. Moving from α-hydroxy ester to α-hydroxy ketone, hydroxyl acetone (entry III.1.a.5) provided similar yield of 80%. Using a secondary alcohol in the case of entry III.1.a.3 provided the highest yield of 96%. In the specific case of entry III.1.a.3 with ethyl lactate as reducing agent, we tested $MeReO_3$ as the catalyst. This change in the catalyst dropped the yield in diethyl tartrate to 55%.

Following these results we used the alcohol reductant which provided the highest yield, ethyl lactate, to a larger survey of diols. (Table III. 1.2).

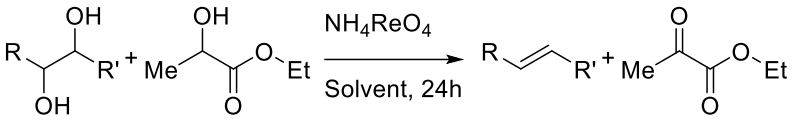
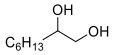
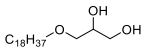
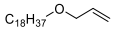
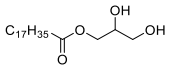
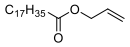
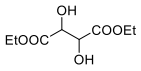


Figure III. 1.5 Activity of ethyl lactate as reducing agent for DODH of diols (1)

Table III. 1.2 Alkene yield using ethyl lactate as reducing agent (Figure III. 1.5)

Entry	Diol (**1**, Figure III. 1.5)	Alkene (**3**, Figure III. 1.5)	1M	0.25M
III.1.2.6			40%	26%
III.1.2.7			21%	34%
III.1.2.8			13%	30%
III.1.2.9			66.5%	88-95%

The alkene yields from 1,2-octanediol (entry III.1.2.1), glycerol monostearate (entry III.1.2.2) and batyl alcohol (entry III.1.2.3), were much lower than that obtained from diethyl tartrate. In these experiments we tried both the usual concentration for the DODH and the reported concentrations for a H-DA reaction (0.25M and 1M respectively). We discovered that the concentrations of the reaction has different effects depending on the diol, but most of the time higher concentration provided lower yield. We could explain this behavior by faster formation of a side product at higher concentration.

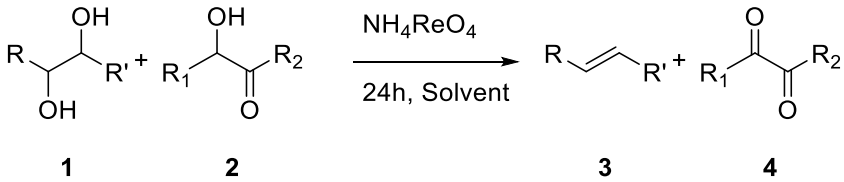
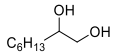
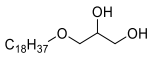
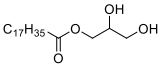
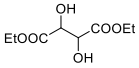


Figure III. 1.6 Activity of other α-hydroxy carbonyl (2) as reducing agent for DODH of glycols (1)

Table III. 1.3 Alkene (3) yield using α-hydroxy carbonyl (2) as reducing agents (Figure III. 1.6)

Entry	Column / **2** (R_1, R_2) / **1**	III.1.3.A Me, OEt	III.1.3.B Me, OH	III.1.3.C H, Me
III.1.3.1		43% (1M)	26%(0.2M) 0%($MeReO_3$)	52%(0.2M) 40%($MeReO_3$)
III.1.3.2		34% (0.25M)	-	-
III.1.3.3		30% (0.25M)	17%(0.2M)	42%(0.2M)
III.1.3.4		88-95% (0.25M)	80%(0.2M)	80%(0.2M)

Ethyl lactate (Column III.1.3.A) was found not to be a really efficient reducing agent on terminal diols. As the other α-hydroxy carbonyl were relatively efficient on DET we tested two of these- lactic acid (Column III.1.3.B) and hydroxyacetone (Column III.1.3.C) on the terminal glycols as well (Table III. 1.3). The alkene yields were worst in the case of lactic acid (Column III.1.3.B) and only slightly improved in the case of hydroxyacetone. We also tried $MeReO_3$ as catalyst for the DODH of 1,2-octanediol (entry III.1.3.1). The $MeReO_3$ DODH reaction did not provide any alkene using lactic acid as reducing agent, but provided similar yield to the NH_4ReO_4 catalyzed reaction using hydroxyacetone.

Several DODH reactions were run on erythritol with these alcohols as reducing agents. No large quantity of butadiene or of DA adducts were detected in any of these reactions. These preliminary results on α-hydroxy carbonyls as reducing agents in the DODH reaction were not encouraging for the development of an efficient tandem DODH-

HDA system. Since these alcohols were efficient on DET we looked at the quantification of the dicarbonyl product formed in these reaction. Although the yields in fumarate were high, we could not find as much of dicarbonyl formed in the reaction. In only a few cases we found small NMR signals (^{1}H and ^{13}C) from the expected dicarbonyl products. For example, entry III.1.1.2 with an 88% yield in DEF, showed a yield of ethyl pyruvate of only 48%. This raised the question of the stability of the dicarbonyl compounds under the reaction conditions. Since the dicarbonyl compounds should react soon after its formation with the diene, we decided to attempt a trapping experiment of the dicarbonyl compound in the HDA cycloadditon. Taking the case of entry III.1.3.1 (NH_4ReO_4 as catalyst), we attempted to trap the ketoaldehyde, methyl glyoxal (**2**, Figure III. 1.7); by adding excess isoprene to the reaction (Figure III. 1.7).

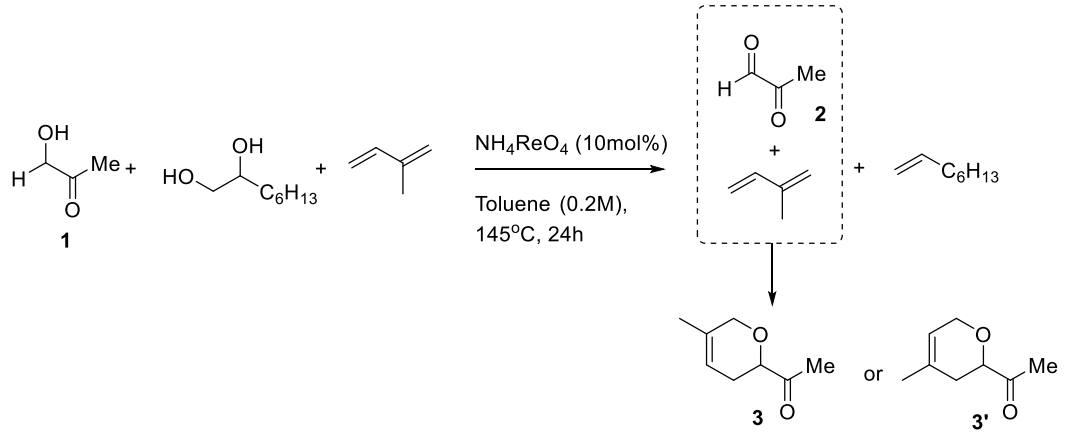


Figure III. 1.7 Trapping experiment of methyl glyoxal (2) by cycloaddition with isoprene

The cycloaddition products (**3** and **3'**, Figure III. 1.7) were not detected by NMR in the reaction mixture. One explanation to this result could be that the cycloaddition process

is slow and that the methyl glyoxal (**2**, Figure III. 1.7) degrades faster under the reaction conditions than the HDA process.

c. Study of the Hetero Diels Alder step

The failure of the trapping experiment raised an important concern about the HDA step in the reaction. We decided, therefore, to study this part of the tandem reaction.

i. α-Dicarbonyls as dienophile

The HDA reaction is often reported as a thermal reaction.[114–116] In order to decrease the temperature of the reaction Lewis acid catalysts have been studied.[117–123] First we started to study the thermal reactivity of α-dicarbonyl as dienophiles (at the DODH reaction temperature) and then we tried some of the reported Lewis acids as additives. Both isoprene and 1,3-butadiene were tested as dienes with ethyl pyruvate and ethyl glyoxalate as dienophiles (Figure III. 1.8).

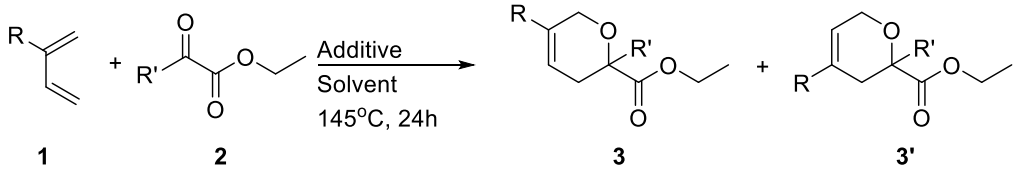


Figure III. 1.8 Study of Hetero-Diel Alder step

The thermal reaction, without a Lewis acid additive, did not occur when toluene was used as a solvent. For both dienophile 2 (Figure III. 1.8), we found traces of 3' (Figure III. 1.8) by GCMS when isoprene was used in a slight excess to play the role of the solvent

in the absence of toluene. The H-DA reaction appears to require high concentrations to work efficiently, which led us to conclude that it is a rather slow reaction and unfavorable when a solvent is employed. For the purpose of the tandem reaction system it is will be difficult to run the DODH reaction in the absence of solvent or to have the diene as solvent and it will be difficult to have an excess of diene over the dienophile due to the stoichiometry of the reaction.

We decided to test if we could catalyze the HDA step with Lewis acids. These reactions were tested in toluene as solvent (1M) using 10mol% of the Lewis acids. None of the tested Lewis acids (Additives: $ZnCl_2$, $AlCl_3$, $Sc(OTf)_3$, $MeReO_3$, Figure III. 1.8) catalysts improved the formation and the yield of **3** or **3'** (Figure III. 1.8). The addition of hydroquinone as a polymerization inhibitor has been studied in of these many cases without success. A variation of different types, volume of solvent were studied as well without seeing much of cycloadduct product (**3** or **3'**, Figure III. 1.8).

In this study of the H-DA reaction between α-dicarbonyl species and simple dienes we have found that the reaction conditions for this cycloaddition are not favorable for a tandem reaction by its requirement of high concentration and an excess of diene (which will be limiting reaction after the DODH reaction step). We have also found that Lewis acids catalyst were not very efficient at catalyzing the reaction under our reaction conditions. In conclusion the chance for a tandem DODH / H-DA reaction looks compromised as the α-carbonyl alcohols do not have great activity as reducing agent on erythreitol.

ii. Benzaldehyde as dienophile

We found a recent report from Bansal's group of a successful HDA cycloaddition reaction with benzaldehyde as the dienophile.[124] We established earlier the efficacy of benzyl alcohol as a reducing agent in the DODH reaction.[46] Although erythritol was not part of this study, we decided to study the HDA reaction between butadiene and benzaldehyde. Since Montmorillonite K-10 was the reported catalyst for the HDA addition, we started by testing it along some other acid additives (p-TsOH, HCOOH) on the cycloaddition of butadiene with benzaldehyde. In these reactions the only observed cycloaddition products were the Diels Alder of butadiene with another of butadiene. Despite this unexpected failure of the acid catalyzed HDA, we continued the study of this cycloaddition without catalyst, with Lewis acid catalysts and even DODH catalysts. Out of these catalyzed attempts only $MeReO_3$ and $Sc(OTf)_3$ appeared to produce traces of the cycloadduct (**1**, Figure III. 1.9).

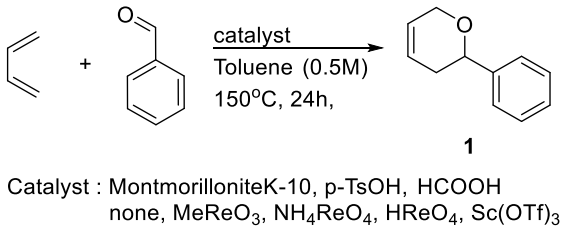


Figure III. 1.9 Hetero-Diel Alder reaction of butadiene and benzaldehyde

Only the $Sc(OTf)_3$ catalyzed reaction mixture showed signals that matched up with the reported NMR spectrum of the expected adduct. The GCMS of the reaction mixture gave a very complicated chromatogram and no matching mass for the product **1** (Figure

III. 1.8). The $Sc(OTf)_3$ catalyzed H-DA would need more experiment but we did not think that the cycloaddition takes place under the tested reaction conditions.

d. Conclusions

This study of the reactivity of α-hydroxy carbonyl as reducing agents in the DODH reaction of simple diols gave only low to moderate yields of olefins. The absence of evidence for the oxidized alcohols may be the result of their potential low stability under the reaction condition. The study of dicarbonyls as dienophiles in H-DA reaction with butadiene under DODH reaction conditions showed formation of the tandem product in few cases. Moreover, the system looks to produce pretty poor yields under the DODH reaction conditions. Attempts to establish benzaldehyde as a dienophile in the HDA step failed as none of the reaction conditions tested gave cycloadducts in a significant quantity. Because of the limited DODH reducing agent activity of these alcohols, the low stability of the dicarbonyl species under the reaction condition, the low yield of the desired HDA, as well as the inactivity of benzaldehyde as dienophile under the reaction conditions, this DODH-HDA tandem system was not studied further.

e. Experimental

i. Reagents and instrumentation

The reaction solvents and rhenium catalysts, ammonium perrhenate and methyltrioxorhenium, were used as received from the suppliers (Sigma Aldrich and Alfa Aesar). The catalysts were stored in a desiccator and regularly placed under vacuum to insure their dryness. The diols- diethyl tartrate, octane diol, glycerol monostearate, batyl

alcohol, and erythritol; the alcohols- lactic acid (2-hydroxypropanoic acid), ethyl glycolate (ethyl 2-hydroxyacetate), ethyl lactate (ethyl 2-hydroxypropanoate), ethyl glycolate (methyl 2-hydroxyacetate) and hydroxyacetone (1-hydroxypropan-2-one); the α-dicarbonyl, ethyl 2-oxopropanoate (ethyl pyruvate), ethyl 2-oxoacetate (ethyl glyoxalate) and benzaldehyde were used as received from Sigma Aldrich, Alfa Aesar and Acros Organic. All of these reagents were flushed with nitrogen for storage (on the shelf or in the refrigerator at 4^{o}C as suggested by suppliers). Butadiene and isoprene were used as received and stored in the refrigerator at 4^{o}C. The Lewis acid and acid catalysts- aluminum chloride, zinc chloride, scandium triflate, para-toluene sulfonic acid and acetic acid- were used directly as received from the suppliers (Sigma Aldrich and Alfa Aesar). Aluminum chloride and zinc chloride were stored in the glove box to keep them dry. The clay catalyst, Montmorillonite K-10, was purchased from Sigma Aldrich and activated under vacuum at 100^{o}C for 24h. ^{1}H NMR spectra were collected on either a Varian Mercury VX-300 MHz or a Varian Mercury VX-400. The NMR spectra were processed using SpinWorks.[102]

ii. Typical reaction conditions

- *DODH reactions*

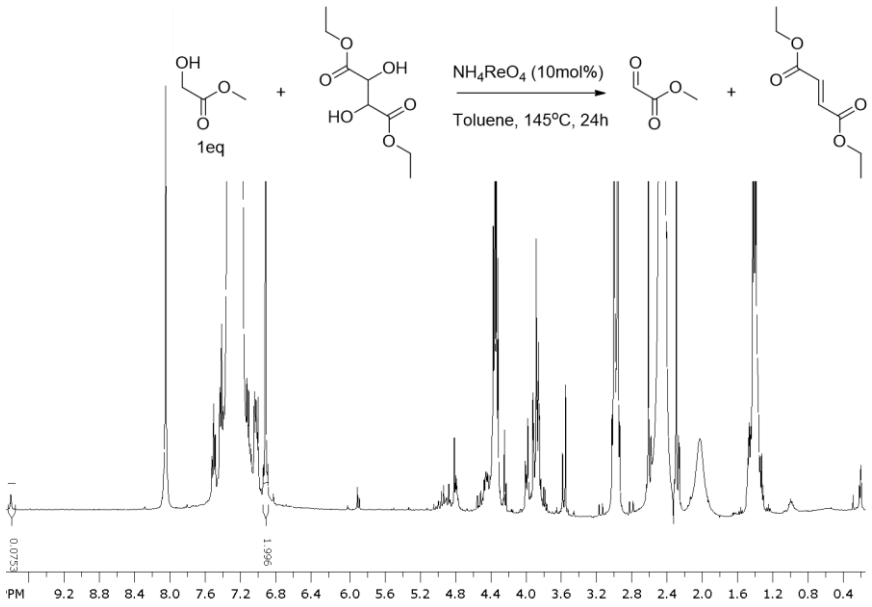
All the reactions were carried in 10 or 15mL sealed pressure tubes (AceGlass or ChemGlass) equipped with a magnetic spin vane. The scale varied from 1 to 0.5 mmol. The reagents- diol, reducing agent (1.1 equiv.) and catalyst (10 mol%), were mixed in 1 to 5 mL of solvent. Nitrogen was bubbled into the solution for 60 seconds before it was carefully screw-capped and placed in a pre-heated oil bath at 150^{o}C for 24h.

- *Hetero Diels-Alder reactions*

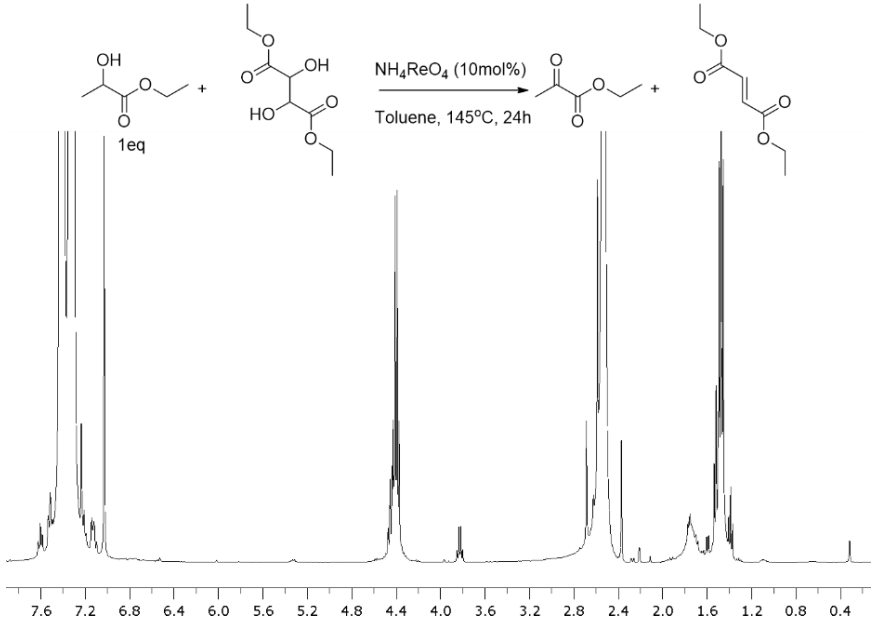
The same reactor tubes were used for the Hetero Diels-Alder reactions. The reagents were loaded into the reactor tube under a nitrogen flow. Butadiene was measured by volume with a gas tight syringe and added to the reactor tube cooled in a -78^{o}C bath to condense it as a liquid. A check of the quantity delivered was performed by weighing the reactor tube before and after the addition of the diene.

iii. Analysis and Quantification

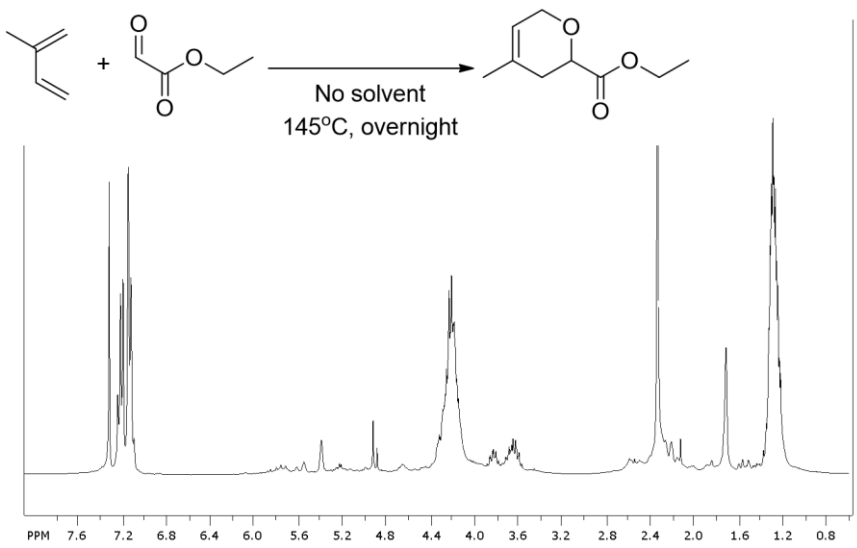
After the reaction the tube was cooled to room temperature. An aliquot of the reaction mixture (100-300 µL) was dissolved in 0.5 mL of $CDCl_3$ and transferred to an NMR tube. In the case of the DODH reaction mixtures 5 µL of an internal standard (DMF or DMSO) was added to the NMR sample for quantification. In the case of Hetero Diels-Alder reaction mixtures when the NMR spectrum was too complicated, a mild vacuum (10 mm Hg) was applied for a few hours to remove the unreacted dienes.

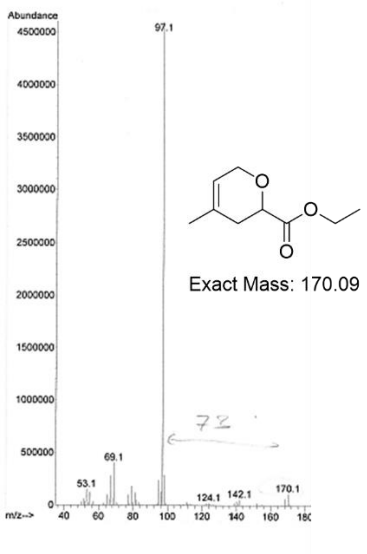


Entry III.1.1.1

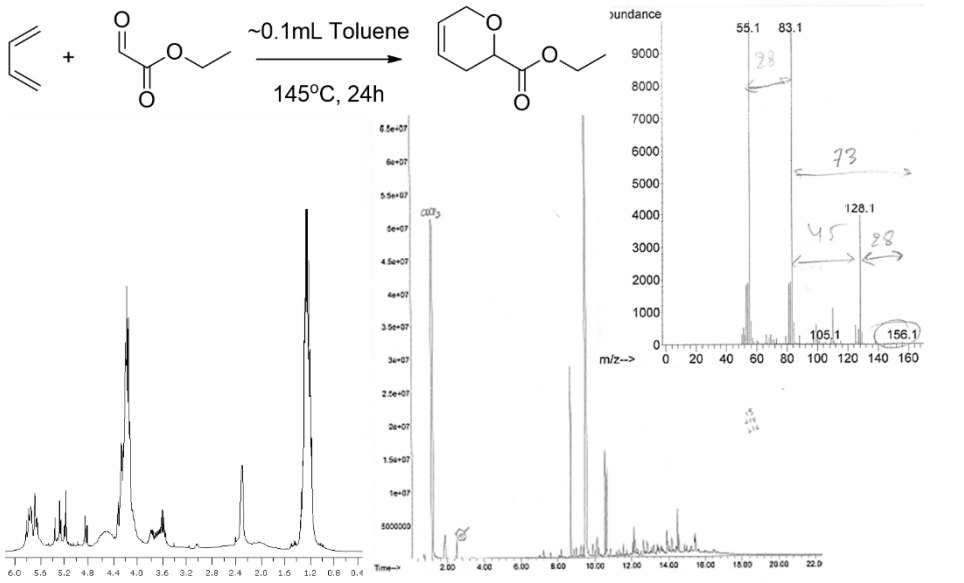


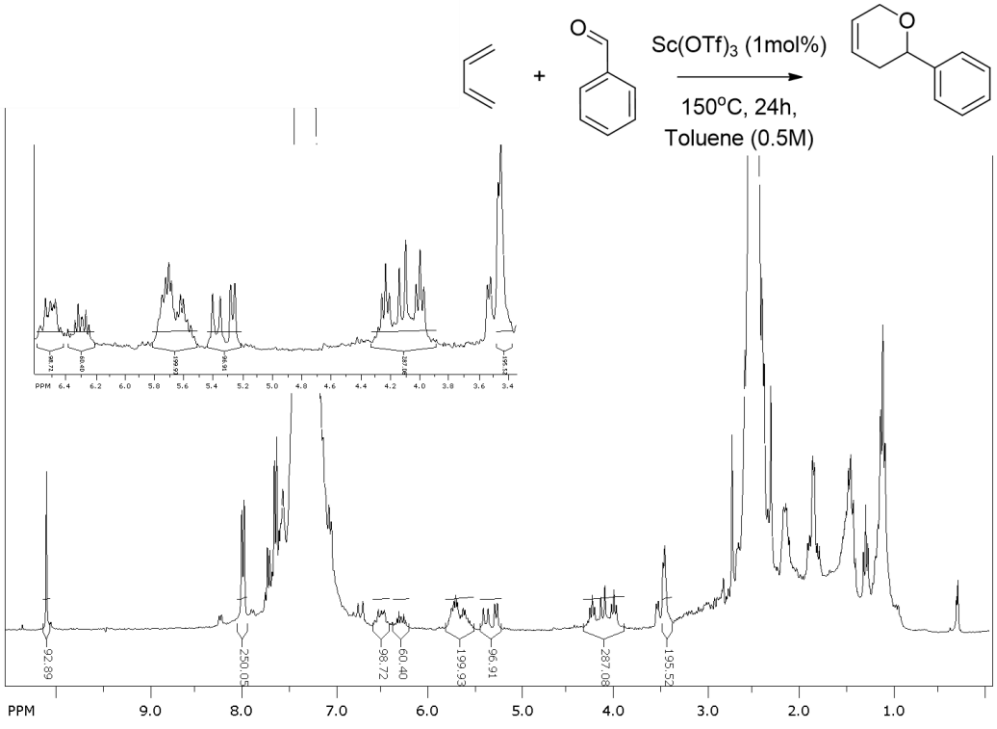
Entry III.1.1.3





Exact Mass: 170.09


~0.1mL Toluene
145°C, 24h
55.1
83.1
73
128.1
105.1
156.1
m/z-->


Sc(OTf)3 (1mol%)
150°C, 24h,
Toluene (0.5M)
92.89
250.05
98.72
60.40
199.93
96.91
287.08
195.52
PPM

2. DODH / Metathesis Tandem Reaction

a. Introduction and Background

i. The metathesis reaction

The olefin metathesis is a reaction which involves the exchange of the alkene vinylic carbons (and substituents) (Figure III. 2.1). This transformation was developed and studied most prominently by Y. Chauvin, R. Grubbs and R. Schrock, who received the Nobel Prize for their contributions. Several catalysts have been reported for the metathesis reaction.[125] These were classified in approximately four generations: from heterogeneous with high valent transition metal halide and titanocene-based catalyst to Schrock tungsten, molybdenum and rhenium arylimido complexes and Grubbs ruthenium with phosphine ligands. This reaction has a lot of potential and applications; ring closing and opening, polymerization, ethenolysis. Olefin metathesis reactions usually require high oxidation state metal catalysts with carbene ligands.

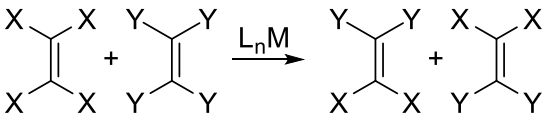


Figure III. 2.1 General metathesis equation

Chauvin and Herisson proposed a mechanism for the alkene metathesis in 1971.[126] In this mechanism the alkene double bond and the transition metal catalyst undergo a [2+2] cycloaddition to form a four membered ring intermediate. This intermediate could then cyclorevert to its original alkylidene form or to a new metal alkylidene and alkene (Figure III. 2.2). The metathesis reaction is used on industrial scale for the formation of high

molecular weight alkenes in the petroleum industry. With the recent development of new metathesis catalyst which tolerate more functional group the metathesis reaction can have applications for drug and polymer synthesis.

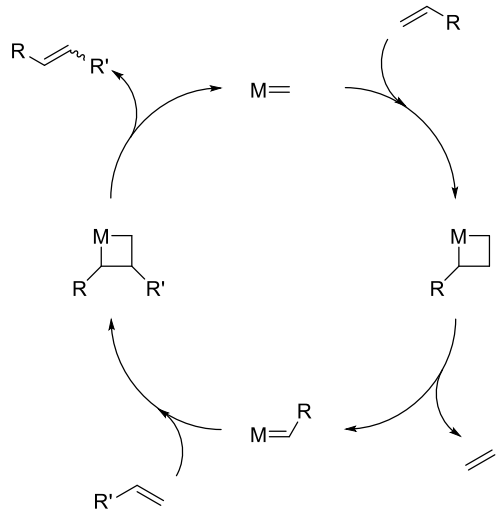


Figure III. 2.2 Metathesis mechanistic cycle

ii. DODH/Alkene Metathesis tandem concept

With the formation of alkenes via the DODH reaction we can see the high potential of an eventual tandem DODH/Olefin Metathesis (Figure III. 2.3). With a majority of product from the DODH reaction containing a terminal alkene this tandem system would allow the formation of high mass alkenes from polyols. Such a process would allow a short chain polyol to form longer chain hydrocarbons which are highly desirable as fuels. It could serve also to create building blocks for synthesis of valuable chemical and drugs. We could also envision using the process on polyols that provides dienes via DODH that could then polymerize or ring close in the alkene metathesis reaction.

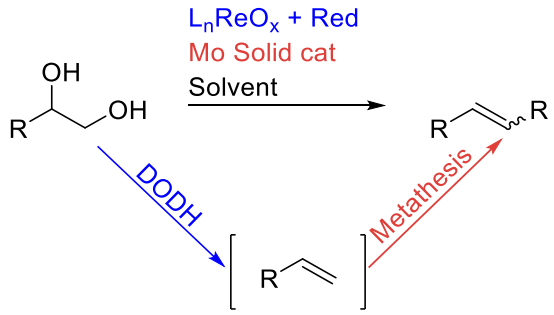


Figure III. 2.3 DODH/ Olefin Metathesis tandem concept

The great sensitivity of most metathesis catalysts towards hydroxylic compounds such as alcohols and water[127] makes a DODH-OM tandem reaction highly challenging. In this section we will describe how we chose a heterogeneous metathesis catalyst, $CoOMoO_3Al_2O_3$, and tested its activity on simple alkenes in the presence of the various DODH reagents, catalyst and products. We found this metathesis catalyst to work on 1-hexene under the DODH reaction conditions, but the catalyst was deactivated by the presence of an alcohol and diol.

b. Study of metathesis reaction under DODH reaction conditions using $CoOMoO_3Al_2O_3$ as catalyst

i. Study of the alkene metathesis step

From the large list of reported catalysts for the metathesis reaction we decided to study the heterogeneous $CoOMoO_3Al_2O_3$ catalyst. Reported in 1966 by L. Turner on 1-butene this catalyst provided a distribution of isomer alkene products from C_2H_4 to C_6H_{12}.[128] The reported reactions conditions for this metathesis reaction system are high temperature from 150°C up to 245°C. The distribution of products depends on the reaction temperature. In order to have an appropriate temperature for the DODH reaction and an

optimum temperature for high carbon contain metathesis products distribution we decided to run our reactions at 170^{o}C. We choose this metathesis system due to its simplicity, commercial availability, its stability in the air and because we thought that as a heterogeneous catalyst it would have less potential for deactivation with the soluble reagents and DODH catalyst. Also we planned to test it as a DODH catalyst since few molybdenum-oxo complexes have been reported for the DODH reaction.[57,60] Finally this catalyst is very inexpensive compared the ruthenium Grubbs catalyst and does not involve any phosphine ligands. Phosphines are good reducing agents for the DODH reaction. Because phosphines are usually expensive and phosphine oxide is a toxic byproduct we try to stay away from phosphine as reducing agent. In the case of a metathesis catalyst with a phosphine ligand the DODH catalyst could react with this ligand deactivating the catalyst or making the need for added phosphine in the system to keep the catalyst active.

After activating the catalyst in a tube furnace in Dr. Resasco's CBME laboratory, we started this study by conducting the metathesis reactions on 1-hexene and styrene using 20 mol% in MoO_3 of the catalyst (Figure III. 2.4) at 170 ^{o}C. The GC and NMR analysis of these reactions showed some high molecular weight internal alkene products showing high GC retention times as major product along with internal alkene proton pattern around 6ppm in the NMR spectrum. In the case of 1-hexene we detected at least two major products, but could not determine the exact length of the carbon chain. In the case of styrene no isomerization of the starting material or product can occur and we could detect both the cis and trans metathesis product, stilbene.

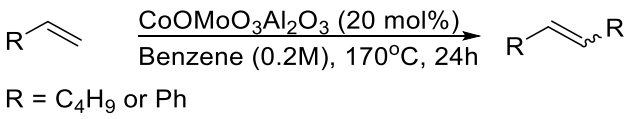


Figure III. 2.4 Study of the metathesis reaction

Having shown that the metathesis reaction works under the tested conditions, we then proceeded to add the reagents required for the DODH reaction. Since we were considering the use of benzyl alcohol[46] as reductant for the DODH reaction of 1,2-hexanediol, we ran metathesis reactions as described in Figure III. 2.4 with added 1,2-hexanediol, benzyl alcohol, benzaldehyde or water (Figure III. 2.5). In each of these cases the metathesis reaction did not take place showing the sensitivity of the catalyst toward hydroxylic compounds. For the specific case of water, a co-product of the DODH reaction, we found that the addition of powdered 4Å molecular sieves could limit the deactivation of the catalyst by water. In the case of reducing agent we can solve the incompatibility of benzyl alcohol with the catalyst by replacing it with any other one reported for the DODH reaction.[15] We found the metathesis reaction to tolerate tetrahydronaphthalene and naphthalene. This hydrogen donor was previously found to be a good reducing agent for the DODH of aliphatic terminal diols (Chapter II).[52,83] Also known as an efficient DODH reducing agent, sodium sulfite[35] and its oxidized product sodium sulfate were also found to be tolerated by the metathesis catalyst. In the case of sulfite as reducing agent 15-crown-5 ether can be added to help its solubility and reactivity as reducing agent. In consequence we also tested the compatibility of the crown ether with the metathesis reaction and found it incompatible. The incompatibility of the metathesis catalyst with the starting diol is more difficult to bypass.

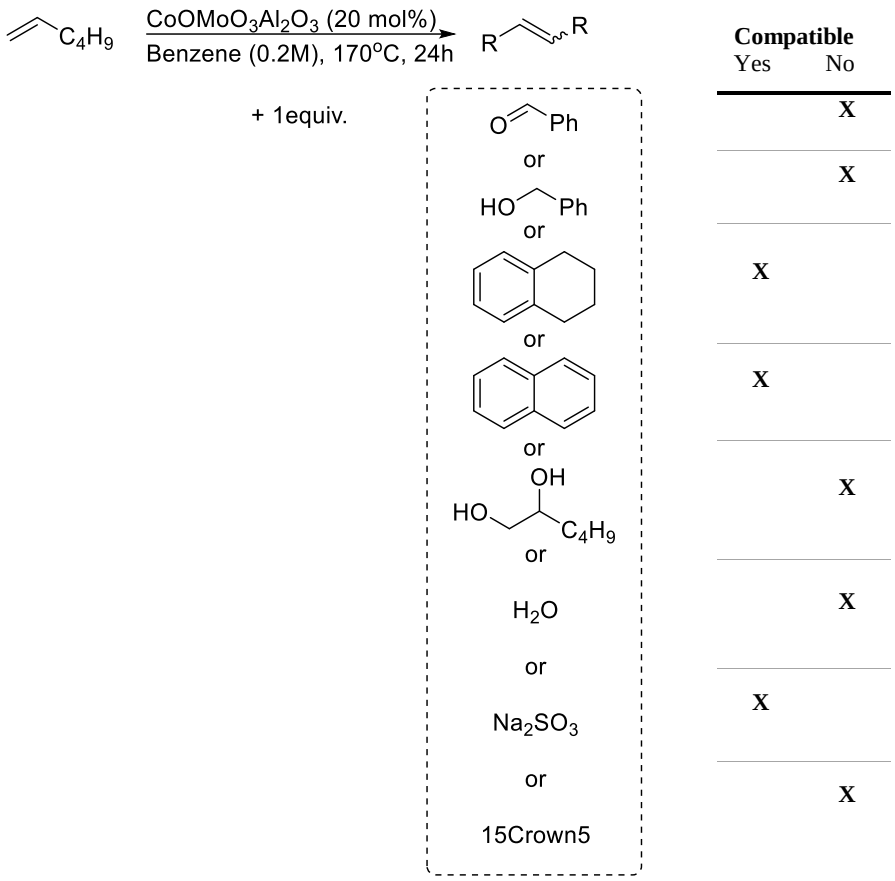


Figure III. 2.5 Tests of compatibility of the metathesis with DODH reagents

ii. Study of $CoOMoO_3Al_2O_3$ as DODH catalyst

We decided to test the activity of the molybdenum-cobalt material as a DODH catalyst. Using sodium sulfite as reducing agent with 1,2-hexanediol we detected a 15% yield of 1-hexene (170°C, 24h, in benzene 0.2M), but no metathesis products by NMR (Figure III. 2.6). This yield is lower than the catalyst loading so it is hard to determine if the catalyst is deactivated or just not able to able to make a full cycle. The low solubility of the reducing agent combined with the heterogeneous catalyst probably makes for very slow reaction. We doubled the catalyst loading (40 mol% in MoO_3), but we did not detect

any alkene products in this case. Thus, under DODH conditions the Co-Mo material was not active for olefin metathesis and had very limited activity as a DODH catalyst. The incompatibility of this metathesis catalyst and 1,2-hexanediol found in the first part of this study might support the low activity of this catalyst for the DODH reaction. We can consider the potential coordination of 1,2-hexanediol to the catalyst. This coordination can be irreversible making the catalyst unavailable to react or the coordinated specie could further react and form an inactive complex.

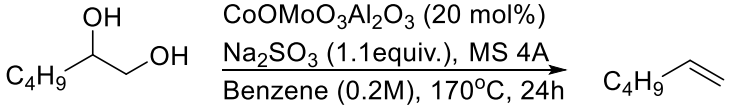


Figure III. 2.6 $CoOMoO_3Al_2O_3$ as DODH catalyst

c. Deoxygenation/Metathesis tandem reaction of styrene oxide

With all of our findings on the compatibility of the DODH reagents and the metathesis catalyst we decided to attempt a tandem reaction starting from an epoxide. In fact we though the epoxide would not deactivate the metathesis catalyst as it has not any exchangeable proton from the alcohol function. The other advantage of starting from an epoxide is the potential for not making an equivalent of water over the deoxygenation step. The deoxygenation (DO) of epoxide to alkene is run under similar reaction conditions than the DODH reaction. We ran this reaction as described Figure III.2.7 on styrene oxide with 10 mol% of rhenium catalyst and 20 mol% (in molybdenum oxide) of the metathesis catalyst and sodium sulfite as reducing agent. The result of this experiment was probed by NMR, GC and GCMS. After 24h the conversion was complete, 100%, we detected by ^{1}H NMR a mix of aldehyde, alkenes and potentially acetals. After a

preparative TLC we had more confidence on the formation of stilbene and we confirmed this result by GCMS. Overall the reaction made several side products with only around 10% in tandem product but it proved the concept of a DODH/Metathesis tandem system. We believe that part of the side reaction came from interaction of the solvent with the reaction. Other solvents should be tested to improve this result.

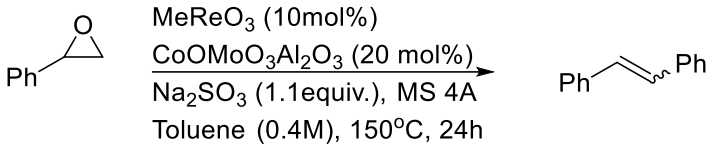


Figure III. 2.7 Deoxygenation/Metathesis tandem reaction

d. Conclusion

Our study of the reagent tolerance on the selected metathesis catalyst demonstrated the low potential for this tandem system to work. In fact even if we could manage to find a reducing agent (and its oxidized product) to be tolerated in the metathesis reaction, the incompatibility of the diol with the molybdenum tri-oxo complex is a major limitation to any combined tandem system. We found the metathesis catalyst to have some activity as DODH catalyst but with lower yield than the catalyst loading. The low solubility of the reducing agent employed in combination with the heterogeneous catalyst could be one explanation to the low yield also the test of a potential crown ether additive demonstrated the deactivation of the metathesis catalyst. Since the product of the DODH reaction that would apply to a tandem system, styrene, hexane, etc., are volatiles one could design a reactor with two zones allowing the volatile material to reach the metathesis catalyst after

removing the water. Also gas such as hydrogen or carbon monoxide could be considered as reducing agents in the DODH reaction.

Starting with an epoxide we obtained DO/Metathesis tandem reaction. Once the reaction would be optimized a larger range of epoxide could be tested, 1,2-hexene oxide for example. These results would then help the general understanding of the tandem reaction.

Several metathesis catalysts have been reported over the years since this reaction was discovered. The alumina-supported $MeReO_3$ could be a good catalyst to test on both DODH and metathesis as it could avoid the use of two different catalysts for the tandem reaction.[129] This tandem system could also be studied further by testing some of the recently reported metathesis catalysts which are getting more and more robust and stable in the presence of water and air such as $RuCl_2PR'_3(=R)$.[130] The high cost of these catalysts would probably not make this system economic for industrial scales.

e. Experimental

i. General information: reagents and instruments.

All reactants and catalysts were obtained commercially and used without further purification. All solvents were ACS grade and were used directly (unless otherwise described in the procedures). ^{1}H NMR spectra were collected on Varian VX300 MHz or VNMRS 400 MHz instruments. The NMR data were processed using SpinWorks[102] and ACD[103] software. Gas chromatograms were collected on a Shimadzu GC-2014 equipped with an AOC 20i+s auto sampler, both with 3% SE-54 packed column, FID and thermal program 40ºC for 5 min; 20 deg/min to 250ºC; then 7 min at 250°C.

ii. Activation of the catalyst

We followed the reported procedure for the activation of the catalyst[128]: 2.0 g of the $CoOMoO_3Al_2Cl_3$ catalyst were placed in a silica tube between two balls of quartz wool. The tube was placed in a horizontal tube furnace. The furnace was set at 550ºC. A stream of dry air was passed through the tube for 1 hour followed by 1.5 hours with a steam of dry nitrogen. The tube was then allowed to cool to room temperature under dry nitrogen. The activated catalyst was then crushed into powder and stored in a glove box. As needed a portion of the catalyst was weighed in the glove box and transferred to the reactor vessel. In the activation process the catalyst changed from a light blue color to a darker deep blue color.

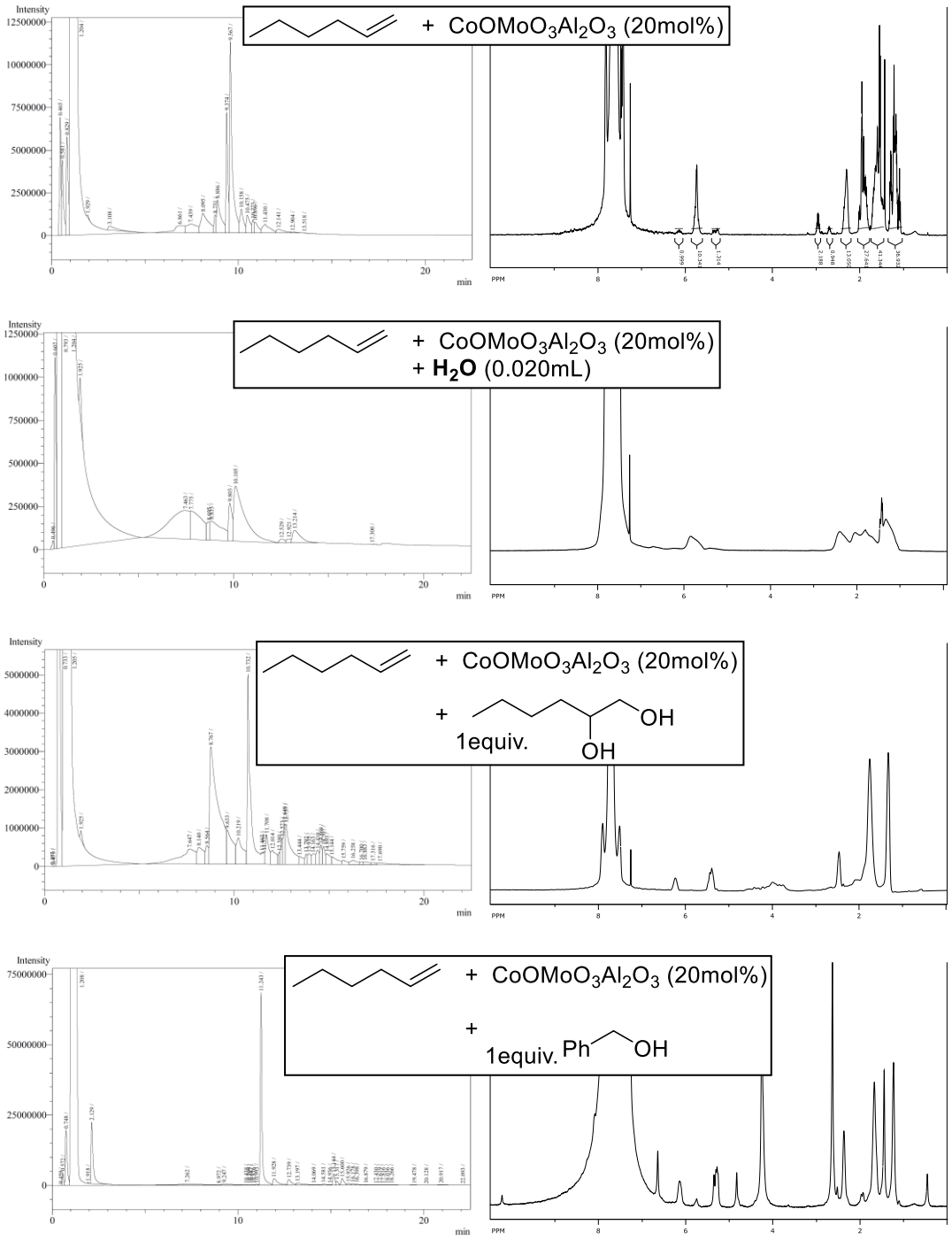
We are grateful to Dr. D. Resasco (CBME) for letting us use the furnace in his laboratory and his postdoctoral fellow Dr. Wang for helping us with the activation process.

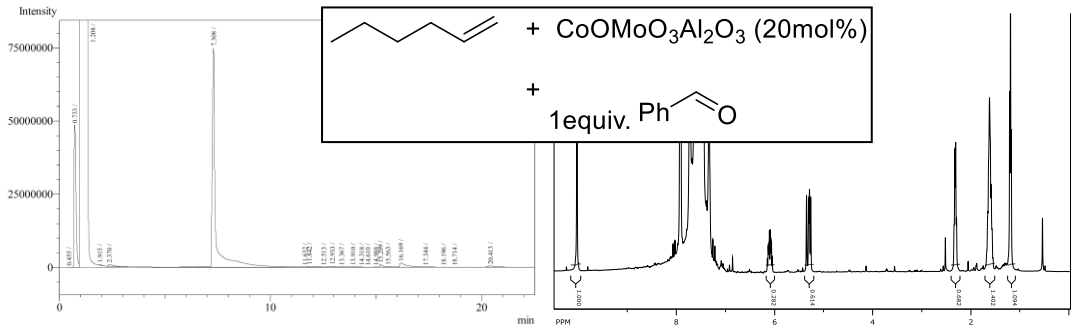
iii. Representative procedure for metathesis reactions.

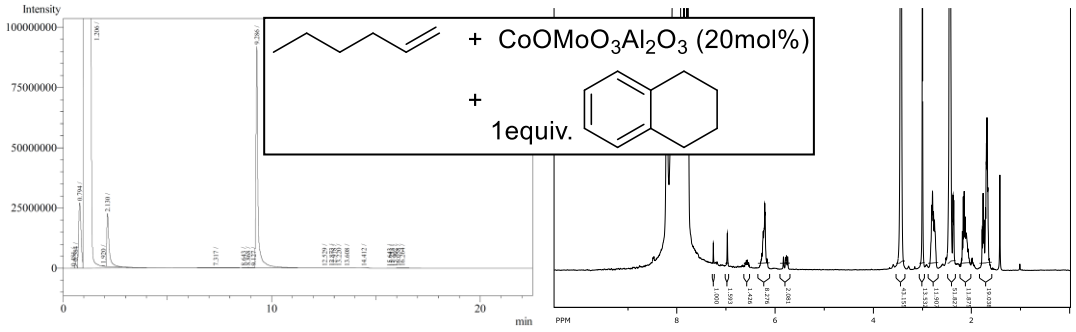
1-Hexene (1.00 mmol, 0.12 mL), $CoOMoO_3Al_2Cl_3$ (0.20 mmol in MoO_3, 100 mg), additives (1.10 mmol), and benzene (2.5 mL) were added to a thick-walled Ace glass reactor tube. A N_2 flow was bubbled into the mixture for at least 60 sec before the Teflon seal was closed. The reactor was placed in an oil bath at 150ºC for 24 h while stirring magnetically. After cooling to room temperature, a 100 µL aliquot of the reaction mixture was removed and added to $CDCl_3$ (0.5 mL) and 2.0 µL DMSO as internal standard for NMR analysis. A 0.5 mL aliquot was collected for GC analysis. All olefinic products

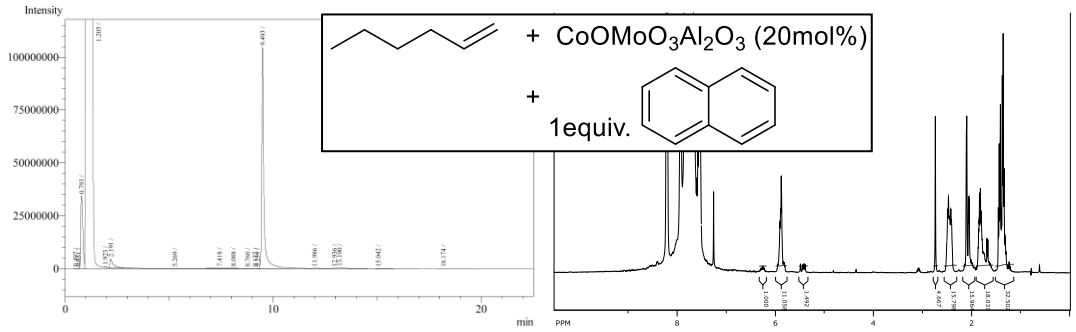
from the metathesis reactions have been previously reported and were identified by comparison of their NMR and GC spectra with authentic samples or published data.

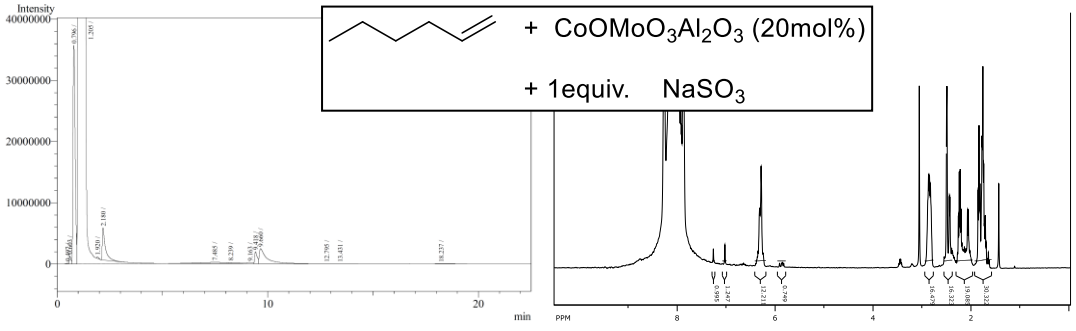
Gas chromatogram **^{1}H NMR Spectrum**

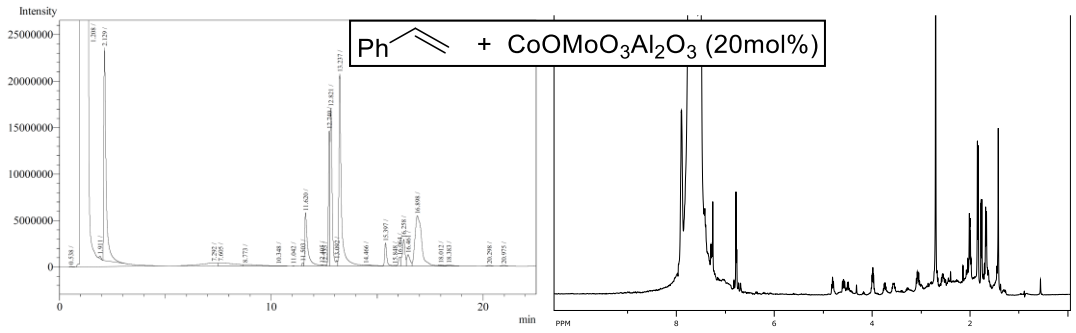



+ $CoOMoO_3Al_2O_3$ (20mol%)
+
1equiv. Ph O
Intensity
min
PPM


+ $CoOMoO_3Al_2O_3$ (20mol%)
+
1equiv.
Intensity
min
PPM

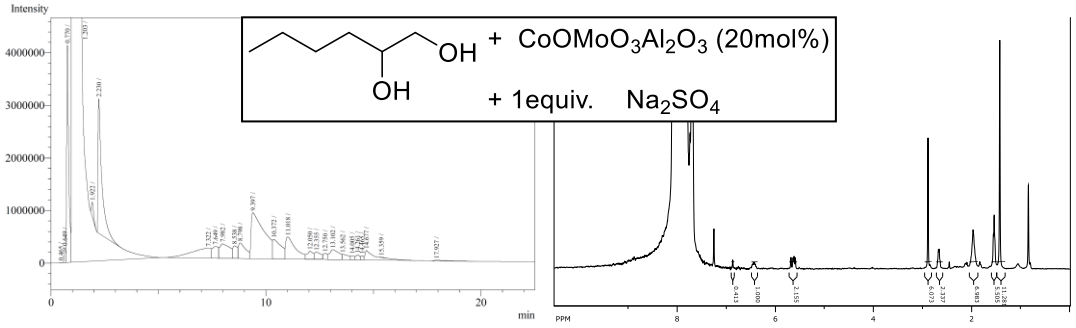

+ $CoOMoO_3Al_2O_3$ (20mol%)
+
1equiv.
Intensity
min
PPM


+ $CoOMoO_3Al_2O_3$ (20mol%)
+ 1equiv. $NaSO_3$
Intensity
min
PPM



iv. Representative procedure for DODH reactions using $CoOMoO_3Al_2Cl_3$ as catalyst.

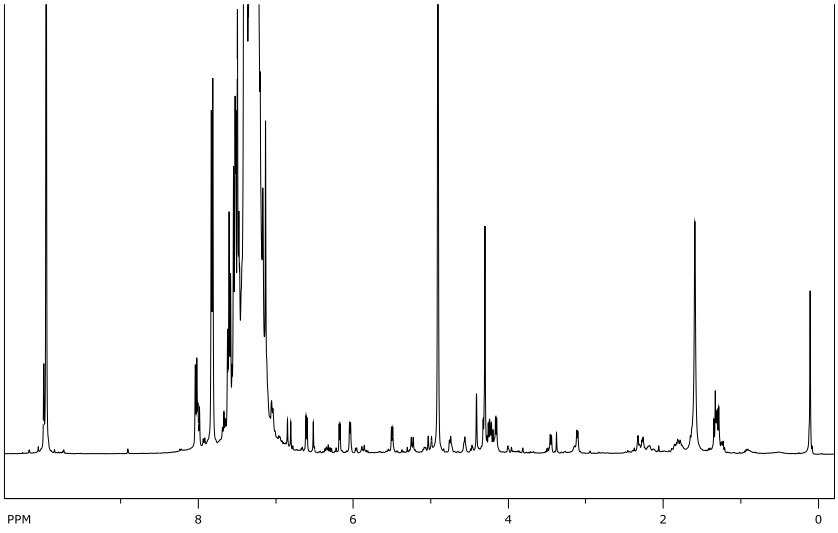
1,2-Hexanediol (1.00 mmol, 0.12 mL), $CoOMoO_3Al_2Cl_3$ (0.20 mmol in MoO_3, 100 mg), sodium sulfite (1.00 mmol, 126 mg) molecular sieves powder 4Å (100 mg), and benzene (2.5 mL) were added to a thick-walled Ace glass reactor tube. A N_2 flow was bubbled into the mixture for at least 60 sec before the Teflon seal was closed. The reactor was placed in an oil bath at 150^{o}C for 24 h while stirring magnetically. After cooling to room temperature, a 100 µL aliquot of the reaction mixture was removed and added to $CDCl_3$ (0.500 mL) and 2.0 µL DMSO as internal standard for NMR analysis. A 0.5 mL aliquot was collected for GC analysis. All olefinic products from the metathesis reactions have been previously reported and were identified by comparison of their NMR and GC spectra with authentic samples or published data.



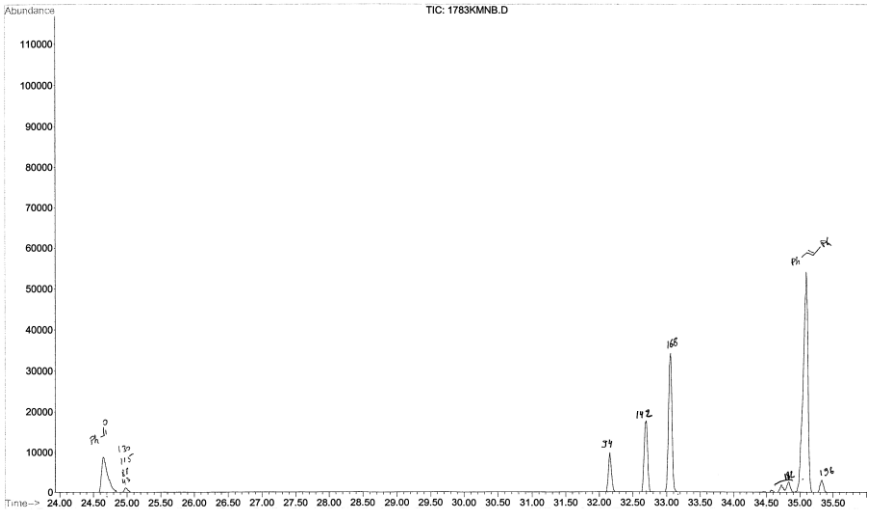
v. Procedure for DO/Metathesis reaction using of 1-hexene oxide

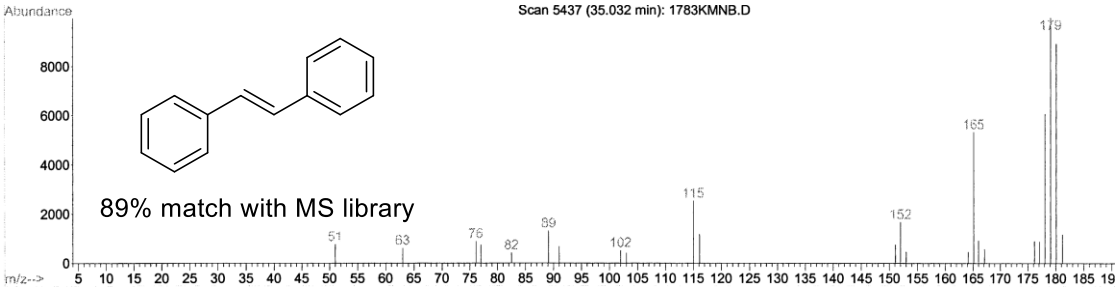
1-Hexene oxide (1.00 mmol, 0.12 mL), $MeReO_3$ (0.10 mol%), $CoOMoO_3Al_2Cl_3$ (0.20 mmol in MoO_3, 100 mg), sodium sulfite (1.00 mmol, 126 mg) molecular sieves powder 4Å (100 mg), and toluene (2.5 mL) were added to a thick-walled Ace glass reactor tube. A N_2 flow was bubbled into the mixture for at least 60 sec before the Teflon seal was closed. The reactor was placed in an oil bath at 150°C for 24 h while stirring magnetically. After cooling to room temperature, 1mL of the reaction was run thru a plug of celite. A 100 µL aliquot of the filtered reaction mixture was added to $CDCl_3$ (0.50 mL) for NMR analysis. A 0.5 mL aliquot was collected for GC and GCMS analysis. GC-MS-EI analyses were performed on a Thermo-Finnigan instrument using a Stabil-wax capillary column.

^{1}H NMR



GCMS





89% match with MS library

3. DODH / Allylation tandem reaction

a. Introduction

i. Allylation background

The allylation reaction is the formal addition of an allylic moiety to a carbonyl group (Figure III. 3.1). The product of this transformation is a homo-allylic alcohol that can used as a bifunctional building block in synthesis. The traditional approach to the synthesis of homo-allylic alcohols is to form first an allylic organometallic reagent which is then added to the carbonyl compound. The high reactivity of the allylic organometallic reagent to moisture and air makes it impractical to scale up. Alternatives to the stoichiometric formation of allylic organometallic reagents were developed in the late 80's. Masuyama and co-workers reported first an allylation reaction using stoichiometric tin chloride ($SnCl_2$) and catalytic palladium (II).[131] The mechanism of this reaction is likely to involve a η^3-allyl-Pd complex which is reduced by tin (II) chloride to form an allyltin intermediate allowing the allyl unit to add to the aldehyde and form product.

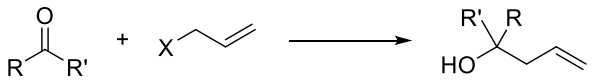


Figure III. 3.1 General allylation reaction equation

More recently in 2011, Dr. Krische at the University of Texas Austin, reported an alcohol mediated carbonyl allylation system catalyzed by an iridium complex (Figure III. 3.2).[132–134] In this reaction an allyl acetate and a primary alcohol (or an aldehyde) undergo C-C coupling. The mechanism of this reaction is likely to involve a nucleophilic allyl-iridium complex.

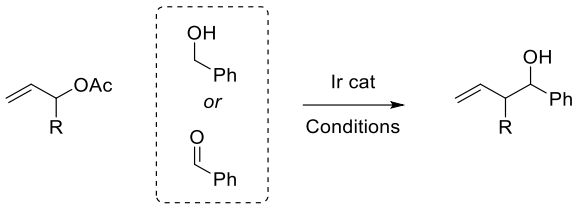


Figure III. 3.2 General carbonyl allylation

ii. Tandem DODH/Allylation concept

The general concept of this tandem DODH/Allylation reaction is to form the allylic alcohol or ester in the DODH reaction (Figure III. 3.3). By using benzyl alcohol as reducing agent simultaneously we will form the carbonyl compound on which the allylic-metal unit can be added making for an atom economical reaction. The final homo-allylic alcohol product will be of much higher value than the glycerol or glycerol derivative and could be further used as a building block for complex product synthesis.

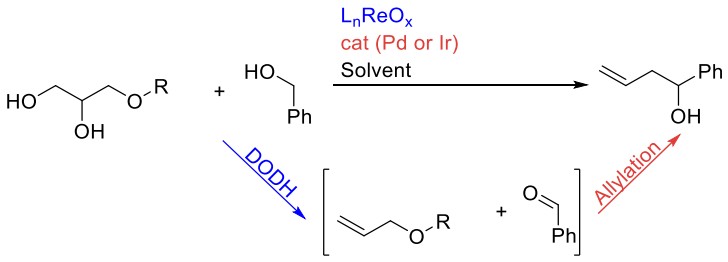


Figure III. 3.3 DODH/Carbonyl-Allylation (CA) tandem concept

iii. DODH/Carbonyl Allylation with Krische system

At the time of Krische's report, our group had discovered the efficacy of benzyl alcohol as a reducing agent for the DODH reaction. In the list of diols we studied an ester derivative of glycerol, glycerol monostearate, which was converted in high yield to an

allyl ester along with benzaldehyde.[46] The similarity of our products from the DODH reaction with the reagents of Krische's system make for a favorable tandem system of the two reactions.

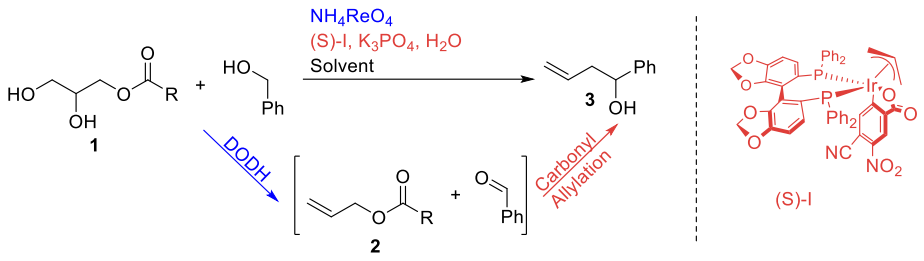


Figure III. 3.4 DODH/Krische Allylation

The general idea for this tandem reaction is to start with the DODH of a glycerol ester, e.g. glyceryl monostearate (**1**, Figure III. 3.3) which produces the allylic ester (**2**, Figure III. 3.3) using benzyl alcohol as the reducing agent and ammonium perrhenate as catalyst. The allylation, catalyzed by the iridium complex (S)-I, can then take place with the aldehyde obtained in the DODH reaction and the allylic pro-nucleophile (**2**, Figure III. 3.3) to provide 1-phenylbut-3-en-1-ol (**3**, Figure III. 3.3). In this tandem reaction the relatively economical glycerol derivative provides a more valuable product via the use of two transition metal catalysts. This system is atom economical since the benzaldehyde formed in the DODH reaction is a reagent in the second reaction. Only the long chain carboxylate from the glycerol ester derivative would be left out of the final product.

In the first part of this section we will describe our approach to testing the compatibility of the reagents for each step.

iv. DODH/Allylation with Masuyama system

With the recent development of a DODH reaction system for glycerol[42,44,83] we also considered the Masuyama allylation to be used in a tandem DODH-CA reaction (Figure III. 3.5). In the Masuyama system tin chloride is used as a stoichiometric reductant with palladium (II) chloride catalyst (either phosphine ligand or bis-benzonitrile and bis-acetonitrile ligands) in dimethyl formamide as solvent. More recently Guo's group reported a modification of the Masuyama allylation using bi-phasic (THF/water) and aqueous media[135] and palladium (II) chloride as the catalyst without any added ligand. Since phosphine is a very good reducing agent in the DODH reaction we wanted to avoid the use of a phosphine based catalyst in the tandem system. The use of triphenyl phosphine as reducing agent was considered, but with the high cost and toxicity of it and it's difficult to recycle triphenyl phosphine oxide byproduct, we wanted to avoid it. In addition we planned on using benzyl alcohol as the reducing agent in this DODH/Allylation tandem system so that we could form the carbonyl species needed for the allylation in the DODH step and achieve an atom economical tandem system. The compatibility of acetonitrile or benzonitrile with the DODH reaction was unknown. In order to limit any potential reactivity of these ligands we will investigate the naked palladium (II) chloride catalyst. The potential activity of tin chloride as a reductant in the DODH reaction will be considered as well since it could compete with benzyl alcohol. The biggest unknown for the Masuyama allylation reaction system is that the reaction proceeds at room temperature, but we planned on conducting it at the typical DODH reaction temperature of 150^{o}C.

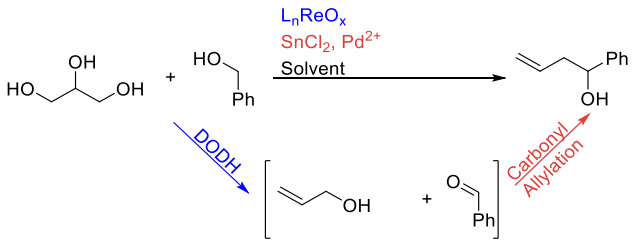


Figure III. 3.5 DODH/Masuyama Allylation

In a second part of this section we will describe our study of each step individually. The allylation will be studied in the potential DODH solvent from toluene and benzene to more polar solvents such as 1-butanol. Tin chloride's activity as a reducing agent will be tested and we will also compare its activity to benzyl alcohol in a competition experiment. Finally we will attempt to combine both reactions in a tandem DODH/Allylation system.

b. DODH/Krische's Allylation

Initially each of the reactions were studied separately and the compatibility of the reagents for each step were evaluated.

i. Allylation step

The reaction conditions for the allylation were utilized from the literature using allyl acetate as the allylic ester. This reaction employed the catalyst (S)-I prepared from bis-1,5-cyclooctadiene chloride diiridium (I), allyl acetate, (S)-SEGPHOS and 4-cyano-3-nitrobenzoic acid. (Figure III. 3.6). The catalyst (S)-I was provided to us by Dr. Krische.

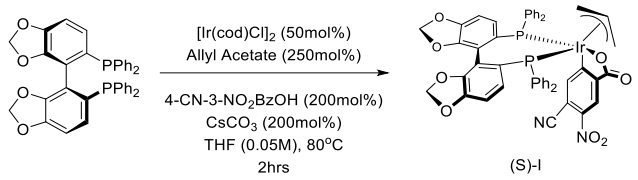


Figure III. 3.6 (S)-I Catalyst preparation

This step was found to have some specific requirements (Figure III. 3.7, R = Ac). In fact the use of potassium triphosphate as a base and an inert atmosphere were two important reaction conditions. The base is needed to deprotonate one of the catalyst intermediates to form an anionic Iridium (I) species that will oxidize and coordinate with the allyl acetate to form the Ir-aryl complex.

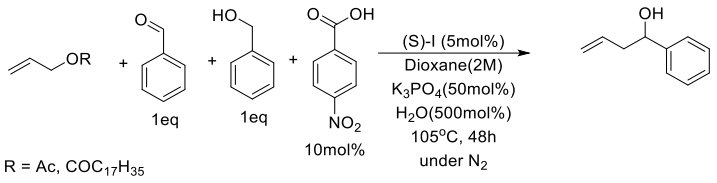


Figure III. 3.7 Study of allylation step

The conditions that we found to be required for the allylation of benzaldehyde with allyl acetate were applied to the isolated alkene product from the DODH of glycerol monostearate (Figure III. 3.7, R = $COC_{17}H_{35}$). Some significant amount of allylation product (~30%) was found in the ^{1}H NMR spectrum. The terminal alkene signals moved up field from 6.7 and 5.2 ppm to 6.5 and 5.0 ppm; the proton next to the hydroxyl moves from 4.6 to 4.4 ppm. Finally, the CH_2 between the unsaturation and the hydroxyl gives a triplet at 2.5 ppm. We also detected some of the allyl ester unreacted in the NMR spectrum. The formation of the product was also confirmed by GCMS with a GC signal at 10.3 min with the right mass.

From these preliminary results on the allylation step, we planned on changing the DODH reaction solvent for dioxane. Following the reaction by NMR it was found that dioxane was not a very good solvent for the DODH reaction. The yield in alkene dropped dramatically below 20%. Toluene was originally reported as solvent for the DODH of this derivative of glycerol so we decided to use a portion of DODH reaction run in toluene to try the allylation step. The ^{1}H NMR analysis of this reaction mixture showed signals at 2.5 ppm for the CH_2 next to the alkene and at 4.6 ppm for the CH-OH group, giving evidence that the allylation product formed. We could then conclude that the DODH reagents are compatible with the allylation reaction system.

To conclude this study of the allylation side of the tandem reaction we found that tripotassium phosphate is needed as a base and an inert atmosphere must be maintained, but also that the allylation reaction tolerates the solvent, products and side products of the DODH reaction.

ii. DODH Step

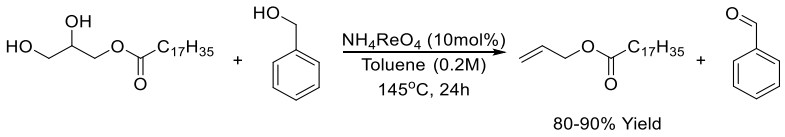


Figure III. 3.8 DODH of Glycerol Monostearate

We reported the DODH of glycerol monostearate using benzyl alcohol as reducing agent and ammonium perrhenate as catalyst with an 80 to 90% yield (Figure III. 3.8).[46] After studying the allylation step, we determined that dioxane is not a suitable solvent for the DODH reaction, so we needed to test the compatibility of the tripotassium phosphate

with the DODH reaction. Since the catalyst, ammonium perrhenate, is slightly acidic our main concern was the deactivation of the rhenium-oxo complex by the tripotassium phosphate. So we ran the DODH reaction under the usual conditions adding the base in the stoichiometry of the allylation system. As we had anticipated, the ^{1}H NMR spectrum of the reaction did not show any protons NMR signals of the DODH alkene product and all the diol was found unreacted.

We decided to screen some milder bases to find one that would be compatible with the DODH system: ammonium hydroxide, sodium carbonate, triethylamine and pyridine (Figure III. 3.9). Ammonium hydroxide was found to allow the DODH reaction to proceed in moderate yield (50% estimate, 150^{o}C, 24h), but when we used this base in place of tripotassium phosphate in the allylation reaction no products were detected by ^{1}H NMR. Also we could see only a very low conversion of the diol with still some strong signals in the 3.5 ppm region.

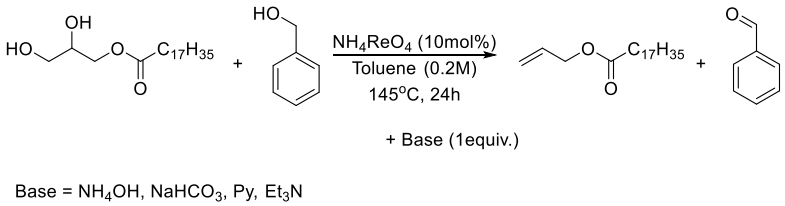


Figure III. 3.9 DODH reaction with added bases

In summary we found the DODH reaction to be incompatible with the base tripotassium phosphate. Even though we found ammonium hydroxide to be compatible with the DODH reaction, this base was found to be unsuitable for the allylation step.

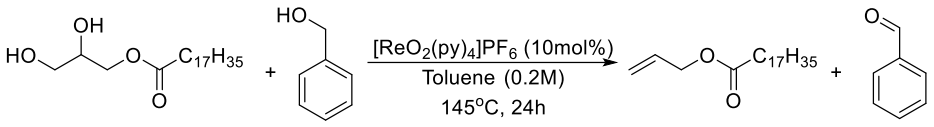


Figure III. 3.10 DODH reaction with trans-$[ReO_2(py)_4]PF_6$ as catalyst and added pyridine

We also tested a potentially base-tolerant DODH catalyst, trans-$[ReO_2(py)_4]PF_6$ (py=pyridine), which has a basic ligand (Chapter III Section 5). This catalyst gave a 70% yield of the DODH alkene product from glycerol monostearate (toluene 0.2M, 150°C, 24h) with benzyl alcohol reductant (Figure III. 3.10). But when we used the catalyst alone or added pyridine to replace tripotassium phosphate in the allylation reaction, we did not observe any signals for the homo-allylic alcohol product in the NMR spectrum. On the other hand the DODH reaction of the glycerol ester with trans-$[ReO_2(py)_4]PF_6$ didn't occur in the presence of the phosphate base (Figure III. 3.11). It is conceivable that the phosphate base reacts with the catalyst (as a ligand or by replacing the anion) making it inactive toward the DODH reaction.

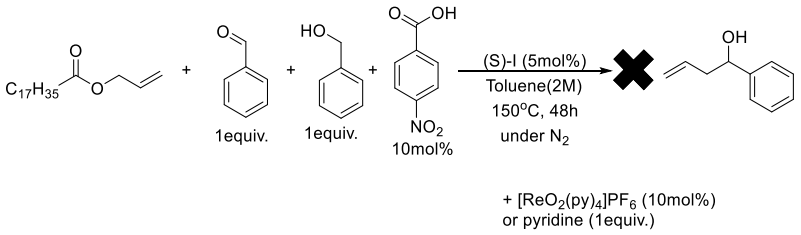


Figure III. 3.11 Carbonyl Allylation Step with added $[ReO_2(py)_4]PF_6$ or pyridine

We found the DODH reaction to be tolerant of pyridine when trans-$[ReO_2(py)_4]PF_6$ was used as catalyst. Unfortunately, neither the catalyst itself nor pyridine could substitute for tripotassium phosphate in the allylation reaction.

iii. Change in the glycerol derivative

The incompatibility of the DODH reaction with the required base for the allylation was a major limitation for the tandem DODH-allylation reactions. In an effort to enable this tandem reaction Dr. Krische suggested a BOC-carbonate derivative of glycerol which could form the base *in situ* upon activation by the Ir-catalyst (Figure III. 3.12). The diol-BOC derivative was prepared from glycerol at room temperature with an excess of di-*tert*-butyl dicarbonate and 4-dimethylaminopyridine (DMAP) as catalyst (Figure III. 3.13).

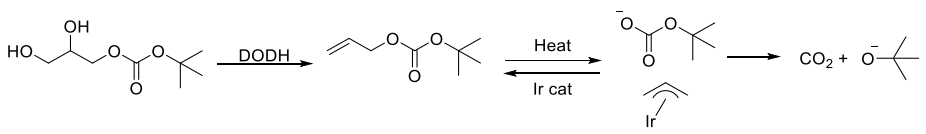


Figure III. 3.12 *In situ* Formation of a Base with BOC Derivative of Glycerol

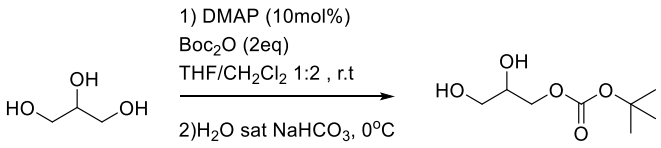


Figure III. 3.13 Synthesis of BOC derivative of glycerol

Since this was a new diol, the DODH step was first tested. Variations of solvents (toluene, dioxane, tetrahydrofuran) and of catalyst (NH_4ReO_4, CH_3ReO_3, trans-$[ReO_2(py)_4]PF_6$ and $[n\text{-}Bu_4N](dipic)VO_2$) were tested with this diol conversion using benzyl alcohol as the reducing agent. In only four of these combinations the NMR analysis of the reaction mixture show alkene and aldehyde products (Table III. 3.1) with yields in alkene from less than 10% and up to 23% (the conversion of this reaction could ne be determined as the starting diol is not soluble in the NMR solvent). The reason for

low yield in alkene could be: 1) a poor solubility of the polyol in the DODH solvent since the most polar solvent, dioxane, gave the highest yield (entry III.3.2) or 2) its product could be unstable at high temperature causing it to degrade or undergo side reactions. With a maximum yield of 23% in alkene and 45% in benzaldehyde in the DODH step, the tandem DODH/Allylation reaction was not attempted. So further efforts to carry out a tandem DODH/Krische'allylation were discontinued.

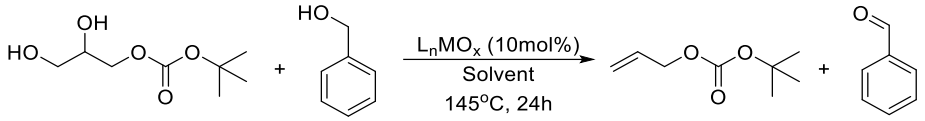


Figure III. 3.14 DODH of the BOC Derivative of Glycerol

Table III. 3.1 DODH Study of the BOC Derivative of Glycerol

entry	Catalyst	Solvent	Yield (%)
III.3.1.1	NH_4ReO_4	Toluene 0.2M dried over Na_2SO_4	12
III.3.1.2		2.5mL Dioxane 0.2M	23
III.3.1.3	trans-$[ReO_2(py)_4]PF_6$	Toluene 0.4M dried over Na_2SO_4 (under N_2)	<10%
III.3.1.4	$MeReO_3$		13

iv. Conclusions

By studying each step individually we discovered that the allylation reaction required potassium triphosphate base and inert atmosphere. The catalytic cycle involves iridium (I), which is air sensitive, and explains the requirement for an inert atmosphere. The base plays a key role in the catalytic cycle by reducing the iridium (III) hydride intermediate.

The use of this base was found to be incompatible with the DODH reaction. We found also that dioxane was not a suitable solvent for the DODH reaction. We found the DODH reaction to be tolerant of ammonium hydroxide. Since most DODH catalysts tested are mildly acidic the presence of a base in the DODH reaction could deactivate the catalyst. Also we found the DODH reaction to tolerate the use of an equivalent of pyridine when a pyridine rhenium (V) oxo complex was employed as catalyst, but pyridine was not an effective substitute for potassium triphosphate in the allylation step. We attempted a variation in the allylic reagent in order to form an equivalent of base in situ, but the BOC derivative of glycerol provided low yield in the DODH reaction itself. We explain the low yield in alkene by the limited solubility of the diol in the reaction solvent and the instability of the BOC derivative at the reaction temperature. Because of these limitations we were not able to combine the DODH reaction and the allylation reaction into an efficient tandem system.

c. DODH/Masuyama's Allylation

In the Masuyama allylation reaction a Pd(II)/Sn(II) co-catalyst promotes the allylic alcohol addition to an aryl aldehyde. In order to obtain allyl alcohol from a DODH reaction we need the inexpensive polyol glycerol. For many years the transformation of this polyol to allyl alcohol was limited by it solubility in the reaction solvent. With the recent report of secondary alcohols as efficient solvents and reducing agent we finally have a promising way to efficiently convert polyols to olefins. Shiramizu and Toste reported a 90% yield of allyl alcohol from glycerol using $MeReO_3$ as catalyst and 3-octanol as reducing agent and solvent.[44] Abu-Omar's group reported a DODH reaction in

which glycerol serves as the diol, the reducing agent and the solvent.[42] More recently in our study of hydroaromatics as DODH reducing agents 1-butanol was used as solvent to convert glycerol to allyl alcohol with indoline as reductant.[83]

In 2004 Guo and co-workers reported an allylation reaction in THF:water in different ratios (from 1:0 to 0:1). They could use water as the solvent in high yield (>90%) by replacing allyl alcohol with allyl chloride. As we wanted to use glycerol as the starting material we focused on their result in a THF:water mixture on allyl alcohol. The DODH of glycerol has not been reported in either THF or water. They also used a stoichiometry of 1 to 2 on aldehyde to alcohol.

We started the study of this tandem reaction system by running the allylation reaction under typical DODH conditions- in benzene at 150ºC (Figure III. 3.15). With this experiment we wanted to determine if the allylation would still occur since it was reported to work at room temperature after several hours. The reaction was analyzed by ^{1}H NMR spectroscopy and showed a little bit of unreacted benzaldehyde with a singlet at 10 ppm and a doublet at 8 ppm. We could see a change in the shape the signal for the terminal alkene protons with a multiplet at 6.3 ppm the two doublets for the CH_2 of the alkene being closer than in allyl alcohol at 5.4 ppm. The allylic CH_2 is expected at 2.5 ppm as a multiplet and the C*H*-OH proton is expected at 4.6 ppm as a triplet; neither of these signals was detected. However, a doublet integrating for 2 (compared to the 6.3 ppm signal) was present at 3.7 ppm, which could be from the ketone **2** (Figure III. 3.15), formed after the allylation of benzaldehyde by the oxidation of the alcohol **1** (Figure III. 3.15). If **1** is oxidized to **2**, it is not easy to see which reagent gets reduced. The only two other signals on in the NMR spectrum were a singlet at 4.3 ppm and a little doublet at 1.7

ppm. In addition allyl alcohol was used in excess, but we did not detect a large amount of unreacted allyl alcohol by NMR. The changes in solvent and temperature most definitely changed the product of the allylation reaction but the formation the ketone **2** was significant as this was a C-C bond formation reaction that took place under similar conditions to the DODH reaction.

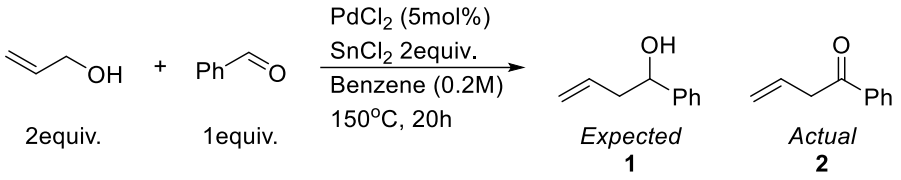


Figure III. 3.15 Allylation reaction in benzene as solvent and at 150ºC

With this result on the allylation step we now had to address the compatibility of the allylation reagents with the DODH reagents. Our biggest concern was the potential activity of tin chloride as a reducing agent in the DODH reaction. We started by testing the activity of $SnCl_2 : 2H_2O$ as a reducing agent for the DODH reaction on diethyl tartrate (Figure III. 3.16). The reaction was analyzed by NMR and we could detect 55% yield of product along with 45% unreacted diol. This demonstrated the ability of tin chloride to act as a reducing agent in the DODH reaction.

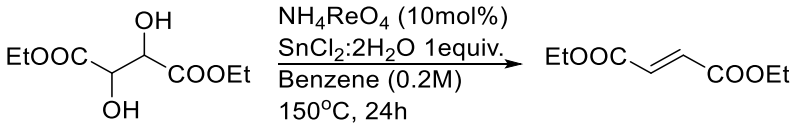


Figure III. 3.16 DODH of DET using $SnCl_2$ as reducing agent

With the demonstration of the activity of tin (II) chloride as reducing agent we decided to test its activity as catalyst for the DODH reaction. We ran the same reaction (Figure III. 3.16) without any rhenium catalyst and 2 equivalents of tin chloride. The NMR analysis of this reaction showed a 67% yield of fumarate. Also we tested tin (II) chloride as catalyst with benzyl alcohol as reducing agent, but we did not detect any diethyl fumarate (singlet at 6.8 ppm) by NMR. Tin chloride and its oxidized product are not "green" chemicals and would not be economical stoichiometrically on industrial scale. A control reaction was run and no DODH reaction was observed when diethyl tartrate is placed at 150^{o}C in benzene 0.2M for 24h). In summary we discovered the ability of tin (II) chloride to be a reducing agent in the rhenium-catalyzed DODH reaction and to convert diethyl tartrate in diethyl fumarate in absence of rhenium catalyst. This is the first report of a DODH reaction driven by a non-transition metal.

Knowing now the ability of tin (II) chloride as a reducing agent on diethyl tartrate we tested it on glycerol. With the poor solubility of glycerol in organic solvents we ran this reaction in a biphasic system with 1 mL of glycerol and 2.5 mL of benzene. We detected 1.2 mmol of allyl alcohol product by NMR. Also we can calculate the turnover number (TON) of the rhenium catalyst to be 24 (Entry III.3.2.1). One issue with this system is to know if tin chloride was the active reducing agent or if the excess glycerol employed could have also taken part in the reaction as reducing agent. Consequently we ran the same reaction without any $SnCl_2$ and obtained only 0.74 mmol of allyl alcohol (Entry III.3.2.2); this corresponds to a 15 TON of the rhenium catalyst. We observed an increase of the TON when $SnCl_2$ was added in the reaction which demonstrated the reducing activity of tin chloride in the DODH reaction.

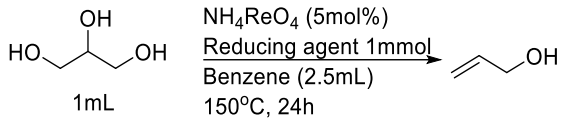


Figure III. 3.17 DODH of glycerol in biphasic media

Table III. 3.2 TON of the DODH in glycerol : benzene solvent mixture

entry	Reducing Agent	mmol of allyl alcohol	TON
III.3.2.1	$SnCl_2$	1.2	24
III.3.2.2	none	0.74	15
III.3.2.3	BnOH	0.87	17

We conducted the same reaction using benzyl alcohol as reducing agent (Entry III.2.3). By NMR we detected 0.87 mmol of allyl alcohol, which corresponds to a TON of 17. This is a slightly higher TON than without additional reducing agent, but lower than when we used $SnCl_2$ as reducing agent. In the case of benzyl alcohol we can observe its product benzaldehyde in the NMR (singlet at 10.0 pm and doublet at 8.0 ppm) and the quantity detected for this reaction was <0.1 mmol, which means clearly that benzyl alcohol was not the primary reducing agent in this DODH reaction.

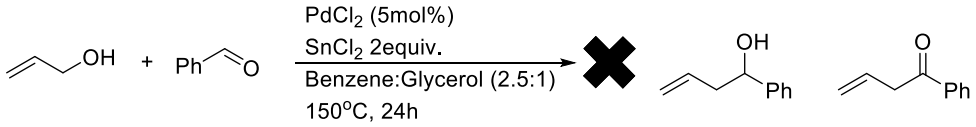


Figure III. 3.18 Allylation reaction in benzene : glycerol biphasic system

With these results on the DODH step we carried out the allylation reaction in a glycerol : benzene solvent mixture (Figure III. 3.18) and 3-octanol (Figure III. 3.19). [44]

We analyzed the reaction mixtures by NMR and did not find sign of allylation product in either one of these reactions.

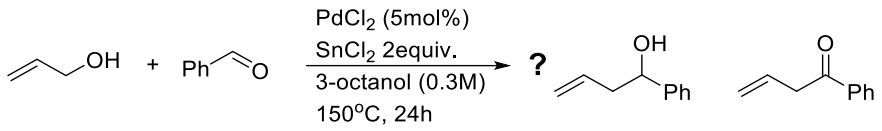


Figure III. 3.19 Allylation step in 3-octanol

Even with little evidence of allylation in 3-octanol we decided to attempt the combined tandem reaction. We first ran this reaction at 150°C for 24h (Figure III. 3.20). The reaction mixture was very complex and the GC chromatogram of it contained several small peaks. We ran the reaction with the same reaction conditions as reported for 3-octanol as reducing agent, at 170°C for only 1.5h. The ^{1}H NMR and GC the reaction mixture was much simpler we estimated the yield of allyl alcohol around 40%. There was no sign of the expected homo-allylic alcohol product of its corresponding ketone.

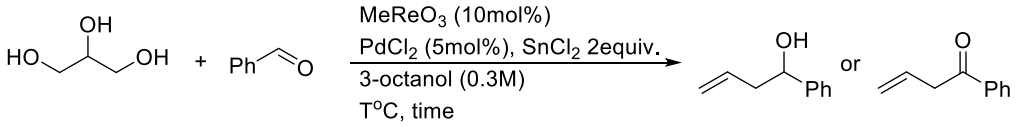


Figure III. 3.20 Tandem DODH/Allylation reaction

We found the solvent, 3-octanol, to dehydrate under these reaction conditions. Subsequently we did some solvent variation with 1-butanol and also dimethoxy ethane (DME) and a poly ethylene glycol (PEG-200) (Figure III. 3.21). 1-Butanol like 3-octanol was not an inert solvent in the reaction. The DME and PEG solvents behaved similarly and required the addition of a reducing agent. Neither benzyl alcohol nor tin chloride

were really efficient reducing agents for the DODH reaction in these solvents (<20% yield). We tried a tandem reaction with additional triphenylphosphine. In the GCMS chromatogram we found a signal at 32.6 min with the same mass as the expected homo-allylic alcohol product. We found a very large amount of solvent derived molecules as well as acetals. With all of these side products from the solvent and the need of an additional expensive and toxic reducing agent, triphenyl phosphine, this reaction was not studied further.

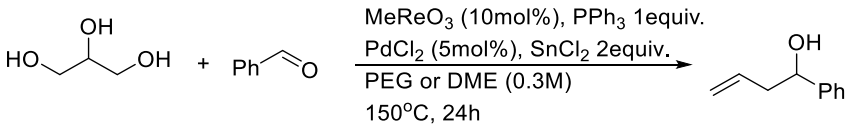


Figure III. 3.21 Tandem DODH/Allylation in PEG or DME solvent

Table III. 3.3 Summary of reaction conditions for attempted allylation and tandem reaction

Reaction	Solvent (0.3M)	Temperature (°C)	Time (h)	Reducing agent
Allylation (Figure III. 3.18, Figure III. 3.19)	Glycerol/Benzene (2.5:1)	150	24	N/A
	3-octanol	150 170	24 1.5	
DODH/Allylation Tandem (Figure III. 3.20, Figure III. 3.21)	3-octanol	150	24	solvent
	1-butanol			$PhCH_2OH$
	DME or PEG-200	150	24	$PhCH_2OH$
				$SnCl_2$
				PPh_3

In summary we studied the potential for a tandem DODH/Masuyama allylation reaction. We found the allylation step to be possible in organic solvents under the DODH reaction conditions and to dehydrogenate. On the study of the DODH step of the reaction

we found benzene : glycerol to be a suitable reaction solvent. In this solvent benzyl alcohol was found to be the primary reducing agent. We also found tin chloride to be a good reducing agent for the DODH reaction of diethyl tartrate and glycerol. The biphasic benzene : glycerol reaction solvent was found to be suitable for the allylation reaction. When the tandem was attempted in 3-octanol we obtained a cleaner reaction mixture when the reaction was run at higher temperature and a short period of time. Also we were still uncertain of the formation of homo-allylic alcohol. Variation of solvent showed the potential for DME and PEG to be suitable but it forced us to add triphenylphosphine as reducing agent in the system. For a reaction run in DME we found in the GCMS clear evidence for the formation a small amount of the desired alcohol but we also detected a large quantity of solvent derived side product. We think that this tandem reaction could have some potential to work better if either system were studied and optimized for a common solvent system.

d. Conclusions

We examined two different allylation reaction systems for a DODH/Allylation tandem reaction. The first one was based of the allylation reaction reported by the Krische group. This reaction used an iridium catalyst along with a base. The base was the major limitation for a tandem reaction as the one reported by Krische and co-worker was not compatible in the DODH reaction. We did find the DODH reaction could tolerate some specific bases, but these were not effective in the allylation step. We also studied a Masuyama allylation system. We discovered the ability of tin chloride to be reducing agent in the DODH reaction. The major limitation a tandem DODH/Masuyama allylation

was found to be the solvent and reducing agent. In fact glycerol required a polar solvent. We found benzene:glycerol to be a suitable solvent for the DODH reaction, but not for the allylation reaction. With all the alcohol (3-octanol, 1-butanol) and diether (DME, PEG-200) solvents tested we could detect large quantities of solvent derived products.

The tandem DODH/allylation reaction is promising and could be further studied. Other base free allylation reactions could be studied[136,137] but the Masuyama allylation system could work if we find a solvent that would allow the DODH reaction of glycerol and not interfere with the reaction. On this last tandem system it would also be highly desirable to have benzyl alcohol as the reducing agent to make it an atom economical reaction.

e. Experimental

i. General information: reagents and instrumentation

All reactants and catalysts were obtained commercially and used without further purification. All solvents were ACS grade and were used directly (unless otherwise described in the procedures). The Iridium catalyst was generously provided by Dr. Krische at the University of Texas Austin. ^{1}H and ^{13}C NMR spectra were collected on Varian VX300 MHz or VNMRS 400 MHz instruments. The NMR data were processed using SpinWorks[102] and ACD[103] software. GC-MS-EI analyses were performed on a Thermo-Finnigan instrument using a Stabil-wax capillary column. Gas chromatograms were collected on a Shimadzu GC-2014 equipped with an AOC 20i+s auto sampler, both with 3% SE-54 packed column, FID and thermal program 40^{o}C for 5 min; 20 deg/min to 250^{o}C; then 7 min at 250°C.

ii. Representative procedure for DODH reactions of Glycerol monostearate

Glycerol monostearate (1.00 mmol, 358 mg), NH_4ReO_4 (0.10 mmol, 27 mg), benzyl alcohol (1.00 mmol, 0.11 mL), and benzene (5 mL) were added to a thick-walled Ace glass reactor tube. Nitrogen was bubbled into the mixture for at least 60 sec before the Teflon seal was closed. The reactor was placed in an oil bath at 150°C for 24 h while stirring magnetically. After cooling to room temperature, a 100 µL aliquot of the reaction mixture was removed and added to $CDCl_3$ (0.6 mL) and 2.0 µL DMSO as internal standard for NMR analysis. This product and the others listed were characterized and quantified using ^{1}H NMR spectroscopy.

^{1}H NMR (300 MHz, $CDCl_3$, δ): 5.9 (m, 1H, CH_2=C*H*-), 5.3 (d, *J*=17.4 Hz, 1H, HC*H*=CH-), 5.2 (d, *J*=10.6 Hz, 1H, *H*CH=CH-), 4.6 (d, *J*=5.0 Hz, 2H, CH_2=CH-C*H*$_2$-), 2.3 (t, *J*=7.4 Hz, 2H, -O-C*H*$_2$-CH_2), 1.6 (m, 4H, -O-CH_2-C*H*$_2$-C*H*$_2$-), 1.3 (m, 30H, -CH_2(C*H*$_2$)$_{14}$-CH_3), 0.9 (t, *J*= 6.2 Hz, 3H, $(CH_2)_{14}$-C*H*$_3$)

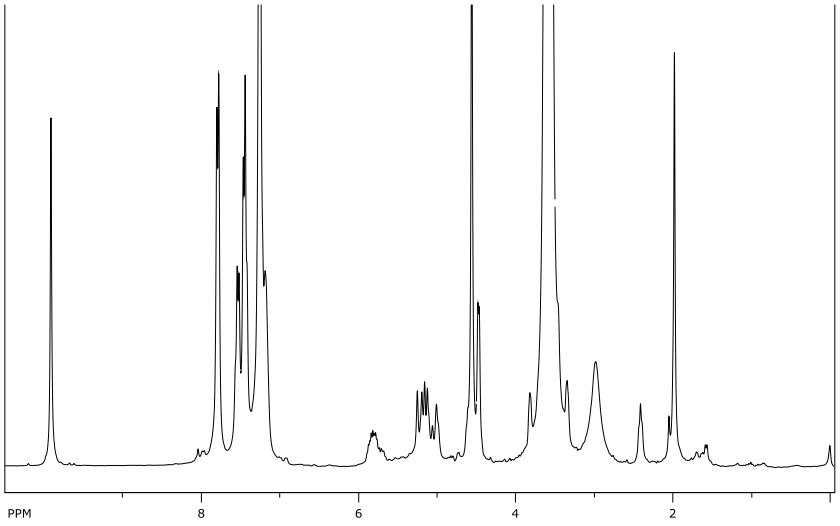
In the case of the reaction run with added base one equivalent of the base was added to the tube as the diol catalyst and solvent were placed in the reactor.

iii. Representative procedure for Krische's allylation reactions

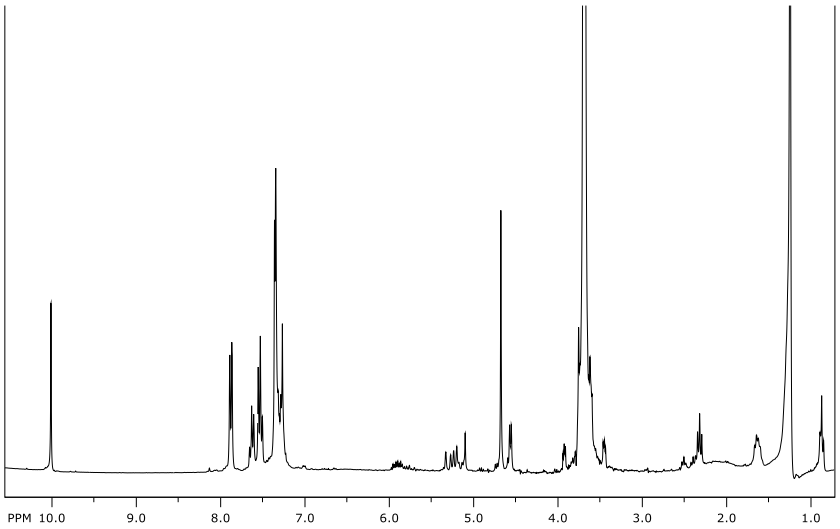
Allyl acetate (1.00 mmol, 0.11 mL), benzyl alcohol (1.00 mmol, 0.11 mL), benzylaldehyde (1.00 mmol, 0.11 mL), 4-nitrobenzoic acid (10 mol%, 17 mg), iridium complex (S)-I (5 mol%, 50 mg) and dioxane (5 mL) were added to a thick-walled Ace glass reactor tube. A N_2 flow was bubbled into the mixture for at least 60 sec before the Teflon seal was closed. The reactor was placed in an oil bath at 105°C for 24 h while

stirring magnetically. After cooling to room temperature, a 100 µL aliquot of the reaction mixture was removed and added to $CDCl_3$ (0.600 mL) and 2.0 µL DMSO as internal standard for NMR analysis. This product and the others listed were characterized and quantified using ^1H NMR spectroscopy.

Allylation on allyl acetate



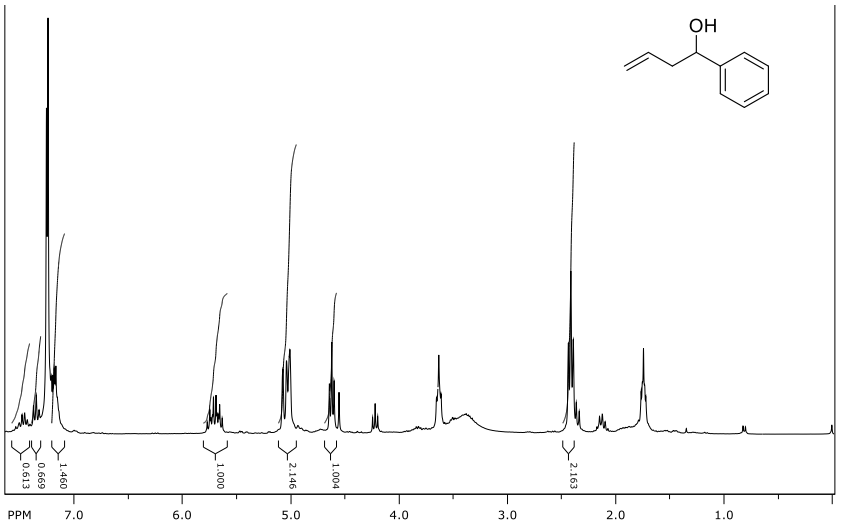
Allylation on allyl monosterate



iv. Synthesis of the benzaldehyde allylation product

Following a literature procedure a solution of benzaldehyde (1.0 equiv.) in anhydrous tetrahydrofuran was added slowly to the Grignard reagent, allyl magnesium bromide (0.1 M in THF, 2 equiv.) at 0°C.[138] The reaction mixture was warmed to room temperature and stirred for 2–12 h. Saturated NH_4Cl aqueous solution was added to the mixture and it was poured into ethyl acetate and extracted with ethyl acetate 2 times. The combined organic layers were washed with brine, dried with Na_2SO_4, filtered, and concentrated. The resulting mixture was treated with sodium bisulfate solution (0.4g in 1 mL of water and 0.11 mL of ethanol) extracted and filtered in order to remove any left over benzaldehyde.[139–141] The residue was purified by silica gel column chromatography (hexane/ethyl acetate). GC analysis (3% SE-54 packed column, thermal program 40°C for 5 min; 20 deg/min to 250°C; then 7 min at 250°C.) of the product showed a retention time of 11.0 min.

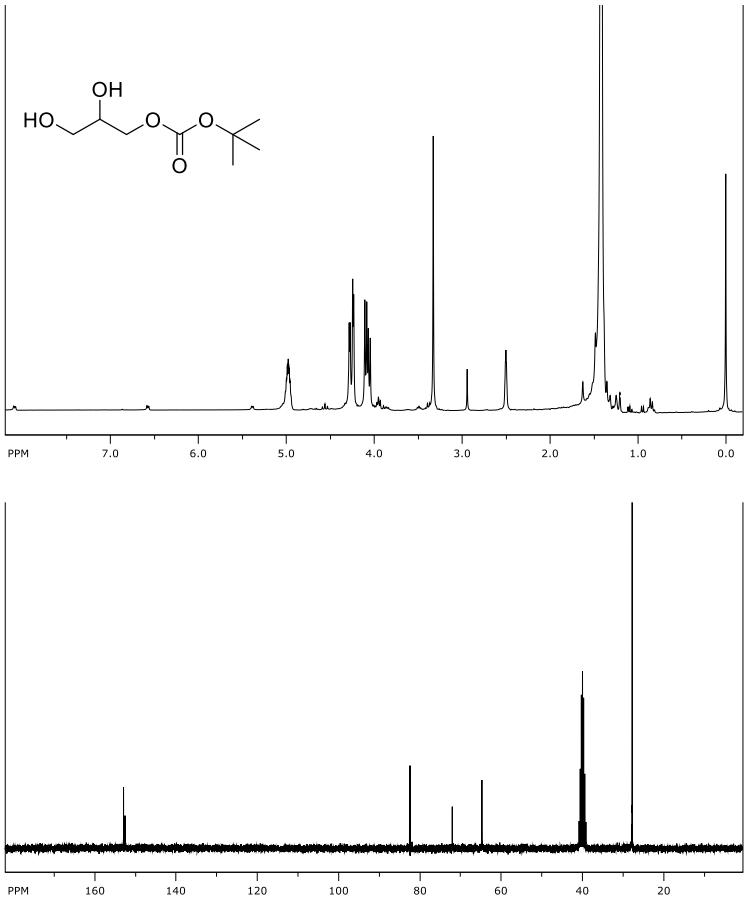
^{1}H NMR (300 MHz, $CDCl_3$): 2.4 (t, J = 6.6 Hz, 2H, CH_2), 4.6 (t, J = 6.6 Hz, 1H, C*H*OH), 5.0 (m, 2H, =CH_2), 5.7 (m, 1H, =C*H*), 7.3-7.7 (m, 5H, C_6H_5);



v. Synthesis of the 1-BOC derivative of glycerol for DODH/ Krische's Allylation

The synthesis of the BOC derivative of glycerol was carried out on a 5 mmol scale using DMAP (10 mol%) and di-tert butyl carbonate (2 equiv.) in a solvent mixture of THF/CH_2Cl_2 (1:2 ratio) at room temperature. After stirring the reaction mixture overnight an equal volume of a saturated aqueous solution of bicarbonate was added at 0°C. The product was then extracted three times with 15 mL of ether and the solvent was removed under reduced pressure. The resulting boc-glycerol is a viscous colorless liquid; 0.79 g, 83% yield.

^{1}H NMR (300MHz, d^6-DMSO): 1.4 (s, 9H, CH_3), 4.0 (dd, J = 6.6 Hz, 2H, CH_2OH), 4.3 (m, 2H, CH_2O), 4.9 (m, 1H, C*H*OH); ^{13}C NMR (300MHz, d^6-DMSO): 154, 72, 65, 28.



vi. Representative procedure for DODH reactions of BOC derivative of Glycerol

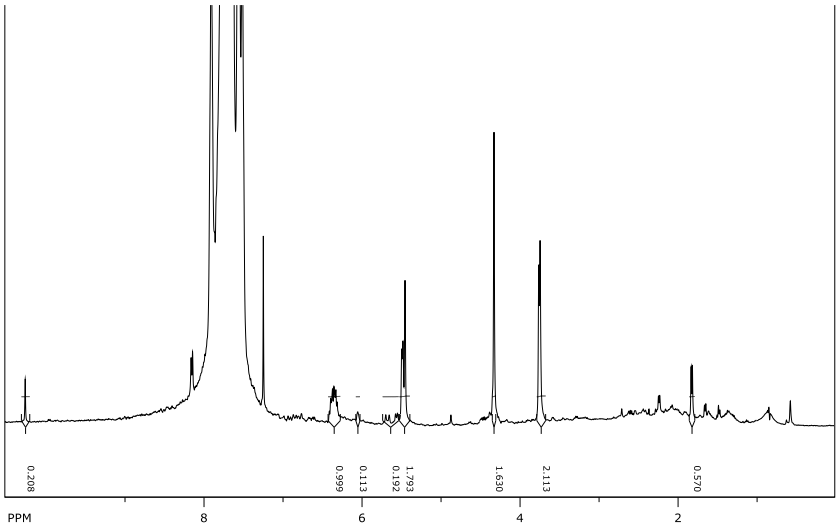
1-Boc derivative of glycerol (1.00 mmol, 192 mg), NH_4ReO_4 (0.10 mmol, 27 mg), benzyl alcohol (1.00 mmol, 0.11 mL), and benzene (5 mL) were added to a thick-walled Ace glass reactor tube. A N_2 stream was bubbled into the mixture for at least 60 sec before the Teflon seal was closed. The reactor was placed in an oil bath at 150°C for 24 h while stirring magnetically. After cooling to room temperature, a 100 µL aliquot of the reaction mixture was removed and added to $CDCl_3$ (0.600 mL) and 2.0 µL DMSO as internal standard for NMR analysis.

vii. Procedure for Masuyama's allylation reaction

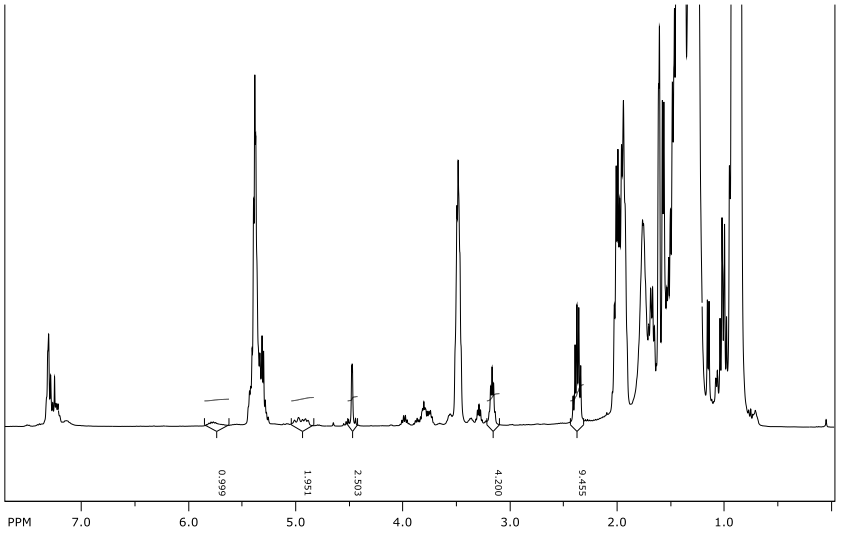
- Benzene as solvent

Allyl alcohol (1.00 mmol, 0.07 mL), benzaldehyde (0.50 mmol, 0.05 mL), tin (II) chloride (1.00 mmol, 190 mg), palladium bis-chloride (0.05 mmol, 9 mg) and 2.5 mL benzene or 3.3 mL 3-octanol were added to a thick-walled Ace glass reactor tube. A N_2 stream was bubbled into the mixture for at least 60 sec before the Teflon seal was closed. The reactor was placed in an oil bath at 150^{o}C for 20 h while stirring magnetically. After cooling to room temperature, a 100 µL aliquot of the reaction mixture was removed and added to $CDCl_3$ (0.6 mL) and 2.0 µL DMSO as internal standard for NMR analysis. This product and the others listed were characterized and quantified using ^{1}H NMR spectroscopy.

In Benzene

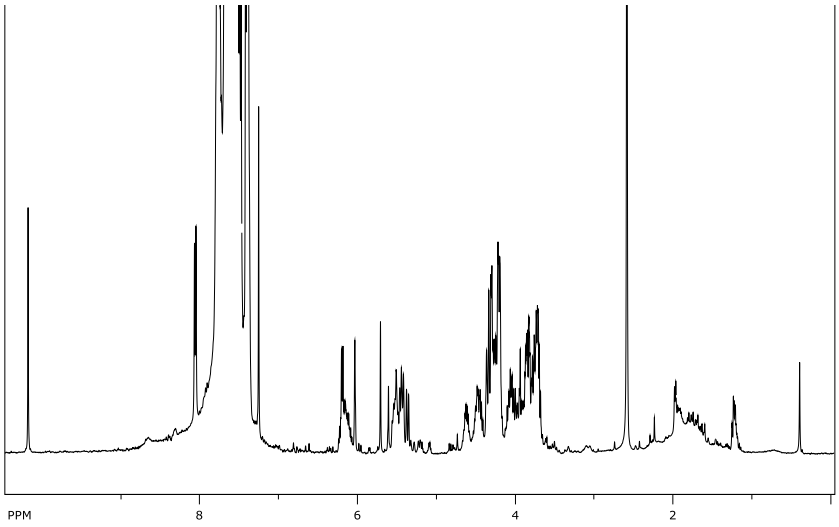


In 3-octanol



- Benzene : Glycerol as solvent

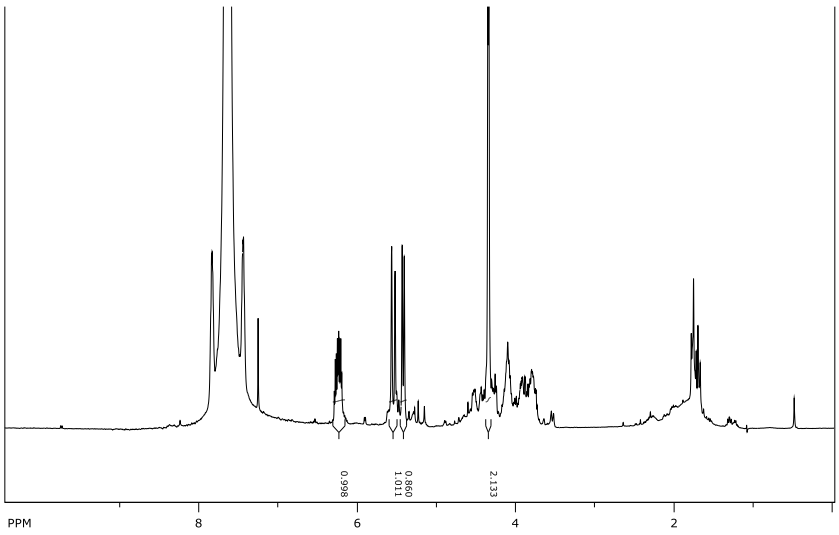
Glycerol (1.0 mL), NH_4ReO_4 (0.05 mmol, 13.4 mg), benzaldehyhde (0.50 mmol, 0.05 mL), tin (II) chloride (1.00 mmol, 190 mg), and benzene (2.5 mL) were added to a thick-walled Ace glass reactor tube. Nitrogen was bubbled into the mixture for at least 60 sec before the Teflon seal was closed. The reactor was placed in an oil bath at 150ºC for 24 h while stirring magnetically. After cooling to room temperature, a 100 µL aliquot of the benzene phase of the reaction mixture was removed and added to $CDCl_3$ (0.6 mL) and 2.0 µL DMF as internal standard for NMR analysis.



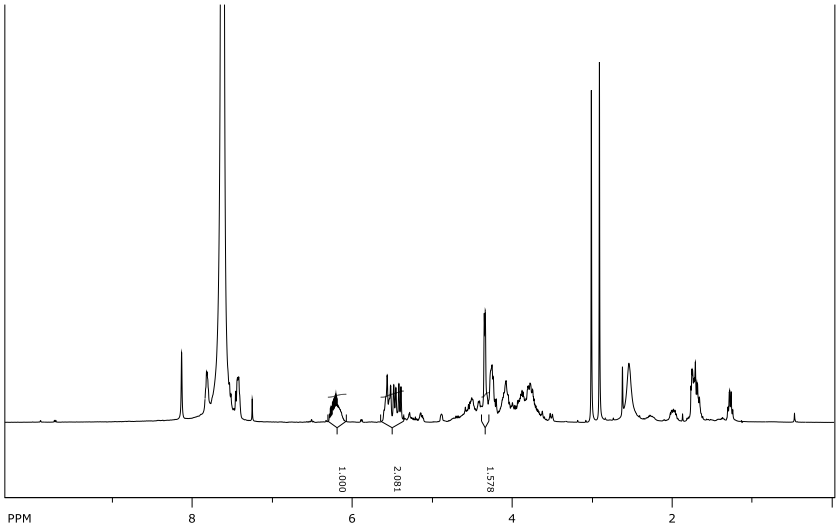
viii. Representative procedure for DODH reactions of Glycerol in Benzene : Glycerol

Glycerol (1.0 mL), NH_4ReO_4 (0.05 mmol, 13 mg), reducing agent {benzyl alcohol (1.00 mmol, 0.11 mL), tin (II) chloride (189 mg), or none}, and benzene (2.5 mL) were added to a thick-walled Ace glass reactor tube. Nitrogen was bubbled into the mixture for at least 60 sec before the Teflon seal was closed. The reactor was placed in an oil bath at 150^oC for 24 h while stirring magnetically. After cooling to room temperature, a 100 µL aliquot of the benzene phase of the reaction mixture was removed and added to $CDCl_3$ (0.6 mL) and 2 µL DMF as internal standard for NMR analysis. A 0.5 mL aliquot of the benzene phase of the reaction mixture was removed and filtered through a little silica plug to remove left over glycerol and particles before being submitted to gas chromatography analysis.

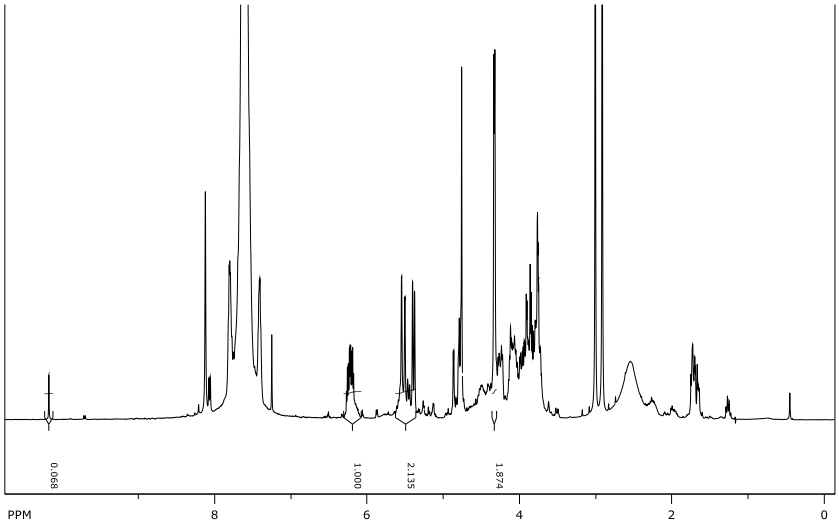
No reducing agent



$SnCl_2$ reducing agent



Benzyl alcohol reducing agent

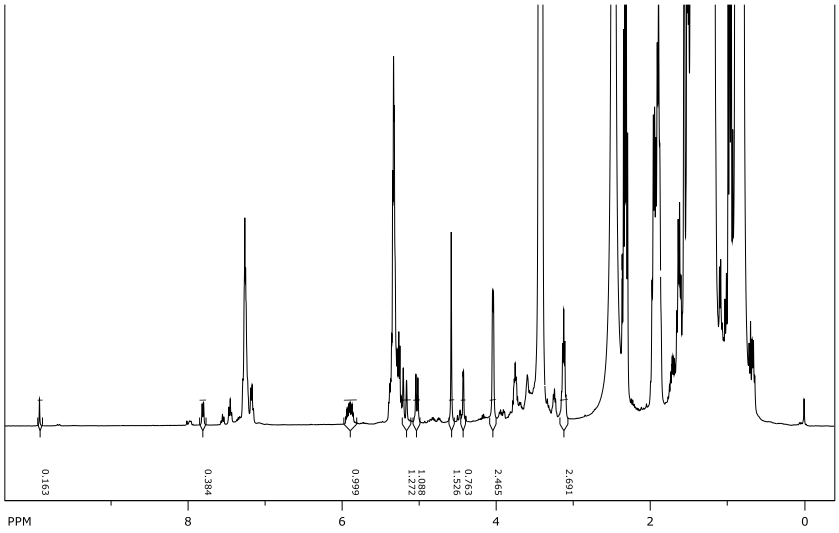


ix. Representative procedure for DODH/ Masuyama's allylation tandem reaction

- 3-octanol as solvent

Glycerol (92 mg, 1.00 mmol), $MeReO_3$ (0.10 mmol, 25 mg), and 3-octanol (3.3 mL) were added to a thick-walled Ace glass reactor tube. Nitrogen was bubbled into the mixture for at least 60 sec before the Teflon seal was closed. The reactor was placed in an oil bath at 150°C for 24 h or 170°C for 1.5h while stirring magnetically. After cooling to room temperature, a 100 µL aliquot of the benzene phase of the reaction mixture was removed and added to $CDCl_3$ (0.6 mL) and 2.0 µL DMF as internal standard for NMR analysis. A 0.5 mL aliquot of the benzene phase of the reaction mixture was removed and filtered through a silica plug to remove left over glycerol and particles before to be submitted to gas chromatography analysis.

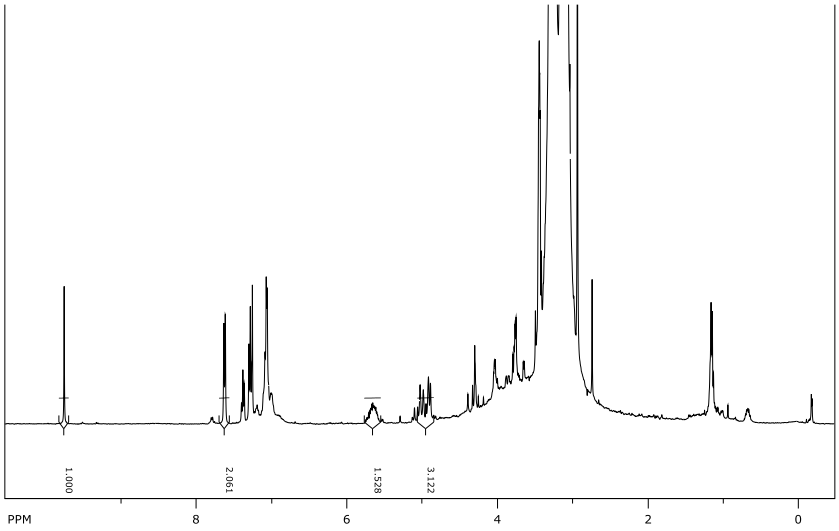
At 170°C for 1.5 h



- DME or PEG as solvent

Glycerol (92 mg, 1.0 mmol), NH_4ReO_4 (0.10 mmol, 27 mg), reducing agent {1.00 mmol; benzyl alcohol (0.11 mL) or tin (II) chloride (189 mg) or triphenylphosphine (262 mg)}, and solvent (2.5 mL; benzene or 1-butanol or DME or PEG-200) were added to a thick-walled Ace glass reactor tube. Nitrogen was bubbled into the mixture for at least 60 sec before the Teflon seal was closed. The reactor was placed in an oil bath at 150°C for 24 h while stirring magnetically. After cooling to room temperature, a 100 µL aliquot of the benzene phase of the reaction mixture was removed and added to $CDCl_3$ (0.6 mL) and 2.0 µL DMF as internal standard for NMR analysis. A 0.5 mL aliquot of the benzene phase of the reaction mixture was collected and filtered on a little silica plug to remove left over glycerol and particles before to be submitted to gas chromatography analysis.

In DME



4. DODH / "Base-free catalytic" Wittig Tandem Reaction

a. Introduction

First discovered in 1954 the Wittig reaction is widely used in organic synthesis.[142] In a Wittig reaction the pre-formed ylid (equation a, Figure III. 4.1) serves as the nucleophile and attacks the aldehyde (equation b, Figure III. 4.1).[143] More recently several studies have attempted to make the Wittig reaction catalytic in phosphine.

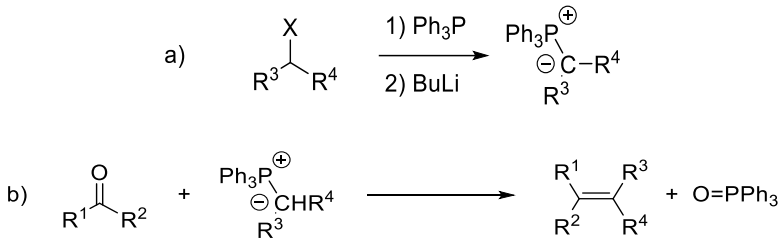


Figure III. 4.1 Formation of the phosphorus ylide and Wittig general scheme

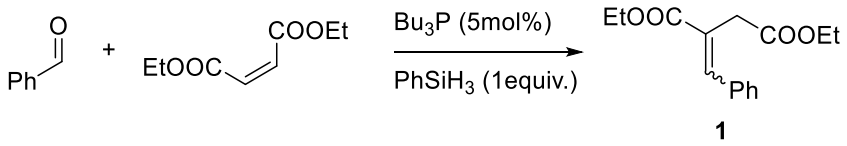


Figure III. 4.2 Werner's base-free catalytic Wittig reaction

A report published in May 2015 caught our attention. In this letter, T. Werner's group describes a "base-free catalytic Wittig reaction".[144] Their system condenses a benzylic aldehyde with diethyl maleate using a catalytic quantity of phosphine and stoichiometric quantity of silane (Figure III. 4.2). Werner et al. speculated on the possible catalytic cycle of this reaction: Phosphine adds to the alkene via a Michael addition, this intermediate can form the ylid by a hydrogen shift. The ylid can then react with the aldehyde in a Wittig transformation releasing the product and phosphine oxide. The silane can then

reduce the phosphine oxide back to phosphine (Figure III. 4.3). The other interesting feature of the reaction is the favored E selectivity in the product.

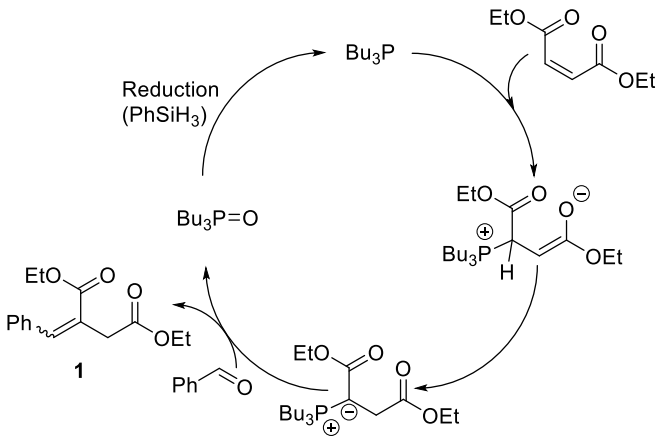


Figure III. 4.3 Proposed mechanism for reaction

Although it is debatable whether this reaction can be called a Wittig reaction or not, we could see in this system the potential for tandemizing it with our DODH system. In fact, in 2012, we conducted a study of benzyl alcohol as DODH reducing agent.[46] One of the diols used in this study was diethyl tartrate (and provided a very high yield in diethyl fumarate (99%). The reaction conditions for our DODH system, benzene, 150°C, 24h are really similar those reported by Werner for his reaction. We therefore planned to develop a DODH/Werner-Wittig tandem reaction.

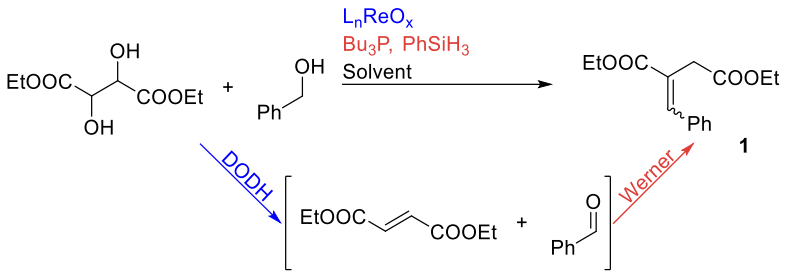


Figure III. 4.4 DODH/ "base free catalytic" Wittig tandem reaction concept

b. Study of the tandem system

Because this tandem system would require mixing several reagents and since the compatibility of these was uncertain, we took a step-by-step approach. Our first experiment was conducted at the concentration and temperature of the DODH reaction. It consisted of taking a portion of the DODH reaction mixture (99% yield of diethyl fumarate and 85% in benzaldehyde) without any treatment and adding to it the phosphine reagent for Werner's reaction in stoichiometric quantity (Figure III. 4.5). This reaction was a success and gave 84% yield in the desired product **1** ,Figure III. 4.5, and 99% conversion of the benzaldehyde present in the DODH reaction mixture. (Conversion determined by NMR)

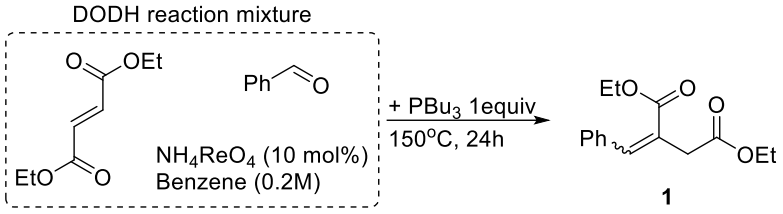


Figure III. 4.5 Compatibility test of Bu_3P with DODH mixture

We concluded that the DODH products and left over catalyst didn't interfere with the Werner-Wittig reaction. Our follow up experiment was to run the tandem reaction starting from diethyl tartrate using the phosphine reagent stoichiometrically along with the DODH reactants and catalyst. This reaction produced no coupling product **1**, Figure III. 4.6, no benzaldehyde, and a very small amount of the fumarate product. From the ^1H NMR spectrum we concluded that the presence of a large quantity of PBu_3 had promoted trans-esterification of the tartrate starting material and the benzyl alcohol.

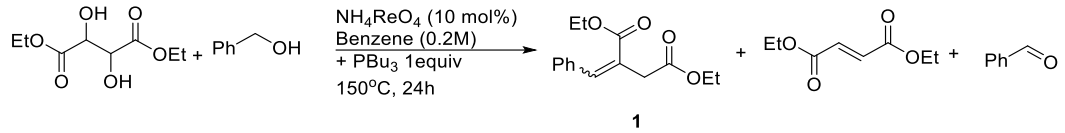


Figure III. 4.6 Tandem reaction using Bu_3P as stoichiometric reagent

Since the phosphine should be used only in a catalytic amount when using silane stoichiometrically, we decided to continue the study and ran an experiment using a portion of a DODH product mixture as in Figure III. 4.5, but this time we used only 5 mol% of the phosphine and one equivalent of phenyl silane. This reaction worked less efficiently than the previous one, which used a stoichiometric amount of tributyl phosphine, giving a 37% yield of the tandem product **1**. This last result shows some compatibility of the silane to the DODH products and catalyst. As previously, we ran the tandem reaction starting from the diol and the alcohol. NMR analysis of the reaction mixture showed no tandem product **1**, but indicated an 84% yield of the fumarate DODH product along with a 57% yield of benzaldehyde (Figure III. 4.6). The DODH reaction then was not much affected by the addition of PBu_3. Although this reagent did not react to form any tandem product **1**. This means that in the DODH reaction this reagent was used in a side reaction making it unavailable for the second reaction. We can speculate that this reagent could be a reducing agent during the DODH reaction. This could explain the lower yield of benzaldehyde compared to the yield of fumarate as well as the unavailability of these for the tandem reaction. We noticed also a small amount of free ethanol in the ^1H NMR spectrum, which showed that some trans-esterification reaction may have taken place as well.

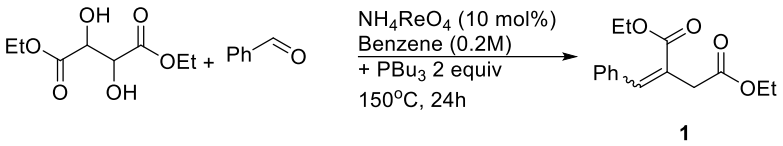


Figure III. 4.7 Tandem DODH/ catalytic Wittig

In order to understand where the incompatibilities are in this system we tried the tandem reaction using PBu_3 as both reducing agent for the DODH and reagent for the Werner-Wittig reaction, Figure III. 4.7. In this experiment an equivalent of benzaldehyde was added for the second step. This reaction was successful. We were able to have both the DODH and stoichiometric Werner-Wittig work in a single pot giving a high yield of 90% of **1**. This proves the viability of the concept, but the use of a stoichiometric quantity of phosphine for each of the steps is a drawback as this is an expensive and toxic reagent.

We tested then if phenyl silane could be used as a regenerative reagent for the phosphine in both the DODH and Werner-Wittig reactions. We attempted to use catalytic phosphine in the DODH/ Werner-Wittig reaction tandem reaction. We ran this reaction with PBu_3 (10 mol%), 2.2 equivalents of the silane and an equivalent of benzaldehyde (Figure III. 4.8). The ^1H NMR of the reaction mixture did not show any desired tandem product, **1**. We did observe a large quantity of the DODH product (>80% yield). This demonstrated that DODH reaction occurred in the presence of the phosphine and silane. In this reaction we noticed an unusual pressure release when opening the reactor. Suspecting that hydrogen was being produced by the silane reaction with H_2O form in the DODH reaction we ran the DODH/Werner-Wittig tandem reaction with added of activated molecular sieves 4Å powder. In this reaction again we could detect a large quantity of DODH product (diethyl fumarate) but no Wittig product **1**. We can then

conclude that silane is reacting with something else in the reaction. In consequence the tandem reaction using a catalytic amount of phosphine reagent would not be possible until we find a way to efficiently remove this side reaction involving the silane.

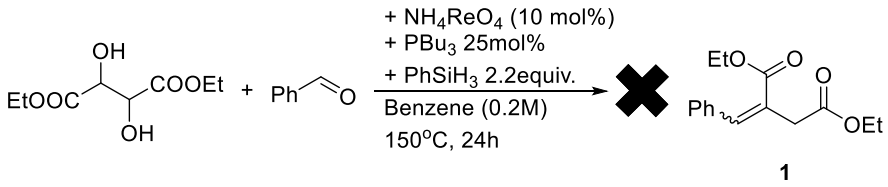


Figure III. 4.8 Tandem DODH/Werner-Wittig and Werner-Wittig reaction using catalytic phosphine

c. Conclusions

In summary, we were able to obtain a high yielding tandem DODH / "base free" Wittig reaction using phosphine as stoichiometric reagent. This is the first efficient and selective DODH / C-C bond formation tandem reaction not involving a Diels-Alder cycloaddition and proves the actual concept of this tandem system. We have discovered the compatibility of the oxo-rhenium DODH catalyst with tributylphosphine. The use of the silane looks to be incompatible with the DODH reaction. With the limited scope of this tandem reaction and the use of stoichiometric phosphine the tandem reaction was not studied further.

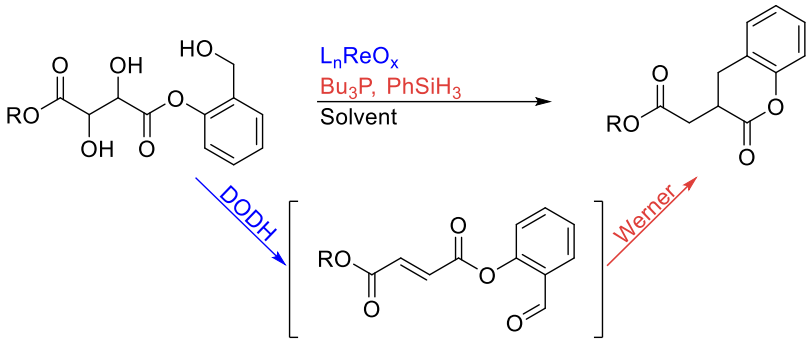


Figure III. 4.9 Potential intramolecular DODH / "base free" Wittig

This DODH / "base free" Wittig could have some applications in the synthesis of succinate derivatives. Succinates are be used as polymer building block and for drugs synthesis. This system could be made more attractive by finding the right reagents to make it catalytic in phosphine. In addition this system would be greener if the benzaldehyde used in the Wittig step was formed in the DODH reaction by using benzyl alcohol as reducing agent. One strategy could be to have a benzyl alcohol unit on ester of the tartrate derivative making it more reactive as a reducing agent in the DODH reaction (Figure III. 4.9). This will then make the Wittig reaction intramolecular. Variations in the diol and/or in the starting alcohol (reducing agent) could also be considered to open the tandem reaction to a more applications (Figure III. 4.10).

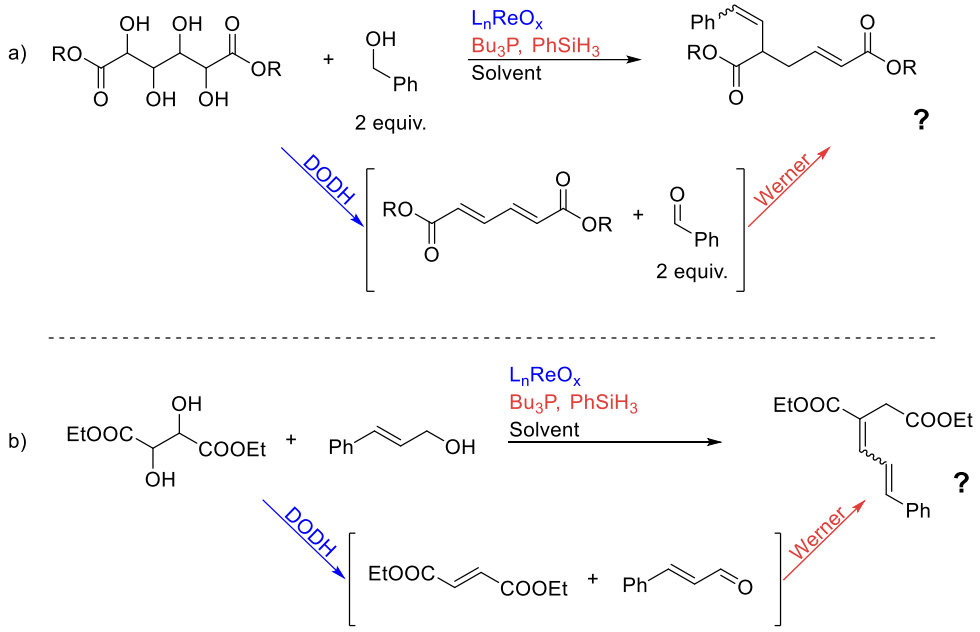


Figure III. 4.10 Variations in the diol and/or alcohol reducing agent

d. Experimental

i. General information: reagents and instruments

All reactants and catalysts were obtained commercially and used without further purification. All solvents were ACS grade and were used directly (unless otherwise described in the procedures). ^{1}H and ^{13}C NMR spectra were collected on Varian VX300 MHz or VNMRS 400 MHz instruments. The NMR data were processed using SpinWorks[102] and ACD[103] software.

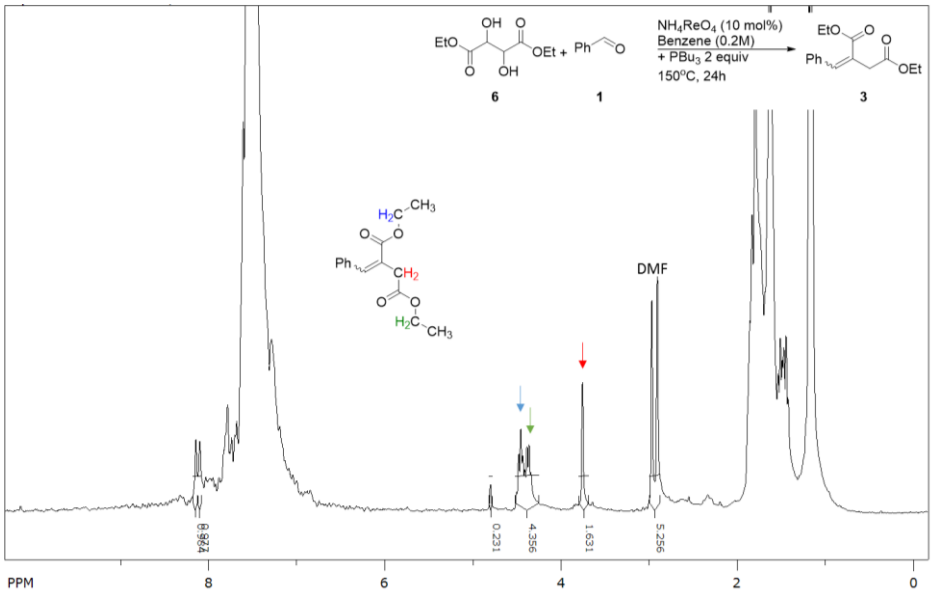
ii. Procedure for DODH / catalytic Wittig reaction from DODH reaction mixture

Diethyl tartrate (2.00 mmol, 0.34 mL), NH_4ReO_4 (0.20 mmol, 54 mg), benzyl alcohol (1.00 mmol, 0.20 mL) and benzene (10 mL) were added to a thick-walled Ace glass

reactor tube. Nitrogen was bubbled into the mixture for at least 60 sec before the Teflon seal was closed. The reactor was placed in an oil bath at 150^{o}C for 24 h while stirring magnetically. After cooling to room temperature, 5 mL of the reaction mixture was mixed with tributyl phosphine (1.00 mmol, 0.25 mL). A N_2 flow was bubbled into the mixture for at least 60 sec before the Teflon seal was closed. The reactor was placed again in an oil bath at 150^{o}C for 24 h while stirring magnetically. After cooling to room temperature, 100 µL of the reaction mixture was removed and added to $CDCl_3$ (0.5 mL) and 2.0 µL DMSO as internal standard for ^{1}H NMR analysis.

iii. Procedure for DODH / catalytic Wittig reaction using PBu_3 as reducing agent and stoichiometric Wittig reagent (Figure III. 4.6 and Figure III. 4.7)

Diethyl tartrate (1.00 mmol, 0.17 mL), NH_4ReO_4 (0.10 mmol, 27 mg), benzaldehyde (1.00 mmol, 0.10 mL), tributyl phosphine (1.00 mmol, 0.20 mL or 2.00 mmol, 0.49 mL) and benzene (5 mL) were added to a thick-walled Ace glass reactor tube. A N_2 flow was bubbled into the mixture for at least 60 sec before the Teflon seal was closed. The reactor was placed in an oil bath at 150^{o}C for 24 h while stirring magnetically. After cooling to room temperature, a 100 µL aliquot of the reaction mixture was removed and added to $CDCl_3$ (0.5 mL) and 2.0 µL DMSO as internal standard for ^{1}H NMR analysis.



NMR spectrum of the reaction on Figure III. 4.6

iv. Procedure for DODH / catalytic Wittig reaction using PBu_3 as a catalyst with diphenyl silane

Diethyl tartrate (1.00 mmol, 0.17 mL), NH_4ReO_4 (0.10 mmol, 27 mg), benzaldehyde (1.00 mmol, 0.10 mL), tributyl phosphine (0.10 mmol, 24 µL), diphenyl silane (2.5mmol, 0.46 mL) and benzene (5 mL) were added to a thick-walled Ace glass reactor tube. Nitrogen was bubbled into the mixture for at least 60 sec before the Teflon seal was closed. The reactor was placed in an oil bath at 150°C for 24 h while stirring magnetically. After cooling to room temperature, a 100 µL aliquot of the reaction mixture was removed and added to $CDCl_3$ (0.5 mL) and 2.0 µL DMSO as internal standard for ^1H NMR analysis.

5. DODH/Heck Tandem Reactions

a. Introduction and Background

i. The Heck reaction

The Heck reaction is the coupling of an alkene with an unsaturated halide using a combination of base and palladium catalyst (Figure III. 5.1). First reported in 1971 by Mizoroki T. the reaction was extensively studied and developed by R. Heck, E. Negishi and A. Suzuki.[145] This reaction was significant for two reasons: 1) it was the first reported C-C bond forming transformation following a Pd(0)/Pd(II) catalytic system; and 2) it is a formal substitution on a planar sp^2 carbon. The catalytic cycle of the palladium in the Heck reaction was describe starting with palladium (0) (Figure III. 5.2). The aryl halide adds to the palladium by an oxidative addition. This step would be follow by the insertion of the terminal alkene between the metal center and the aryl group. The product is then released to leave a palladium (II) hydride specie. The base would then reduce the metal center to regenerate palladium (0).

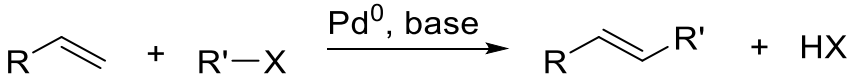


Figure III. 5.1 General Heck reaction

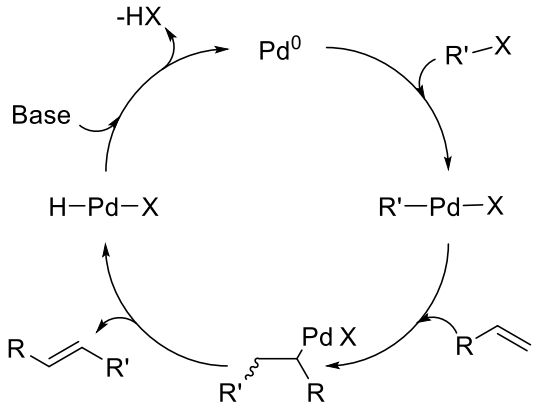


Figure III. 5.2 Heck catalytic cycle

ii. DODH/Heck Tandem Concept

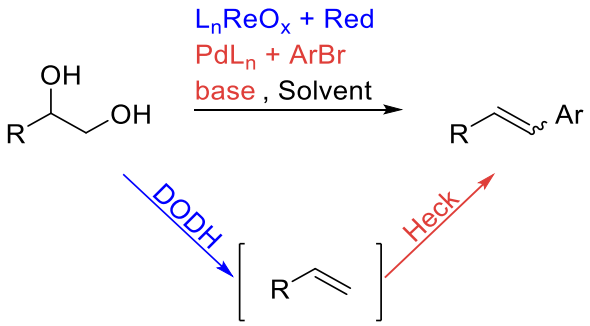


Figure III. 5.3 DODH/Heck tandem concept

In this tandem system we envisioned the formation of a terminal alkene by the deoxydehydration of its corresponding diol. Then in the presence of base, palladium catalyst and aryl bromide this alkene would be subsequently transformed in a Heck reaction (Figure III. 5.3). This tandem system does not utilize the side product of the DODH reaction (from the reducing agent) in the second reaction. If the tandem process works, we could use para substituted benzyl alcohols as reducing agent for the DODH reaction and as aryl halide for the Heck reaction (Figure III. 5.4). The DODH/Heck tandem reaction would provide alkenes products which could be used as a building block

for drug synthesis. We will focus on using benzyl alcohol as a reducing agent in the DODH reaction. This tandem system is an important challenge due to the required basic conditions for the reaction. In this section we will describe how we tried first to use a pyridine-based rhenium oxo complex to serve as the DODH catalyst and to provide the base in the Heck reaction. We studied first each reaction individually to evaluate the potential for a combined tandem system. The requirement for a base in the Heck coupling step was assessed by choosing a base-compatible DODH catalyst and the major limitation was found to be the solvent for the reaction.

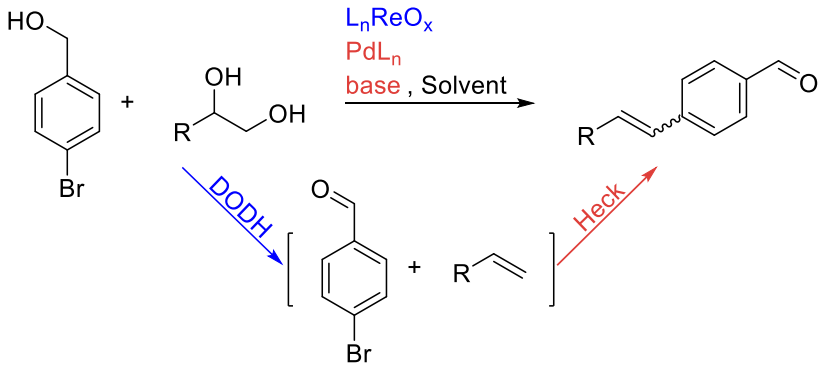


Figure III. 5.4 DODH/Heck tandem reaction with the reducing agent and aryl halide provided by one reagent

b. Study of the DODH step

In order to obtain a functioning DODH/Heck tandem system we needed to adjust and choose the DODH reaction conditions carefully. In most reported DODH reaction the rhenium oxo complex used trend to be slightly acidic but the heck reaction required added base. In his dissertation, J. Michael McClain reported a study of the activity of $ReO_2(py)_4^{+}X^{-}$ for the DODH reaction.[146] He found this catalyst to have similar activity to the previously reported rhenium oxo complexes using sulfite as reducing agent for the

DODH conversion of styrene glycol and 1,2-octane diol, but with benzyl alcohol as reductant a much better result (80% yield in 1-octene) was obtained than previously reported with ammonium perrhenate (50%). He also found this catalyst to be more reactive when hexaflorophosphate was its counter ion. McClain also investigated the mechanism of the DODH reaction using this $ReO_2(py)_4^{+-}PF_6$ catalyst, including the influence of additives on the reaction rate, finding that the addition of 1 to 5 equivalent of pyridine (with respect to the amount of rhenium complex) increased the rate of reaction. This was the first report of a DODH reaction under basic conditions.

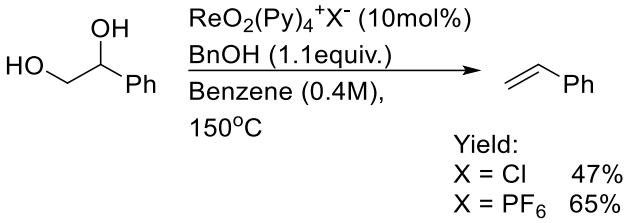


Figure III. 5.5 DODH reaction system using $ReO_2(Py)_4^{+-}X$ as catalyst

We started our experimental study by repeating the DODH reaction on styrene glycol at higher concentration (0.4 M) as it would be required in the Heck system. We tested both the chloride and hexafluorophosphate counter ion catalysts (Figure III. 5.5). We found the latter to be more effective with a 65% yield. We then ran the same reaction with added base and we found that use of 1 to 5 equivalents (with respect to the diol) of either potassium bicarbonate or pyridine did not lower significantly the yields. Since several reported Heck systems required more polar media, we also tested the DODH reaction in dimethylformamide (DMF) and dimethyl acetamide (DMA). These solvents greatly affected the yield (<10%) and the conversion (>90%) of the reaction. Therefore,

a tandem DODH / Heck system would have a very low chance of providing high yields if run in such solvents.

c. Study of the Heck step

After some searches for reported base-free Heck systems, we found a report from Bhargava'group which described the Heck coupling of 2-bromopyridine with styrene without added base using bis(acetonitrile)dichloro palladium ($Pd(CH_3CN)_2Cl_2$) as catalyst.[147] We believe the base required in the Heck coupling reaction here is the substituted pyridine substrate ($PyrH^+$ pKa=5). As we envisioned use of a pyridine-rhenium complex for the DODH reaction step, the use of pyridine in the Heck step looked like a reasonable choice. In their report Bhargava' group used more polar solvents such as dimethylformamide (DMF) and dimethyacetamide (DMA), but with toluene as solvent they did not detect any Heck coupling product.

We were concerned about the Bhargava system for two reasons: 1) the stoichiometry of alkene to halide (2:1); and 2) the required polar solvent. The first point means that the alkene should have been formed in excess to have only part of it to be transformed in the Heck reaction. Therefore, we decided to test Bhargava's Heck system with a 1 to 1 ratio of alkene to halide in order to determine if the reaction could still work and if there was any decrease in the yield.

We ran a few experiments under Bhargava's reaction conditions in order to determine the potential Heck reaction conditions that could be appropriate for a DODH / Heck tandem system. We started by testing the effectiveness of a 1:1 alkene:organic halide ratio in the Heck reaction (Figure III. 5.6). Under the previously reported conditions a very

low conversion of styrene (~10% conversion) was observed (7% yield). Thus, we found that this reaction was not efficient with only a stoichiometric quantity of alkene.

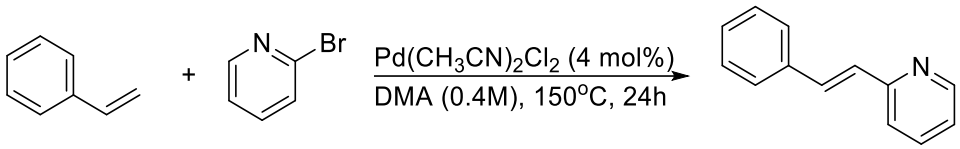


Figure III. 5.6 Test of stoichiometric on Heck coupling

We also tested the efficacy of the system when an equivalent of pyridine and an equivalent of bromobenzene were used instead of the 2-bromopyridine (Figure III. 5.7). This worked in a similar way as the reaction using 2-bromopyridine; we could detect a limited amount of stilbene (5%) and a large quantity of unreacted styrene. We also tested this reaction in benzene and could not detect any stilbene.

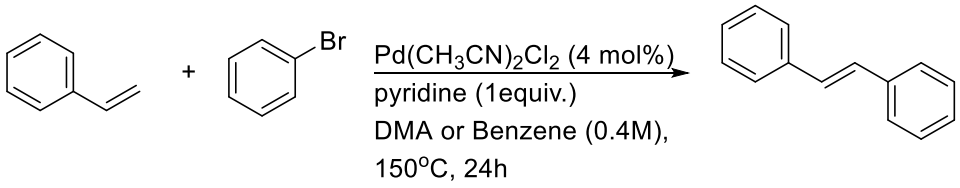


Figure III. 5.7 Test of the Heck reaction using pyridine as additive

The variations of reagents stoichiometry and solvent affected the Heck reaction and provided low yield in alkene product. With these results on the Heck side the DODH/Heck tandem reaction was not attempted.

d. Conclusion

After investigating both reaction sides of this tandem system we found significant limitations that prevented the achievement of a DODH/Heck tandem reaction. Although the addition of 1 to 5 equivalents of a base did not appreciably affect the efficiency of the DODH reaction, the DODH reaction was found to be incompatible with DMF or DMA as solvent. On the other side we found the Heck reaction to proceed with either bromopyridine or the bromobenzene along with 1 equivalent of pyridine in the system but providing very low yield. This Heck coupling system, however, was ineffective in a non-polar organic solvent such as benzene.

We can then conclude that the solvent is a limiting factor for this tandem system to work. Some more study of polar solvent DODH systems such as DMA or DMF would be required to obtain a compatible system. If such a solvent were found, it would need to be tested on the Heck reaction to evaluate if the tandem DODH-Heck system could work. Another limiting factor could be the reaction stoichiometry which means that the stilbene might be required to be in excess to increase substantially the yield of the Heck reaction.

e. Experimental

i. General information: reagents and instruments.

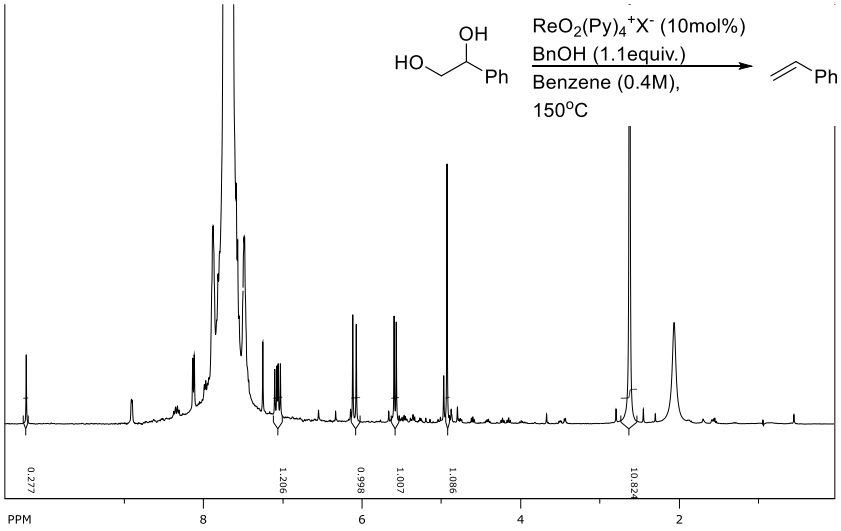
Most reactants were obtained commercially and used without further purification. The rhenium catalysts were synthesized according to literature reports.[148] Styrene was distilled under vacuum (10 mm Hg) and stored at -80 ^{o}C. All solvents were ACS grade and were used directly (unless otherwise described in the procedures). ^{1}H and ^{13}C NMR

spectra were collected on Varian VX300 MHz or VNMRS 400 MHz instruments. The NMR data were processed using SpinWorks[102] and ACD[103] software.

ii. Representative procedure for DODH reactions.

Styrene glycol (1.00 mmol, 138 mg), $ReO_2(py)_4^{+-}PF_6$ (0.10 mmol, 68 mg), benzyl alcohol (1.00 mmol, 0.11 mL), and benzene (2.5 mL) were added to a thick-walled Ace glass reactor tube. A N_2 flow was bubbled into the mixture for at least 60 sec before the Teflon seal was closed. The reactor was placed in an oil bath at 150 ^oC for 24 h while stirring magnetically. After cooling to room temperature, a 100 µL aliquot of the reaction mixture was removed and added to $CDCl_3$ (0.5 mL) and 2.0 µL DMSO as internal standard for NMR analysis. All olefinic products from the DODH reactions have been previously reported and were identified by comparison of their NMR spectra with authentic samples or published data.

DODH Reaction of styrene glycol with $ReO_2(py)_4^{+-}PF_6$ as catalyst



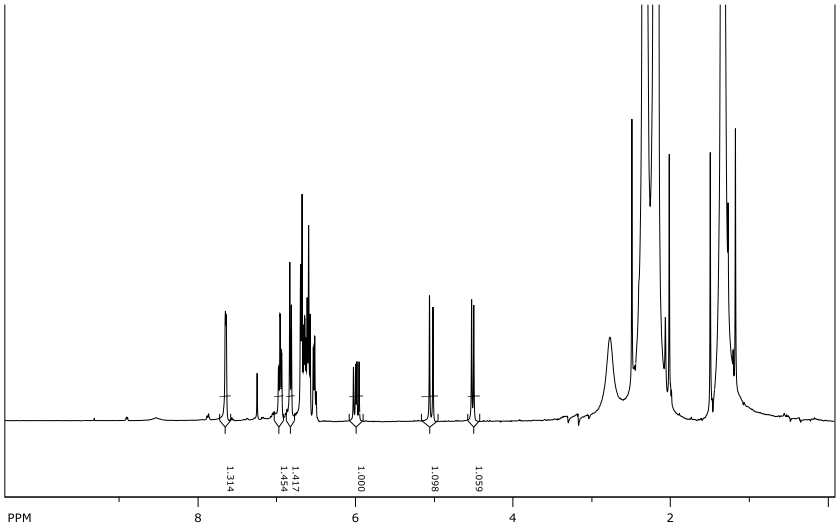
iii. Representative procedure for Heck reactions.

Styrene (1.00 mmol, 0.11 mL), $PdCl_2(CH_3CN)_2$ (0.04 mmol, 10 mg), 2-bromo pyridine (1.10 mmol, 0.09 mL), and DMA (2.5 mL) were added to a thick-walled Ace glass reactor tube. Nitrogen gas was bubbled into the mixture for at least 60 sec before the Teflon seal was closed. The reactor was placed in an oil bath at 150^{o}C for 24 h while stirring magnetically. After cooling to room temperature, a 100 µL aliquot of the reaction mixture was removed and added to $CDCl_3$ and 2.0 µL DMSO as internal standard for NMR analysis. All olefinic products from the DODH reactions have been previously reported and were identified by comparison of their NMR spectra with authentic samples or published data.

trans-stilbene : ^{1}H-NMR (300 MHz, $CDCl_3$): 7.5 (m, 4H), 7.3 (m, 4H), 7.2 (m, 2H), 7.1 (s, 2H)

2-styrylpyridine : ^{1}H-NMR (300 MHz, $CDCl_3$): 8.6 (d, J = 4.02H_Z, 2H), 7.6 (m, 4H), 7.3 (m, 4H) 7.1 (m, 2H)

Heck Reaction of styrene with 2-bromopyridine



6. DODH/Hydroacylation Tandem Reaction

a. Introduction

iv. Hydroacylation Background

The hydroacylation reaction is the addition of an aldehyde to an alkene by C-C bond formation (Figure III. 6.1). This reaction is usually catalyzed by either rhodium, ruthenium, nickel, palladium or iridium transition metal complexes. It is a completely atom economical process since all of the atoms of the two reactants are incorporated into the single product.[149] In the late 60's Ohno and Wilkinson discovered the decarbonylation of aldehydes by the use of a stoichiometric amount of Wilkinson's complex ($RhCl(PPh_3)_3$).[150,151] Sakai and co-workers reported the first hydroacylation as an intramolecular process.[152] Because of the catalytic cycle of Wilkinson's catalyst the intermolecular hydroacylation is competing with the decarbonylation reaction (Figure III. 6.2). It was Suggs in 1978 who first described the suppression of the decarbonylation by employing β-chelating aldehyde.[153] This discovery allowed the development of the intramolecular hydroacylation reaction.

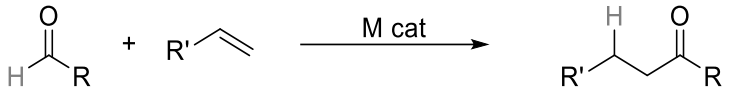


Figure III. 6.1 General Hydroacylation equation

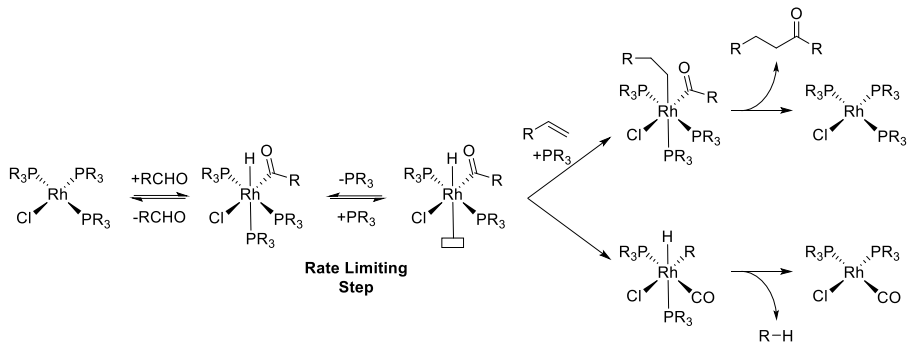


Figure III. 6.2 Rhodium catalyst mechanism; Hydroacylcation and Decarbonylation

Other catalysts such as ruthenium or iridium complexes can facilitate selective intermolecular hydroacylation on non-chelating aldehydes. This is possible because a C-H oxidative addition step is involved in the mechanism with these metal complexes.

v. Tandem DODH/Hydroacylation Concept

The general idea of the DODH/Hydroacylation tandem reaction is to form both of the hydroacylation reactants, alkene and aldehyde, in the DODH reaction to make the tandem reaction completely atom efficient (Figure III. 6.3). We already had established the reaction conditions for the DODH reaction using benzyl alcohol as reducing agent.[46] Subsequently we started our investigation on tandem DODH-hydroacylation by looking at the literature to find compatible reactions conditions for the hydroacylation on simple alkenes with aryl aldehydes. Watanabe and co-workers reported hydroacylations using ruthenium dodecacarbonyl as catalyst.[154,155] They studied the reaction conditions for cyclic and terminal linear alkenes with benzaldehyde. Their system will present multiple challenges; 1) the yields are generally low (50% maximum); and 2) the ratio of alkene to aldehyde is 8 to 1. In this system they also used carbon monoxide as ligand for the catalyst

which made us hopeful that this gas could function as the reducing agent for the DODH reaction, more equivalents of alkene would form than of aldehyde. In addition the side product in the DODH reaction would be CO_2, the only atoms lost in the tandem reaction. The use of carbon monoxide as a reducing agent was studied in the presence of hydrogen in the DODH/hydroformylation tandem study section 7 Chapter III. Also to date there is only one report of carbon monoxide as a DODH reducing agent from Gopaladasu and Nicholas and this system uses a vanadium catalyst.[66]

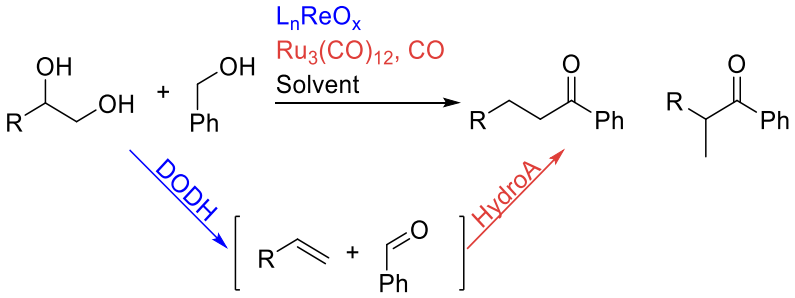


Figure III. 6.3 DODH/Hydroacylation tandem concept

With all of the uncertainty of a potential intermolecular tandem DODH/hydroacylation reaction we also imagined an intramolecular version. For this intramolecular system we thought about making a glycerol ether derivative of ortho-hydroxyl benzyl alcohol (Figure III. 6.4) as a model substrate. This substrate would carry both the diol and the reducing agent for the DODH reaction. The allyl aldehyde product of this DODH reaction could undergo intramolecular hydroacylation to provide the heterocyclic ketone.

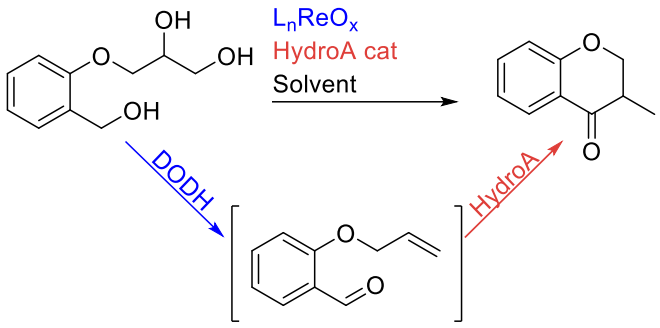


Figure III. 6.4 Intramolecular DODH/Hydroacylation tandem concept

In either of inter- and intramolecular DODH/hydroacylation tandem reactions the products would be of high value and would be applicable to organic synthesis. The intermolecular DODH/Hydroacylation produces arylketones. Arylketones are commonly used in the preparation of pharmaceutical molecules and materials. They can also act as useful building blocks in organic chemistry.[156] The intramolecular DODH/hydroacylation provides flavone derivatives. Flavones are attractive molecules as they have several biological activities such as antioxidant, anti-tumor, anti-proliferative, estrogenic, anti-microbial, acetyl cholinesterase, and anti-inflammatory. They are also used in cancer, cardiovascular disease and neurodegenerative disorders.[157]

In this section we will cover the studies of these two potential DODH/Hydroacylation systems. In the first part we describe our results on the study of the intermolecular hydroacylation reaction step. Then we describe the synthesis and the DODH activity of the glycerol ether derivative of ortho-hydroxyl benzyl alcohol.

b. Intermolecular DODH/Hydroacylation

In the reported system by Watanabe's group cyclohexene was used as the solvent as well as reagent (Figure III. 6.5).[155] The choice of the alkene as solvent would be difficult

to apply on the DODH side of the tandem system. Also before attempting any tandem reactions we decided to study if the hydroacylation reaction would still work using a 1:8 ratio of aldehyde to alkene but with benzene as a solvent (Figure III. 6.5) to be closer to the known reaction conditions for the DODH reaction. Under these conditions the hydroacylation never took place; we found only unreacted aldehyde and alkene in the ^{1}H NMR spectrum after reactions under either 200 or 300 psi CO at 185^{o}C after two to four days.

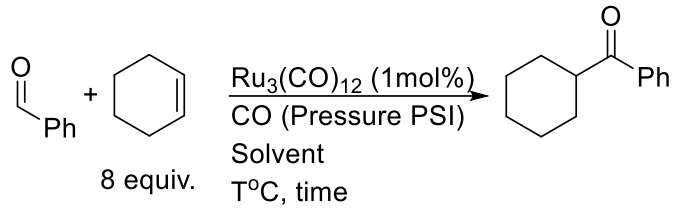


Figure III. 6.5 General Hydroacylation of cyclohexene and benzaldehyde

Table III. 6.1 Reported and Attempted Hydroacylations

	Reported	Attempted
Reaction Conditions	$Ru_3(CO)_{12}$ (1mol%), CO (285 PSI), 200^{o}C, 48h	$Ru_3(CO)_{12}$ (1mol%) CO (200-300 PSI), Benzene (0.2M), 185^{o}C, 2-4 days

From these preliminary results on the use of additional solvent in the hydroacylation reaction it is difficult to envision an efficient intermolecular DODH/hydroxylation reaction with these hydroacylation reaction conditions. To overcome this problem we could study a different hydroacylation catalyst. Indeed rhodium and cobalt cyclopentadiene complexes have been reported to be efficient for the hydroacylation of 1:1 ratio of alkene to aldehyde using toluene as solvent (Figure III. 6.6).[149]

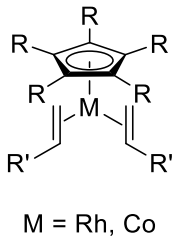


Figure III. 6.6 Hydroacylation catalyst

c. Intramolecular DODH/Hydroacylation

From our observations in the study of intermolecular hydroacylation we imagined a way to bypass some of the obstacles and limitations of the hydroacylation reaction by making the reaction intramolecular. The intramolecular version should compensate for the unfavorable entropy change of the intermolecular reaction. In fact the intramolecular hydroacylation has been more widely studied and could provide more options for reaction conditions and should allow us to avoid the use of a large excess of one of the reagents.

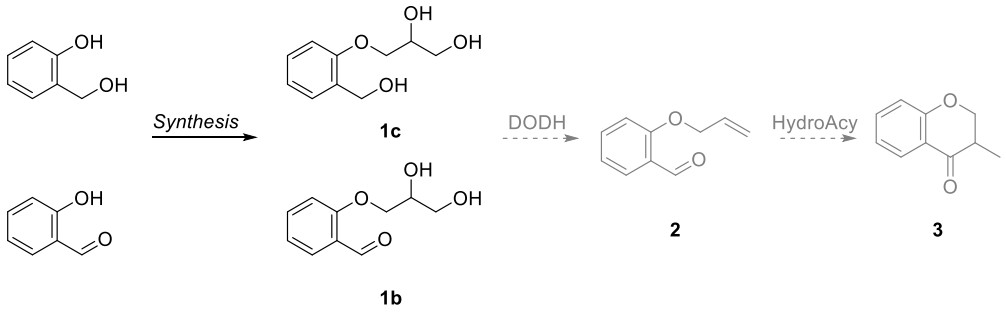


Figure III. 6.7 Intramolecular DODH/Hydroacylation study plan

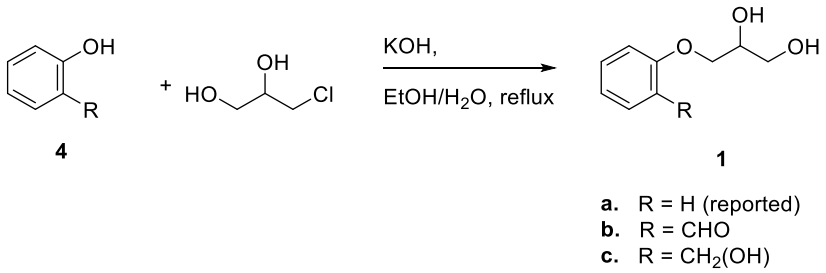


Figure III. 6.8 General synthesis of compound 1

In order to have an intramolecular hydroacylation the DODH reaction must produce a product alkene with a formyl group in the same molecule. According to this idea we found a synthesis procedure for **1a** (Figure III. 6.8)[158] and planned the synthesis of **1b** and **1c** (Figure III. 6.7) neither of which had been prepared before. First we carried out the synthesis of **1b** starting from salicylaldehyde (**4b**, Figure III. 6.8) as reported for phenol itself (80% yield). Then we ran the DODH reaction of **1b** using benzyl alcohol as reducing agent (Figure III. 6.9) under the usual conditions. ^{1}H NMR analysis of this reaction mixture did not indicate the presence of any allylic benzaldehyde product **2.** Instead, we detected the formation of a cyclic acetal **5** (singlet at 6.3 ppm) resulting from an intramolecular reaction. This product is not too surprising since the DODH catalyst, ammonium perrhenate, is acidic and in the past we have detected acetal formation under these conditions.[46] In the same way we designed this polyol to later favor the intramolecular hydroacylation reaction from this diol, **1b**, and the acetal formation would be entropically favored as well. The formation of this acetal was reported previously.[159]

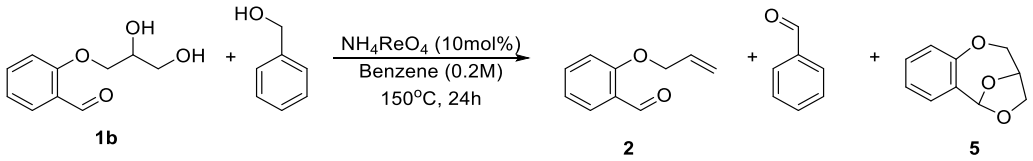


Figure III. 6.9 DODH of <u>1b</u>

Using the procedure reported for **1a**, we then prepared **1c** starting from salicylalcohol (**4c**, Figure III. 6.8) (76% yield). This compound was characterized by ^{1}H NMR. We did not expect the benzylic hydroxyl to be reactive in this step as its pKa is about 16 vs. the pKa of the phenol is around 10 and the pKa of the conjugate acid of the base potassium

hydroxide is around 15. We tested the DODH reaction of this polyol **1c** (Figure III. 6.10) employing the usual reaction conditions- benzene 0.2M, ammonium perrhenate (10 mol%), 150^{o}C, 24h, entry III.6.2.1. We did not observe the formation of **2**. It was difficult to estimate the conversion as **1c** is not soluble in the reaction solvent benzene nor the NMR solvent chloroform-*d*. We then decided to run the reaction in a more polar solvent, 1-butanol, since it was previously used for the DODH of glycerol with indoline as reducing agent.[83] For this reaction in 1-butanol we used methyl trioxorhenium (10 mol%) as the catalyst at 150^{o}C for 24h; entry 2.2, the NMR spectrum in DMSO-d^{6}. revealed a set of signals for a terminal alkene (multiplet at 6 ppm and two doublets at 5.5 and 5.3 ppm), but no signal was present around 10 ppm for an aldehyde. However, we detected a singlet at 5.6 ppm indicative of an acetal. Apparently, the solvent 1-butanol formed an acetal with the aldehyde product. We can then conclude that the DODH of **1c** gave about an 80% yield, but the product **2** formed an acetal **6,** Figure III. 6.11, with the solvent. Since we are studying this polyol in order to use it in a tandem DODH/Hydroacylation reaction, the conversion of the aldehyde to acetal would not allow the hydroacylation step of the tandem reaction. In an attempt to have a suitable solvent for the DODH of the polyol **1c** we tested 1,2-dimethoxy ethane. Matt Slief, an undergraduate student in our laboratory, briefly studied this solvent for the DODH of polyols such as xylitol with some limited success (~20% yield of diene). In the DODH of **1c** in 1,2-dimethoxy ethane (0.3M), 10 mol % ammonium perrhenate, 150^{o}C , 24h; entry III.6.2.3, we could detect a small amount of allylic product (<10 % yield), but no signal was detected for an aldehyde.

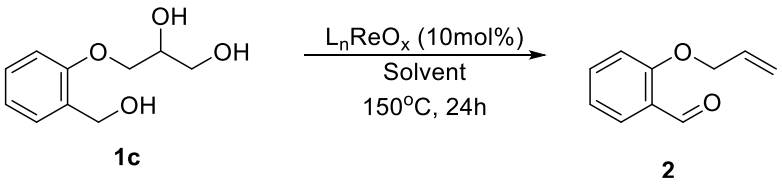


Figure III. 6.10 DODH of 1c

Table III. 6.2 Reaction conditions tested on the DODH of 1c

Entry	Catalyst	Solvent	Yields
III.6.2.1	NH_4ReO_4	benzene	0%
III.6.2.2	$MeReO_3$	1-butanol	80% **6**
III.6.2.3	NH_4ReO_4	1,2-dimethoxy ethane	<10%

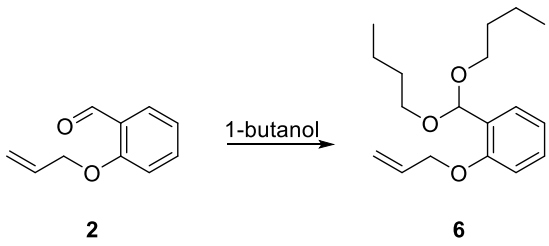


Figure III. 6.11 Reaction of 2 with 1-butanol to form acetal 6

Our study of the reactivity of **1b** and **1c** in the DODH reaction demonstrated they're ineffective at producing compound **2**. The diol **1b** directly formed an intramolecular acetal before the DODH reaction has a chance to even start. The polyol **1c** has a low solubility in regular DODH solvent such as benzene. The DODH of **1c** was very efficient in more polar solvent, 1-butanol, but this solvent was reactive with the product and formed an acetal with the aldehyde making it unavailable for a potential tandem reaction. Our attempt of using a 1,2-dimethoxyethane as solvent showed limited quantity of DODH product and some evidence of reactivity of this solvent in these reaction conditions. It

would then require a study of more solvents to optimize the DODH step for the formation of **2** and without further reaction. Before going in this direction we decided to collect reference for the hydroacylation of **2**. We discovered in a report from Glorius and co-workers the inefficiency of the intramolecular hydroacylation of analogs of **2** (Figure III. 6.12).[160] They described the hydroacylation of **2'** with 56% when employing 20 mol% of N-heterocyclic carbene (**NHC-1**) and 40 mol% of 1,8-Diazabicyclo[5.4.0]undec-7-ene (**DBU**) additives. In light of the required ligand and additive in the hydroacylation step we decided not to pursue the study of a DODH-Hydroacylation tandem reaction.

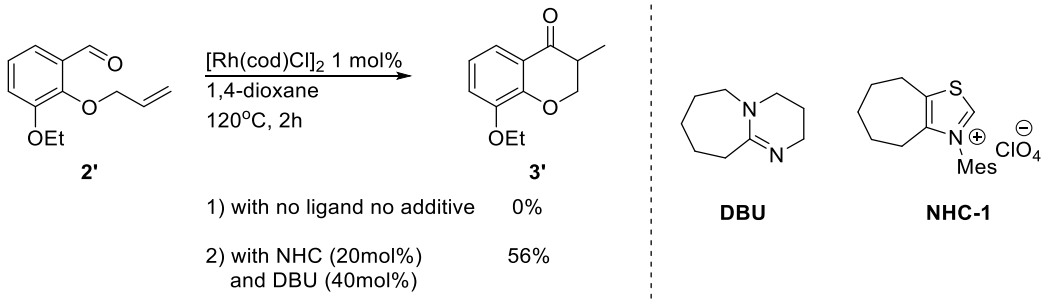


Figure III. 6.12 Reported hydroacylation by Glorius and co-worker

d. Conclusions and future prospects

We studied both inter and intramolecular potential DODH/Hydroacylation reaction systems. We did not observe appreciable hydroacylation product in the Ru-catalyzed intermolecular reaction between cyclohexene and benzaldehyde. The stoichiometry of the reagents and solvent/molarity of the reaction are the main parameters that we think that are limiting the hydroacylation reaction in this case.

In order to favor the hydroacylation reaction step we decided to attempt the reaction in an intramolecular system with glycerol ether derivatives of salicyl aldehyde and alcohol. We tested the DODH reaction step on these polyols. We found the salicyl alcohol

derivative of glycerol to undergo DODH in 1-butanol reaction with 80% yield. Although the allyl ether salicyl aldehyde product reacted with the solvent to form an acetal. With this type of further transformation of the product the hydroacylation would not be able to take place in a tandem system. Also when we investigated the reported reaction conditions for a similar intramolecular hydroacylation system we found that commercially available rhodium catalyst such as $[Rh(cod)Cl]_2$ would require the use of a **NHC-1** and **DBU** to provide 56% yield in the heterocyclic ketone. We think that both **DBU** and the **NHC-1** additive could interact with the DODH reaction or could have unpredicted activity in the DODH reaction.

A study of rhenium and NHC ligand could benefit to this tandem reaction system. Recently Chongmin and co-worker have reported the first **NHC** cationic perrhenium complex for the DODH reaction and could be used to start a compatibility study of **NHC-1** with the DODH reaction system by making a **NHC-1**:NH_4ReO_4 complex.[161] It would be even desirable to have the same **NHC** ligand in the hydroacylation and DODH catalyst. The need and use for **DBU** as an additive would still have to be assessed.

In the case of the successful intramolecular DODH/hydroacylation tandem reaction we can envision an increase of its scope by replacing glycerol for xylitol or other polyols such as glyceric or gluconic acids (Figure III. 6.13). These polyols have already been studied for the DODH reaction. Since flavones have reported bioactive potentials in cancer and cardiovascular treatments[157] these tandem products would be very attractive.

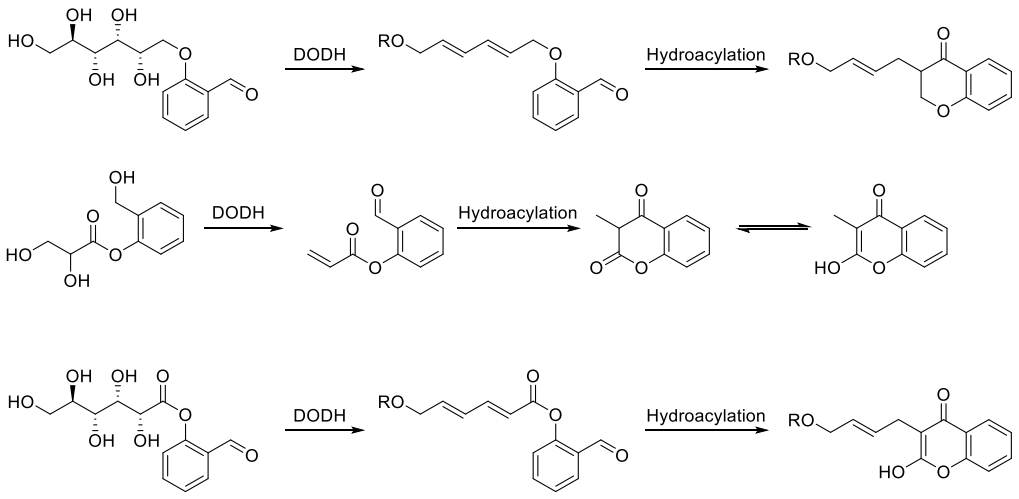


Figure III. 6.13 Potential scope study for intramolecular DODH/hydroacylation

e. Experimental

i. General information: reagents and instruments.

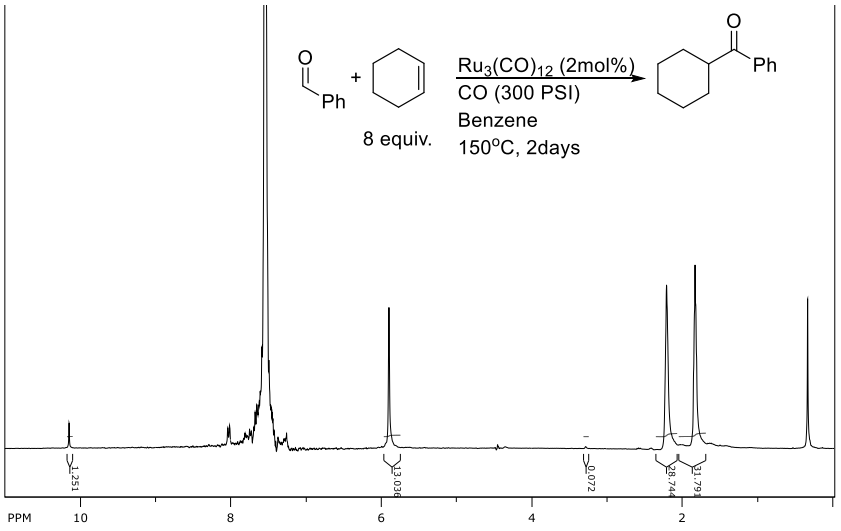
Most reactants were obtained commercially and used without further purification. All solvents were ACS grade and were used directly (unless otherwise described in the procedures). ^{1}H and ^{13}C NMR spectra were collected on Varian VX300 MHz or VNMRS 400 MHz instruments. The NMR data were processed using SpinWorks[102] and ACD[103] software.

ii. Representative procedure for intermolecular hydroacylation reactions.

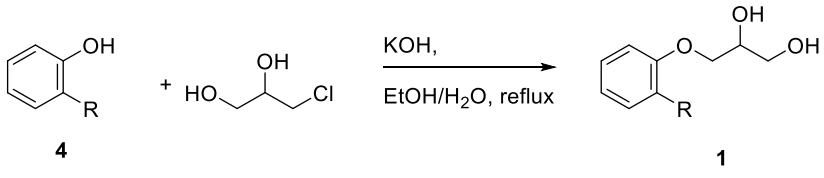
Benzaldehyde (4.00 mmol, 0.41 mL), cyclohexene (32.0 mmol, 3.2 mL), $Ru_3(CO)_{12}$ (0.07 mmol, 44 mg) and benzene (20 mL) were added to a stainless-steel Parr reactor. The reactor was purged three times with carbon monoxide before being pressurized to 300 PSI and placed in an oil bath at 190^{o}C for 2 to 4 days while stirring magnetically.

After cooling to room temperature, the pressure was released in a fume hood and a 100 µL aliquot of the reaction mixture was removed and added to $CDCl_3$ (0.5 mL) for ^1H NMR analysis.

Intermolecular hydroacylation reactions



*iii. Synthesis of compound **1b** and **1c***



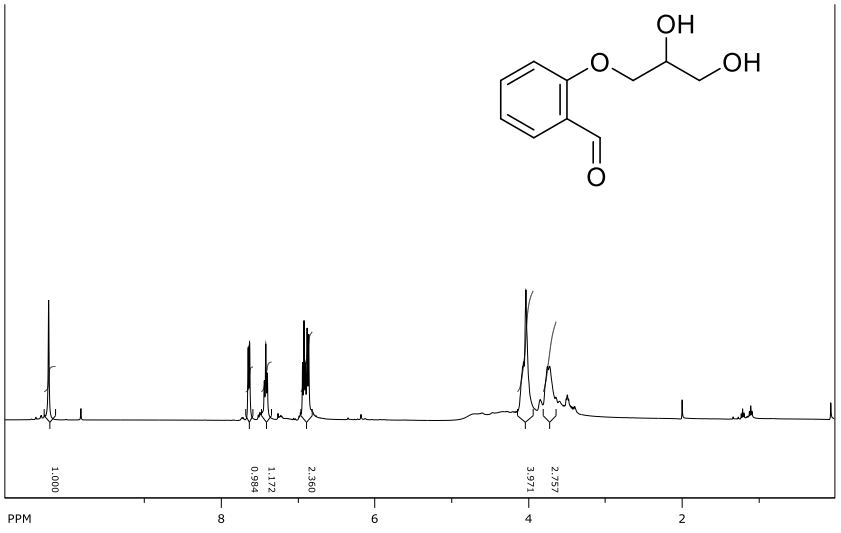
a. R = H (reported)
b. R = CHO
c. R = $CH_2(OH)$

General synthesis scheme for 1

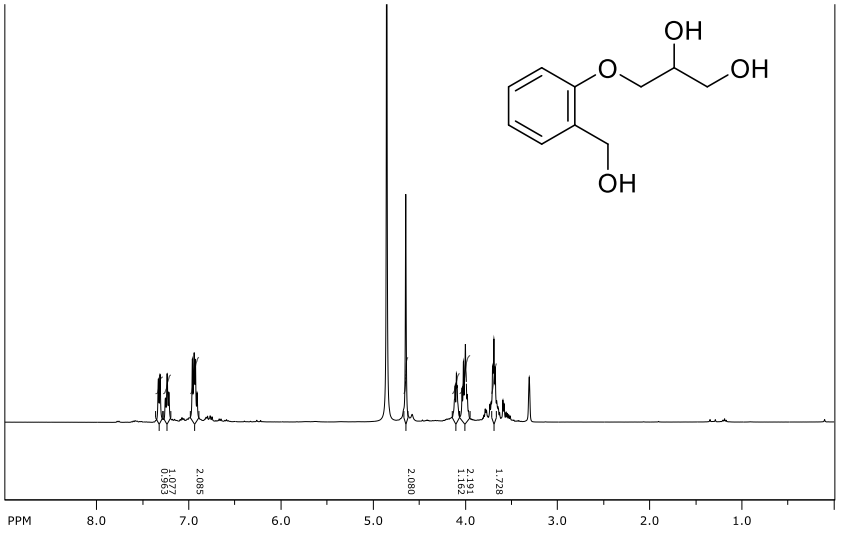
We followed the same literature procedure for the synthesis of **1a** from phenol and 3-chloropropane-1,2-diol for the synthesis of **1b** and **1c**.

A solution of KOH (3.5 g, 6.25 mmol, 1.25 equiv.) in H_2O (1 mL) was added to a solution of the appropriate phenol (5.0 mmol, 1.0 equiv.; 0.53 mL salicylaldehyde or 621 mg salicyl alcohol) in EtOH (3 mL). The resulting mixture was heated under reflux for 10 min. Then, a solution of 3-chloro-1,2-propanediol (6.0 mmol, 0.50 mL, 1.2 equiv.) in EtOH (0.5 mL) was slowly added and the mixture was further heated under reflux until completion, 16 h. The ethanol was then removed under reduced pressure and Et_2O was added, along with more water. The aqueous phase was extracted twice with Et_2O and the combined organic layers were dried over $MgSO_4$, filtered and evaporated under reduced pressure. Both **1b** and **1c** were pale yellow oils.

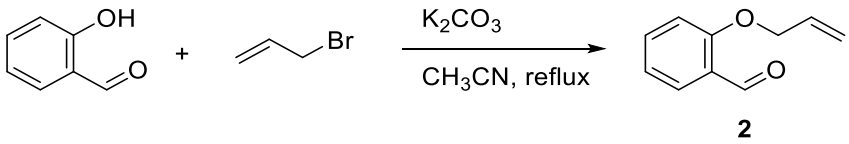
1b ^{1}H NMR (400 MHz; $CDCl_3$): 10.3 (s, 1H), 7.6 (dd, J = 1.61, 7.68 Hz, 1H), 7.4 (td, J = 1.66, 8.56 Hz 1H), 6.9 (t, J = 7.68 Hz, 1H), 4.1 (m, 4H), 3.8 (m, 1H).



1c ^{1}H NMR (400 MHz; MeOH-d^4): 7.3 (d, J = 6.85 Hz, 1H), 7.2 (t, J = 8.22 Hz, 1H), 6.9 (m, 2H), 4.6 (s, 2H), 4.1 (m, 1H), 4.0 (m, 2H), 3.7 (m, 2H).



*iv. Synthesis of compound **2***

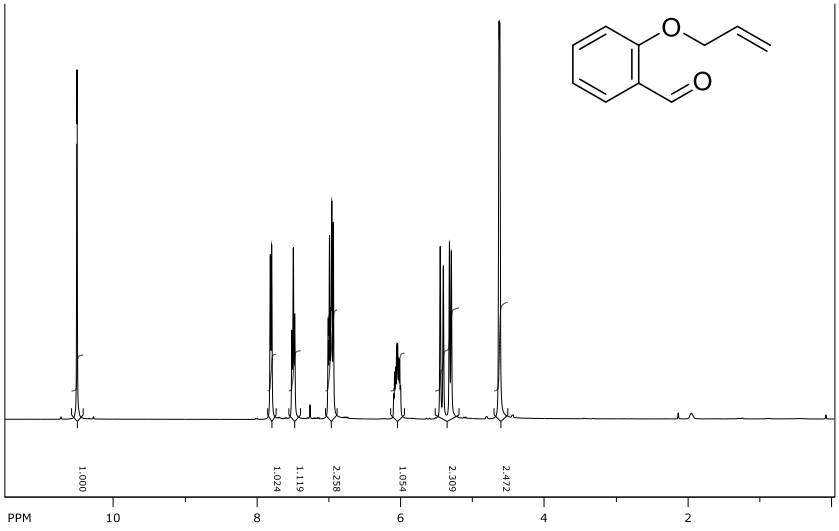


2

We followed the same literature procedure for the synthesis of **2** from salicyl aldehyde and allyl bromide.[162]

Salicylaldehyde (0.27 mL, 2.5 mmol), allyl bromide (0.28 mL, 3.3 mmol) and potassium carbonate (520 mg, 3.8 mmol) were mixed in acetonitrile (10 mL) and the reaction mixture was heated to 60 °C (reflux, 3 h). The mixture was cooled to room temperature and diluted with ethyl acetate. The reaction mixture was washed with saturated aqueous ammonium chloride, 1 M aqueous sodium hydroxide and brine. The separated organic phase was dried over Na_2SO_4 and the solvent was removed to give the title compound (404 mg, 100%) as a pale yellow oil.

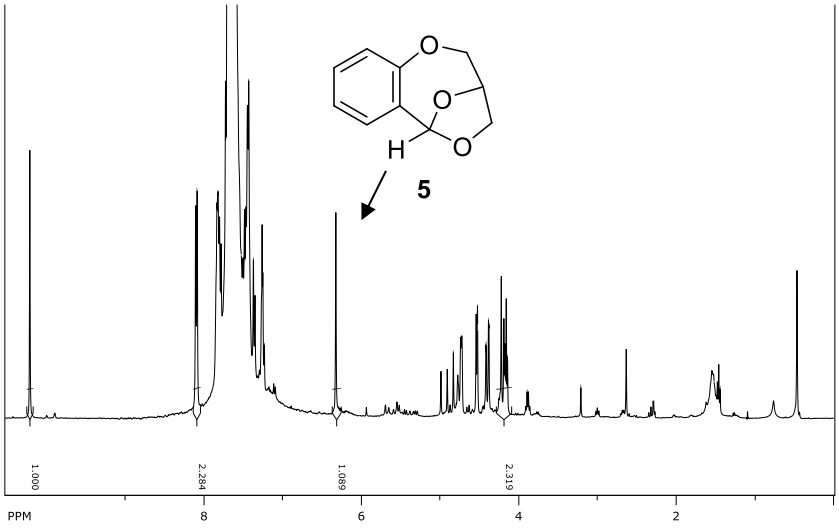
^{1}H NMR (400 MHz; $CDCl_3$): 10.5 (s, 1H), 7.8 (d, J = 7.8 Hz, 1 H), 7.5 (dd, J = 8.1, 7.8 Hz, 1 H), 6.9 (m, 2H), 6.0 (m, 1H), 5.4 (d, J = 17.4 Hz, 1 H), 5.3 (d, J = 10.5 Hz, 1H), 4.6 (d, J = 4.8 Hz, 2H);



v. Representative procedure for DODH reactions.

Compound **1b** (1.00 mmol, 198 mg), NH_4ReO_4 (0.10 mmol, 25 mg), benzyl alcohol (1.00 mmol, 0.11 mL), and benzene (5 mL) were added to a thick-walled Ace glass reactor tube. A N_2 flow was bubbled into the mixture for at least 60 sec before the Teflon seal was closed. The reactor was placed in an oil bath at 150 ^{o}C for 24 h while stirring magnetically. After cooling to room temperature, a 100 µL aliquot of the reaction mixture was removed and added to $CDCl_3$ (0.5 mL) and 2.0 µL DMSO as internal standard for NMR analysis. The resulting spectrum was compared to the expected product (**2**).

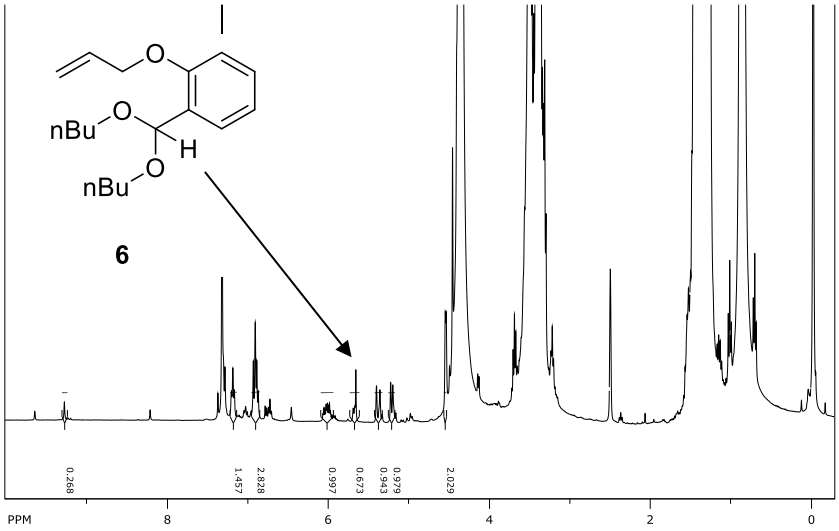
*[1]H NMR DODH reaction of 1b (*Figure III. 6.9*)*



Reported ^{1}H NMR for **5**[159] (300MHz, $CDCl_3$): 7.3–7.2 (m, 2H), 7.0–6.9 (m, 2H), 6.0 (s, 1H), 4.7–4.6 (m, 1H), 4.3–4.2 (m, 2H), 4.0–3.9 (m, 2H)

Compound **1c** (1.00 mmol, 198 mg), $MeReO_3$ (0.10 mmol, 24 mg) and 1-butanol (3.3 mL) were added to a thick-walled Ace glass reactor tube. A N_2 flow was bubbled into the mixture for at least 60 sec before the Teflon seal was closed. The reactor was placed in an oil bath at 150 ^{o}C for 24 h while stirring magnetically. After cooling to room temperature, a 100 µL aliquot of the reaction mixture was removed and added to DMSO-d^6 (0.5 mL) and 2.0 µL DMSO as internal standard for NMR analysis. The resulting spectrum was compared to the expected product **2**.

^{1}H NMR of the reaction entry 2 table 2



^{1}H NMR for **6** (400MHz, DMSO-d^{6}): 7.2 (m, 1H), 6.9 (m, 3H), 6.0 (m, 1H), 5.6 (s, 1H), 5.4 (d, J = 10.75 Hz, 1H), 5.2 (d, J = 5.25 Hz, 1H), 4.5 (d, J = 1.75 Hz, 2H)

7. DODH/Hydroformylation Tandem Reaction

a. Introduction and Background

i. The hydroformylation reaction

The hydroformylation reaction was discovered in 1938 by Otto Roelen.[163] It is a metal-catalyzed process in which an alkene reacts with CO and H_2 and is transformed into an aldehyde by the addition of a formyl group and a hydrogen to the alkene double bond (Figure III. 7.1). Because of the formation of a carbon-carbon bond in this process, this reaction has been the focus of many studies. The aldehyde formed can be oxidized to the carboxylic acid or it can be hydrogenated to the alcohol. These products are key building blocks for the synthesis of plastics, detergents, surfactants, lubricants and dialkyl phthalate plasticizers,[164] making the hydroformylation reaction an important industrial process.

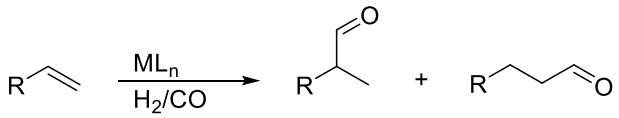


Figure III. 7.1 General Hydroformylation reaction

The initial hydroformylation reaction discovered by Roelen was the transformation of ethylene into propanal catalyzed by cobalt tetracarbonyl hydride under an atmosphere of hydrogen and carbon monoxide gas. The system was first improved by the use of phosphine ligands on the cobalt catalyst. A major improvement to the hydroformylation reaction was made with the discovery of rhodium catalysts in the 1970's.[164] These highly active precious metal catalysts were found to be particularly efficient on small chain

alkenes, eight carbons or less. Nowadays most hydroformylation processes are catalyzed by triarylphosphine rhodium complexes.

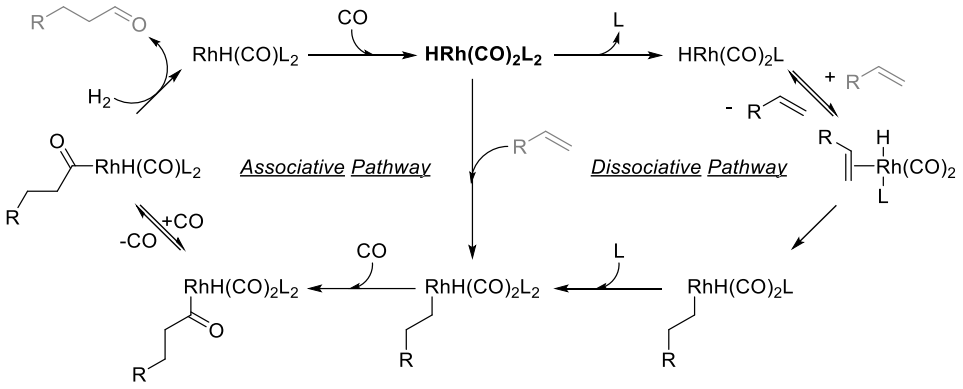


Figure III. 7.2 Rhodium catalyzed hydrofomylation mechanistic cycle

Depending on the catalyst used, hydroformylation reactions are run at temperatures between 40 and 200^{o}C under high pressures, from 10 to 100 atmospheres, of a carbon monoxide and hydrogen mixture.[165] Terminal alkenes are more reactive than internal alkenes. These conditions make the hydroformylation process an attractive reaction to be coupled with deoxydehydration.

The rhodium-based catalytic cycle is believed to follow either an associative or dissociative pathway (Figure III. 7.2). In either of these pathways the alkene coordinates to the metal-hydride followed by migratory insertion of the olefin to form metal-alkyl after which CO insert into metal-alkyl. With the oxidative addition of hydrogen and reductive elimination of the aldehyde product the catalyst is regenerated. Depending on the catalyst and/or the alkene unsymmetrical alkene can form both normal (linear) and iso (branched) aldehyde product and result from the way alkene is inserting into the metal hydride bond (M-O).

ii. DODH/Hydroformylation tandem concept

A tandem DODH/hydroformylation (DODH/HF) reaction is to start with a C_n linear terminal vicinal diol to form a terminal olefin via the deoxydehydration process that could then undergo hydroformylation to provide a linear and/or branched C_{n+1} aldehyde (Figure III. 7.3). In an ideal case the hydrogen and carbon monoxide gas mixture could also serve as the reducing agent in the DODH process. Other reported DODH reducing agent could be considered also as long as these or their products will not disturb the subsequent hydroformylation step. Our main concern in this tandem system is the compatibility of the high oxidation state rhenium complex with the low oxidation state rhodium complex.

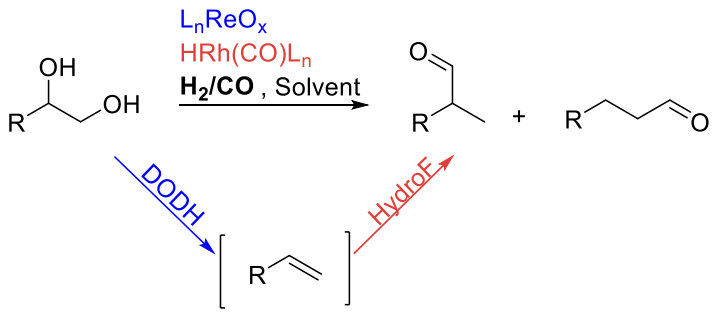


Figure III. 7.3 DODH/Hydroformylation tandem concept

In this section we will describe the preliminary studies conducted to evaluate the potential of a hydrogen and carbon monoxide gas mixture as reducing agent in the DODH reaction. As a model diol we studied the DODH reaction of 1,2-hexanediol. The hydroformylation of 1-hexene has been well studied and provides several catalyst and condition options. We will then report our study of the hydroformylation reaction of 1-hexene before reporting the results obtained for the DODH/hydroformylation tandem reaction.

b. Hydrogen and Carbon monoxide as DODH reducing agents

Hydrogen was reported as an effective reducing agent for the deoxygenation of epoxides catalyzed by $MeReO_3$ by Abu-Omar and co-workers.[33] When applied to the DODH of 1,2-hexanediol this reducing agent had only 18% yield in alkene (Figure III. 7.4). At higher pressure, 300 psi, the main product detected was hexane (50% Yield). More recently carbon monoxide was also reported as a reducing agent for the DODH reaction by Gopaladasu and Nicholas with a vanadium-oxo catalyst.[66]

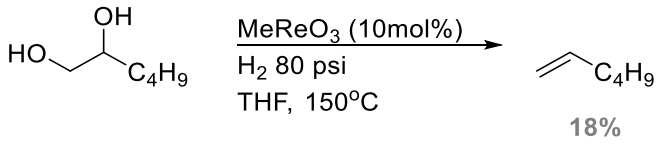


Figure III. 7.4 Abu-Omar DODH of 1,2-hexanediol with H_2 as reducing agent

We tested several reaction conditions (catalyst, time, temperature, pressure; Figure III. 7.5) for the DODH of 1,2-hexanediol using hydrogen and carbon monoxide as reducing agent (Table III. 7.1). We started by mimicking the reported reaction conditions which used hydrogen as reducing agent and we used methyl trioxorhenium as catalyst (entries 1.1-1.2). We observed the same 30% yield (95% conversion) after 22.5h and 6h. Variations of the rhenium catalyst entries 1.3 to 1.6 did not improve the yield with a maximum of 30% and up to 90% conversion. We also tried the vanadium complex reported effective for DODH with carbon monoxide as reducing agent, but with the gas mixture of hydrogen and carbon monoxide the yield dropped to 24% with 90% conversion (entries 1.7 and 1.9). When ammonium perrhenate was employed as catalyst we could see a drop in the diol conversion (21%) with approximately 20% yield after

24h. We let the reaction going for 48h and found 43% yield in alkene with 81% conversion.

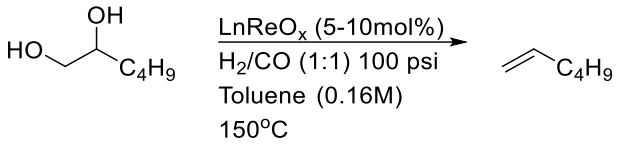


Figure III. 7.5 DODH of 1,2-hexanediol using H_2/CO as reducing agent

Table III. 7.1 Results of the DODH of 1,2-hexane diol (Figure III. 7.5) with hydrogen and carbon monoxide under various reaction conditions

Entry	L_nMO_x	Time	Alkene Yield[a]	Diol Conversion[a]
III.7.1.1	$MeReO_3$	22.5h	30%	95%
III.7.1.2		6 h	30%	95%
III.7.1.3	$ReOCl_3(PPh_3)_3$	24 h	<10%	>90%
III.7.1.4	$IReO_2(PPh_3)_3$	24 h	17%	>90%
III.7.1.5[b]			30%	>90%
III.7.1.6	n-Bu_4NReO_4	Up to 4 days	0%	>51%
III.7.1.7[c]	Bu4N(LVO_2)[g]	4 days	24%	>90%
III.7.1.8[d]			0%	>90%
III.7.1.9[e]	NH_4ReO_4	24 h	20%	21%
III.7.1.10[f]		48 h	43%	81%

a) Yield and conversion determined by NMR using DMSO or DMF as internal standard, b) 185°C, c) 180°C, d) 300 psi 180°C, e) results expressed as ration alkene to diol, f) 3:1 H_2/CO ratio; g) L=(salicyl-2-thiophenyl-hydrazide)

In an attempt to improve the activity of the H_2/CO gas mixture as reducing agent we investigated potential hydrogen activating reagent. The challenge of using such additive in the reaction is to activate the hydrogen without favoring the alkene hydrogenation reaction. In fact if we were to employ the usual solid additive such as palladium on carbon

we might help activation of the hydrogen toward the DODH reaction but it might also reduce the alkene formed to the saturated hydrocarbon. Subsequently we turned to catalyst with are reported to activate hydrogen selectively toward carbonyl reduction. One such catalyst is known as Shvo's catalyst.[166] It is a bi ruthenium complex which dissociates in solution into two monomers with complementary reactivity (Figure III. 7.6). One of these monomers carries two hydrogen atoms when the second one is lacking hydrogens. Both of these monomers are involve in the catalytic cycle of aldehyde reduction (Figure III. 7.7).

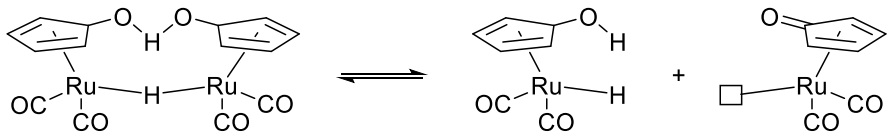


Figure III. 7.6 Shvo's Ruthenium catalyst dissociation equilibrium

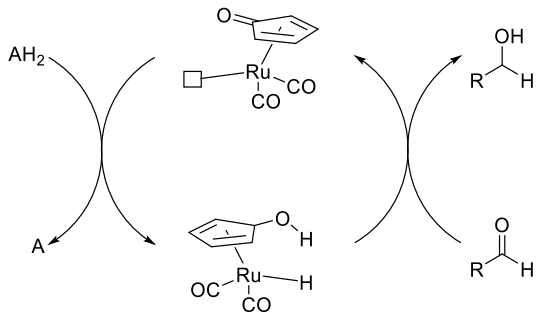


Figure III. 7.7 Shvo's catalyst cycle for hydrogen activation in aldehyde reduction

Economical iron analogues of this bi ruthenium catalyst (Figure III. 7.6) were developed. Also after some research on the topic we decided to synthesize and test the iron carbonyl complex **1** (Figure III. 7.8). We tested the DODH of 1,2-hexane diol with 10 mol% of **1** (Figure III. 7.8) and we did not detect any conversion of the diol. We also

tested the same reaction with 10 mol % of benzyl alcohol. The added alcohol is to play the role of a reducing agent in the DODH reaction which could then be regenerated by **1-H2** (Figure III. 7.9). In this reaction we detected benzaldehyde, benzyl alcohol, unreacted diol and acetal (of diol with benzaldehyde) but no alkene. We can then conclude that 1 was not efficient to activate hydrogen for the DODH of 1,2-hexanediol even with a catalytic quantity of alcohol.

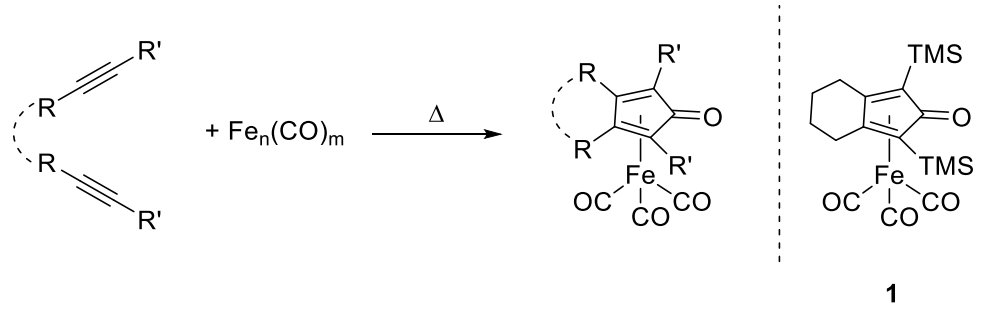


Figure III. 7.8 Synthesis of iron analogues to Shvo's catalyst

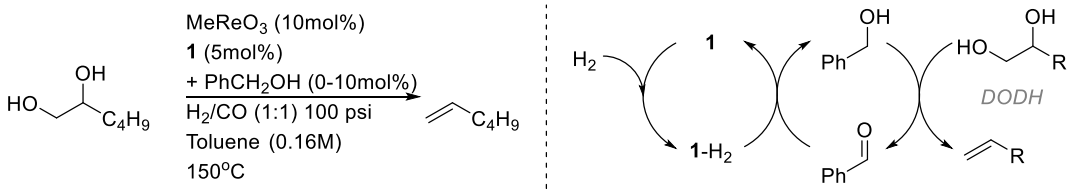


Figure III. 7.9 DODH of 1,2-hexanediol using 1 as hydrogen activating catalyst

In summary we found a very limited DODH activity of the hydrogen/carbon monoxide mixture with this set of oxo-metal complexes with a maximum yield of 30% and 95% conversion. In many cases the conversion of the diol was high but the yield was low indicating that a side reaction of the diol, possibly dehydration/hydrogenation or oxidation, was competing. We attempted to ease the activation of hydrogen by adding an iron carbonyl complex but the overall reaction was not improved. To effectively use

hydrogen and carbon monoxide for both DODH and hydroformylation we would have to identify new catalysts or co-catalysts to improve the activity of hydrogen and carbon monoxide as reducing agent. As a last resort we would consider the use of an alternative efficient reducing agent for the DODH part of the tandem reaction.

c. Hydroformylation of 1-hexene

From the numerous reaction conditions reported for the hydroformylation of 1-hexene we choose to test two common and commercially available catalysts; $HRh(CO)(PPh_3)_3$ and $Co_2(CO)_8$ (Table III. 7.2).[165] In these reactions we detected by ^1H NMR a variety of products including isomerized alkenes, aldehydes, alcohols and acetals (Figure III. 7.10).

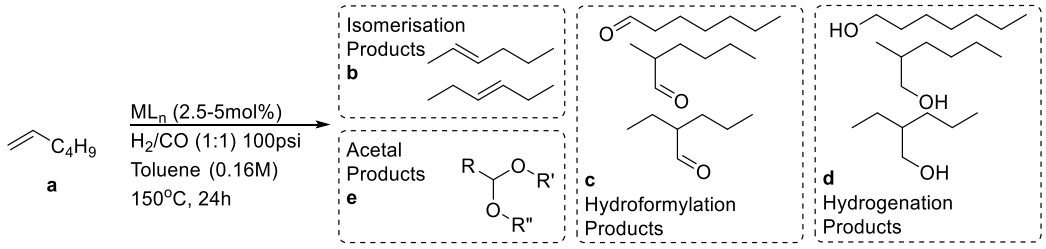


Figure III. 7.10 Hydroformylation of 1-hexene

Table III. 7.2 Results of the hydroformylation of 1-hexene

Entry	ML_n	Additive	Products ratio[a]				
			a	b	c	d	e
III.7.2.1[b]	$HRh(CO)(PPh_3)_3$	-	0.1	**5.3**	1.6	2.0	1.0
III.7.2.2[b]		DPPE 25 mol%	0.2	0.3	**2.8**	0.9	**5.8**
III.7.2.3[b]		PPh_3 100 mol%	0.2	0.3	**3.6**	0.8	**5.1**
III.7.2.4[c]	$Co_2(CO)_8$	-	0.2	**8.7**	1.0	0	0
III.7.2.5[c]		500 psi	**6.7**	3.3	0	0	0

a)Ratios obtained by ^{1}H NMR, b) 2.5 mol% of catalyst, c) 5 mol% of catalyst

When we used the rhodium catalyst without additives, entry III.7.2.1, we found by ^{1}H NMR the internal (isomerized) alkene to be the major component of the reaction mixture along with some hydroformylation product (ratio b:c, 5.3:1.6). Pittman and Hirao reported the use of added 1,2-bis(diphenylphosphino)ethane (dppe) ligand in the reaction improved the yield of the hydroformylation reaction. We tried dppe as an additive in the reaction, entry III.7.2.2, and observed a major improvement in the alkene conversion; the major products of this reaction were aldehydes and acetals. We presume that the alcohols are formed in the reaction by reduction of the aldehydes in the presence of hydrogen; the alcohols can then form acetals with the aldehydes present in the reaction. Overall the ratio of alkenes to hydroformylation derived products is 0.5 to 9.5. This result demonstrate a good selectivity to the hydroformylation reaction.

Considering the use of this diphosphine-catalyst combination in a tandem DODH-HF reaction, we recognize that the presence of free phosphine could serve as a stoichiometric reductant for DODH.[23] Accordingly, we tested the hydroformylation of 1-hexene with

added PPh_3 (1 equivalent) (entry III.7.2.3).[23] In this reaction we observed a similar product distribution as in the reaction with added dppe. The use of triphenylphosphine could now be considered for the tandem reaction, although its cost and the formation of useless triphenylphosphine oxide would not be ideal.

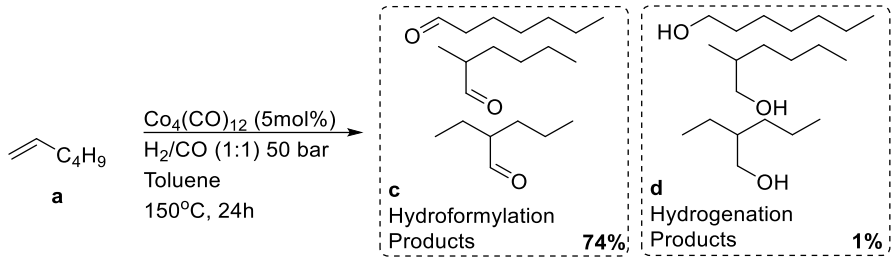


Figure III. 7.11 Pakkanen Hydroformylation of 1-hexene [167]

With these considerations in mind we also tested a phosphine-free cobalt catalyst for hydroformylation. We started by using the same reaction conditions as with the rhodium catalyst, entry 2.4. In this case we didn't see any hydroformylation derived product. The major product found in this reaction was internal alkenes resulting from isomerization. We tested the reaction at higher pressure, 500 psi, and temperature 150°C entry 2.5. Under these conditions we found much less isomerization of the alkene but no product from hydroformylation. With our previous observation on the negative effect of the addition of base to the DODH reaction (Sections 3&5 Chapter III) we wanted to avoid the use of triethyl amine in the DODH/hydroformylation reaction system.

In summary, we found $HRh(CO)(PPh_3)_2$ to be a good hydroformylation catalyst and it worked even better in the presence of added phosphine, which opened some potential for a DODH/Hydroformylation reaction. We also tested phosphine-free dicobalt

octacarbonyl as a hydroformylation catalyst but found it ineffective under DODH conditions.

d. Tandem DODH/Hydroformylation

Our finding that added triphenylphosphine (PPh_3) improved the hydroformylation reaction yield and knowing the potential of triphenylphosphine as reducing agent in the DODH reaction, we decided to attempt the tandem DODH/HF reaction on 1,2-hexane diol. In order to insure the activity of triphenylphosphine as a reducing agent with the DODH catalyst we decided to use a known triphenylphosphine rhenium complex $IReO_2(PPh_3)_2$.[168] This catalyst was found to be active with PPh_3 as the reducing agent in our alcohol reductive coupling/deoxygenation project.[169]

First we tested the DODH reaction of 1,2-hexanediol using triphenylphosphine as reducing agent (Figure III. 7.12) with $IReO_2(PPh_3)_2$ as catalyst (in the presence of H_2/CO). Analyzing this reaction by NMR we found a 33% yield of 1-hexene and 15% of 2- and 3-hexene. Overall this makes for 48% of alkene product. We could also detect 52% of unreacted alcohol. The reaction is selective toward the DODH although a third of the alkene isomerized. With a conversion equal to the yield we can anticipate more alkene with more time if the catalyst is still active.

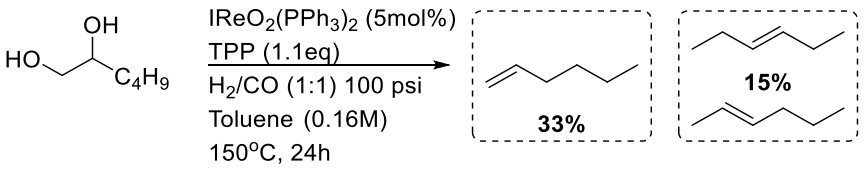


Figure III. 7.12 DODH of 1,2-hexanediol with PPh_3 as reducing agent

With these results in hand we tested a tandem DODH/hydroformylation of 1,2-hexanediol (Figure III. 7.12). In the reaction we used 5 mol% of the $IReO_2(PPh_3)_2$, 2.5 mol% of the $HRh(CO)(PPh_3)_3$, 2 equivalents of triphenylphosphine in toluene and we pressurized the reaction to 100 psi with (1:1) ratio of hydrogen and carbon monoxide. We analyzed this reaction by NMR, GC and GCMS and found less than 10% of unreacted diol, 10% yield of alkenes, 16% of aldehydes, 13% of reduced aldehyde (alcohols) and 16% acetals (Figure III. 7.13). We presume that the acetals formed from the reaction of the starting diol with the aldehydes formed in the hydroformylation. This reaction could be run longer in order react the last 10% of diol. The catalyst loading could also be increased a little in case either one of the rhenium complex or rhodium complex were deactivate. The hydrogenation of the aldehyde hydroformylation product could be studied in order to understand how we could favor or disfavor this reaction. By effectively favoring the formation of these alcohols we could eventually limit the formation of acetals. Overall this tandem DODH/hydroformylation reaction worked moderately well with an overall 45% yield in various tandem products (aldehydes, alcohols and acetals).

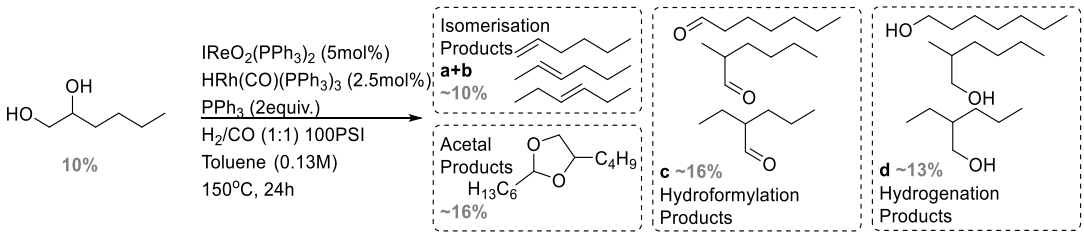


Figure III. 7.13 DODH/Hydroformylation tandem reaction of 1,2-hexane diol

After we observed low selectivity in the tandem reaction with 1,2-hexanediol we decided to make some variation in the starting diol. Phenyl-1,2-ethane diol should form

styrene in the DODH reaction, which has no option to isomerize, making only two possible hydroformylation products. Using the same reaction conditions we tested the tandem DODH/Hydroformylation reaction on phenyl-1,2-ethanediol (Figure III. 7.14). In this reaction we observed no unreacted diol and only 5% yield in alkene. The aldehyde products were found in 50 and 23% yields for the terminal and branched aldehyde respectively. We also found a 5% yield of acetal. This makes an overall 78% yield in tandem product. In this case we did not observe any reduction of the aldehyde products to alcohols.

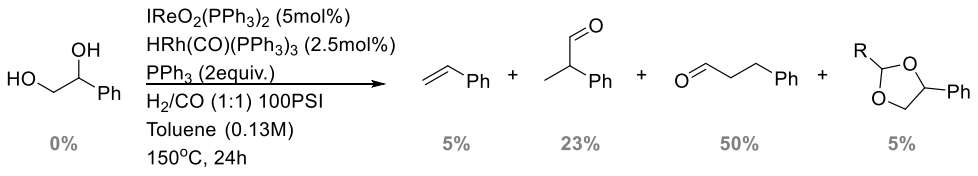


Figure III. 7.14 DODH/Hydroformylation tandem reaction of phenyl-1,2-ethanediol

In order to extend the substrate scope of this tandem DODH/HF reaction and to simplify the product distribution we tried the DODH/hydroformylation tandem reaction on cis-1,2-cyclooctane diol since it was demonstrated by Ahmad, Chapman and Nicholas that only the cis diol is reactive in the DODH reaction.[35] Using the same reaction conditions we observed no unreacted diol, 83% yield of cyclooctene, 7% of aldehyde and 8% of alcohol (Figure III. 7.15). No acetal was detected in this reaction. Overall we found only 15% of DODH/hydroformylation tandem products with this diol. We ran this reaction for a longer time in the eventuality of a slow hydroformylation step, but it did not improve the yield of tandem products. In fact, the hydroformylation reaction has been reported to be more efficient on terminal alkenes than internal alkenes. With no increase

in the product distribution after three days of reaction we suspect deactivation of the rhodium catalyst.

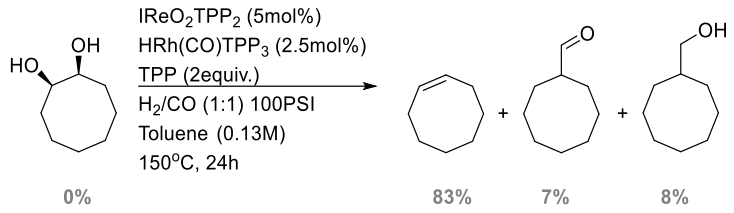


Figure III. 7.15 DODH/Hydroformylation tandem reaction of cis-1,2-cyclooctane diol

Under these reaction conditions the DODH/hydroformylation reaction was alsos attempted on diethyl tartrate, hydrobenzoin (PhCH(OH)-CH(OH)Ph) and cis-1,2-cyclohexanediol. The first two did undergo DODH and we could detect their alkene product, but no hydroformylation took place. When the hydroformylation of the DODH products, diethyl fumarate and cis stilbene, was attempted, the reaction did not occur. Therefore these alkenes are not very reactive toward hydroformylation. In the attempted tandem DODH/HF on cis-1,2-cyclohexanediol we did not detect any diol conversion in the ^{1}H NMR. Previously this diol was used in DODH reaction using $MeReO_3$ as catalyst with Na_2SO_3 as reducing agent, this reaction required 48 hours reaction time to obtain 25% yield in alkene. We can then conclude that the DODH reaction of this diol is slow and that in our case the change in catalyst and reducing agent might not be optimum for the DODH of cis-1,2-cyclohexanediol.

In summary we were able to obtain successful tandem DODH/hydroformylation reactions on three diols- 1,2-hexane diol, 1-phenyl-1,2-ethane diol and cis-1,2-cyclooctane diol. The tandem reaction on 1,2-hexanediol provided a good result with a

high ratio of hydroformylation derived products such as branched and linear products as well as the potential for alkene isomerization and aldehyde. The reaction of 1-phenyl-1,2-ethane diol provided the best yield and selectivity in aldehyde without further reduction to alcohol. Finally the reaction of cis-1,2-cyclooctane diol was found to mostly produce the DODH alkene product, possibly the result of low hydroformylation reactivity of this cyclic alkene.

e. Conclusion

In conclusion, we found the 1:1 mixture of hydrogen and carbon monoxide to have low activity as a DODH reducing agent with a maximum of 30% yield of hexene from hexanediol at 95% conversion. We studied the hydroformylation step and found $HRh(CO)(PPh_3)_2$ was the most efficient catalyst and provided a high yield when phosphines were additives in the reaction. Since triphenyl phosphine is a well-known DODH reducing agent we studied the DODH/hydroformylation tandem reaction on 1,2-hexanediol, 1-phenyl-1,2-ethanediol and cis-1,2-cyclooctanediol. The product distribution and selectivity were different for each of these diols. But we did observe moderate to good overall yields of tandem derived products (aldehydes, alcohols and acetals) for 1,2-hexanediol (45% overall yield) and 1-phenyl-1,2-ethanediol (78% overall yield). The cyclic diol provided a low overall yield in tandem products (15% overall yield).

These successful tandem reaction attempts demonstrate the compatibility of higher oxidation state rhenium and lower oxidation state rhodium tandem catalysts. It has been only few prior examples of high and low oxidation state co-catalysis/compatibility. In

fact most dual catalyst system use metal of close low oxidation state: $[Rh(cod)Cl]_2$/$[Ir(cod)Cl]_2$ for amine synthesis, $Pd(PPh_3)_4$/Grubb II for the synthesis of cycloalkenes.[170,171]

Future work could cover a larger survey of diols such as polyols (glycerol or xylitol for example) and the study of other hydroformylation catalyst such as $Ru_3(CO)_{12}$-2,2'-bipyridine or Rh_2O_3 or $PtCl_2$ [165] which would not require a phosphine ligand. The potential of other DODH reducing agents could then be considered such as sodium sulfite or secondary or benzyl alcohols. These reducing agents would make for a more economic and environmentally friendly reaction system. The most desirable reducing agent remains the hydrogen and carbon monoxide mixture and it could be reconsidered with future DODH report or with the use of co-catalysts to activate hydrogen in the reaction. The idea of using a co-catalyst to activate H_2 or CO could be attempted using the original ruthenium Shvo's catalyst.

f. Experimental

i. General information: reagents and instruments.

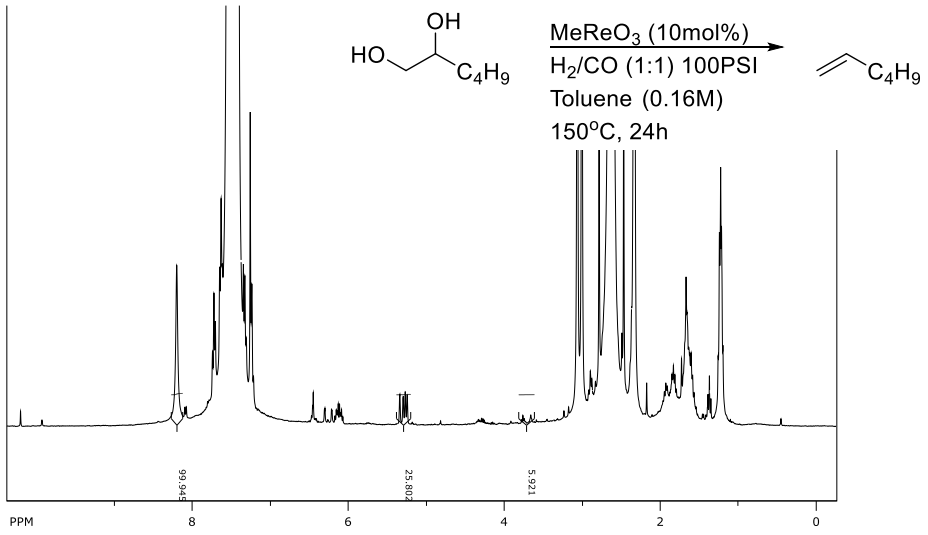
All reactants and catalysts were obtained commercially and used without further purification. All solvents were ACS grade and were used directly (unless otherwise described in the procedures). ^{1}H NMR spectra were collected on Varian VX300 MHz or VNMRS 400 MHz instruments. The NMR data were processed using SpinWorks[102] and ACD[103] software. Gas chromatograms were collected on a Shimadzu GC-2014 equipped with an AOC 20i+s auto sampler, both with 3% SE-54 packed column, FID and thermal

program 40°C for 5 min; 20 deg/min to 250°C; then 7 min at 250°C. GC-MS-EI analyses were performed on a Thermo-Finnigan instrument using a Stabil-wax capillary column.

ii. Representative procedure for DODH reactions using H_2/CO as reducing agent

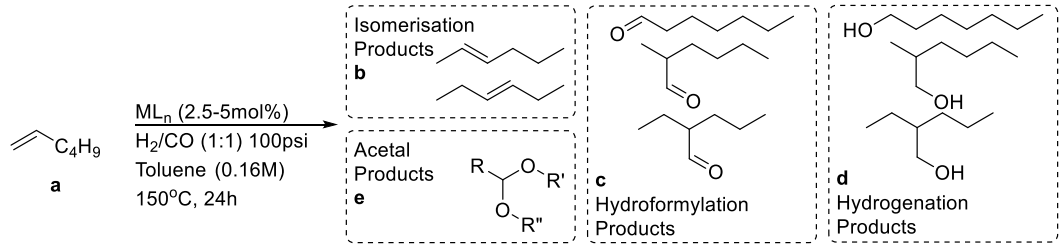
1,2-Hexanediol (1.00 mmol, 0.12 mL), NH_4ReO_4 (0.10 mmol, 27 mg) and toluene (7.5 mL) were added to a 150 mL Fischer Porter Tube. The reactor was closed and nitrogen was bubbled into the mixture *via* the dip tube for at least 60 sec. The reactor was pressured with hydrogen to 50 psi then with carbon monoxide to 100 psi (CO tank regulator delivering 150 psi). The reactor was placed in an oil bath at 150°C for 24 h while stirring magnetically. After cooling to room temperature, a 100 µL aliquot of the reaction mixture was removed and added to $CDCl_3$ (0.6 mL) and 2.0 µL DMF as internal standard for NMR analysis.

Entry III.7.1.1

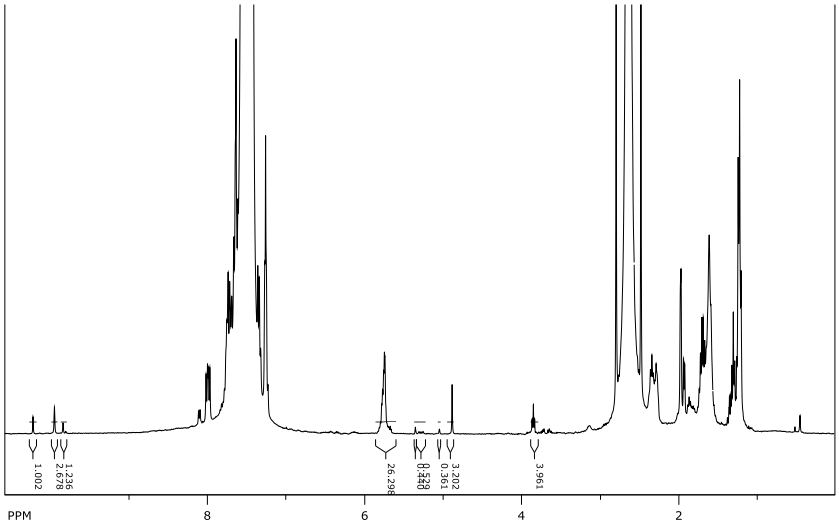


iii. Representative procedure for hydroformylation of 1-hexene

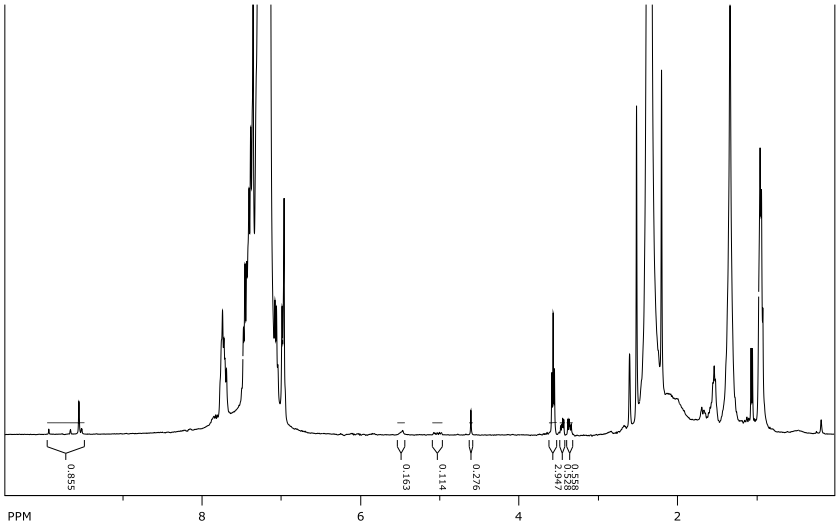
1-Hexene (1.00 mmol, 0.13 mL), $HRh(CO)(PPh_3)_3$ (0.025 mmol, 23 mg) and toluene (7.5 mL) were added to a 150 mL Fischer Porter Tube. The reactor was closed and nitrogen was bubbled into the mixture *via* the dip tube for at least 60 sec. The reactor was pressured with hydrogen to 50 psi then with carbon monoxide to 100 psi (CO tank regulator delivering 150 psi). For higher pressure the reaction was run in a Parr stainless steel reactor. The reactor was placed in an oil bath at 150°C for 24 h while stirring magnetically. After cooling to room temperature, a 100 µL aliquot of the reaction mixture was removed and added to $CDCl_3$ (0.600 mL) and 2.0 µL DMF as internal standard for NMR analysis.



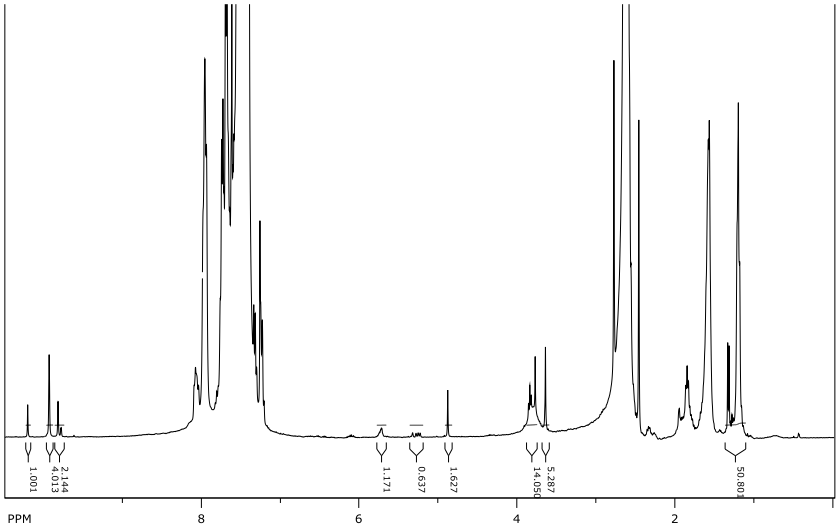
Entry III.7.2.1 with $HRh(CO)(PPh_3)_3$, no additive



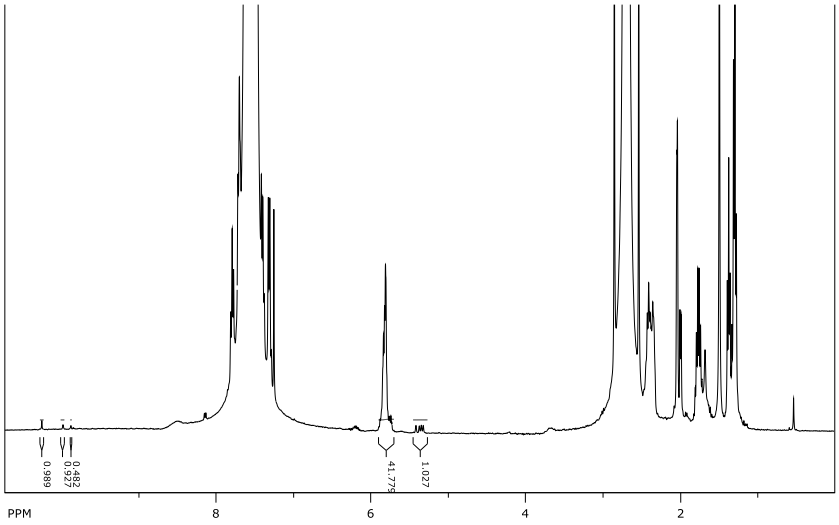
Entry III.7.2.2 with HRh(CO) (PPh_3)$_3$, and dppe 25mol%



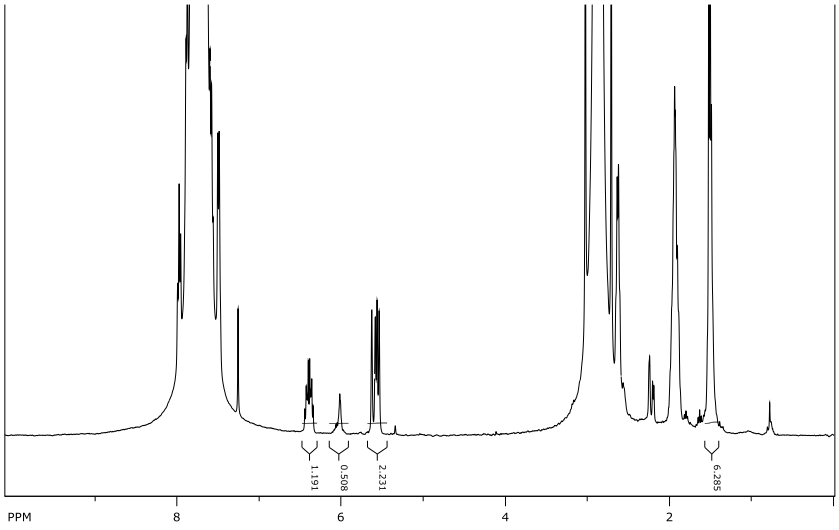
Entry III.7.2.3, with HRh(CO) (PPh_3)$_3$, PPh_3 (100mol%)



Entry III.7.2.4 with $Co_2(CO)_8$, 100 psi



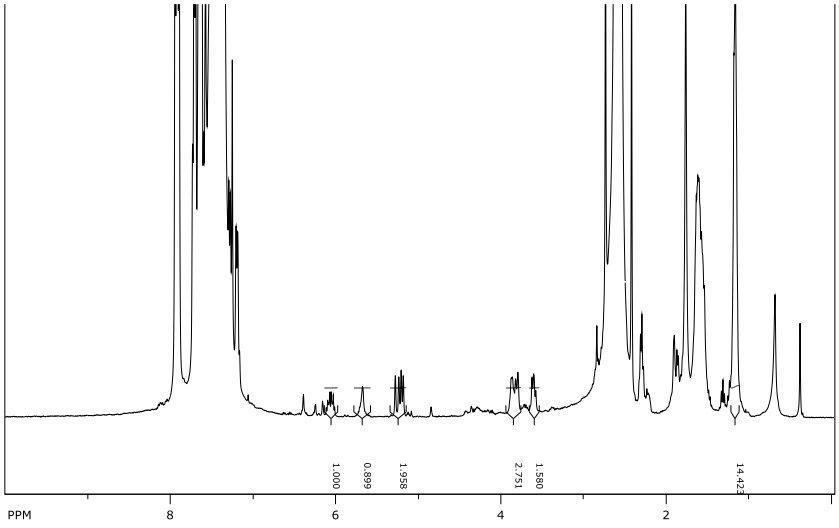
Entry III.7.2.5 with $Co_2(CO)_8$, 500 psi



iv. Procedure for the DODH of 1,2-hexanediol catalyzed by $IReO_2(PPh_3)_2$ and triphenyl phosphine as reducing agent

1,2-Hexanediol (1.00 mmol, 0.13 mL), $IReO_2(PPh_3)_2$ (0.005mmol, 4 mg), triphenyl phosphine (1.00 mmol, 262 mg) and toluene (7.5 mL) were added to a 150 mL Fischer

Porter Tube. The reactor was closed and nitrogen was bubbled into the mixture *via* the dip tube for at least 60 sec. The reactor was pressured with hydrogen to 50 psi then with carbon monoxide to 100 psi (CO tank regulator delivering 150 psi). For higher pressure the reaction was run in a stainless steel reactor. The reactor was placed in an oil bath at 150ºC for 24 h while stirring magnetically. After cooling to room temperature, a 100 µL aliquot of the reaction mixture was removed and added to $CDCl_3$ (0.6 mL) and 2.0 µL DMF as internal standard for NMR analysis.



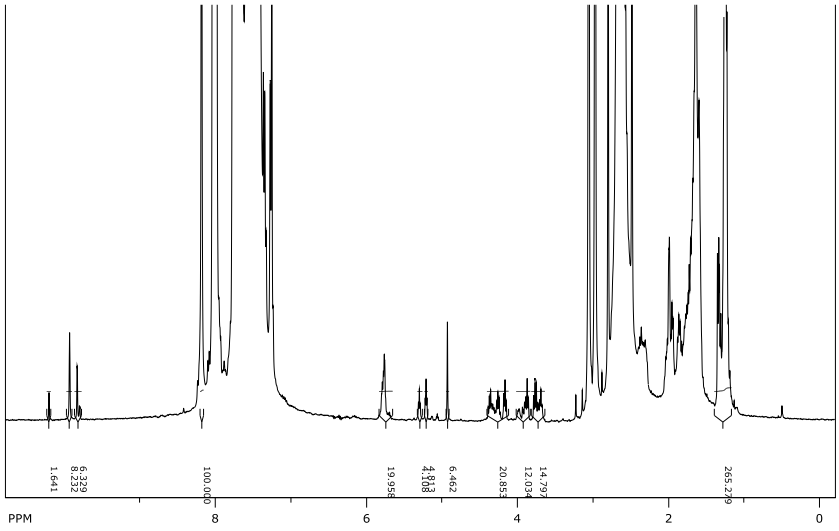
v. Representative procedure for DODH/hydroformylation tandem reactions

The glycol (1.00 mmol) [1,2-hexanediol (0.12 mL) [or 1-phenyl-1,2-ethanediol (138 mg) or cis-1,2-cyclooctanediol (144 mg)], $IReO_2(PPh_3)_2$ (0.005 mmol), $HRh(CO)(PPh_3)_3$ (0.025 mmol, 23 mg), triphenyl phosphine (2.00 mmol, 524 mg) and toluene (7.5 mL) were added to a 150 mL Fischer Porter Tube. The reactor was closed and nitrogen was bubbled into the mixture *via* the dip tube for at least 60 sec. The reactor was pressured

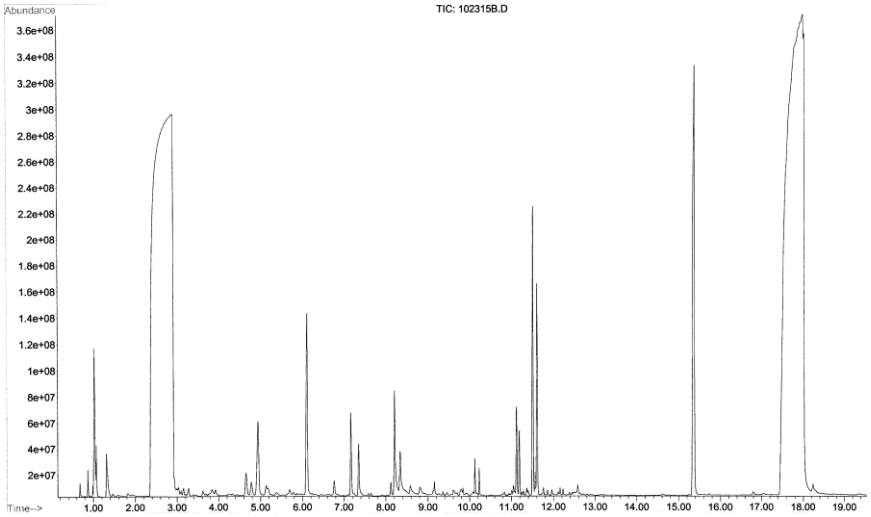
with hydrogen to 50 psi then with carbon monoxide to 100 psi (CO tank regulator delivering 150 psi). For higher pressure the reaction was run in stainless steel reactor. The reactor was placed in an oil bath at 150ºC for 24 h while stirring magnetically. After cooling to room temperature, a 100 µL aliquot of the reaction mixture was removed and added to $CDCl_3$ (0.6 mL) and 2.0 µL DMF as internal standard for NMR analysis. 0.5mL of the reaction mixture was submitted to GC and/or GCMS.

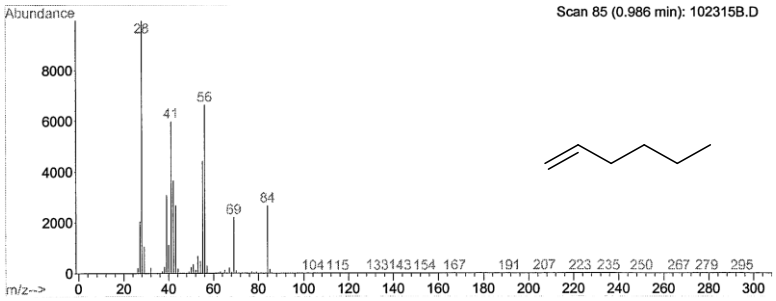
*Tandem DODH-HF on 1,2-hexanediol (*Figure III. 7.13*)*

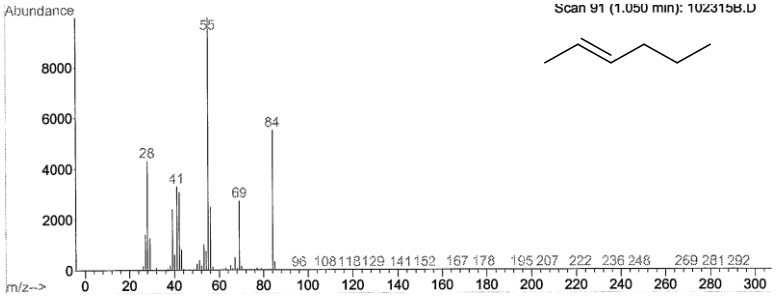
^{1}H NMR

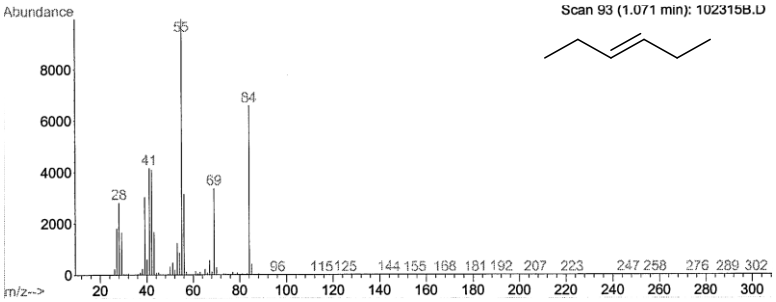


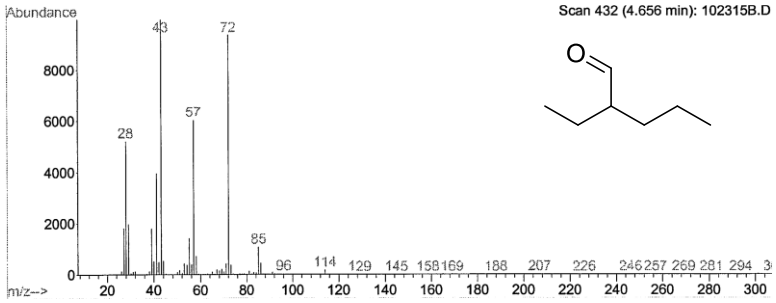
GCMS

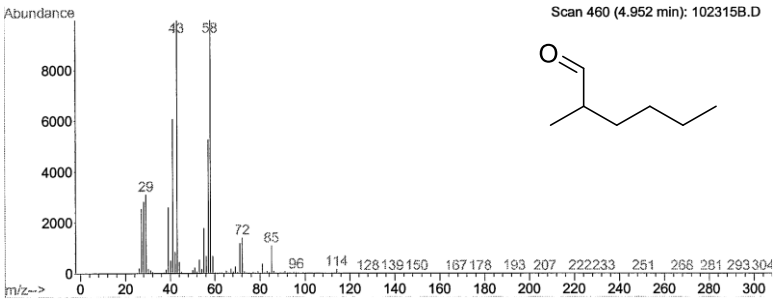


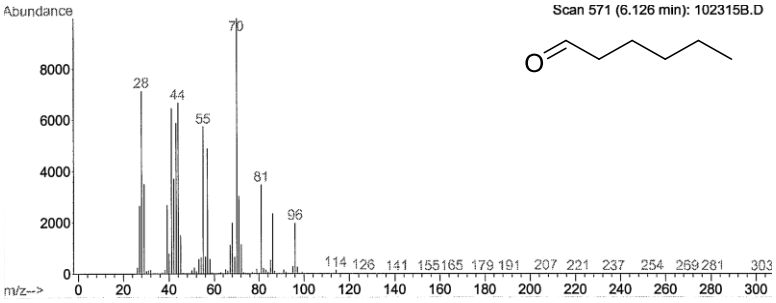

Abundance
Scan 85 (0.986 min): 102315B.D
28
41
56
69
84
m/z-->

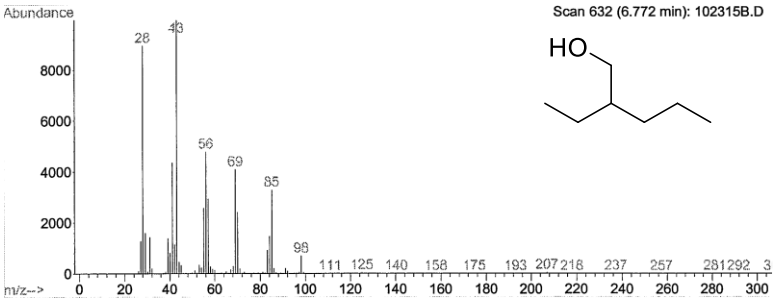

Abundance
Scan 91 (1.050 min): 102315B.D
55
84
28
41
69
m/z-->

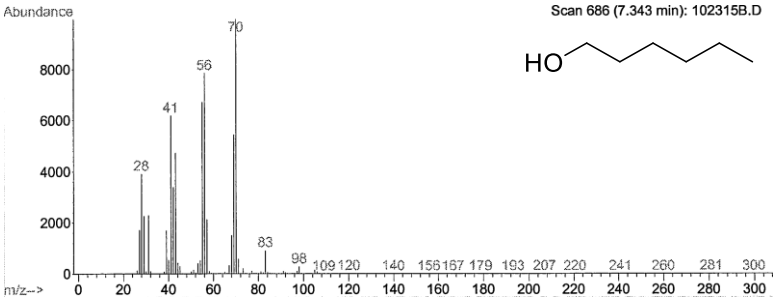

Abundance
Scan 93 (1.071 min): 102315B.D
55
84
41
69
28
m/z-->


Abundance
Scan 432 (4.656 min): 102315B.D
43
72
O
57
28
85
m/z-->


Abundance
Scan 460 (4.952 min): 102315B.D
43
58
O
29
72
85
m/z-->

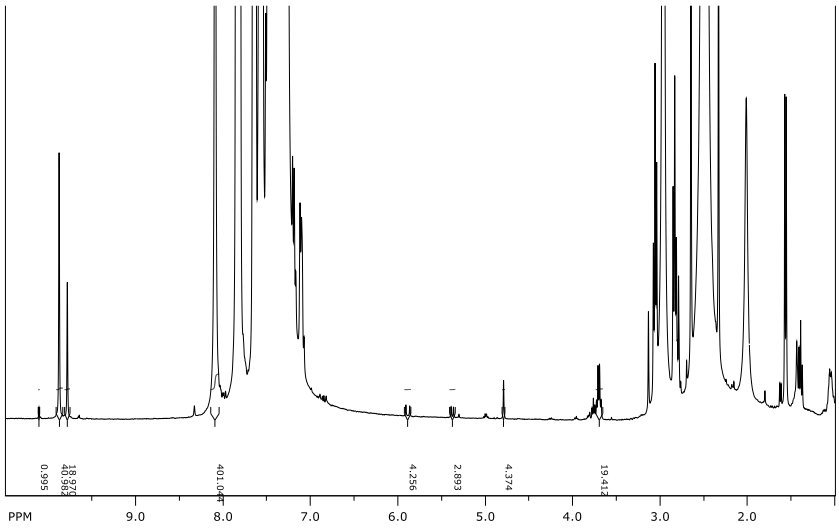




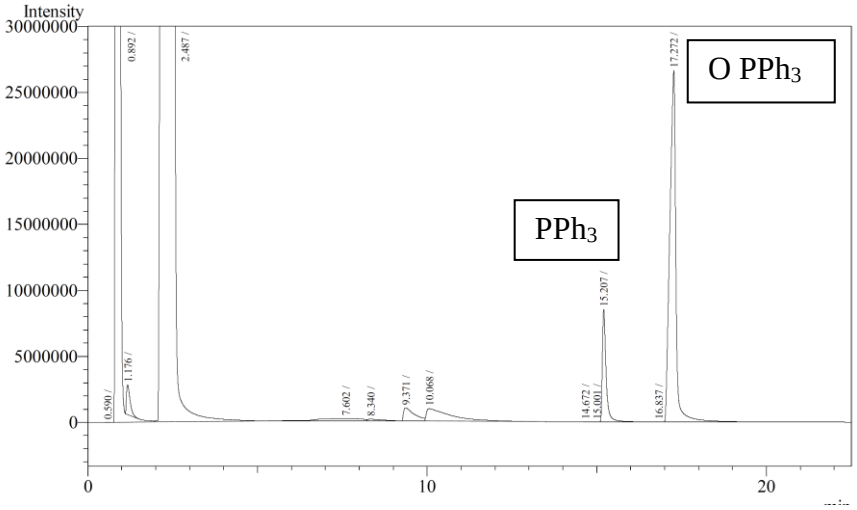


Tandem DODH-HF on 1-phenyl-1,2-ethanediol

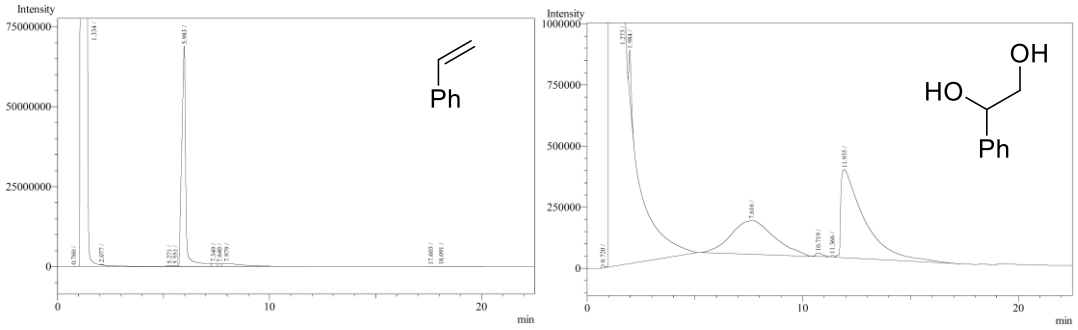
^{1}H NMR



GC

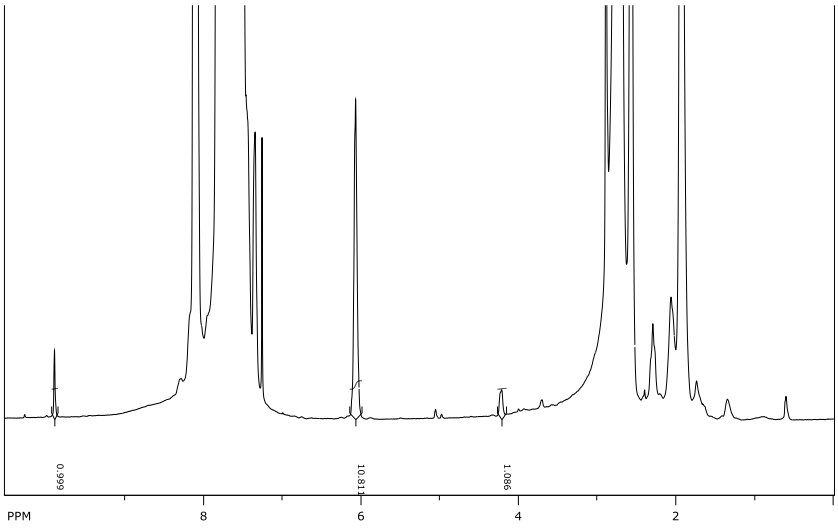


GC references:

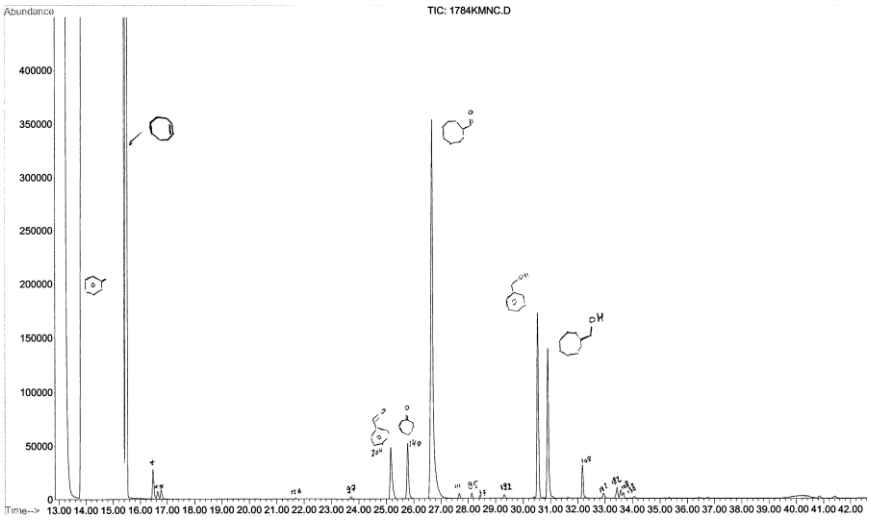


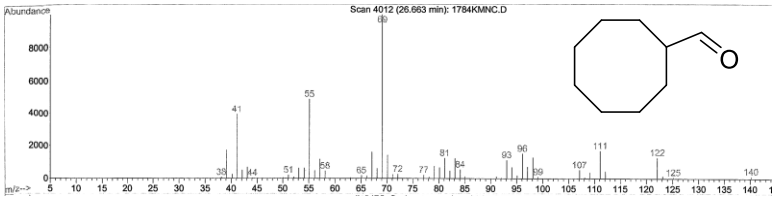
Tandem DODH-HF on cis-1,2-cyclooctanediol

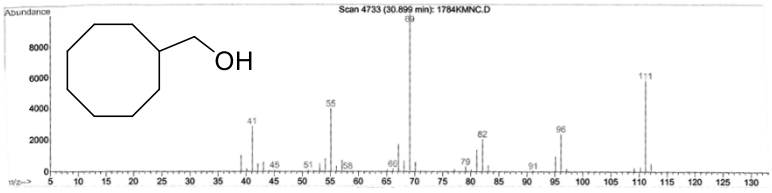
^{1}H NMR



GCMS


TIC: 1784KMNC.D
Abundance
Time-->


Scan 4012 (26.663 min): 1784KMNC.D
Abundance
m/z-->


Scan 4733 (30.899 min): 1784KMNC.D
Abundance
OH
m/z-->

Chapter IV. Mechanistic Study of $IReO_2TPP_2$-Promoted Reaction of Alcohols with Triphenylphosphine

1. Introduction and Background

We described in Chapter I the multiple efforts made in the development of selective chemical transformations of biomass-derived, oxygen-rich feedstocks by re-functionalizing C-O bonds.[3,172] As shown in Figure I.1.1 dehydration and deoxygenation processes allow reduction of the oxygen content and therefore an energy increase of carbohydrates and derived sugar alcohols.[8,173–176] In addition to the DODH reaction which we described in detail already, hydrodeoxygenation (HDO, Figure IV.1) is one such reaction that is practiced in chemical industry and in the laboratory.[10,177–179] The HDO of activated mono-alcohols (benzylic/allylic/tertiary) can be effected by H_2/Pd-C[180–182] or reaction with Lewis acid/hydridic reagents, proceeding via carbocations. Heterogeneous metal- and metal-oxide catalysts, e.g. Pd-C, Ra-Ni and MoS_xO_y, WO_x, ReO_x are used industrially for the HDO of unactivated alcohols and phenols,[183–185] but these reactions require severe conditions and often have limited product selectivity.[186–188] The homogeneously catalyzed HDO of alcohols is rather little known, but terminal glycols have been converted to terminal alcohols with modest selectivity by low valent Ru-complexes.[13,189] Recently, the selective HDO of aryl ethers[190] and phenols,[191] having strong Csp^2-O bonds, has been disclosed, catalyzed by nickel and iridium complexes.

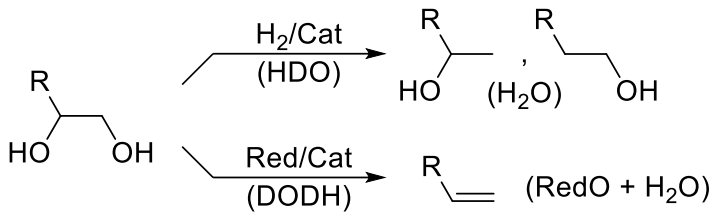


Figure IV.1 Hydrodeoxygenation (HDO) and Deoxydehydration (DODH) of alcohols

Oxo-metal complexes have been used in catalytic dehydration,[192,193] deoxydehydration,[15] and oxidation[194,195] of alcohols. From these reported systems we thought about of using this ability of oxo-metal complex to activate C-O bonds for the deoxygenation of mono-alcohols. At first G. Kasner and J. M. McClain carried out a stoichiometric reaction of an oxo-Re(v) species, $IReO_2TPP_2$ (**1**)[168], with the activated alcohol benzhydrol, $Ph_2CH(OH)$. They were hoping to demonstrate the ability of this rhenium oxo complex to deoxygenate this alcohol, but after 24h at 150°C in benzene the major product they observed was the hydrocarbon dimer; 1,1,2,2-tetraphenylethane, $Ph_2CHCHPh_2$, in 90% yield (Figure IV.2a). The only other organic product they detected in the reaction mixture was the dibenzhydrol ether $(Ph_2CH)_2O$ (5% yield).

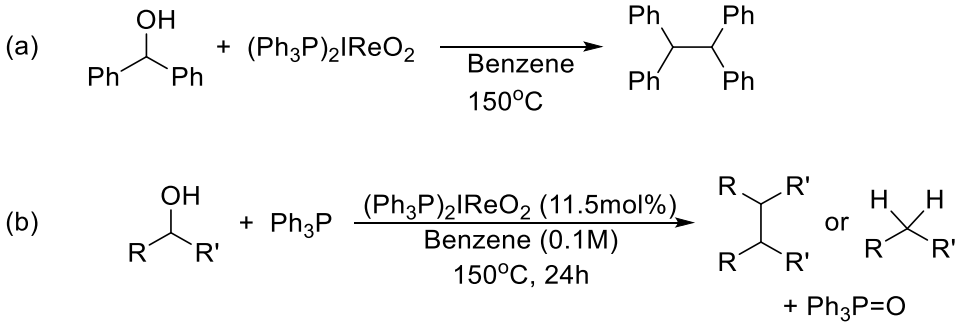


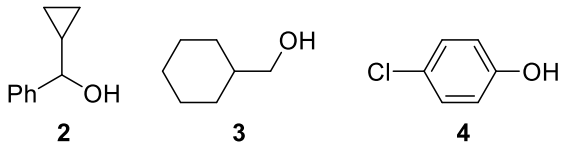
Figure IV.2 Deoxygenation (DO) and reductive coupling (RC) of alcohols

They were able to run this reaction under catalytic conditions using 11.5 mol% of **1**, and triphenylphosphine as stoichiometric reducing agent giving the dimer in 80% yield.

With Gabrielle we were able to decrease the catalyst loading to 1 mol% with 90% yield in dimer after 168h. We also expanded the scope of alcohol substrates for the reaction (Table IV.1). In a similar way with 11.5% of **1** fluorenol (entry IV.1.3) provided bifluorenyl in 91% yield. Mixed coupling between benzhydrol and fluorenol provided a mixture of homo and hetero coupled products (entry VI.1.4). The slightly less activated 1-phenylethanol provided 43% yield in dimer product after a longer reaction time along with 56% yield in ketone (entry IV.1.5). Cinnamyl alcohol, $PhCHCHCH_2OH$, was reactive as well and provided a 64% yield of isomeric diene dimers (entry IV.1.6). The isomeric alcohol 1-phenyl propan-1-ol (entry IV.1.7) gave a similar yield and product distribution as cinnamyl alcohol. The non-benzylic activated alcohol sorbyl alcohol reacted to give a 62% yield of tetraene dimers (entry IV.1.8). The reaction on triphenylmethanol and benzoin, an α-hydroxyketone, entry IV.1.9 and entry IV.1.10, gave in each case as the major product the deoxygenated hydrocarbon, instead of the dimer. Finally benzyl alcohol (entry IV.1.11) gave after 95h at 150^{o}C a mixture of dimers ($PhCH_2CH_2Ph$, PhCHCHPh), deoxygenation product (toluene), ether $(PhCH_2)_2O$ and benzaldehyde (98% conversion).

The cyclopropyl-phenylmethanol **2** was largely unreacted after 168h at 150^{o}C under the same reaction conditions (PPh_3/**1** in benzene) and only a trace of dimer product was formed without being fully characterized. The alcohol could have help us to probe if the reaction mechanism involves a radical. A radical formation on the carbon next to the cyclopropyl ring would resonate making the three membered ring open. Without surprise the primary, unactivated alcohols cyclohexane methanol **3** and para chlorophenol **4** did

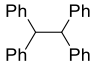
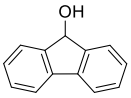
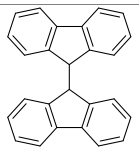
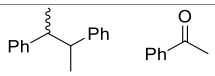
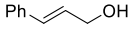
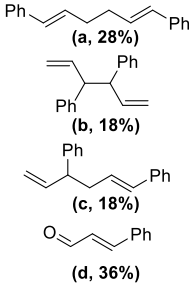
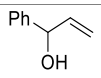
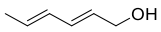
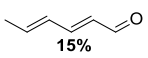
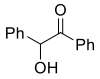
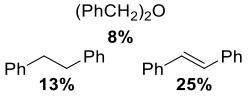
not react under these conditions (100 h at 150°C in benzene) due to their stronger C-O bonds.



2 **3** **4**

Figure IV.3 Other alcohols tested 2, 3 and 4

Table IV.1 Deoxygenation and reductive coupling of alcohols by $PPh_3/IReO_2(PPh_3)_2$ (1)[a]

Entry	Substrate	Products & Yields[b,f]
IV.1.1 IV.1.2[d]		 **80% (65%)[c]** **90%**
IV.1.3		 **91%**
IV.1.4	 + 9-fluorenol (1:1)	 $R^1=R^2$=Ph **24%** $R^1=R^2$=9-fluorenyl **48%** R^1=Ph, R^2=9-flurenyl **13%**
IV.1.5		 **43%** **56%** **(1:1 meso : *d,l*)**
IV.1.6		 **(a, 28%)** **(b, 18%)** **(c, 18%)** **(d, 36%)**
IV.1.7		**a (30%), b (17%), c (17%)**
Entry	Substrate	Products & Yields[b,f]
IV.1.8		C_{12}-tetraenes (isomers) **62%**  **15%**
IV.1.9		 **75%**
IV.1.10		 **92%**
Entry	Substrate	Products & Yields[b,f]
IV.1.11 e		Ph−CH_3 Ph−CHO **29%** **23%** $(PhCH_2)_2O$ **8%**  **13%** **25%**

a) 0.1M reactants (ROH and PPh_3), 0.011M **1**, benzene solvent, 150°C (sealed tube), 24h. b) Yields determined by ^1H NMR integration with Me_2NCHO or CH_2ClCH_2Cl internal standard. c) Isolated yield after column chromatography. d) 1mol% **1**, 168h. e) 92h reaction time f) PPh_3 was almost entirely consumed for the ROH to R-H reactions, but ca. 50% remained for the ROH to R-R reactions

The formation of dimer product under these condition can be called a reductive coupling (RC) of alcohol. The RC process and also the catalytic deoxygenation (DO) have not been much described using homogeneous transition metal catalysis. The deoxygenation of activated alcohols was reported using stoichiometric Cp_2TiCl[196] and $W^{ii}Cl_2(PMe_3)_4$[197], and catalytic PMHS/$PdCl_2$.[198] Only the stoichiometric RC of activated alcohols by reduced Ti-compounds[199–202] and La/Me_3SiCl,[203] and a Cu-catalyzed La/Me_3SiCl variant have been reported.[204]

In the initial publication[169] on these results we proposed a possible catalytic cycle for the deoxygenation and reductive coupling reactions (Figure IV.1), beginning with association of the alcohol with **1** to give an alkoxo-hydroxo rhenium species **A**. Such complexes have been suggested intermediates for other oxo-metal-mediated alcohol reactions, e.g. dehydration, oxidation and allylic alcohol isomerization.[192,193,205–208] From the complex **A** R-H and/or R-R could be produced via concerted or stepwise oxidative elimination[§] generating an oxidized Re(vii) species, $IReO_3TPP_2$ (**C**); **C** could then be reduced by the phosphine to regenerate **1**. Alternatively, another alcohol molecule could coordinate to **A** making an oxo-dialkoxo species **B** (similar complexes have been described).[209–212] Complex **B** could then undergo oxidative elimination to produce the dimer. Analogous alkoxide or –glycolate reduced metal species were reported for the catalytic HDO of alcohols and phenols by heterogeneous reducible solid metal oxides[186–188] and the homogeneous oxo-metal catalyzed deoxydehydration of glycols[23,33,35,36,41,45,46,83]and epoxide deoxygenation.[33,213]

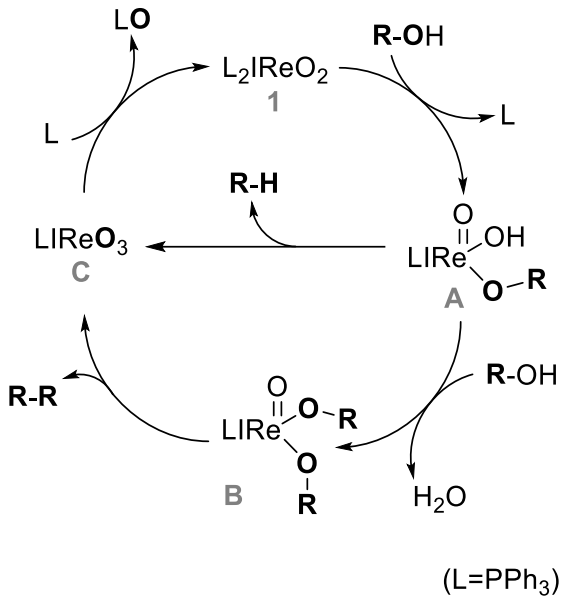


Figure IV.4 Possible catalytic cycle for deoxygenation and reductive coupling

One the most interesting parts of the mechanism is the C-O bond breaking step. In reported stoichiometric DO and RC reactions this step was suggested to take place via the generation of organic radicals by the metal-alkoxide complex.[214] Our oxo-Re-catalyzed reductive coupling reaction was facilitated by the presence of aryl and vinyl substituents on the alcohol, showed limited regioselectivity with allylic alcohols, and the selectivity toward deoxygenation (entries IV.1.9 and IV.1.10) could support the formation of Re-alkoxo intermediates (**A** or **B**) and derived carbon-radicals. Also experiments conducted by Gabrielle were inconclusive to implicate C-radical intermediates (Figure IV.5). The reaction entry IV.1.1 was carried out in the presence of 1-2 equivalents of hydrogen donors and radical traps 1,4-cyclohexadiene, 9,10-dihydroanthracene or xanthene,[215,216] without any significant change in the dimer yield (80 ± 5%) or the H-donors derived products (Figure IV.5).

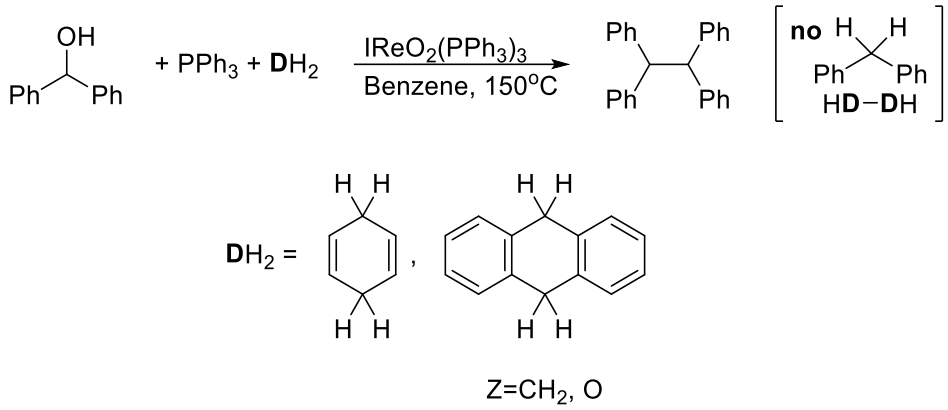
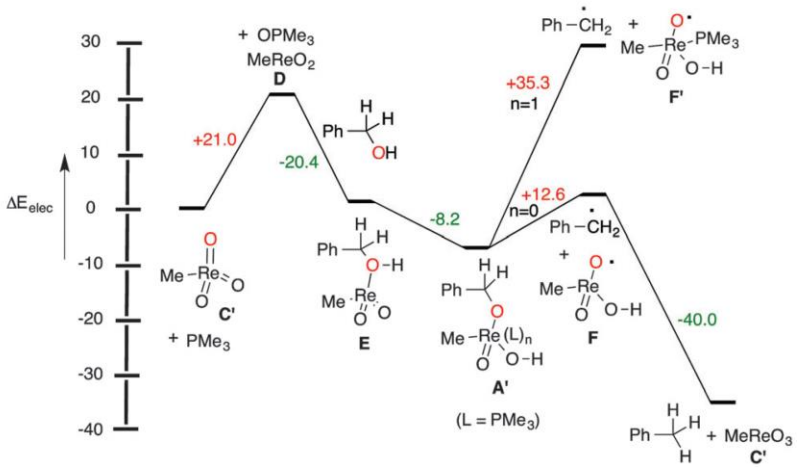


Figure IV.5 (Non)Effect of H-Donors on reductive coupling

Prof. Nicholas conducted an initial DFT computational study of the deoxygenation of $PhCH_2OH$ by the model catalyst $MeRe^{vii}O_3$ (**C'**). He found the mechanistic pathway in Figure IV.6for **1** to be exoergic at each stage from $MeRe^{v}O_2$ (**D**) via intermediates **E**, **A'** and **C'** (Figure IV.6). The C-O bond in alkoxy-ReO_x species is indicated to be much weaker by a calculated dissociation energy of only 13 kcal/mol for conversion of $PhCH_2$-ORe(O)Me(OH) (**A'**) to benzyl radical and **F**, which increases to 35 kcal for the more accurate model intermediate for catalyst **1**, $PhCH_2$-ORe(O)Me(OH)(PMe_3) (**A'->F'**). This energy is still much lower than for $PhCH_2$-OH homolysis (81 kcal).[217] While either homolytic or non-homolytic pathways for C-O cleavage in the DO and RC reactions may be operative, a weakened C-O bond in an intermediate Re-alkoxide was suggested to be the likely source of catalytic activation.



B3LYP method and LANL2DZ/6-31G(d) basis sets

Figure IV.6 Calculated energetics of $MeReO_2$-promoted alcohol deoxygenation

The catalytic RC and DO system we have uncovered offers a way to reductively convert alcohols to hydrocarbons under neutral condition avoiding pre-functionalization of the alcohol.[218–222] This reaction could have a lot of potential for the conversion of biomass derived alcohols to organic platform chemicals and to provide an alternative to the Guerbert reaction.[223]

Gabrielle Kasner is currently working on expanding the substrate scope and to find more practical and economical reductant/catalyst pairs. Dr. Nicholas is expanding the DFT calculations. In this chapter I describe my recent (unpublished) efforts to identify the reactive intermediates and the catalytic pathway involved

2. Results

a. Study of the catalyst in solution; ligand dissociation

A solution of $IReO_2(PPh_3)_2$ (Figure IV.7) in benzene-d^6 was prepared under nitrogen and wrapped in aluminum foil to avoid any potential interaction with air and light. The

first observation was a color change of the solution from the purple color of the original solid catalyst to a crimson red after only 30 minutes. After a day in the solvent the color was light brown to yellow; past one day the sample was bright yellow (Figure IV.8a).

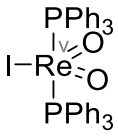


Figure IV.7 Pre-catalyst $IReO_2(PPh_3)_2$

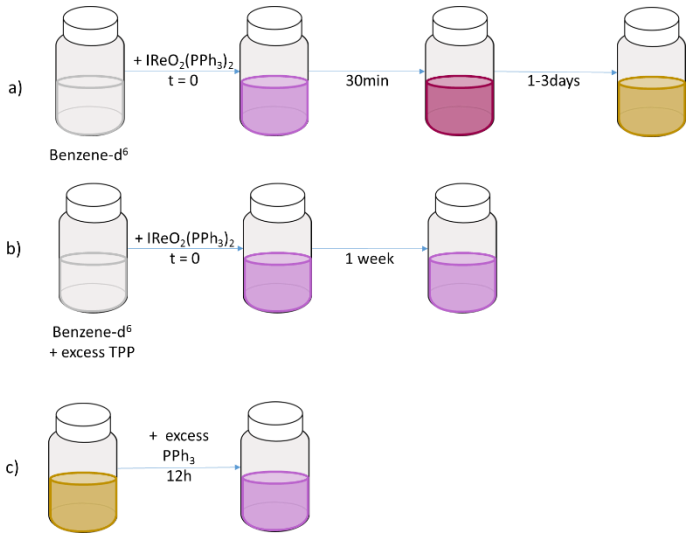
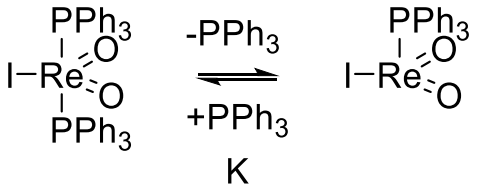


Figure IV.8 Color changes of the pre-catalyst $IReO_2(PPh_3)_2$ in solution

Since the pre-catalyst has phosphine ligands we were also able to probe what was happening during these color changes by ^{31}P NMR. The starting Re^{V} complex has a symmetrical structure (C_2 crystallographic symmetry, intermediate between trigonal-bipyramidal and square-pyramidal)[168] and thus only one phosphorus NMR signal with a chemical shift of 4.6 ppm. After 30 min when the sample had turned into a crimson color, in addition to the signal of the starting complex we could detect two new phosphorous

signals at -5 ppm and -11.0 ppm. The peak at -5 ppm corresponds to NMR shift for free triphenylphosphine. We followed the evolution of the ^{31}P spectrum of the sample as the color changed over time; the closer the color was to yellow the larger the two shielded signals became. After 3 days, the phosphorous signal of the starting complex was very small and the two other signals were dominant.

Our interpretation of these observations is that one of the triphenylphosphine ligands of the $IReO_2(PPh_3)_2$ complex dissociates from the metal center when dissolved in benzene. In order to confirm this we added $IReO_2(PPh_3)_2$ to a solution containing approximately 5 equivalents of triphenylphosphine in benzene-d^6. This sample did not change color and stayed purple for over a week (Figure IV.8b) and its ^{31}P NMR spectrum showed a strong signal at 4.6 ppm from $IReO_2(PPh_3)_2$ and only traces of the two signals observed previously. To probe further whether the process was reversible an excess of triphenylphosphine (~5 equivalents) was added to a bright yellow sample of $IReO_2TPP_2$ in benzene (0.01 mol/L) that had aged for 3 days. In less than an hour the sample darkened to a crimson color (Figure IV.8c) and overnight the solution was back to the original purple color of $IReO_2TPP_2$. In the ^{31}P NMR spectrum the signal at 4.6 ppm was again predominant and the -11.0 ppm signal was very small.



Purple *Yellow*

Figure IV.9 Pre-catalyst ligand dissociation equilibrium in solution

From the observed behavior of $IReO_2(PPh_3)_2$ in solution we speculated on the potential dissociation of a phosphine ligand in solution. This ligand dissociation is not clearly mentioned in the literature. A report from Chung and co-worker suggested the intermediacy of $IReO_2(PMe_3)$ as a potential active catalyst for hydrosilylation of carbonyls starting from $IReO_2(PMe_3)_2$, but they provided only the calculated energy for this dissociation (7.3 kcal/mol).[224] As this process can be stopped or reversed by adding an excess of triphenylphosphine, we concluded that the two species are equilibrium. In the alcohol reductive coupling reaction (RC) the Re^{v} oxo-complex is used in catalytic quantity (1-10 mol%) and triphenylphosphine in two equivalents (100 mol%). From our observations of the catalyst behavior in the presence and absence of added phosphine we conclude that the $IReO_2(PPh_3)_2$ form of the catalyst would be favored under catalytic reaction conditions.

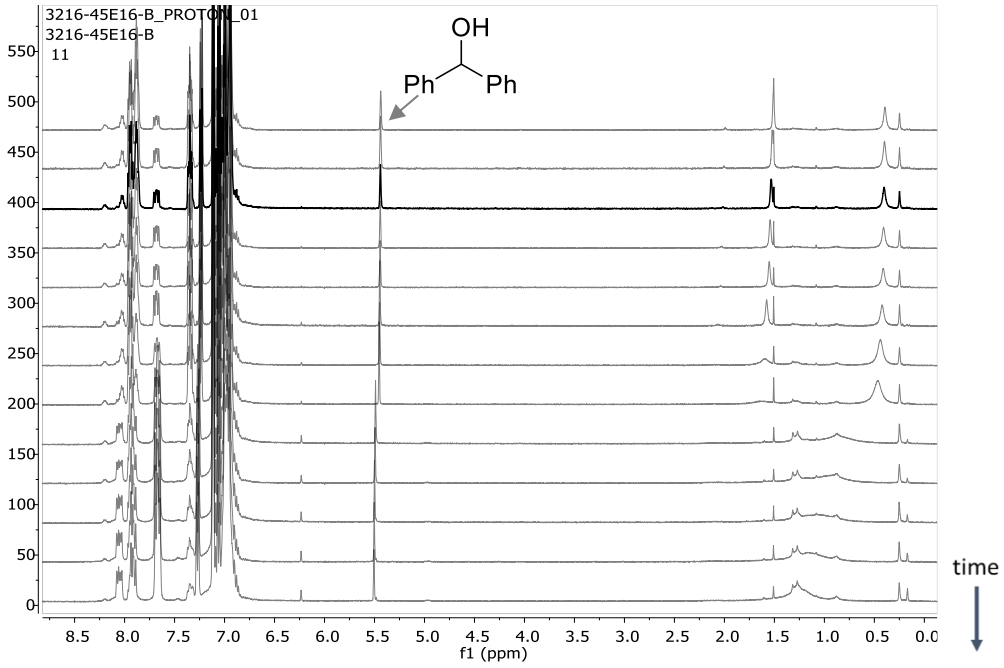
In order probe the mechanism of the RC reaction we carried out a series of stoichiometric reactivity experiments to elucidate the sequence of pre-catalyst transformations in the presence of either or both reactants.

b. Stoichiometric reaction NMR study: $IReO_2(PPh_3)_2$ and benzhydrol

We started the study of the interaction of the pre-catalyst with alcohols by a series of experiments at room temperature. We intended with these experiments to observe potential key intermediates of the catalytic cycle. We prepared first a set of three samples with a stoichiometric quantity of alcohol and pre-catalyst in a sealed NMR tube purged with nitrogen with benzene-d^6 as solvent: A, one without additional reagent; B, one with the pre-catalyst aged in the solvent to dissociate PPh_3; and C, one with a 1:1 alcohol +

PPh_3. We kept these sample at room temperature for several weeks and followed the changes overtime by ^{1}H and ^{31}P NMR spectroscopy.

- A [1:1:1 ratio of $IReO_2(PPh_3)_2$ + $Ph_2CH(OH)$ + PPh_3]
- B [1:1 ratio of $IReO_2(PPh_3)_2$ + $Ph_2CH(OH)$]
- C [1:1 ratio of {$IReO_2(PPh_3)$+free PPh_3} + $Ph_2CH(OH)$]



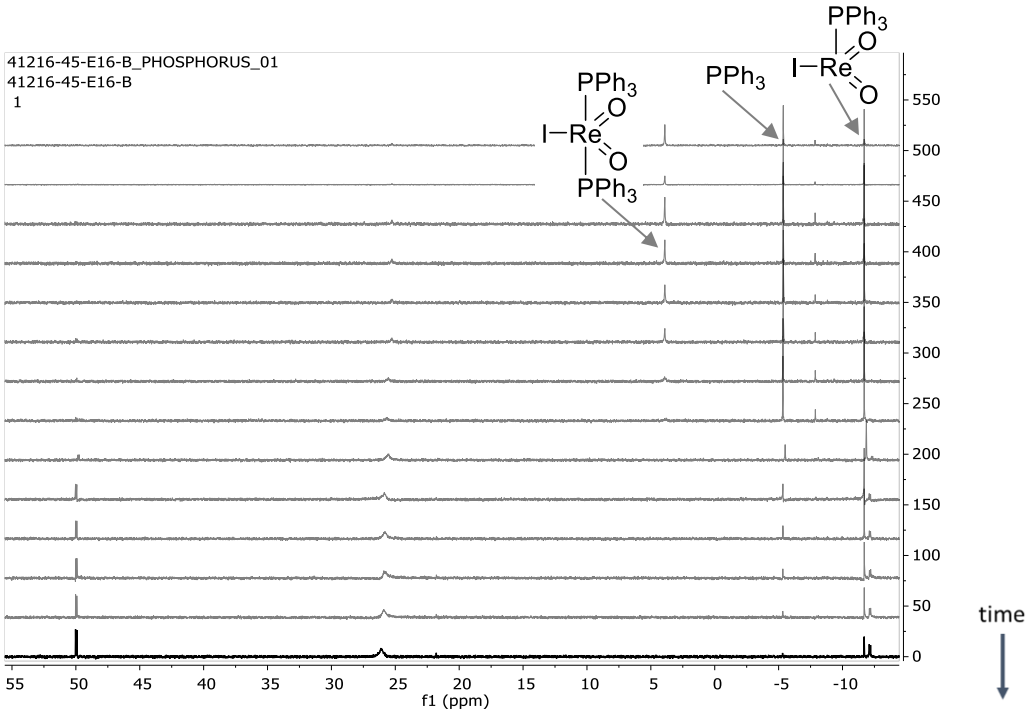


Figure IV.10 ^{1}H (left) and ^{31}P (right) NMR spectra of sample B over a month

The three samples evolved in a similar way and changed color from purple to yellow. The only difference we observed was in the rate of these changes from sample to sample- C was the fastest, then B, and A was the slowest. In the ^{1}H NMR spectra we observed a new singlet at 6.23 ppm and in the ^{31}P NMR spectra we detected PPh_3 dissociation and the formation of a new signal at -7.16 ppm. Later we also saw the formation of phosphine oxide at 25.4 ppm and a set of two doublets at 50.66 ppm and -11.46 ppm (J_{PP}= 16 Hz). These new NMR signals demonstrate reaction of the catalyst with benzhydrol and the formation of new species. The formation of some triphenylphosphine oxide is evidence of a redox process occurring in the NMR tube overtime and at room temperature.

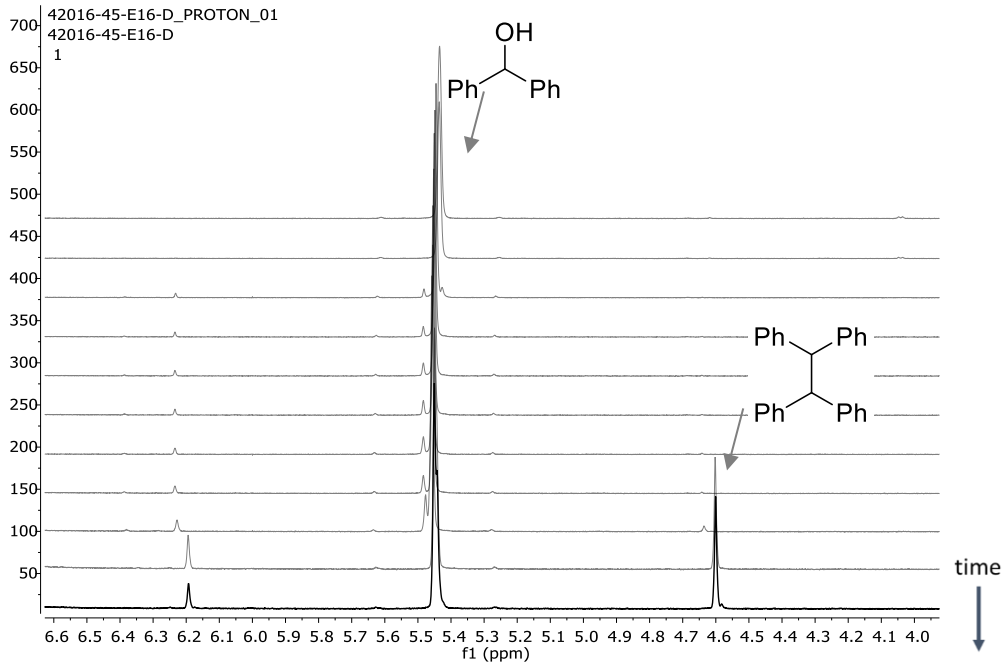
After several weeks no more changes were observed in the NMR spectrum. Then sample **B** was warmed to 50^{o}C. After many days at this moderate temperature the dimer product was not detected, but a color change from yellow to bright pink was. This color

change corresponded to the appearance of a signal at 9.6 ppm in the ^{1}H NMR spectrum and a broad ^{31}P NMR signal in the phosphine oxide region ~27-24 ppm. We added more PPh_3 (5 equivalents) to this sample and observed an immediate color change to yellow and overnight to purple. Both of these colors are close to the color of the mono PPh_3 $ReIO_2$ catalyst and starting catalyst the bis-PPh_3 $ReIO_2$ catalyst.

Following these stoichiometric experiments we prepared two additional samples in a similar way but using an excess of benzhydrol - 5 and 10 equivalents (D and E).

- D [1:5 ratio of $IReO_2(PPh_3)_2$ + $Ph_2CH(OH)$]
- E [1:10 ratio of $IReO_2(PPh_3)_2$ + $Ph_2CH(OH)$]

In these experiments at room temperature similar but faster changes in the proton and phosphorus NMR spectra were observed. When sample [D] was heated at 50°C, the dimeric product $Ph_2CHCHPh_2$ was detected (4.7 ppm, s, C*H*) after about 32h.



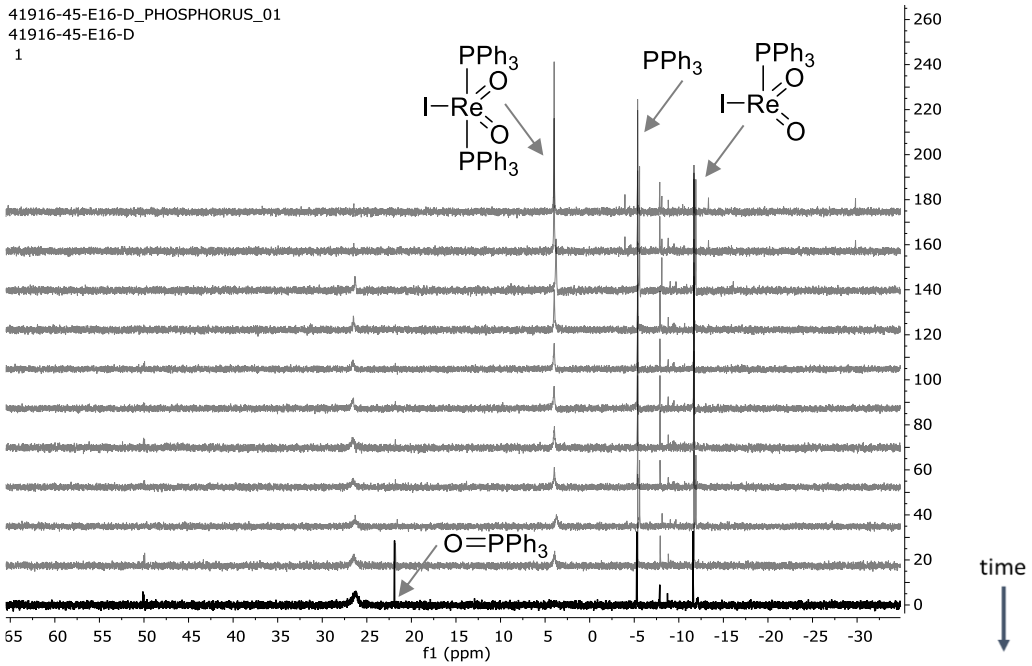


Figure IV.11 ^{1}H (left) and ^{31}P (right) NMR spectra of sample D room temperature to 50ºC

The set of two doublets in the ^{31}P NMR (50.66 ppm, -11.46 ppm) formed only in the sample containing the alcohol. Each of these shows a J coupling of 15 Hz. This value is too low to be from a direct P-P bond and is more typical of a ^{2}J or ^{3}J phosphorous-phosphorous coupling.[225] With chemical shifts of ~50 and ~ -12 ppm a complex with a (PPh_3)Re(O=PPh_3) subunit is suggested (Figure IV.12). Indeed the -12 ppm peak is really near that of the mono PPh_3-$ReIO_2$ complex (~11 ppm) and the 50 ppm signal is downfield of O=PPh_3 (at 25 ppm), in the region of some reported phosphine oxide metal-complexes.[226,227] To further support this assignment we decided to prepare a reaction sample with a 1:5 ratio of $IReO_2(PPh_3)_2$ to O=PPh_3. After 24h this sample solution was yellow and the same pair of doublets in the ^{31}P NMR spectrum was observed. The structure assigned to this rhenium complex is thus (PPh_3)ReO_2I($OPPh_3$).

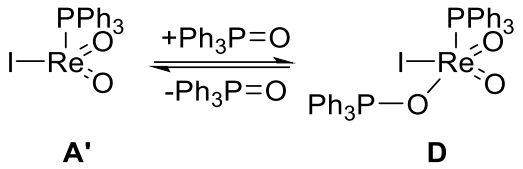


Figure IV.12 Formation of phosphine oxide-rhenium complex

Mass spectrum, ESI+/- and APCI+/-, of samples E and B_2 were collected but with both of these ionization methods we observed only one mass signal with a Re isotope pattern (^{185}Re 37.4% and ^{187}Re 62.6%) in the ESI – and this mass (1170.94 m/z) does not match a reasonable formulas for an alcohol-rhenium complex or a phosphine-rhenium-phosphine oxide complex.

IR spectra of most of the samples (A – E) were collected in order to compare at least the rhenium-oxo absorptions in the 900-1000 cm^{-1} region. With samples in benzene we used a liquid cell to acquire IR spectra for which we had to substrate the benzene but the subtraction would not work as liquid IR of benzene has several broad signals. After all the potential new signals we found were too small to allow a clear interpretation.

The stoichiometric interactions of the pre-catalyst and benzhydrol were studied in detail without obtaining as much information as we hoped for, particularly to characterize species derived from the coordinated alcohol. We decided vary the alcohols to include both unreactive and reactive ones in the reductive coupling, namely ethanol, benzyl alcohol, 1-phenylethanol, and cinnamyl alcohol. Some of these were chosen because their protons would NMR couple and show splitting patterns in the ^{1}H NMR. The samples containing $(PPh_3)_2ReO_2I$ together with ethanol or benzyl alcohol changed color overnight from purple to green; the sample with cinnamyl alcohol followed the same color changes after two days; the sample with 1-phenylethanol changed color from purple to crimson

after two days. In the ^{1}H NMR spectra of the samples that changed to green- ethanol, benzyl alcohol and cinnamyl alcohol- two new sets of the protons appeared from molecules derived of the starting alcohol. The largest signals were from the free (uncomplexed) alcohols and the two new sets of signals were shifted substantially up field (Δ(ppm) from 1.1 to 1.7) of the free alcohol. The integrated H-NMR signals for these peaks in the samples containing ethanol and benzyl alcohol was about 1:2 and about 1:5 with cinnamyl alcohol. These signals are assigned to alkoxide rhenium complexes, LRe-O-C$\underline{H}_2$-R.[168,228,229] In the case of 1-phenylethanol after a week we could see the formation of one set of similar alcohol derived species in very small quantity (<10%).

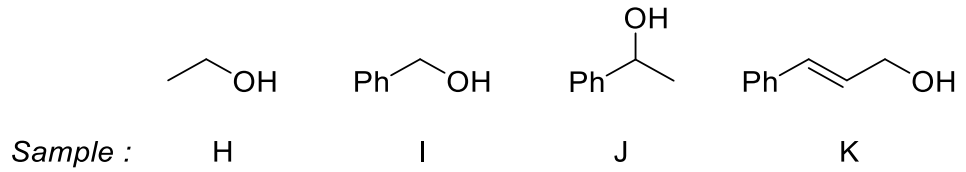


Figure IV.13 List of the alcohols studied

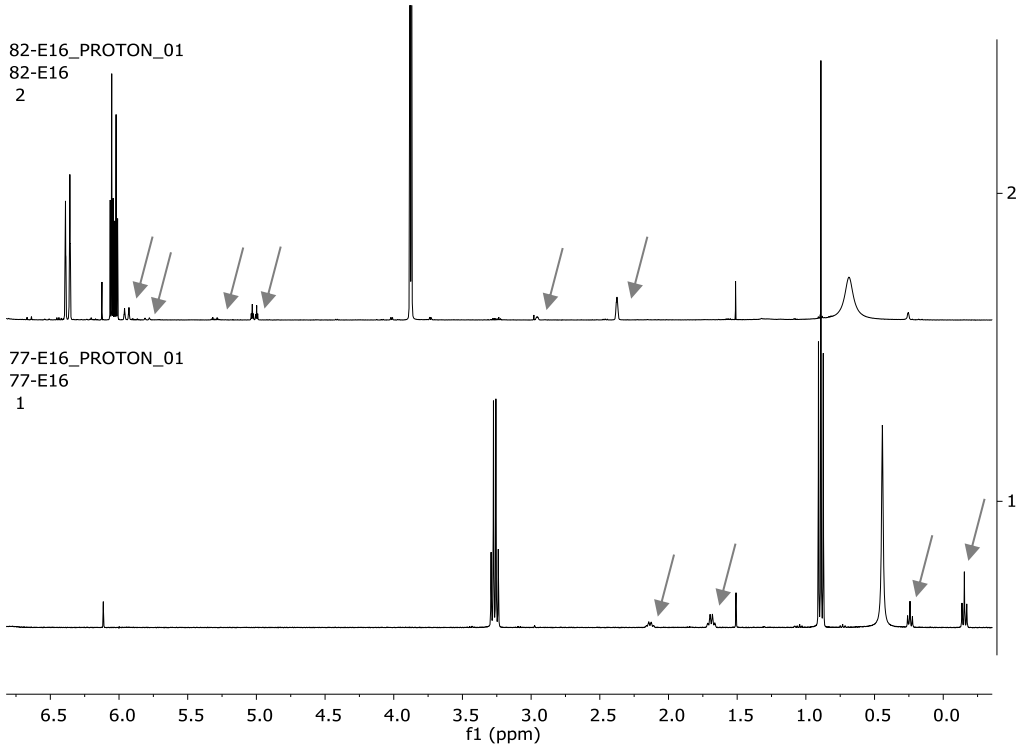


Figure IV.14 ^{1}H NMR spectra of sample [PhCHCHCH$_2$OH + 1] (top) and [CH$_3$CH$_2$OH + 1] (bottom) with 5:1 ratio of alcohol to rhenium complex

ROH[a]		EtOH		PhCH$_2$OH	PhCH(OH)CH$_3$		PhCHCHCH$_2$OH		Ph$_2$CH(OH)
		Shift[b]	J[c]	Shift[b]	Shift[b]	J[c]	Shift[b]	J[c]	Shift[b]
New signals in ROH + IReO$_2$(PPh$_3$)$_2$ Sample	^{1}H	2.12 q 0.24 t 1.67 q -0.16 t	6.99 6.99	3.56 s 2.70 s	3.62 q 3.21 q 2.03 s 6.61 d 0.87 d 0.73 d 1.07 d 0.23 m 0.52 d	6.5 6.85 7.14 6.60 6.65 1.47	5.94 d 5.00 dt 2.36 s 6.10 s	15.99 3.91	6.25 s, 4.97 m small 1.08 s
	^{31}P[d]	**-7.45** **-10.65**		**-6.76** **-10.93**	**-3.97** -7.88 -8.12 -8.82 -9.34 **-14.11**		-6.88, **-10.45**		72.66 **49.97** d,(J_{PP}=16) 21.79 -7.93 -8.81 -9.57 -10.65 **-12.14** d,(J_{PP}=16)

a) 1:5 IReO$_2$(PPh$_3$)$_2$ to ROH in 0.8 mL d^6-benzene, b) Shift in ppm, c) J coupling in Hz d) Strongest signals bolded

Table IV.2 New signals in ^{1}H and ^{31}P NMR of ROH/IReO$_2$(PPh$_3$)$_2$ samples

A singlet was found near 6.1 ppm for the samples with ethanol and cinnamyl alcohol, which is similar to the 6.23 ppm signal in the samples containing benzhydrol. In the cases of the two other alcohols, benzyl alcohol and 1-phenylethanol, we found a multiplet, seemingly a doublet of doublets at 6.5 ppm. This signal could be a CH proton but we are lacking evidence to make a definitive assignment.

In parallel with the proton NMR spectra studies ^{31}P NMR spectra were also acquired for each of these samples. The presence of these two sets of alcohol derived protons correlated with the presence of a large signal at -10.5 to -10.9 ppm and a smaller one at -7 to -6 ppm in the ^{31}P NMR spectrum. Only the ^{31}P NMR spectrum of [1-phenylethanol + $IReO_2(PPh_3)_2$] sample showed more signals, very similar to the [benzhydrol+ $IReO_2(PPh_3)_2$] sample, between -7 and -10 ppm and also with an additional strong phosphorus signal at -14.11 ppm.

From these observations we suggest that two different types of intermediate complexes are formed; one for each set of new ethylic signals. With the different ratios of these proton signals we can imagine that only one molecule of alcohol is coordinated to two different rhenium species (II, Figure IV.15) with one favored over the other, or that we have close to a 1:1 ratio of these rhenium complexes with one that has two alcohol units coordinated to it (I, Figure IV.15).

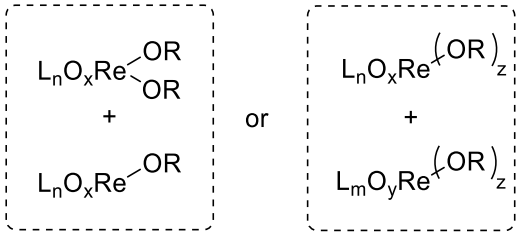


Figure IV.15 Potential complexes formed with alcohols

In an attempt to address if we are looking at case I or II in Figure IV.15 we varied the ratio of rhenium to alcohol in two samples with 1:2 and 1:10 ratios. In fact by providing more or less alcohol equivalents to the catalyst in the case of I, Figure IV.15 we observed a variation of the integration of the ethylic protons by favoring/disfavoring the mono or dialkoxi complex. Such variations in the ratio of catalyst to alcohol were made with ethanol. We observed a different rate of color changes between each of these two samples (1:10 faster than 1:2). After 24h the integrations value were collected for each of the new ethylic proton sets. The ratio of the two new CH_2 signals was not much different for each of these samples (Table IV.3). This result shows the independency of the alcohol coordination to this concentration. Subsequently we are more likely to be in the case of II, Figure IV.15 with both rhenium complexes having the same number of alkoxy group coordinated.

CH_2 ratio **1**:EtOH	CH_3CH_2OH 3.26 ppm	2.13 ppm	1.68 ppm
1:2	1.28	0.29	0.43
1:5	4.19	0.25	0.56
1:10	9.32	0.25	0.42

Table IV.3 Integration ratios of new CH_2 signals in ethanol/catalyst samples

Now these complexes could have one or two phosphine ligands attached as well. But it seems logical to anticipate that the larger proton signal (also the most up field one for ethanol, benzyl alcohol and cinnamyl alcohol) goes with the larger phosphorus signal (-10.5 to -10.9 ppm), leaving the -6 to -7 ppm phosphorus signal related to the other alcohol derived proton signal.

c. Kinetic study

The kinetic study of the reductive coupling of benzhydrol required some adjustment of the reaction conditions. A higher boiling point solvent than benzene, chlorobenzene (PhCl), was tested and it provided the same yield (~ 80%, Figure IV.16 with T = 150 ^{o}C). With this solvent we also able to decrease the temperature to the boiling point of chlorobenzene (Figure IV.16, T = 125 ^{o}C) and obtain a 75% yield.

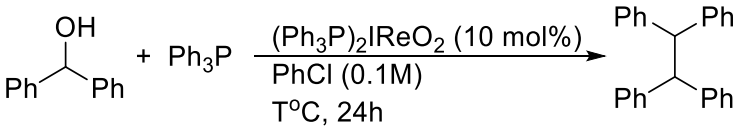
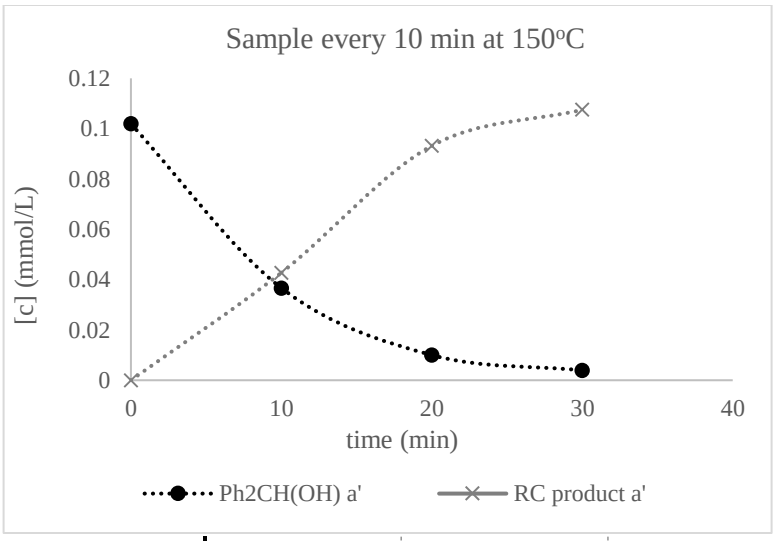


Figure IV.16 Reductive coupling of benzhydrol in chlorobenzene

We planned on following the reaction by NMR over time. In order to have an accurate quantification we needed to add an internal standard to the reaction mixture and to make sure the standard does not react in the reaction. Hexamethylbenzene and cyclooctane were good candidates as internal standard. We tested their accuracy by running the reductive coupling reaction of benzhydrol with an added quantity of internal standard. Both of the reactions hexamethylbenzene and cyclooctane were efficient and spectators in the reaction. We choose hexamethylbenzene for its higher boiling point (265^{o}C) over cyclooctane (149^{o}C).

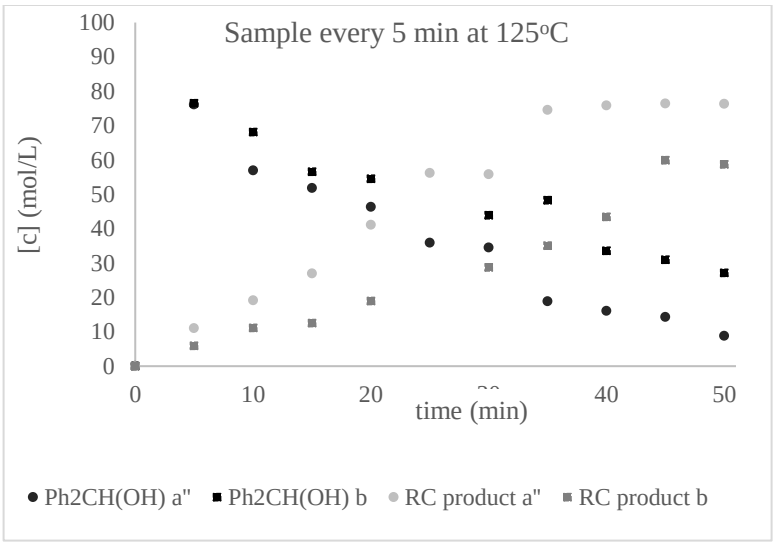
We started the kinetic study by running the reaction at 150^{o}C and taking a sample every 10 min (Figure IV.17). In this set of data points we discovered that under these reaction conditions the reaction was almost complete within 30 minutes. Since we would like to study the initial reaction rates we would have to look at the first 10 min of the reaction.



mmol/L	[$IReO_2TPP_2$]	[$Ph_2CH(OH)$]	[PPh_3]
a’	10	100	100

Figure IV.17 Kinetic plot 1

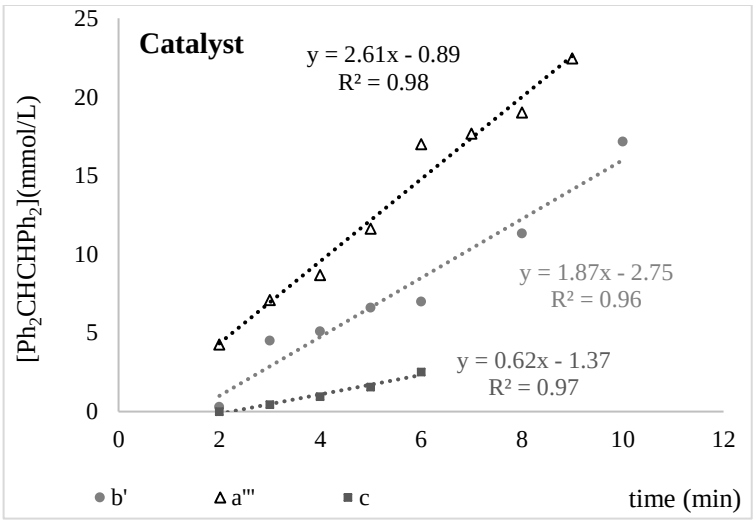
We lowered the temperature to 125ºC and the sampling time to every 5 min (Figure IV.18). This time we tried two different concentration of catalyst (0.01 and 0.005 mol/L). After 50 min the reaction was nearly complete giving about 75% yield of the dimer product for the higher concentration of the catalyst and about 60% for the lower concentration of catalyst. These sets showed that at 125ºC the initial rate period in is in the first 15 min of reaction.



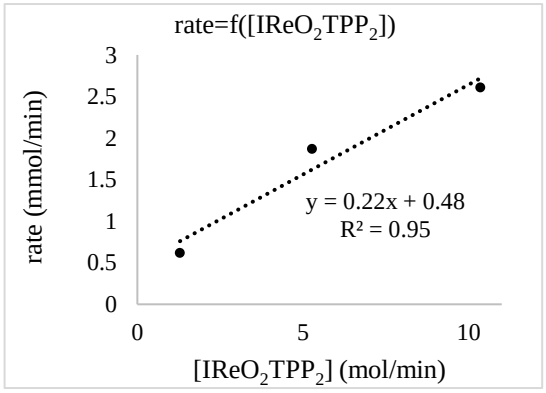
mmol/L	$[IReO_2TPP_2]$	$[Ph_2CH(OH)]$	$[PPh_3]$
● a''	10	100	100
■ b'	5		

Figure IV.18 Kinetic plot 2

Subsequently the reaction at the same temperature (125ºC) was run but we took samples every minute (Figure IV.19) which allowed us finally to observe the initial rate of the reaction. Having three components in the reaction, $IReO_2TPP_2$, $Ph_2CH(OH)$ and PPh_3, several sets of reaction varying only the concentration of one component at a time were run. Staring by keeping the alcohol and reducing agent at a fixed concentration (0.10 M) the catalyst was changed with concentrations at 0.01, 0.005 and 0.001 M; (Figure IV.19). From this catalyst concentration variation we could see a clear trend in the rate- the rate increased with an increase of the catalyst concentration. With such a clear trend we plotted: rate=f($[catalyst]^n$) and varied n to find the reaction order in the catalyst. Having only three points in this data set the exact order could not be determined between 1 and ½.



mmol/L	$[IReO_2TPP_2]$	$[Ph_2CH(OH)]$	$[PPh_3]$
■ c	1		
● b’	5	100	100
Δ a’’’	10		



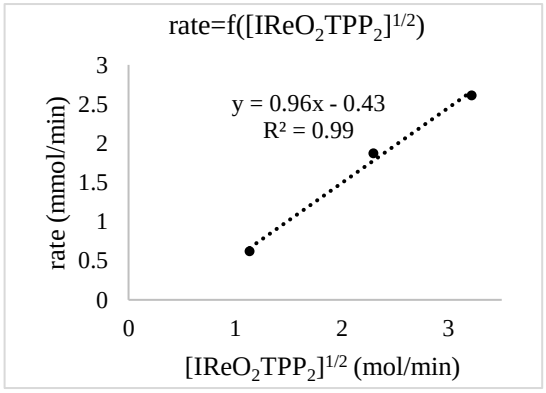
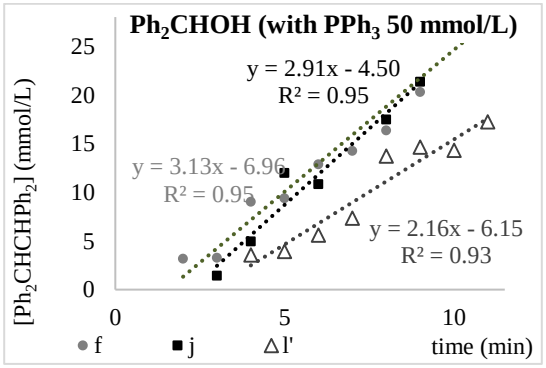


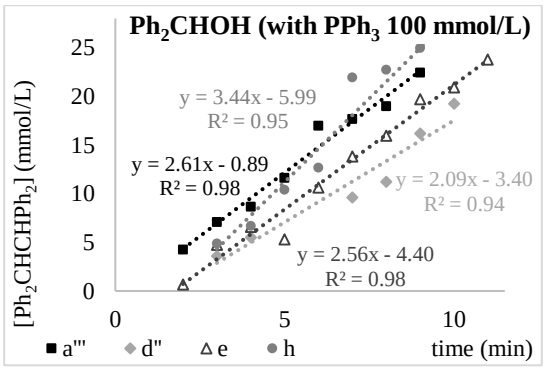
Figure IV.19 Kinetic plot 3

The same procedure of sampling every minute with the reaction running at 125ºC was applied to various concentrations of benzhydrol with a catalyst concentration of 0.01 M and for three different of triphenyl phosphine concentrations (Figure IV.20). In these plots there wasn't a systematic trend such as the one found for the catalyst concentration variation. Only in the case of $[PPh_3]$ = 0.2 M the reaction looked to have a dependency in

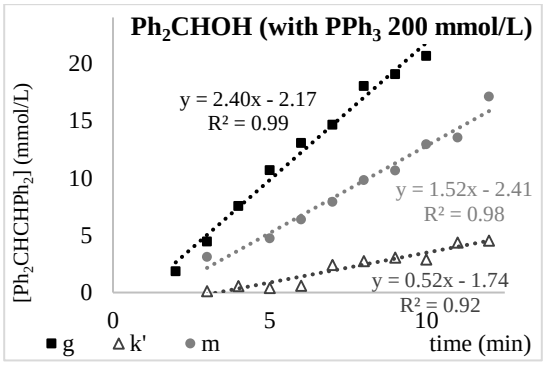
the alcohol, but this dependency is not linear as the rate is highest for the intermediate concentration of alcohol (0.1 M) and the lowest for the highest concentration of alcohol (0.2 M).



mmol/L	[IReO$_2$TPP$_2$]	[Ph$_2$CH(OH)]	[PPh$_3$]
■ j	10	50	50
● f		100	
Δ l’		200	



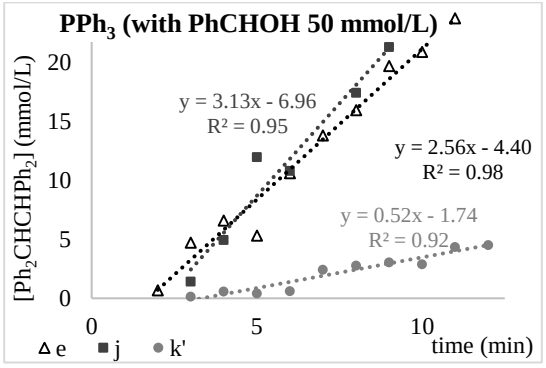
mmol/L	[IReO$_2$TPP$_2$]	[Ph$_2$CH(OH)]	[PPh$_3$]
Δ e	10	50	100
■ a’’’		100	
◆ d’’		200	
● h		500	



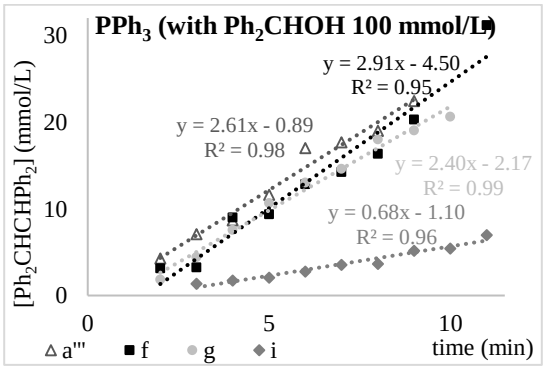
mmol/L	[IReO$_2$TPP$_2$]	[Ph$_2$CH(OH)]	[PPh$_3$]
Δ k’	10	50	200
■ g		100	
● m		200	

Figure IV.20 Kinetic plot 4

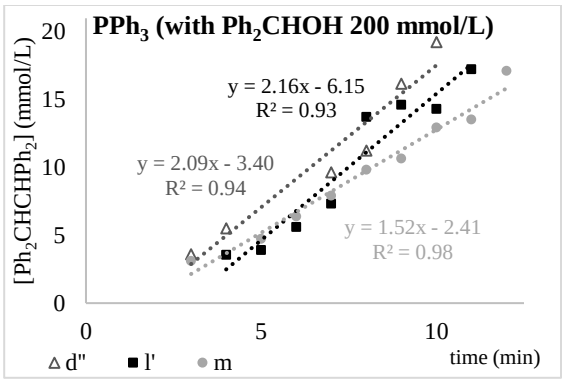
In the variations of triphenylphosphine molarity for a fix concentration of catalyst and alcohol we did not observe too much a general trend like in the plots with the alcohol variations. Only the highest molarity of the triphenylphosphine (0.5 mol/L) decreased the rate drastically (Plot : **PPh_3 (with Ph_2CHOH 100 mmol/L)**). Also when the molarity of alcohol was the lowest (0.05 mol/L) with the molarity of 0.2 mol/L of triphenylphosphine we saw a decrease of rate of the product formation (Plot: **PPh_3 (with Ph_2CHOH 100 mmol/L)**).



mmol/L	$[IReO_2TPP_2]$	$[Ph_2CH(OH)]$	$[PPh_3]$
■ j	10	50	50
Δ e			100
● k’			200



mol/L	$[IReO_2TPP_2]$	$[Ph_2CH(OH)]$	$[PPh_3]$
■ f	10	100	50
Δ a’’’			100
● g			200
◆ i			500



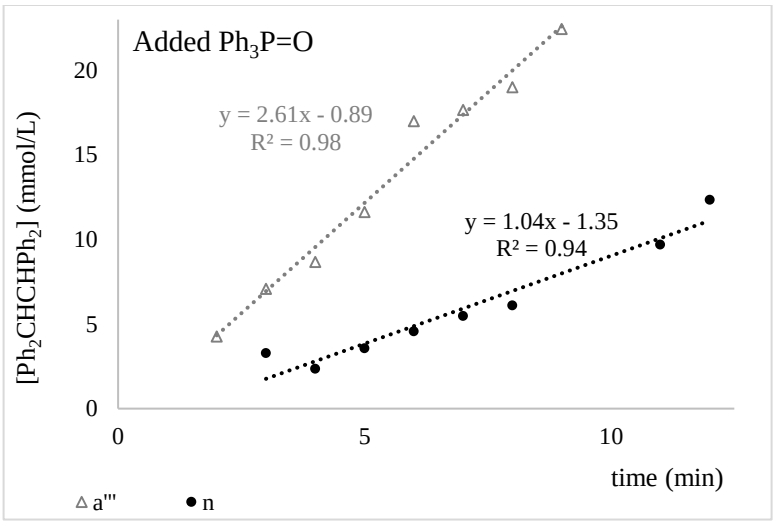
mol/L	[$IReO_2TPP_2$]	[$Ph_2CH(OH)$]	[PPh_3]
■ l’	10	200	50
Δ d’’			100
● m			200

Figure IV.21 Kinetic plot 5

In both the triphenylphosphine and alcohol concentration dependency plots we could not see any clear and linear trend of the rate of product formation. The concentration in reagents employed in these reactions were similar to the actual RC reaction conditions. At these concentrations of catalyst the independence of rate on phosphine and alcohol concentrations may indicate that the catalyst is "saturated". It could be of importance as usually kinetic studies are run with bigger differences of concentrations of the reactants. We can see that when the alcohol concentrations is low compare to the concentration of triphenylphosphine we could detect a drop in the rate of reaction. A high concentration of triphenylphosphine in the reaction significantly decreased the rate. With 0.1 and 0.05 mol/L concentrations of alcohol the rates found were similar but for 0.2mol/L concentration the rate decreased. We determined in the NMR stoichiometric experiments (Chapter IV.2.b) that the release of one of the PPh_3 ligands on the rhenium complex is first step for the reaction to proceed. We also determined that this dissociation was reversible (Chapter IV.2.a) and that an excess of triphenylphosphine disfavored this dissociation. The inhibition of the reaction by large quantity of PPh_3 in the kinetic study could then reflect the disfavored equilibrium of the ligand dissociation. Triphenyl phosphine could also have a role in other catalytic cycle’s intermediates since it is the

reducing agent of the reaction. All these data show that the mechanism of this reaction is complex and might involve both the triphenylphosphine and the alcohol in one or more interconversions of intermediates before or in the turnover-limiting step.

Triphenyl phosphine is used in the reaction as reducing agent. Over the catalytic cycle it would form triphenylphosphine oxide and this co-product of the reaction would accumulate after each catalyst turn over. The oxide is known to be a potential ligand for the rhenium complex and we have found evidence of the phosphine oxide-rhenium-phosphine complex in the stoichiometric study (Figure IV.12). With both of these observations one more reaction was run in which was added triphenylphosphine oxide (0.5 mol/L) (Figure IV.22) and monitored dimer formation overtime (at 125^{o}C taking a sample every minute). In this reaction we observed a decrease of the reaction rate. This behavior demonstrates an inhibition effect of triphenylphosphine oxide in the reaction therefore either the presence of large quantity the oxide disfavors the equilibrium step in which it is released or it interacts with the catalyst in an equilibrium forming an inactive rhenium complex.



mmol/L	[IReO$_2$TPP$_2$]	[Ph$_2$CH(OH)]	[PPh$_3$]	[O=PPh$_3$]
Δ a'''	10	100	100	0
● n				500

Figure IV.22 Kinetic plot 6

d. Computational results summary of (PPh$_3$)$_2$ReO$_2$I + MeOH (by K. Nicholas)

In light of the observations in the stoichiometric and kinetic study Dr. Nicholas started a DFT study of the IReO$_2$(PPh$_3$)$_2$ catalyzed reductive coupling reaction (Figure IV.23). Benzhydrol was replaced by methanol in order to decrease the calculation time. All the calculated energies are electronic energies, not corrected for zero point energy, temperature, solvation or entropy. The first step; the ligand dissociation (**1**->**1'**) as we observed in the stoichiometric experiments; has an energy penalty of 16.9 kcal/mol (ΔG would be substantially lower because of positive entropy change). The coordination of the alcohol to the rhenium center (**1'** -> **2**) is a favorable step with an energy change of -8.4 kcal/mol. On this intermediate **2** a second alcohol can coordinate to provide dialkoxy species **3** with the release of H$_2$O. From this dialkoxide complex **3** many pathways are

possible. However the concerted transition states for C-O/C-C bond-breaking/making could not be located. The other transition states between intermediates are not shown either. The direct formation of the methyl radical by breaking the C-O bond in **3** is up hill with 41.6 kcal/mol. $\cdot CH_3$ and Re^{v} **4a** could then form the dimer (C-C bond formation) product and a rhenium (vii) trioxo **5a** which would be reduced back the starting rhenium (v) complex (**1'**).

The reduction of the metal center of **3** by triphenylphosphine could occur to form a Re^{iii} dialkoxide intermediate **4b** with a penalty of only 7.3 kcal/mol. This Re^{iii} complex could form the radical $\cdot CH_3$ the same way as (**3** -> **4a**) to form **5b**. This C-O bond breaking step is again up hill and **5b** was found to have similar C-O bond dissociation energy compared to **4a**. Combining the $\cdot CH_3$ radical and Re^{iii} alkoxide **5b** could then allow the formation of the C-C bond to make dimer and provide **1'** back.

The two pathways described above involve rhenium dialkoxide intermediates, but alkyl-alkoxide-rhenium complexes arising from alkyl group migration to Re could also be intermediates. This would form by breaking one of the C-O bond and making a Re-C bond (**4b** -> **4b'**) with an overall -14.6 kcal/mol. The $\cdot CH_3$ radical and Re alkyl **5b'** can form from **4b'** with a penalty of 35.6 kcal/mol. Similar path with the formation of alkyl-alkoxide-rhenium complex can be obtained from **3** (**3** -> **4c**) with only a 27 kcal/mol penalty. The complex 4c releases the dimer and Re^{vii} **5a** in a stepwise or concerted transition state that is not yet located.

In all these proposed pathways the calculated energies between the catalyst intermediates are fairly reasonable. In fact with Dr. Nicholas computational results in our publication[169] we can anticipate that an activated alcohol would lower energies of C-O

bond breaking steps. The C-O bond breaking steps are the most uphill in energy (therefore rate-limiting) and the C-C bond forming steps were the most downhill in energy. The steps involving alcohol coordination, phosphine dissociation and oxo-Re reduction by PR_3 are generally moderately endo/exothermic.

These computational results provide a nice overall picture of the energies for each potential catalyst intermediates although it does not provide the energy of the transition state.

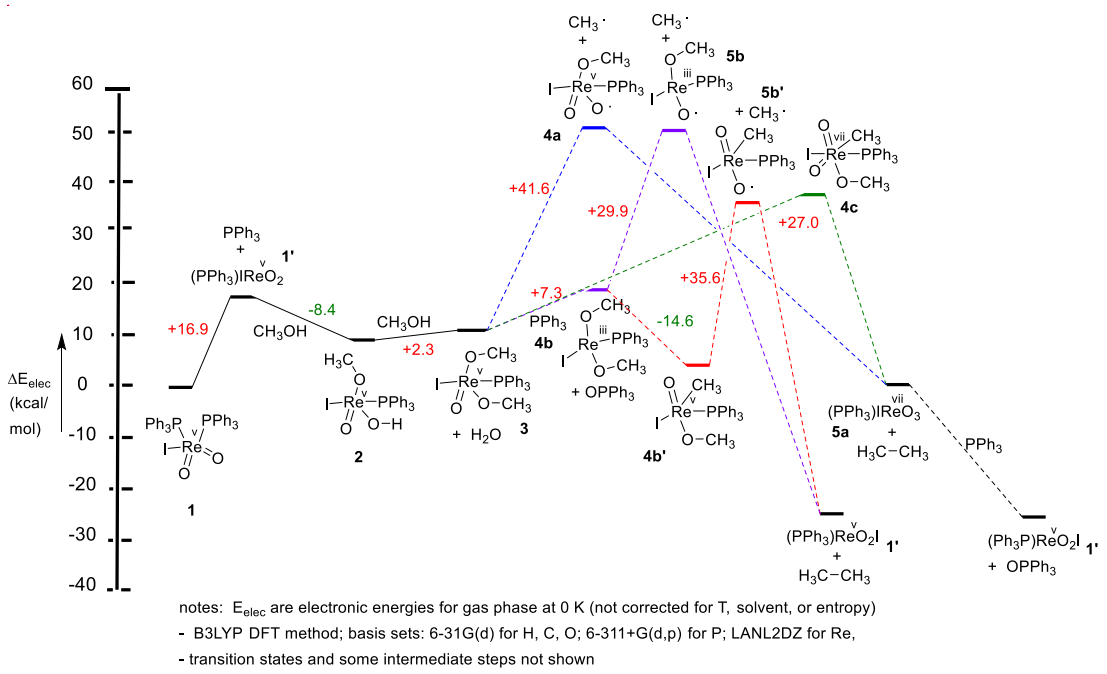


Figure IV.23 DFT study of the $IReO_2(PPh_3)_2$ catalyzed reductive coupling *(by Dr. Nicholas)*

3. Discussion and Conclusions

In the publication we described the reductive coupling of a survey of alcohols (Figure IV.24). We saw how the most activated alcohols were the most reactive; benzhydrol, fluorenol. Less activated alcohols took more time to provide reductive coupling, sorbic alcohol, 1-phenylethanol, benzyl alcohol. Cinnamyl alcohol and 1-phenylpropenol

provide a similar isomer product distribution. In the case of 1-phenylethanol we detected a 1:1 mixture of meso and chiral dimer product. Triphenylmethanol and benzoin underwent deoxygenation instead of reductive coupling. Cyclopropyl-phenylmethanol reacted a little after a very long period of time at 150^{o}C. This result added to the radical trap experiments, which had shown no effect of hydrogen donors in the reductive coupling of benzhydrol, are not providing evidence for radical involvement in the mechanism.

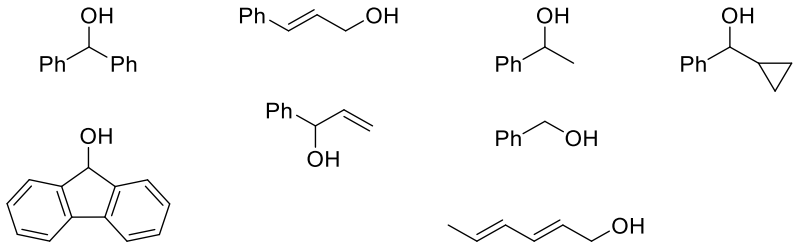


Figure IV.24 List of reactive alcohols in reductive coupling reaction

With all the data we have collected we can try to draw a better picture of the possible reductive coupling reaction mechanism. The reaction begins with an equilibrium between **A** and **A'** by the dissociation of a triphenylphosphine ligand of the pre-catalyst **A** (Figure IV.25). We observed this dissociation when the catalyst was in solution in an equilibrium. We saw in the stoichiometric experiment how one of the ligands had to be dissociated before new metal complexes could be detected. We know from the kinetic study that triphenylphosphine can have an inhibitory effect on reaction rate and we can see in this equilibrium how **A** is favored over **A'** in the presence of excess phosphine. Subsequently we believe that **A'** is the active catalyst.

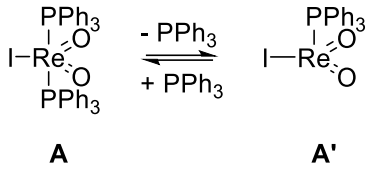


Figure IV.25 Pre-catalyst A to active catalyst A' equilibrium

From the stoichiometric experiments involving the pre-catalyst, alcohols and phosphine we could see with the different alcohols that the alcohol coordinates to the rhenium center. We detected two sets of alcohol-derived protons and new phosphine complexes having a different ratio. We think they represent two different rhenium complexes. Each set could come from **B1** and **B2** depending on if the coordinated alcohol transfers its proton to one of the rhenium oxo groups or not (Figure IV.26). The ratio we observe is then the equilibrium reached between **B1** and **B2** with the highest ratio being the more abundant of the two species.

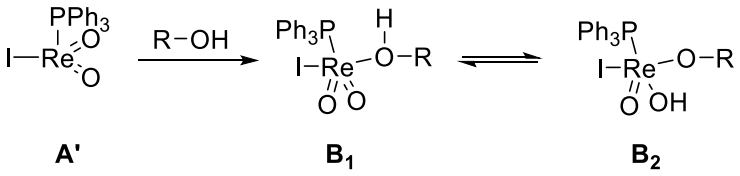


Figure IV.26 Alcohol coordination forming to species B1 and B2

Another possibility seen for the two sets of alcohol derived protons could be an equilibrium between a monoalkoxy **B2** or dialkoxy **C** rhenium complex. In the complex **C** each alcohol group would be equivalent by the structure's symmetry to have the same ^{1}H NMR shift and splitting pattern.

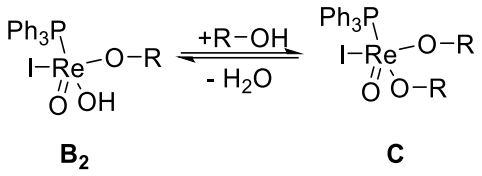


Figure IV.27 Possible equilibrium between a mono (B₂) and bis (C) alkoxy rhenium complex.

The limited effect found in changing the ratio of alcohol to rhenium complex disfavored the potential involvement of equilibrium between a mono alkoxyde and dialkoxyde intermediate (**B₂** ⇔ **C**). The alkoxy-Re complex detected are both carrying the same number of coordinated alcohol.

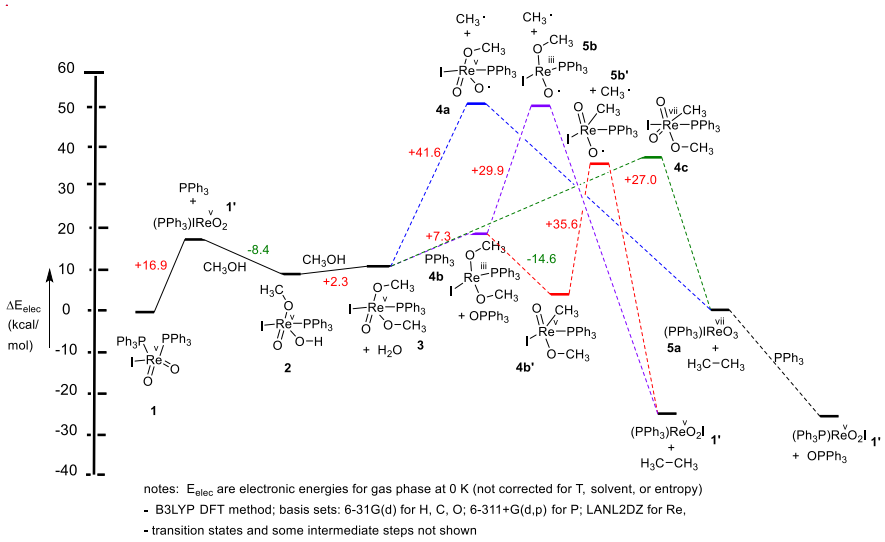


Figure IV.23 DFT study of the $IReO_2(PPh_3)_2$ catalyzed reductive coupling *(by Dr. Nicholas)*

From the alkoxy-rhenium complexes (B_1, B_2 or C) we can suggest that the reductive coupling could take place directly to form dimer. In his DFT calculation Dr. Nicholas has not found yet a transition state for concerted oxidative elimination to form dimer from dialkoxy-Re. The experimental low regio- and stereoselectivity argues against a concerted process. Therefore we might be looking at a stepwise C-O cleavage and C-C

bond formation. ReO-R homolysis was calculated to have low bond energies in addition Peters and co-worker reported experimental evidences of molybdenum alkoxide homolysis to radicals for the formation Mo/Ti μ-oxo complexes.[214] If this does occur, the dimer could form by rapid rebound:

$$R\cdot + R\text{-}O\text{-}Re \rightarrow R\text{-}R + O{=}Re$$

However we could not see any effect of hydrogen donors in the reaction demonstrating that no radical was trapped which argue against a 'free' radical. The only potential explanation to support the dissociation and rebound of a radical without being trapped would be a solvent cage effect.

The formation of alkyl rhenium complex could be possible as well (30 to 35 kcal/mol) **C** to **F** or **C'** to **F'** (depending on when the reduction happens). With the formation of such an alkyl complex the number of bonds between the phosphine and the proton is lower than three. In the literature such an alkyl-phosphine metal complex would show a large ^{1}H NMR J_{PH} coupling (6 to 12 Hz).[230] We did not detect such large coupling in the proton spectra of the multiple reactions in this study. From this observation it is then unlikely that such an alkyl-rhenium complex is formed under these conditions (room temperature and concentration).

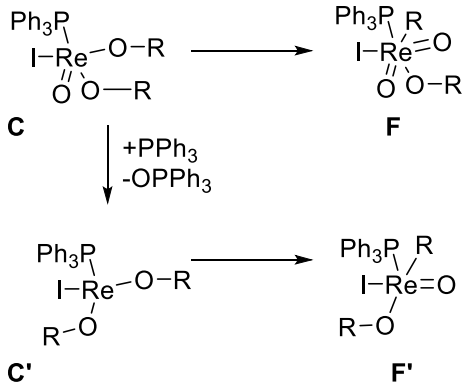


Figure IV.28 Possible formation of Re-alkyl complexes F and F'

We also ruled out the possibility to form a stable alkoxy-hydride rhenium complex intermediate (Figure IV.29) because hydride protons would have a very specific shift (3-4 ppm) and would also be close enough to the phosphorous ligand to show a J_{PH} coupling (~30 Hz)[231]. We did not observe such a proton signal in the several NMR monitoring experiments that we ran.

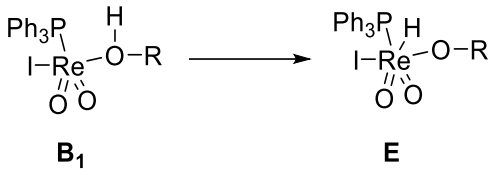


Figure IV.29 Possible formation of rhenium hydride intermediate E

From the stoichiometric NMR experiments we know that triphenylphosphine oxide does not form until the alcohol interacts with the catalyst. Therefore there is no reduction of the metal center before the alcohol coordinates with the catalyst. Also we could see some triphenylphosphine oxide before any dimer was formed.

We also observed the formation of rhenium species which had two chemically different phosphine coordinated and coupling to each other. From the chemical shifts of these signals and the same signals in the sample of pre-catalyst **A** mixed with excess triphenylphosphine oxide we think this rhenium intermediate does not involve the alcohol. The coordination of phosphine oxide to the catalyst was further confirmed by the inhibition effect of the added phosphine oxide in a kinetic reaction set. In addition we found that adding triphenylphosphine in sample **D** would regenerate **A**.

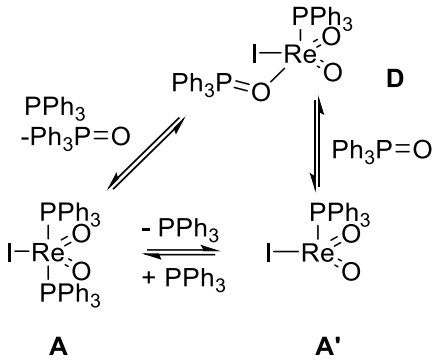


Figure IV.30 Formation of PPh_3-Re-$OPPh_3$ D rhenium complex

With the variation of alcohol in the stoichiometric experiments we noticed how the primary alcohol (ethanol, benzyl alcohol, cinnamyl alcohol) were the fastest to show color and NMR changes and the secondary alcohols (1-phenylethanol and benzhydrol) were the slowest to change. With triphenylphosphine as ligand the rhenium center the steric hindrance of the secondary alcohol could slow their stoichiometric reaction or it could also make the alkoxy-rhenium intermediate less stable. In the actual reductive coupling reaction the secondary alcohol benzhydrol provided as high yields as cinnamyl alcohol so this primary/secondary alcohol effect is noticeable only in the stoichiometric experiments. Also the dimer formation depends on the activation of the R-OM bond. This bond strength can be affected by resonance and delocalization in the developing radical which are both possible with benzhydrol and cinnamyl alcohol and would affect the rate-limiting step.

The kinetic study has informed us of a clear catalyst dependence even though we could not tell with confidence if the catalyst order was 1 or ½. Since we used concentrations near the actual reaction concentration we were not in the optimum condition to probe the kinetics of the alcohol and triphenylphosphine. Nonetheless we

detected an inhibition effect of triphenylphosphine and the alcohol when used in excess. The kinetic results demonstrated a complex mechanism which could involve both the triphenylphosphine and the alcohol in one or more intermediates before or in the turnover-limiting step.

From our experiment and computation results we could give a possible reaction mechanism (Figure IV.31). The rhenium pre-catalyst **A** from the active catalyst **A'** by the dissociation of triphenylphosphine. **A'** can then form coordinated alcohol rhenium complex $\mathbf{B_1}$ by the coordination of one alcohol or a dialkoxy-rhenium complex **C** by the coordination of two alcohols. $\mathbf{B_1}$ is in equilibrium with the hydroxyl-alkoxy-rhenium complex $\mathbf{B_2}$. With the intervention of a second alcohol and triphenylphosphine $\mathbf{B_2}$ would form the dimer product, triphenylosphine oxide and **A'**. The dialkoxide-rhenium complex **C** could be reduced by triphenylphosphine to make a rhenium (iii) dialkoxy complex **C'**. This complex **C'** would then form the dimeric product and **A'**. The formation of triphenylphosphine oxide over the cycle could favor the formation of complex **D** which can be in equilibrium with **A** in the presence of triphenylphosphine or **A'**.

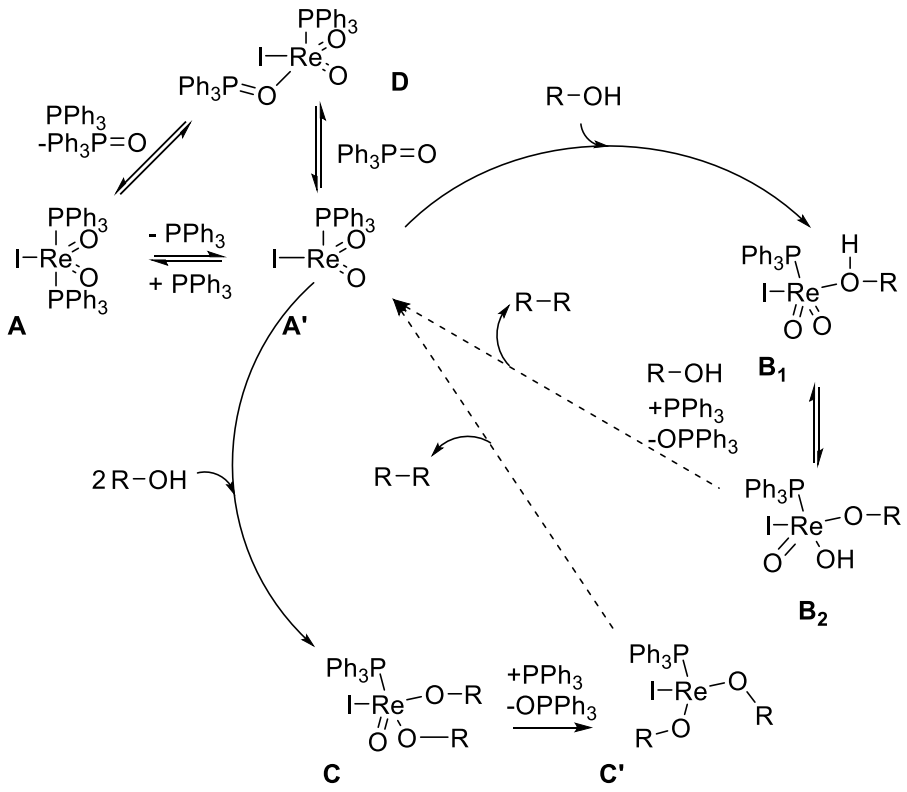


Figure IV.31 Possible mechanistic pathway

We have collected a lot of mechanistic information on the alcohol reductive coupling reaction but we still lack conclusive data that show how the C-O bond is breaking and how the dimer C-C bond is forming to have a full picture of the mechanistic cycle. More experiments in the laboratory and with computational tools could help to fill the catalyst cycle. The reductive coupling reaction on (R)-1-phenylethanol would be informative to understand if the C-O/C-C breaking/making is concerted of stepwise by determining first if the stereo center of the alcohol is retained during the reaction by measuring its optical rotation before and after the reaction. In fact the products of the reaction are two diastereomers, one meso and one chiral (RR and SS). We could detect both of them by NMR with a 1:1 ratio since each of diastereomers have different NMR spectrum. The detection of both diastereomers is not relevant to the mechanism although the

determination the chiral products distribution (RR and/or SS) would be indicating a concerted or stepwise mechanism. By isolating the chiral product and measuring its optical purity we could determine if the reaction favored the RR or SS chiral product (Figure IV.32). More kinetic reactions could be run using para substituted benzylic alcohols in order to build a Hammett plot. Such a plot could indicate with its slope, ρ, if the reaction transition state is sensitive ($\rho \neq 0$) or not ($\rho = 0$) to negative ($\rho > 0$) or positive charge ($\rho < 0$). This will inform us of the nature of the C-O bond breaking.

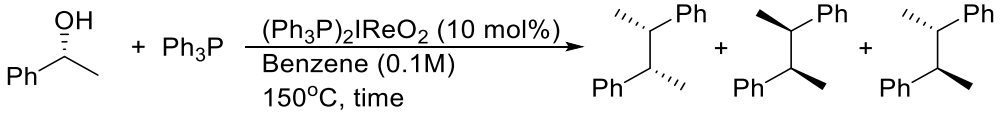


Figure IV.32 Reductive coupling of (R)-1-phenylethanol

4. Experimental

a. General information: reagents and instruments.

All reactants and catalysts were obtained commercially and used without further purification. All solvents were ACS grade and were used directly (unless otherwise described in the procedures). ^{1}H, ^{2}H and ^{13}C NMR spectra were collected on Varian VNMRS 400 MHz and VNMRS 500 MHz instruments. The NMR data were processed using MestReNova[232] and ACD[103] software. Gas chromatograms were collected on a Shimadzu GC-2014 equipped with an AOC 20i+s auto sampler, both with 3% SE-54 packed column, FID and thermal program 40^{o}C for 5 min; 20 deg/min to 250^{o}C; then 7 min at 250^{o}C.

b. Catalyst synthesis

The catalyst (**1**) was synthesized in two steps following a literature procedure.[233] Only the starting material was changed from perrhenic acid to ammonium perrhenate.

i. Synthesis of $I_2ReO(OEt)(PPh_3)_2$

Ammonium perrhenate (white crystal) (1.0 g, 3.7 mmol) and triphenylphosphine (5 g, 19 mmol) were added to a mixture of 56% hydriodic acid solution (5 mL) and ethanol (30 mL). The reaction was brought to reflux for 15 min. Green crystals formed in the solution. These crystals were filtered off, washed with ethanol and dried under high vacuum (1-5 mmHg). The yield was nearly quantitative. The product was stored in a dedicator over $CaCl_2$.

*ii. Synthesis of $IReO_2(PPh_3)_2$ (**1**)*

$I_2ReO(OEt)(PPh_3)_2$ (1.0 gr, 0.97 mmol) of was added to a mixture of acetone (50 mL) and water (2 mL). The green suspension was magnetically stirred at room temperature. After an hour the suspended crystals changed color to violet. These crystals were filtered off and washed with cold acetone. The product was recrystallized from 1:1 benzene / hexanes (Process: at 100°C until dilution and slow temperature decrease to room temperature followed by vacuum filtration and rinsed with cold hexane and overnight under high vacuum 5-1 mmHg) giving a yield of 80%. The product was then stored in a dedicator over $CaCl_2$.

c. Study of the catalyst in solution; ligand dissociation

Each sample was prepared with about 1 mL of benzene-d^6 and 4 mg of $IReO_2(PPh_3)_2$ under N_2 (5 mM). First we tested the evolution of samples over time with and without aluminum foil wrap to check for any potential effects of light. After establishing that light did not make any difference for these samples, we did not wrap the samples in the rest of the study.

For the samples in which we added triphenylphosphine 26 mg was used.

d. NMR Stoichiometric Experiments

i. Representative procedure: Sample B

$IReO_2(PPh_3)_2$ (**1**) (0.006 mmol, 5 mg) and benzhydrol (60 µL of 0.06 M solution in d^6-benzene), (alcohol/catalyst ratio in the table below) were added into 0.74 mL of d^6-benzene in a thick-walled NMR tube. The NMR tube was caped and purged (vacuum

pumped then back filled with N_2 three times) and finally placed under argon. The tube was left at room temperature for several weeks. The changes over time were followed by ^{1}H and ^{31}P NMR.

After a month at room temperature and no more noticeable changes B and D were placed in an oil bath at 50°C. The changes were followed by ^{1}H and ^{31}P NMR about every 16 h.

Sample[a]	ROH	
	R	equiv.[b]
A[c]	Ph_2CH	1
B	Ph_2CH	1
C[d]	Ph_2CH	1
D	Ph_2CH	5
E	Ph_2CH	10
G[e]	-	0
H	Et	5
I	$PhCH_2$	5
J	PhCHMe	5
K	$PhCHCHCH_2$ OH	

a) with **1** (6 µmol, 5 mg) in 0.8 mL d^6-benzene; b) relative to **1**; c) with 1 mmol (26 mg) of PPh_3; d) catalyst **1** was left in solvent 3 days for ligand dissociation; e) with 1 mmol (28 mg) of $OPPh_3$

- ^{13}C NMR signals in $\mathbf{B_2}$:

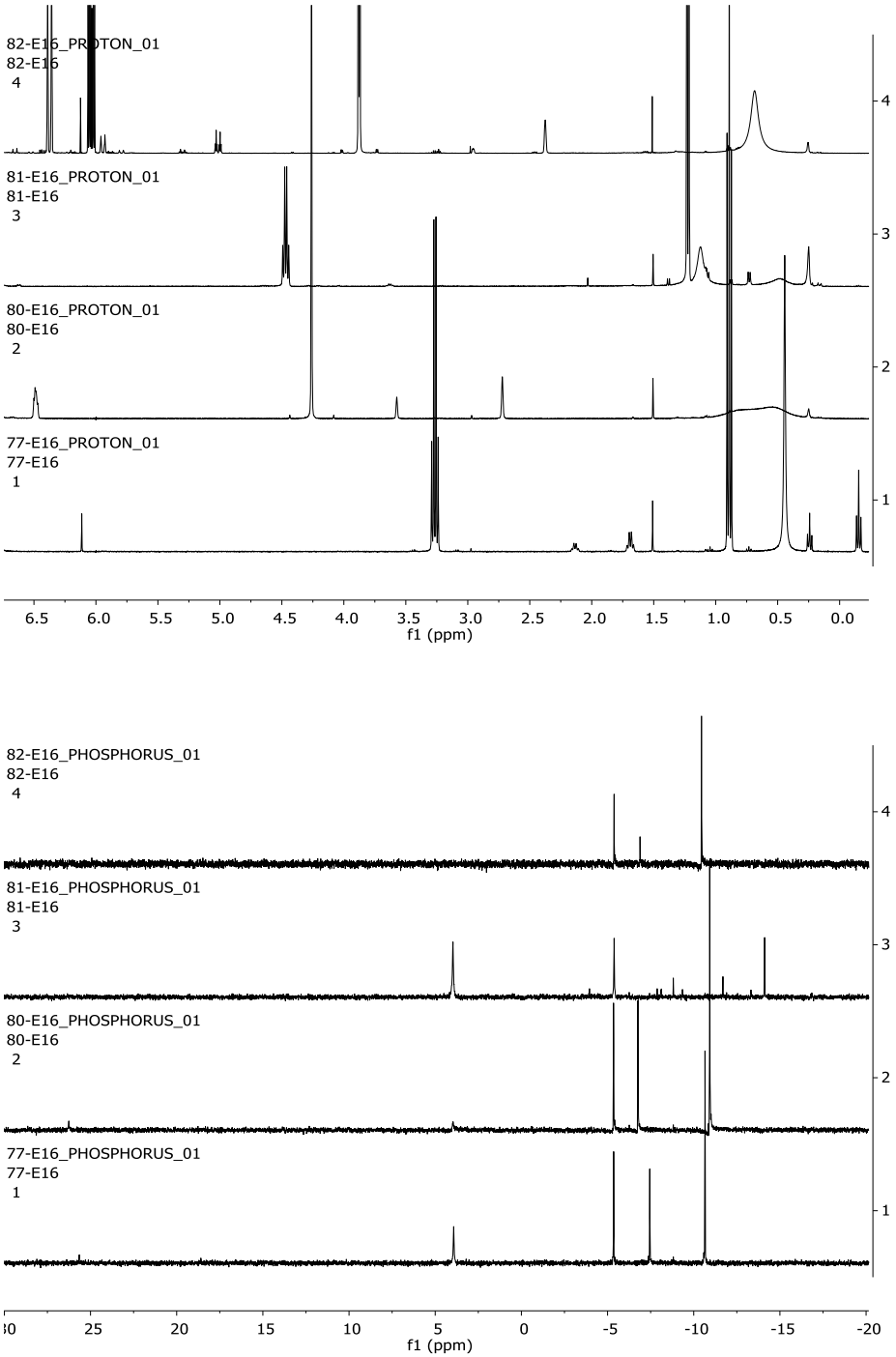
30, 76*, 127*, 127*, 127.5 *d(J_{CP}<2 Hz)*, 128 *d(J_{CP}<2 Hz)*, 128 *d(J_{CP}=2.29 Hz)*, 128.2, 128.3, 128.35, 128.4, 128.45 *d(J_{CP}~2 Hz)*, 128.5, 128.6 *d(J_{CP}=5.34 Hz)*, 128.7, 128.8, 128.9, 129.1*, 129.4, 129.7, 131.1 *d(J_{CP}=2.29Hz)*, 131.2 *d(J_{CP}~2 Hz)*, 132 *d(J_{CP}=9.92 Hz)*, 133.1 *d(J_{CP}=2.29 Hz)*, 133.7, 133.9 *d(J_{CP}=19.84 Hz)*, 134.0 *d(J_{CP}=11.44 Hz)*, 134.4 *d(J_{CP}=9.16 Hz)*, 135 *t(J_{CP}=4.4 Hz)*, 144.6*

ROH = *

ROH	EtOH		$PhCH_2OH$	$PhCH(OH)CH_3$		$PhCHCHCH_2OH$		$Ph_2CH(OH)$
	Shift (ppm)	J(Hz)	Shift (ppm)	Shift (ppm)	J(Hz)	Shift (ppm)	J (Hz)	Shift (ppm)
Free ROH	3.3 q CH_2, 0.9 t CH_3	6.99	4.3 s CH_2	4.5 q CH, 1.2 d CH_3	6.41	6.4 d PhCH, 6.0 dt CH, 3.9 d CH_2	15.94 5.43	5.5 s CH_2
With $IReO_2(PPh_3)_2$	2.1 q CH_2, 0.2 t CH_3	6.99	3.6 s CH_2	3.6 q CH, - d CH_3	6.5	5.9 d PhCH, 5.0 dt CH 2.4 s CH_2	15.99 3.91	
	1.7 q CH_2, -0.2 t CH_3	6.99	2.7 s CH_2	3.2 q CH, - d CH_3	6.85			
				2.0 s, 6.6 d	7.14			
				0.9 d, 0.7 d 1.1 d 0.2 m, 0.5 d	6.60, 6.65 1.47 - 10.41	6.10 s		6.3 s, 4.9 m small, 1.1 s

$IReO_2(PPh_3)_2$ with:	^{31}P NMR Signals [b]
Ph_2CHOH[a]	72.7, {**49.97**, d, J_{PP}=16 Hz}, **25.5**, 21.8, **-5.4**, -7.9, -8.8, -9.6, -10.7, **-11.7**, {**-12.14**, d, J_{PP}=16 Hz}
$PhCH(OH)CH_3$	**-3.9**, **-5.4**, -7.9, -8.1, -8.8, -9.3, -11.7, **-14.1**
$PhCH_2(OH)$	**-5.3**, **-6.8**, **-10.9**, -11.7
$PhCHCHCH_2OH$	**-5.4**, -6.9, **-10.5**
EtOH	25.7, **-5.3**, **-7.5**, **-10.7**, -11.7
References: PPh_3	**-5.3**
$O=PPh_3$	**25.4**
$IReO_2(PPh_3)_2$	**4.57**
$[IReO_2PPh_3+PPh_3]$	**-5.4, -11.7**

a) After 3-4days at room temperature; the major signals are bolded, b) After only 16h at 50°C,



^{1}H and ^{31}P NMR spectra of the samples H, I, J and K (from bottom to the top)

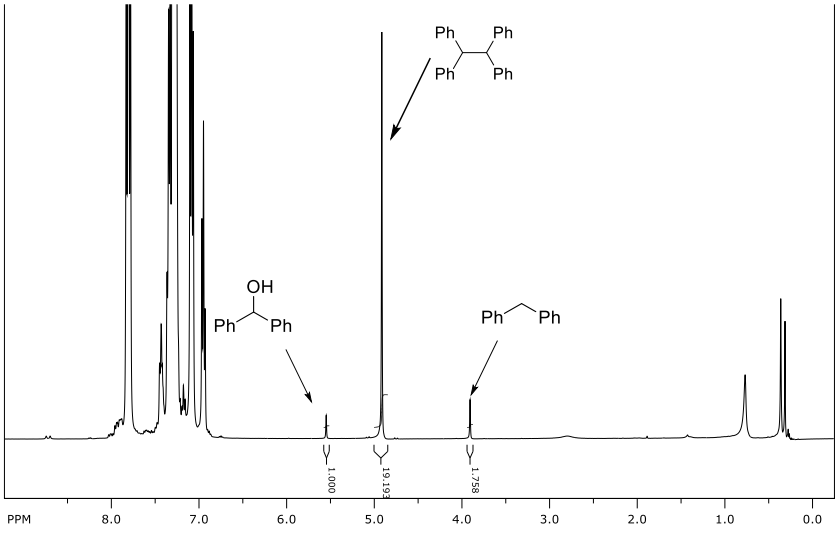
e. Kinetic experiments

i. Solvent test

Benzhydrol (0.10 mmol, 18 mg), triphenylphosphine (0.10 mmol, 26 mg) and the catalyst **1** (10 mol%, 9 mg) in PhCl (1 mL) were added to a thick-walled Ace glass reactor tube. A N_2 stream was bubbled into the mixture for at least 60 sec before the Teflon seal was closed. The reactor was placed in an oil bath at 125^{o}C for 24h. After cooling to room temperature, a 100 μL aliquot of the reaction mixture was removed and added to $CDCl_3$ and 2.0 μL DMF as internal standard for NMR analysis. 0.5 mL of the reaction was submitted for GC analysis.

$Ph_2CHCHPh_2$ ^{1}H NMR (400MHz, $CDCl_3$): 7.5-7.1 (m, 20H, Ar), 4.7 (s, 2H, C*H*)

^{1}H NMR



ii. Internal standard test

Benzhydrol (0.05 mmol, 9 mg), triphenylphosphine (0.05 mmol, 13 mg) and the catalyst **1** (10 mol%, 9 mg) in *d*^{6}-benzene (0.50 mL) were added to a NMR tube along with an internal standard of hexamethylbenzene (3 mg) or cyclooctane (2 μL)]. The NMR tube

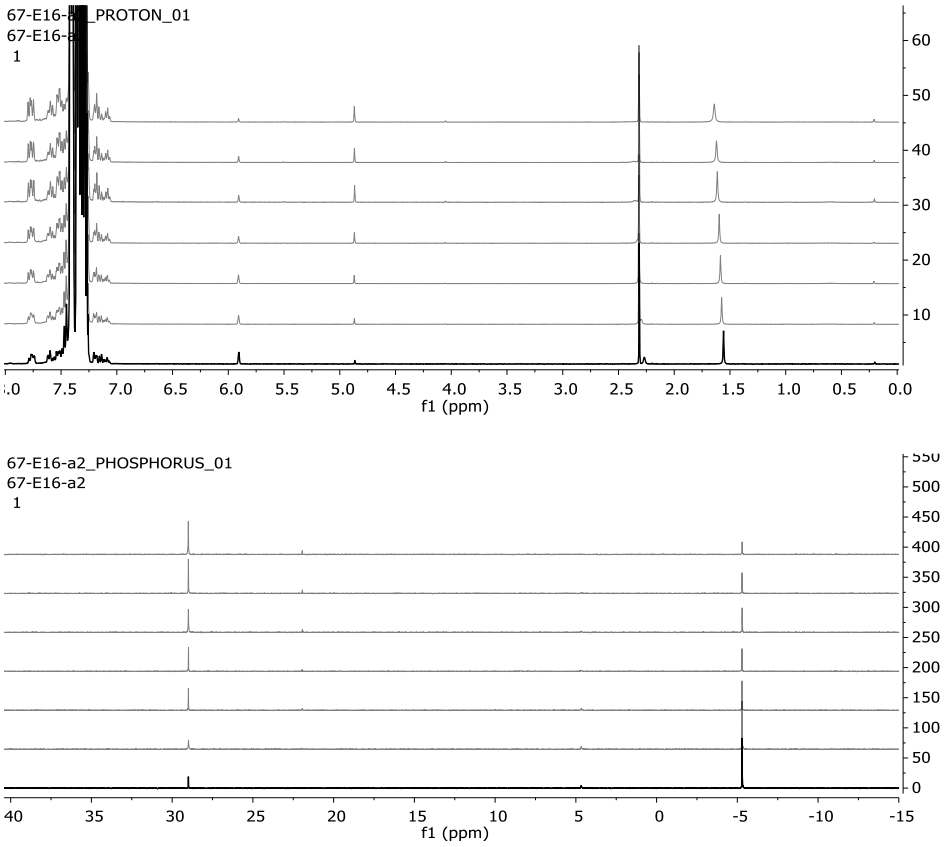
was flushed with N_2 for at least 60 sec before being closed. The NMR tube was placed in an oil bath at 125^{o}C for 24h. After cooling to room temperature, the NMR tube was wiped with hexanes on a towel and analyzed.

iii. Kinetic samples preparation

In a 1 dram vial **1**, benzhydrol and triphenylphosphine (quantities in the table below) were mixed with 0.9 mL of distilled chlorobenzene (stored over molecular sieves 4Å) and 0.1 mL of hexamethyl benzene (0.1 M) was added. The vial was caped and mixed on the vortexer for 20 seconds. The sample was then immediately split into 10 NMR tubes (0.10 mL in each tube). After capping the tubes they were placed in a preheated oil bath, 125^{o}C and a timer was started. An NMR tube was removed from the oil bath every minute starting at 2 minutes. As soon as the tube was removed it was placed in an ice bath and 0.5 mL of $CDCl_3$ was added. The tubes were wiped with hexane on a towel to remove the oil. The NMR tubes remained in ice or in the freezer until the NMR spectra were acquired.

Sample [a]	$IReO_2(PPh_3)_2$		$Ph_2CH(OH)$		PPh_3	
	mmol	mg	mmol	mg	mmol	mg
a[b], a''[c], a'''	0.01	8.7	0.10	18.4	0.10	26.3
b[c], b'	0.005	4.35	0.10	18.4	0.10	26.3
c	0.001	0.87	0.10	18.4	0.10	26.3
d	0.01	8.7	0.20	36.8	0.10	26.3
e	0.01	8.7	0.05	9.2	0.10	26.3
f	0.01	8.7	0.10	18.4	0.05	13.1
g	0.01	8.7	0.10	18.4	0.20	52.6
h	0.01	8.7	0.50	92.0	0.10	26.3
i	0.01	8.7	0.10	18.4	0.50	131.5
j	0.01	8.7	0.05	9.2	0.05	13.1
k	0.01	8.7	0.05	9.2	0.20	52.6
l	0.01	8.7	0.20	36.8	0.05	13.1
m	0.01	8.7	0.20	36.8	0.20	52.6
n[d]	0.01	8.7	0.1	18.4	0.1	26.3

a) in [0.9 mL PhCl + 0.1 mL Me_6Ph (0.16 M in PhCl)]; b) 150°C, sample every 10 min; c) 125°C, sample every 5 min; d) with $OPPh_3$ (0.50 mmol, 136 mg)



Representative ^{1}H and ^{31}P NMR spectra of the samples taken overtime (a'')

f. IR sampling

IR spectra were acquired with a liquid cell on a Bruker FT-IR instrument. The background was done with the atmosphere and an IR spectrum of the solvent benzene was collected in order to overlap with the sample solution spectra. Samples from the stoichiometric NMR experiments (A, B, E) were used to collect IR spectra. Authentic samples were prepared by dissolving the reference compound in similar concentrations (**1**, benzhydrol, triphenylphosphine, and triphenylphosphine oxide.

g. MS sampling

Sample E from the stoichiometric NMR experiments was submitted for ESI+ and ESI-. Sample B from the stoichiometric NMR experiments was submitted for APCI+ and APCI-.

References

1. Corma, A., Iborra, S. & Velty, A. Chemical Routes for the Transformation of Biomass into Chemicals. *Chem. Rev.* **107,** 2411–2502 (2007).
2. Huber, G. W., Iborra, S. & Corma, A. Synthesis of Transportation Fuels from Biomass: Chemistry, Catalysts, and Engineering. *Chem. Rev.* **106,** 4044–4098 (2006).
3. Chheda, J. N., Huber, G. W. & Dumesic, J. A. Liquid-Phase Catalytic Processing of Biomass-Derived Oxygenated Hydrocarbons to Fuels and Chemicals. *Angew. Chem. Int. Ed.* **46,** 7164–7183 (2007).
4. Top Value Added Chemicals from Biomass: Volume I - Results of Screening for Potential Candidates from Sugars and Synthesis Gas.
5. Agirrezabal-Telleria, I., Gandarias, I. & Arias, P. L. Heterogeneous acid-catalysts for the production of furan-derived compounds (furfural and hydroxymethylfurfural) from renewable carbohydrates: A review. *Catal. Today* **234,** 42–58 (2014).
6. Mascal, M. & Nikitin, E. B. Towards the Efficient, Total Glycan Utilization of Biomass. *ChemSusChem* **2,** 423–426 (2009).
7. Yang, W. & Sen, A. One-Step Catalytic Transformation of Carbohydrates and Cellulosic Biomass to 2,5-Dimethyltetrahydrofuran for Liquid Fuels. *ChemSusChem* **3,** 597–603 (2010).
8. Mascal, M. & Nikitin, E. B. Dramatic Advancements in the Saccharide to 5-(Chloromethyl)furfural Conversion Reaction. *ChemSusChem* **2,** 859–861 (2009).

9. Binder, J. B. & Raines, R. T. Simple Chemical Transformation of Lignocellulosic Biomass into Furans for Fuels and Chemicals. *J. Am. Chem. Soc.* **131,** 1979–1985 (2009).

10. Ruppert, A. M., Weinberg, K. & Palkovits, R. Hydrogenolysis Goes Bio: From Carbohydrates and Sugar Alcohols to Platform Chemicals. *Angew. Chem. Int. Ed.* **51,** 2564–2601 (2012).

11. Deng, W., Tan, X., Fang, W., Zhang, Q. & Wang, Y. Conversion of Cellulose into Sorbitol over Carbon Nanotube-Supported Ruthenium Catalyst. *Catal. Lett.* **133,** 167–174 (2009).

12. Yan, N., Zhao, C., Luo, C., Dyson, P., Liu, H. & Kou, Y., One-Step Conversion of Cellobiose to C6-Alcohols Using a Ruthenium Nanocluster Catalyst. *J. Am. Chem. Soc.* **128,** 8714–8715 (2006).

13. Schlaf, M., Ghosh, P., Fagan, P. J., Hauptman, E. & Bullock, R. M. Catalytic Deoxygenation of 1,2-Propanediol to Give n-Propanol. *Adv. Synth. Catal.* **351,** 789–800 (2009).

14. Metzger, J. O. Catalytic Deoxygenation of Carbohydrate Renewable Resources. *ChemCatChem* **5,** 680–682 (2013).

15. Boucher-Jacobs, C. & Nicholas, K. M. in *Selective Catalysis for Renewable Feedstocks and Chemicals* (ed. Nicholas, K. M.) 163–184 (Springer International Publishing, 2014).

16. Dethlefsen, J. R. & Fristrup, P. Rhenium-Catalyzed Deoxydehydration of Diols and Polyols. *ChemSusChem* **8,** 767–775 (2015).

17. Raju, S., Moret, M.-E. & Klein Gebbink, R. J. M. Rhenium-Catalyzed Dehydration and Deoxydehydration of Alcohols and Polyols: Opportunities for the Formation of Olefins from Biomass. *ACS Catal.* **5,** 281–300 (2015).

18. Liu, S., Yi, J. & Abu-Omar, M. M. in *Reaction Pathways and Mechanisms in Thermocatalytic Biomass Conversion II* (eds. Schlaf, M. & Zhang, Z. C.) 1–11 (Springer Singapore, 2016).

19. Crank, G. & Eastwood, F. Derivatives of orthoacids. II. The preparation of olefins from 1,2-diols. *Aust. J. Chem.* **17,** 1392–1398 (1964).

20. Ando, M., Ohhara, H. & Takase, K. A Mild and Stereospecific Conversion of Vicinal Diols into Olefins Via 2-Methoxy-1,3-Dioxolane Derivatives. *Chem. Lett.* **15,** 879–882 (1986).

21. Bergman, R. G., Ellman, J. A., Arceo Rebollo, E. & Marsden, P. C. Method of Converting a Polyol to an Olefin. (2009).

22. Arceo, E., Marsden, P., Bergman, R. G. & Ellman, J. A. An efficient didehydroxylation method for the biomass-derived polyols glycerol and erythritol. Mechanistic studies of a formic acid-mediated deoxygenation. *Chem. Commun.* 3357 (2009). doi:10.1039/b907746d

23. Cook, G. K. & Andrews, M. A. Toward Nonoxidative Routes to Oxygenated Organics: Stereospecific Deoxydehydration of Diols and Polyols to Alkenes and Allylic Alcohols Catalyzed by the Metal Oxo Complex (C5Me5)ReO3. *J. Am. Chem. Soc.* **118,** 9448–9449 (1996).

24. Gable K. P. & Ross B. in *Feedstocks for the Future* **921,** 143–155 (American Chemical Society, 2006).

25. Raju, S., Jastrzebski, J. T. B. H., Lutz, M. & Klein Gebbink, R. J. M. Catalytic Deoxydehydration of Diols to Olefins by using a Bulky Cyclopentadiene-based Trioxorhenium Catalyst. *ChemSusChem* **6,** 1673–1680 (2013).

26. Raju, S., Jastrzebski, J., Lutz, M., Witteman, L., Dethlefsen, J., Fristrup, P., Moret, M. & Gebbink, R. Spectroscopic Characterization of a Monomeric, Cyclopentadienyl-Based Rhenium(V) Dioxo Complex. Inorg. Chem. 54, 11031–11036 (2015).

27. Gable, K. P. & Phan, T. N. Extrusion of Alkenes from Rhenium(V) Diolates: Energetics and Mechanism. *J. Am. Chem. Soc.* **116,** 833–839 (1994).

28. Gable, K. P. & Juliette, J. J. J. Extrusion of Alkenes from Rhenium(V) Diolates: The Effect of Substitution and Conformation. *J. Am. Chem. Soc.* **117,** 955–962 (1995).

29. Gable, K. P. & Juliette, J. J. J. Hammett Studies on Alkene Extrusion from Rhenium(V) Diolates and an MO Description of Metal Alkoxide−Alkyl Metal Oxo Interconversion. *J. Am. Chem. Soc.* **118,** 2625–2633 (1996).

30. Gable, K. P., AbuBaker, A., Zientara, K. & Wainwright, A. M. Cycloreversion of Rhenium(V) Diolates Containing the Hydridotris(3,5-dimethylpyrazolyl)borate Ancillary Ligand. *Organometallics* **18,** 173–179 (1999).

31. Gable, K. P. & Zhuravlev, F. A. Kinetic Isotope Effects in Cycloreversion of Rhenium (V) Diolates. *J. Am. Chem. Soc.* **124,** 3970–3979 (2002).

32. Nakagiri, T., Murai, M. & Takai, K. Stereospecific Deoxygenation of Aliphatic Epoxides to Alkenes under Rhenium Catalysis. *Org. Lett.* **17,** 3346–3349 (2015).

33. Ziegler, J. E., Zdilla, M. J., Evans, A. J. & Abu-Omar, M. M. H_2 -Driven Deoxygenation of Epoxides and Diols to Alkenes Catalyzed by Methyltrioxorhenium. *Inorg. Chem.* **48,** 9998–10000 (2009).

34. Bi, S., Wang, J., Liu, L., Li, P. & Lin, Z. Mechanism of the $MeReO_3$ -Catalyzed Deoxygenation of Epoxides. *Organometallics* **31,** 6139–6147 (2012).

35. Ahmad, I., Chapman, G. & Nicholas, K. M. Sulfite-Driven, Oxorhenium-Catalyzed Deoxydehydration of Glycols. *Organometallics* **30,** 2810–2818 (2011).

36. Vkuturi, S., Chapman, G., Ahmad, I. & Nicholas, K. M. Rhenium-Catalyzed Deoxydehydration of Glycols by Sulfite. *Inorg. Chem.* **49,** 4744–4746 (2010).

37. Al-Ajlouni, A. M., Günyar, A., Zhou, M.-D., Baxter, P. N. W. & Kühn, F. E. Adduct Formation of Dichloridodioxidomolybdenum(VI) and Methyltrioxidorhenium(VII) with a Series of Bidentate Nitrogen Donor Ligands. *Eur. J. Inorg. Chem.* **2009,** 1019–1026 (2009).

38. Xu, Z., Zhou, M., Drees, M., Chaffrey-Millar, H., Herdtweck, W. & Kühn, F. Mono- and Bis- Methyltrioxorhenium(VII) Complexes with Salen Ligands: Synthesis, Properties, Applications. *Inorg. Chem.* **48,** 6812–6822 (2009).

39. Rietveld, M. H. P., Nagelholt, L., Grove, D., Veldman, N., Spek, A., Rauch, M., Herrmann, W. & van Koten G., Synthesis of methyltrioxorhenium(VII) arylamine complexes and mono- and bis(ortho)-chelated arylaminorhenium(VII) trioxides. *J. Organomet. Chem.* **530,** 159–167 (1997).

40. Liu, P. & Nicholas, K. M. Mechanism of Sulfite-Driven, $MeReO_3$ -Catalyzed Deoxydehydration of Glycols. *Organometallics* **32,** 1821–1831 (2013).

41. Arceo, E., Ellman, J. A. & Bergman, R. G. Rhenium-Catalyzed Didehydroxylation of Vicinal Diols to Alkenes Using a Simple Alcohol as a Reducing Agent. *J. Am. Chem. Soc.* **132,** 11408–11409 (2010).

42. Yi, J., Liu, S. & Abu-Omar, M. M. Rhenium-Catalyzed Transfer Hydrogenation and Deoxygenation of Biomass-Derived Polyols to Small and Useful Organics. *ChemSusChem* **5,** 1401–1404 (2012).

43. Canale, V., Tonucci, L., Bressan, M. & d'Alessandro, N. Deoxydehydration of glycerol to allyl alcohol catalyzed by rhenium derivatives. *Catal. Sci. Technol.* **4,** 3697–3704 (2014).

44. Shiramizu, M. & Toste, F. D. Deoxygenation of Biomass-Derived Feedstocks: Oxorhenium-Catalyzed Deoxydehydration of Sugars and Sugar Alcohols. *Angew. Chem. Int. Ed.* **51,** 8082–8086 (2012).

45. Shiramizu, M. & Toste, F. D. Expanding the Scope of Biomass-Derived Chemicals through Tandem Reactions Based on Oxorhenium-Catalyzed Deoxydehydration. *Angew. Chem. Int. Ed.* **52,** 12905–12909 (2013).

46. Boucher-Jacobs, C. & Nicholas, K. M. Catalytic Deoxydehydration of Glycols with Alcohol Reductants. *ChemSusChem* **6,** 597–599 (2013).

47. Liu, S., Senocak, A., Smeltz, J., Yang, L., Wegenhart, B., Yi, J., Kenttamaa, H., Ison, E. & Abu-Omar M. M. Mechanism of MTO-Catalyzed Deoxydehydration of Diols to Alkenes Using Sacrificial Alcohols. *Organometallics* **32,** 3210–3219 (2013).

48. Qu, S., Dang, Y., Wen, M. & Wang, Z.-X. Mechanism of the Methyltrioxorhenium-Catalyzed Deoxydehydration of Polyols: A New Pathway Revealed. *Chem. – Eur. J.* **19,** 3827–3832 (2013).

49. Dethlefsen, J. R. & Fristrup, P. In Situ Spectroscopic Investigation of the Rhenium-Catalyzed Deoxydehydration of Vicinal Diols. *ChemCatChem* **7,** 1184–1196 (2015).

50. Wu, D., Zhang, Y. & Su, H. Mechanistic Study on Oxorhenium-Catalyzed Deoxydehydration and Allylic Alcohol Isomerization. *Chem. – Asian J.* n/a-n/a (2016). doi:10.1002/asia.201600118

51. Michael McClain, J. & Nicholas, K. M. Elemental Reductants for the Deoxydehydration of Glycols. *ACS Catal.* **4,** 2109–2112 (2014).

52. Denning, A. L., Dang, H., Liu, Z., Nicholas, K. M. & Jentoft, F. C. Deoxydehydration of Glycols Catalyzed by Carbon-Supported Perrhenate. *ChemCatChem* **5,** 3567–3570 (2013).

53. Sandbrink, L., Klindtworth, E., Islam, H.-U., Beale, A. M. & Palkovits, R. ReOx/TiO2: A Recyclable Solid Catalyst for Deoxydehydration. *ACS Catal.* **6,** 677–680 (2016).

54. Emsley, J. *Rhenium is one of the rarest elements in the Earth's crust with an average concentration of ca. 7 parts per billion by weight, making it the 77th most abundant element in Earth's crust. Nature's Building Blocks: An A-Z Guide to the Elements*. (Oxford University Press, 2011).

55. *Molybdenum's abundance in the earth's crust is 1.2 parts per million by weight. Concise Encyclopedia Chemistry*. (De Gruyter, 1994).

56. Hills, L., Moyano, R., Montilla, F., Pastor, A., Galindo, A., Alvarez, E., Machetti, F. & Pettinari, C., Dioxomolybdenum(VI) Complexes with Acylpyrazolonate Ligands: Synthesis, Structures, and Catalytic Properties. *Eur. J. Inorg. Chem.* **2013,** 3352–3361 (2013).

57. Dethlefsen, J. R., Lupp, D., Oh, B.-C. & Fristrup, P. Molybdenum-Catalyzed Deoxydehydration of Vicinal Diols. *ChemSusChem* **7,** 425–428 (2014).

58. Maradur, S. & Nicholas, K. M. unpublished results, 2012. (2012).

59. Lupp, D., Christensen, N. J., Dethlefsen, J. R. & Fristrup, P. DFT Study of the Molybdenum-Catalyzed Deoxydehydration of Vicinal Diols. *Chem. – Eur. J.* **21,** 3435–3442 (2015).

60. Dethlefsen, J. R., Lupp, D., Teshome, A., Nielsen, L. B. & Fristrup, P. Molybdenum-Catalyzed Conversion of Diols and Biomass-Derived Polyols to Alkenes Using Isopropyl Alcohol as Reductant and Solvent. *ACS Catal.* **5,** 3638–3647 (2015).

61. Beckerle, K., Sauer, A., Spaniol, T. P. & Okuda, J. Bis(phenolato)molybdenum Complexes as Catalyst Precursors for the Deoxydehydration of Biomass-Derived Polyols. *Polyhedron* doi:10.1016/j.poly.2016.03.053

62. Emsley, J. *Vanadium's abundance in the earth's crust is 120 parts per million by weight. Nature's Building Blocks: An A-Z Guide to the Elements*. (Oxford University Press, 2011).

63. Chapman, G. & Nicholas, K. M. Vanadium-catalyzed deoxydehydration of glycols. *Chem. Commun.* **49,** 8199 (2013).

64. Chapman, G. & Nicholas, K. M. unpublished results. (2014).

65. Galindo, A. DFT Studies on the Mechanism of the Vanadium-Catalyzed Deoxydehydration of Diols. *Inorg. Chem.* **55,** 2284–2289 (2016).

66. Gopaladasu, T. V. & Nicholas, K. M. Carbon Monoxide (CO)- and Hydrogen-Driven, Vanadium-Catalyzed Deoxydehydration of Glycols. *ACS Catal.* **6,** 1901–1904 (2016).

67. Zhang, Y. & LI, X. Chemical process to convert mucic acid to adipic acid. (2015).

68. Li, X. *et al.* Highly Efficient Chemical Process To Convert Mucic Acid into Adipic Acid and DFT Studies of the Mechanism of the Rhenium-Catalyzed Deoxydehydration. *Angew. Chem. Int. Ed.* **53,** 4200–4204 (2014).

69. Zhang, H., Li, X., Ang, E., Zhang, Y. & Zhao, H., Production of Adipic Acid from Sugar Beet Residue by Combined Biological and Chemical Catalysis. *ChemCatChem* n/a–n/a (2016). doi:10.1002/cctc.201600069

70. Ota, N., Tamura, M., Nakagawa, Y., Okumura, K. & Tomishige, K. Performance, Structure, and Mechanism of ReOx–Pd/CeO2 Catalyst for Simultaneous Removal of Vicinal OH Groups with H2. *ACS Catal.* 3213–3226 (2016). doi:10.1021/acscatal.6b00491

71. Ota, N., Tamura, M., Nakagawa, Y., Okumura, K. & Tomishige, K. Hydrodeoxygenation of Vicinal OH Groups over Heterogeneous Rhenium Catalyst Promoted by Palladium and Ceria Support. *Angew. Chem. Int. Ed.* **54,** 1897–1900 (2015).

72. Geary, L. M., Chen, T.-Y., Montgomery, T. P. & Krische, M. J. Benzannulation via Ruthenium-Catalyzed Diol–Diene [4+2] Cycloaddition: One- and Two-

Directional Syntheses of Fluoranthenes and Acenes. *J. Am. Chem. Soc.* **136,** 5920–5922 (2014).

73. Liu, S. *et al.* Mechanism of MTO-Catalyzed Deoxydehydration of Diols to Alkenes Using Sacrificial Alcohols. *Organometallics* **32,** 3210–3219 (2013).
74. Dethlefsen, J. R. & Fristrup, P. In Situ Spectroscopic Investigation of the Rhenium-Catalyzed Deoxydehydration of Vicinal Diols. *ChemCatChem* n/a-n/a (2015). doi:10.1002/cctc.201403012
75. Moores, A., Poyatos, M., Luo, Y. & Crabtree, R. H. Catalysed low temperature H2 release from nitrogen heterocycles. *New J. Chem.* **30,** 1675–1678 (2006).
76. Reddy, B. M., Han, D.-S., Jiang, N. & Park, S.-E. Dehydrogenation of Ethylbenzene to Styrene with Carbon Dioxide Over ZrO2-based Composite Oxide Catalysts. *Catalysis Surveys from Asia* **12,** 56–59 (2008).
77. Mayer, J. M. Understanding Hydrogen Atom Transfer: From Bond Strengths to Marcus Theory. *Acc. Chem. Res.* **44,** 36–46 (2011).
78. Karki, M., Araujo, H. & Magolan, J. Dehydroaromatization with V2O5. *Synlett* **24,** 1675–1678 (2013).
79. Lee, E. H. Iron Oxide Catalysts for Dehydrogenation of Ethylbenzene in the Presence of Steam. *Catal. Rev.* **8,** 285–305 (1974).
80. Chen, S., Lu, G. & Cai, C. Iridium-Catalyzed C-3 Allylation of Indoles with Allylic Alcohols Promoted by a Brønsted Acid. *Synthesis* **46,** 1717–1724 (2014).
81. Waidmann, C. R. *et al.* Slow Hydrogen Atom Transfer Reactions of Oxo- and Hydroxo-Vanadium Compounds: The Importance of Intrinsic Barriers. *J. Am. Chem. Soc.* **131,** 4729–4743 (2009).

82. Matsuo, T. & Mayer, J. M. Oxidations of NADH Analogues by cis-[RuIV(bpy)2(py)(O)]2+ Occur by Hydrogen-Atom Transfer Rather than by Hydride Transfer. *Inorg. Chem.* **44,** 2150–2158 (2005).

83. Boucher-Jacobs, C. & Nicholas, K. M. Oxo-Rhenium-Catalyzed Deoxydehydration of Polyols with Hydroaromatic Reductants. *Organometallics* **34,** 1985–1990 (2015).

84. Sun, D., Hubig, S. M. & Kochi, J. K. Electron-transfer pathway for photoinduced Diels–Alder cycloadditions. *J. Photochem. Photobiol. Chem.* **122,** 87–94 (1999).

85. Ono, N. *et al.* Synthesis of Phthalocyanine Fused with Bicyclo[2.2.2]octadienes and Thermal Conversion into Naphthalocyanine. *HETEROCYCLES* **74,** 835 (2007).

86. Ishihara, A., Sutrisna, I. P., Ifuku, M., Qian, E. W. & Kabe, T. Elucidation of Hydrogen Mobility in Coal Using a Fixed Bed Flow Reactor -Hydrogen Transfer Reaction between Tritiated Hydrogen, Coal, and Tetralin-. *Energy Fuels* **16,** 1483–1489 (2002).

87. Zhang, Z.-G., Okada, K., Yamamoto, M. & Yoshida, T. Hydrogenation of anthracene over active carbon-supported nickel catalyst. *Catal. Today* **45,** 361–366 (1998).

88. Pajak, J. & Brower, K. R. Kinetic isotope effects and pressure effects in several hydrogen-transfer reactions of tetralin and related compounds. *J. Org. Chem.* **50,** 2210–2216 (1985).

89. Soltani Rad, M. *et al.* One-Pot Synthesis of N-Alkyl Purine, Pyrimidine and Azole Derivatives from Alcohols using Ph3P/CCl4: A Rapid Route to Carboacyclic Nucleoside Synthesis. *Synthesis* **2009,** 3067–3076 (2009).

90. Kimura, T. *et al.* Effects of N-allyl-substituted purines on the drug-induced sleep and spontaneous activity. *Res. Commun. Psychol. Psychiatry Behav.* **15,** 30–40 (1990).

91. Daly, J. W., Padgett, W. L. & Shamim, M. T. Analogs of caffeine and theophylline: effect of structural alterations on affinity at adenosine receptors. *J. Med. Chem.* **29,** 1305–1308 (1986).

92. DeClercq, E. in *Advances in antiviral drug design* **1,** 88–164 (Press, Greenwich, 1993).

93. Reppe, D. W. & Ufer, D. H. Verfahren zur Herstellung von Aminoverbindungen Process for the preparation of amino compounds. (1940).

94. Johnson, H. E. Process for the production of 3-indole-propionic acids. (1962).

95. Nishiguchi, T., Imai, H., Hirose, Y. & Fukuzumi, K. Transfer hydrogenation and transfer hydrogenolysis: VIII. Hydrogen transfer from amines to olefins catalyzed by heterogeneous and homogeneous catalysts. *J. Catal.* **41,** 249–257 (1976).

96. Wechsler, D., Cui, Y., Dean, D., Davis, B. & Jessop, P. G. Production of H2 from Combined Endothermic and Exothermic Hydrogen Carriers. *J. Am. Chem. Soc.* **130,** 17195–17203 (2008).

97. Nishiguchi, T., Imai, H. & Fukuzumi, K. Cleavage of Aralyl and Oxygen Nitrogen Bonds by the Hydrogen Transfer from Organic Compounds Catalyzed by Noble Metal Salts. *Chem. Lett.* **6,** 1113–1114 (1977).

98. Chowdhury, A. D. *et al.* Towards a Practical Development of Light-Driven Acceptorless Alkane Dehydrogenation. *Angew. Chem. Int. Ed.* **53,** 6477–6481 (2014).

99. Herrmann, W. A., Weichselbaumer, G. & Herdtweck, E. Mehrfachbindungen zwischen hauptgruppenelementen und übergangsmetallen: LXVII. Zur kenntnis der 'metallsäure' methyl(trioxo)rhenium(VII): adduktbildung mit amin-basen und aromaten. die struktur des anilin-komplexes CH3ReO3·H2NC6H5. *J. Organomet. Chem.* **372,** 371–389 (1989).

100. Abu-Omar, M. M. & Espenson, J. H. Facile Abstraction of Successive Oxygen Atoms from Perchlorate Ions by Methylrhenium Dioxide. *Inorg. Chem.* **34,** 6239–6240 (1995).

101. Gut, I. G. & Wirz, J. 3H-Indol. *Angew. Chem.* **106,** 1240–1243 (1994).

102. Marat, K. *SpinWorks 4*. (University of Manitoba : Winnipeg Canada).

103. *ACD/Structure Elucidator*. (Advanced Chemistry Development, Inc., 2014).

104. Diels, O. & Alder, K. Synthesen in der hydroaromatischen Reihe. *Justus Liebigs Ann. Chem.* **460,** 98–122 (1928).

105. Grieco, P. A. & Larsen, S. D. Iminium Ion-Based Diels–Alder Reactions: N-Benzyl-2-Azanorborene. *Org. Synth.* **68,** 206 (1990).

106. Roush, W. R. in *Comprehensive Organic Synthesis* (ed. Fleming, I.) 513–550 (Pergamon, 1991).

107. Tang, Y. *et al.* Strategies and approaches for constructing 1-oxadecalins. *Tetrahedron* **62,** 10785–10813 (2006).

108. Jung, E. J., Park, B. H. & Lee, Y. R. Environmentally benign, one-pot synthesis of pyrans by domino Knoevenagel/6π-electrocyclization in water and application to natural products. *Green Chem.* **12,** 2003–2011 (2010).

109. Kumar, S. *et al.* Synthesis, Photochromic Properties, and Light-Controlled Metal Complexation of a Naphthopyran Derivative. *Org. Lett.* **10,** 3761–3764 (2008).

110. Rawat, M., Prutyanov, V. & Wulff, W. D. Chromene Chromium Carbene Complexes in the Syntheses of Naphthopyran and Naphthopyrandione Units Present in Photochromic Materials and Biologically Active Natural Products. *J. Am. Chem. Soc.* **128,** 11044–11053 (2006).

111. Delbaere, S., Micheau, J.-C. & Vermeersch, G. NMR Kinetic Investigations of the Photochemical and Thermal Reactions of a Photochromic Chromene. *J. Org. Chem.* **68,** 8968–8973 (2003).

112. McKee, T. C. *et al.* New Pyranocoumarins Isolated from Calophyllum lanigerum and Calophyllum teysmannii. *J. Nat. Prod.* **59,** 754–758 (1996).

113. McKee, T. C. *et al.* Pyranocoumarins from Tropical Species of the Genus Calophyllum: A Chemotaxonomic Study of Extracts in the National Cancer Institute Collection. *J. Nat. Prod.* **61,** 1252–1256 (1998).

114. Stambouli, A., Chastrette, M. & Soufiaoui, M. Reactions de cycloaddition [4 + 2] sous micro - ondes des derives du glyoxal. *Tetrahedron Lett.* **32,** 1723–1724 (1991).

115. Garrigues, B., Laurent, R., Laporte, C., Laporterie, A. & Dubac, J. Microwave-Assisted Carbonyl Diels-Alder and Carbonyl-Ene Reactions Supported on Graphite. *Liebigs Ann.* **1996,** 743–744 (1996).

116. in *Organic Chemistry* (ed. Weinreb, D. L. B. and S. M.) **47,** 94–119 (Elsevier, 1987).

117. Johannsen, M. & Joergensen, K. A. Asymmetric hetero Diels-Alder reactions and ene reactions catalyzed by chiral copper(II) complexes. *J. Org. Chem.* **60,** 5757–5762 (1995).

118. Evans, D. A., Tregay, S. W., Burgey, C. S., Paras, N. A. & Vojkovsky, T. C2-Symmetric Copper(II) Complexes as Chiral Lewis Acids. Catalytic Enantioselective Carbonyl−Ene Reactions with Glyoxylate and Pyruvate Esters. *J. Am. Chem. Soc.* **122,** 7936–7943 (2000).

119. Jankowski, K. & Luce, R. Reactions de quelques dienes avec le pyruvate dðhyle en presence de AlCl3. *Tetrahedron Lett.* **15,** 2069–2071 (1974).

120. Aggarwal, V. K., Vennall, G. P., Davey, P. N. & Newman, C. Trifluoromethanesulfonic Acid, an Efficient Catalyst for the Hetero Diels-Alder Reaction and an Improved Synthesis of Mefrosol. *Tetrahedron Lett.* **38,** 2569–2572 (1997).

121. Dintzner, M. R. *et al.* Montmorillonite clay-catalyzed hetero-Diels–Alder reaction of 2,3-dimethyl-1,3-butadiene with benzaldehydes. *Tetrahedron Lett.* **48,** 1577–1579 (2007).

122. Hanamoto, T., Sugimoto, Y., Jin, Y. Z. & Inanaga, J. Scandium(III) Perfluorooctanesulfonate [$Sc(OPf)_3$] : A Novel Catalyst for the Hetero Diels–Alder Reaction of Aldehydes with Non-Activated Dienes. *Bull. Chem. Soc. Jpn.* **70,** 1421–1426 (1997).

123. Zhu, Z. & Espenson, J. H. Aqueous Catalysis: Methylrhenium Trioxide (MTO) as a Homogeneous Catalyst for the Diels−Alder Reaction. *J. Am. Chem. Soc.* **119,** 3507–3512 (1997).

124. Sogani, N., Sinha, P. & Bansal, R. K. Hetero-Diels–Alder reaction of aromatic aldehydes catalyzed by titanium tetrachloride: computational and experimental results. *Tetrahedron* **70,** 735–741 (2014).

125. Hoveyda, A. H. & Zhugralin, A. R. The remarkable metal-catalysed olefin metathesis reaction. *Nature* **450,** 243–251 (2007).

126. Jean-Louis Hérisson, P. & Chauvin, Y. Catalyse de transformation des oléfines par les complexes du tungstène. II. Télomérisation des oléfines cycliques en présence d'oléfines acycliques. *Makromol. Chem.* **141,** 161–176 (1971).

127. Hong, S. H. & Grubbs, R. H. Highly Active Water-Soluble Olefin Metathesis Catalyst. *J. Am. Chem. Soc.* **128,** 3508–3509 (2006).

128. Bradshaw, C. P. C., Howman, E. J. & Turner, L. Olefin dismutation: Reactions of olefins on cobalt oxide-molybdenum oxide-alumina. *J. Catal.* **7,** 269–276 (1967).

129. Salameh, A., Baudouin, A., Basset, J.-M. & Copéret, C. Tuning the Selectivity of Alumina-Supported (CH3)ReO3 by Modifying the Surface Properties of the Support. *Angew. Chem. Int. Ed.* **47,** 2117–2120 (2008).

130. Tomasek, J. & Schatz, J. Olefin metathesis in aqueous media. *Green Chem.* **15,** 2317 (2013).

131. Takahara, J. P., Masuyama, Y. & Kurusu, Y. Palladium-catalyzed carbonyl allylation by allylic alcohols with stannous chloride. *J. Am. Chem. Soc.* **114,** 2577–2586 (1992).

132. Gao, X., Townsend, I. A. & Krische, M. J. Enhanced anti-Diastereo- and Enantioselectivity in Alcohol-Mediated Carbonyl Crotylation Using an Isolable Single Component Iridium Catalyst. *J. Org. Chem.* **76,** 2350–2354 (2011).

133. Gao, X., Han, H. & Krische, M. J. Direct Generation of Acyclic Polypropionate Stereopolyads via Double Diastereo- and Enantioselective Iridium-Catalyzed Crotylation of 1,3-Diols: Beyond Stepwise Carbonyl Addition in Polyketide Construction. *J. Am. Chem. Soc.* **133,** 12795–12800 (2011).

134. Kim, I. S., Han, S. B. & Krische, M. J. anti-Diastereo- and Enantioselective Carbonyl Crotylation from the Alcohol or Aldehyde Oxidation Level Employing a Cyclometallated Iridium Catalyst: α-Methyl Allyl Acetate as a Surrogate to Preformed Crotylmetal Reagents. *J. Am. Chem. Soc.* **131,** 2514–2520 (2009).

135. Tan, X.-H., Hou, Y.-Q., Shen, B., Liu, L. & Guo, Q.-X. SnCl2/PdCl2-mediated aldehyde allylation in fully aqueous media. *Tetrahedron Lett.* **45,** 5525–5528 (2004).

136. Hirashita, T., Kambe, S., Tsuji, H., Omori, H. & Araki, S. Direct Preparation of Allylic Indium(III) Reagents from Allylic Alcohols via a Reductive Transmetalation of π-Allylnickel(II) with Indium(I) Iodide. *J. Org. Chem.* **69,** 5054–5059 (2004).

137. Fontana, G., Lubineau, A. & Scherrmann, M.-C. Investigation of the aqueous transmetalation of π-allylpalladium with indium salt: the use of the Pd(OAc)2–TPPTS catalyst. *Org. Biomol. Chem.* **3,** 1375–1380 (2005).

138. Lee, S.-M., Lee, W.-G., Kim, Y.-C. & Ko, H. Synthesis and biological evaluation of α,β-unsaturated lactones as potent immunosuppressive agents. *Bioorg. Med. Chem. Lett.* **21,** 5726–5729 (2011).

139. Betterton, E. A., Erel, Y. & Hoffmann, M. R. Aldehyde-bisulfite adducts: prediction of some of their thermodynamic and kinetic properties. *Environ. Sci. Technol.* **22,** 92–99 (1988).

140. Kjell, D. P., Slattery, B. J. & Semo, M. J. A Novel, Nonaqueous Method for Regeneration of Aldehydes from Bisulfite Adducts. *J. Org. Chem.* **64,** 5722–5724 (1999).

141. Pandit, C. & Mani, N. Expedient Reductive Amination of Aldehyde Bisulfite Adducts. *Synthesis* **2009,** 4032–4036 (2009).

142. Wittig, G. & Schöllkopf, U. Über Triphenyl-phosphin-methylene als olefinbildende Reagenzien (I. Mitteil. *Chem. Ber.* **87,** 1318–1330 (1954).

143. Wittig, G. From Diyls to Ylides to my Idyll. *Nobel Lect.* (1979).

144. Schirmer, M.-L., Adomeit, S. & Werner, T. First Base-Free Catalytic Wittig Reaction. *Org. Lett.* **17,** 3078–3081 (2015).

145. Beletskaya, I. P. & Cheprakov, A. V. The Heck Reaction as a Sharpening Stone of Palladium Catalysis. *Chem. Rev.* **100,** 3009–3066 (2000).

146. McClain, J. M. I. Survey of Catalyst and Reductant Effects on Oxorhenium Catalyzed Deoxydehydration of Glycols, PhD. Dissertation. *Dep. Chem. Biochem. Univ. Okla.* (2015).

147. Lakshmi Kantam, M., Vishnuvardhan Reddy, P., Srinivas, P. & Bhargava, S. Ligand and base-free Heck reaction with heteroaryl halides. *Tetrahedron Lett.* **52,** 4490–4493 (2011).

148. Booysen, I. N. Rhenium(V)-Imido complexes with potentially multidentate ligands containing the amino group. (Nelson Mandela Metropolitan University Faculty of Science, 2007).

149. Leung, J. C. & Krische, M. J. Catalytic intermolecular hydroacylation of C–C π-bonds in the absence of chelation assistance. *Chem. Sci.* **3,** 2202–2209 (2012).

150. Tsuji, J. & Ohno, K. Organic syntheses by means of noble metal compounds XXI. Decarbonylation of aldehydes using rhodium complex. *Tetrahedron Lett.* **6,** 3969–3971 (1965).

151. Baird, M. C., Nyman, C. J. & Wilkinson, G. The decarbonylation of aldehydes by tris(triphenylphosphine)chlororhodium(I). *J. Chem. Soc. Inorg. Phys. Theor.* 348–351 (1968). doi:10.1039/J19680000348

152. Sakai, K., Ide, J., Oda, O. & Nakamura, N. Synthetic studies on prostanoids 1 synthesis of methyl 9-oxoprostanoate. *Tetrahedron Lett.* **13,** 1287–1290 (1972).

153. Suggs, J. W. Isolation of a stable acylrhodium(III) hydride intermediate formed during aldehyde decarbonylation. Hydroacylation. *J. Am. Chem. Soc.* **100,** 640–641 (1978).

154. Kondo, T., Akazome, M., Tsuji, Y. & Watanabe, Y. Ruthenium complex catalyzed intermolecular hydroacylation and transhydroformylation of olefins with aldehydes. *J. Org. Chem.* **55,** 1286–1291 (1990).

155. Kondo, T., Tsuji, Y. & Watanabe, Y. Ruthenium complex catalyzed intermolecular hydroacylation of olefins. *Tetrahedron Lett.* **28,** 6229–6230 (1987).

156. Wu, H. *et al.* One-Pot Synthesis of Arylketones from Aromatic Acids via Palladium-Catalyzed Suzuki Coupling. *J. Org. Chem.* **81,** 2987–2992 (2016).

157. Singh, M., Kaur, M. & Silakari, O. Flavones: An important scaffold for medicinal chemistry. *Eur. J. Med. Chem.* **84,** 206–239 (2014).

158. Guimond, N., MacDonald, M. J., Lemieux, V. & Beauchemin, A. M. Catalysis through Temporary Intramolecularity: Mechanistic Investigations on Aldehyde-Catalyzed Cope-type Hydroamination Lead to the Discovery of a More Efficient Tethering Catalyst. *J. Am. Chem. Soc.* **134,** 16571–16577 (2012).

159. Janeliunas, D., Daskeviciene, M., Malinauskas, T. & Getautis, V. Study of the interaction of salicyl aldehydes with epichlorohydrin: a simple, convenient, and efficient method for the synthesis of 3,6-epoxy[1,5]dioxocines. *Tetrahedron* **65,** 8407–8411 (2009).

160. Hirano, K., Biju, A. T., Piel, I. & Glorius, F. N-Heterocyclic Carbene-Catalyzed Hydroacylation of Unactivated Double Bonds. *J. Am. Chem. Soc.* **131,** 14190–14191 (2009).

161. Sun, H. *et al.* Imidazolinium Perrhenate-Catalyzed Deoxydehydration of Vicinal Diols to Alkenes. *Chin. J. Org. Chem.* **35,** 1904 (2015).

162. Law, K. R. & McErlean, C. S. P. Extending the Stetter Reaction with 1,6-Acceptors. *Chem. – Eur. J.* **19,** 15852–15855 (2013).

163. Cornils, B., Herrmann, W. A. & Rasch, M. Otto Roelen, Pioneer in Industrial Homogeneous Catalysis. *Angew. Chem. Int. Ed. Engl.* **33,** 2144–2163 (1994).

164. *New Syntheses with Carbon Monoxide | J. Falbe | Springer*.

165. Ojima, I., Tsai, C.-Y., Tzamarioudaki, M. & Bonafoux, D. in *Organic Reactions* (John Wiley & Sons, Inc., 2004).

166. Warner, M. C., Casey, C. P. & Bäckvall, J.-E. in *Bifunctional Molecular Catalysis* (eds. Ikariya, T. & Shibasaki, M.) 85–125 (Springer Berlin Heidelberg, 2011).

167. Alvila, L., Pakkanen, T. A., Pakkanen, T. T. & Krause, O. Comparative study of homogeneous catalytic activity of group 8–9 metal compounds in hydroformylation of 1-hexene. *J. Mol. Catal.* **73,** 325–334 (1992).

168. Ciani, G. F., D'Alfonso, G., Romiti, P. F., Sironi, A. & Freni, M. Rhenium(V) oxide complexes. Crystal and molecular structures of the compounds trans-ReI2O(OR)(PPh3)2 (R = Et, Me) and of their hydrolysis derivative ReIO2(PPh3)2. *Inorganica Chim. Acta* **72,** 29–37 (1983).

169. Kasner, G. R., Boucher-Jacobs, C., McClain, J. M. & Nicholas, K. M. Oxo-rhenium catalyzed reductive coupling and deoxygenation of alcohols. *Chem. Commun.* **52,** 7257–7260 (2016).

170. Lohr, T. L. & Marks, T. J. Orthogonal tandem catalysis. *Nat. Chem.* **7,** 477–482 (2015).

171. Galván, A., Fañanás, F. J. & Rodríguez, F. Multicomponent and Multicatalytic Reactions – A Synthetic Strategy Inspired by Nature. *Eur. J. Inorg. Chem.* **2016,** 1306–1313 (2016).

172. Claude Moreau. Microporous and mesoporous catalysts for the transformation of carbohydrates. *Catal. Fine Chem. Synth.* **4,** 141–156

173. Yang, W. & Sen, A. One-Step Catalytic Transformation of Carbohydrates and Cellulosic Biomass to 2,5-Dimethyltetrahydrofuran for Liquid Fuels. *ChemSusChem* **3,** 597–603 (2010).

174. Zheng, Y., Chen, X. & Shen, Y. Commodity Chemicals Derived from Glycerol, an Important Biorefinery Feedstock. *Chem. Rev.* **108,** (2008).

175. Sun, Y. & Cheng, J. Hydrolysis of lignocellulosic materials for ethanol production: a review. *Bioresour. Technol.* **83,** 1–11 (2002).

176. Stöcker, M. Biofuels and Biomass-To-Liquid Fuels in the Biorefinery: Catalytic Conversion of Lignocellulosic Biomass using Porous Materials. *Angew. Chem. Int. Ed.* **47,** 9200–9211 (2008).

177. Dutta, S. Deoxygenation of Biomass-Derived Feedstocks: Hurdles and Opportunities. *ChemSusChem* **5,** 2125–2127 (2012).

178. Zacher, A. H., Olarte, M. V., Santosa, D. M., Elliott, D. C. & Jones, S. B. A review and perspective of recent bio-oil hydrotreating research. *Green Chem* **16,** 491–515 (2014).

179. Bu, Q. *et al.* A review of catalytic hydrodeoxygenation of lignin-derived phenols from biomass pyrolysis. *Bioresour. Technol.* **124,** 470–477 (2012).

180. Kieboom, A. P. G., De Kreuk, J. F. & Van Bekkum, H. Substituent effects in the hydrogenolysis of benzyl alcohol derivatives over palladium. *J. Catal.* **20,** 58–66 (1971).

181. Sawadjoon, S., Lundstedt, A. & Samec, J. S. M. Pd-Catalyzed Transfer Hydrogenolysis of Primary, Secondary, and Tertiary Benzylic Alcohols by Formic Acid: A Mechanistic Study. *ACS Catal.* **3,** 635–642 (2013).

182. Tsuji, J. & Mandai, T. Palladium-Catalyzed Hydrogenolysis of Allylic and Propargylic Compounds with Various Hydrides. *Synthesis* **1996,** 1–24 (1996).

183. Hong, Y.-K., Lee, D.-W., Eom, H.-J. & Lee, K.-Y. The catalytic activity of Pd/WOx/γ-Al2O3 for hydrodeoxygenation of guaiacol. *Appl. Catal. B Environ.* **150–151,** 438–445 (2014).

184. Li, S., Zhang, B. & Kühn, F. E. Benzimidazolic complexes of methyltrioxorhenium(VII): Synthesis and application in catalytic olefin epoxidation. *J. Organomet. Chem.* **730,** 132–136 (2013).

185. de Souza, P. M. *et al.* Role of Keto Intermediates in the Hydrodeoxygenation of Phenol over Pd on Oxophilic Supports. *ACS Catal.* **5,** 1318–1329 (2015).

186. Martin, A., Armbruster, U., Gandarias, I. & Arias, P. L. Glycerol hydrogenolysis into propanediols using in situ generated hydrogen – A critical review. *Eur. J. Lipid Sci. Technol.* **115,** 9–27 (2013).

187. Tomishige, K., Nakagawa, Y. & Tamura, M. in *Selective Catalysis for Renewable Feedstocks and Chemicals* (ed. Nicholas, K. M.) 127–162 (Springer International Publishing, 2014).

188. Nakagawa, Y., Tamura, M. & Tomishige, K. Catalytic materials for the hydrogenolysis of glycerol to 1,3-propanediol. *J. Mater. Chem. A* **2,** 6688–6702 (2014).

189. Murru, S., Nicholas, K. M. & Srivastava, R. S. Ruthenium (II) sulfoxides-catalyzed hydrogenolysis of glycols and epoxides. *J. Mol. Catal. Chem.* **363–364,** 460–464 (2012).

190. Sergeev, A. G., Webb, J. D. & Hartwig, J. F. A Heterogeneous Nickel Catalyst for the Hydrogenolysis of Aryl Ethers without Arene Hydrogenation. *J. Am. Chem. Soc.* **134,** 20226–20229 (2012).

191. Kusumoto, S. & Nozaki, K. Direct and selective hydrogenolysis of arenols and aryl methyl ethers. *Nat. Commun.* **6,** 6296 (2015).

192. Zhu, Z. & Espenson, J. H. Organic Reactions Catalyzed by Methylrhenium Trioxide: Dehydration, Amination, and Disproportionation of Alcohols. *J. Org. Chem.* **61,** 324–328 (1996).

193. Korstanje, T. J., Jastrzebski, J. T. B. H. & Klein Gebbink, R. J. M. Mechanistic Insights into the Rhenium-Catalyzed Alcohol-To-Olefin Dehydration Reaction. *Chem. – Eur. J.* **19,** 13224–13234 (2013).

194. Luzzio, F. A. in *Organic Reactions* (John Wiley & Sons, Inc., 2004).

195. Murahashi, S.-I. & Komiya, N. in *Ruthenium in Organic Synthesis* (ed. Murahashi, essor S.-I.) 53–93 (Wiley-VCH Verlag GmbH & Co. KGaA, 2004).

196. Diéguez, H. R. *et al.* Weakening C−O Bonds: Ti(III), a New Reagent for Alcohol Deoxygenation and Carbonyl Coupling Olefination. *J. Am. Chem. Soc.* **132,** 254–259 (2010).

197. Crevier, T. J. & Mayer, J. M. C−O Bond Homolysis in a Tungsten Alkoxide: The Mechanism of Alcohol Deoxygenation by WCl2(PMe3)4 and WH2Cl2(PMe3)4. *J. Am. Chem. Soc.* **119,** 8485–8491 (1997).

198. Wang, H. *et al.* Efficient Palladium-Catalyzed C□O Hydrogenolysis of Benzylic Alcohols and Aromatic Ketones with Polymethylhydrosiloxane. *Adv. Synth. Catal.* **355,** 341–347 (2013).

199. van Tamelen, E. E. & Schwartz, M. A. Reductive Coupling of Alcohols to Hydrocarbons. *J. Am. Chem. Soc.* **87,** 3277–3278 (1965).

200. McMurry, J. E. & Silvestri, M. Simplified method for the titanium(II)-induced coupling of allylic and benzylic alcohols. *J. Org. Chem.* **40,** 2687–2688 (1975).

201. Isakov, V. E. & Kulinkovich, O. G. The Head-to-Head ReductiveCoupling of Homoallylic Alcohols Promoted by Titanium(II)-OlefinComplexes. *Synlett* 0967–0970 (2003). doi:10.1055/s-2003-39300

202. Karunakar, G. V. & Periasamy, M. A simple method for the conversion of propargyl alcohols to symmetrical 1,5-diynes using low valent titanium reagents. *Tetrahedron Lett.* **47,** 3549–3552 (2006).

203. Nishino, T., Nishiyama, Y. & Sonoda, N. Deoxygenative Dimerization of Benzylic and Allylic Alcohols, and Their Ethers and Esters Using Lanthanum Metal and Chlorotrimethylsilane in the Presence of a Catalytic Amount of Iodine and Copper(I) Iodide. *Bull. Chem. Soc. Jpn.* **76,** 635–641 (2003).

204. Nishino, T., Nishiyama, Y. & Sonoda, N. Lanthanum metal-assisted deoxygenative coupling of alcohols. *Tetrahedron Lett.* **43,** 3689–3691 (2002).

205. Rappe, A. K. & Goddard, W. A. Hydrocarbon oxidation by high-valent Group VI oxides. *J. Am. Chem. Soc.* **104,** 3287–3294 (1982).

206. Bellemin-Laponnaz, S., Gisie, H., Le Ny, J. P. & Osborn, J. A. Mechanistic Insights into the Very Efficient [ReO3OSiR3]-Catalyzed Isomerization of Allyl Alcohols. *Angew. Chem. Int. Ed. Engl.* **36,** 976–978 (1997).

207. Herrmann, A. T., Saito, T., Stivala, C. E., Tom, J. & Zakarian, A. Regio- and Stereocontrol in Rhenium-Catalyzed Transposition of Allylic Alcohols. *J. Am. Chem. Soc.* **132,** 5962–5963 (2010).

208. Jacob, J., Espenson, J. H., Jensen, J. H. & Gordon, M. S. 1,3-Transposition of Allylic Alcohols Catalyzed by Methyltrioxorhenium. *Organometallics* **17,** 1835–1840 (1998).

209. DuMez, D. D. & Mayer, J. M. Rhenium(V) Oxo-Alkoxide Complexes: Syntheses and Oxidation to Aldehydes. *Inorg. Chem.* **34,** 6396–6401 (1995).

210. Paulo, A., Domingos, A., Marcalo, J., Pires de Matos, A. & Santos, I. Reactivity of a Tetrakis(pyrazolyl)borate Oxorhenium Complex. *Inorg. Chem.* **34,** 2113–2120 (1995).

211. Boehm, G., Wieghardt, K., Nuber, B. & Weiss, J. Coordination chemistry of rhenium(V), -(IV), and -(III) with the macrocyclic ligands 1,4,7-triazacyclononane (L) and its N-methylated derivative (L'). Crystal structures of [LReCl3]Cl, [L2Re2Cl2(.mu.-Cl)(.mu.-OH)]I2.cntdot.2H2O, [L2Re2I2(.mu.-O)2]I2.cntdot.2H2O, and [L'2Re2Cl4(.mu.-O)]ZnCl4. Effect of .pi.-donors on the Re-Re bond distance. *Inorg. Chem.* **30,** 3464–3476 (1991).

212. Seisenbaeva, G. A. *et al.* Homo- and hetero-metallic rhenium oxomethoxide complexes with a M4(μ-O)2(μ-OMe)4 planar core—a new family of metal alkoxides displaying a peculiar structural disorder. Preparation and X-ray single crystal study. *J. Chem. Soc. Dalton Trans.* 2762–2768 (2001). doi:10.1039/B103287A

213. Gable, K. P. & Brown, E. C. Rhenium-Catalyzed Epoxide Deoxygenation: Scope and Limitations. *Synlett* 2243–2245 (2003).

214. Peters, J. C. *et al.* Assembly of Molybdenum/Titanium μ-Oxo Complexes via Radical Alkoxide C−O Cleavage. *J. Am. Chem. Soc.* **118,** 10175–10188 (1996).

215. Bass, K. C. Hydrogen Abstraction by Benzyl Radicals. *Nature* **201,** 700–701 (1964).

216. Mayer, J. M. Hydrogen Atom Abstraction by Metal−Oxo Complexes: Understanding the Analogy with Organic Radical Reactions. *Acc. Chem. Res.* **31,** 441–450 (1998).

217. Dinda, S., Genest, A. & Rösch, N. O2 Activation and Catalytic Alcohol Oxidation by Re Complexes with Redox-Active Ligands: A DFT Study of Mechanism. *ACS Catal.* **5,** 4869–4880 (2015).

218. McLaughlin, M. P., Adduci, L. L., Becker, J. J. & Gagné, M. R. Iridium-Catalyzed Hydrosilylative Reduction of Glucose to Hexane(s). *J. Am. Chem. Soc.* **135,** 1225–1227 (2013).

219. Yasuda, M., Onishi, Y., Ueba, M., Miyai, T. & Baba, A. Direct Reduction of Alcohols: Highly Chemoselective Reducing System for Secondary or Tertiary Alcohols Using Chlorodiphenylsilane with a Catalytic Amount of Indium Trichloride. *J. Org. Chem.* **66,** 7741–7744 (2001).

220. Mayr, H. & Dogan, B. Selectivities in ionic reductions of alcohols and ketones with triethylsilane/trifluoroacetic acid. *Tetrahedron Lett.* **38,** 1013–1016 (1997).

221. Adlington, M. G., Orfanopoulos, M. & Fry, J. L. A convenient one-step synthesis of hydrocarbons from alcohols through use of the organosilane-boron trifluoride reducing system. *Tetrahedron Lett.* **17,** 2955–2958 (1976).

222. Barton, D. H. R., Blundell, P., Dorchak, J., Jang, D. O. & Jaszberenyi, J. C. The invention of radical reactions. Part XXI. Simple methods for the radical deoxygenation of primary alcohols. *Tetrahedron* **47,** 8969–8984 (1991).

223. Kozlowski, J. T. & Davis, R. J. Heterogeneous Catalysts for the Guerbet Coupling of Alcohols. *ACS Catal.* **3,** 1588–1600 (2013).

224. Chung, L. W., Lee, H. G., Lin, Z. & Wu, Y.-D. Computational Study on the Reaction Mechanism of Hydrosilylation of Carbonyls Catalyzed by High-Valent Rhenium(V)−Di-oxo Complexes. *J. Org. Chem.* **71,** 6000–6009 (2006).

225. Kühl, O. in *Phosphorus-31 NMR Spectroscopy* (ed. Kühl, O.) 7–23 (Springer Berlin Heidelberg, 2008).

226. Dean, P. A. W., Phillips, D. D. & Polensek, L. A 31P nmr spectroscopic study of complexation of tin(II) and lead(II) by some phosphines, phosphine oxides, and related ligands, with the 31P nuclear magnetic resonance spectra of two tetratertiary phosphine tetraoxides and the analogous tetra-sulfides and -selenides. *Can. J. Chem.* **59,** 50–61 (1981).

227. Hursthouse, M. B., Levason, W., Ratnani, R. & Reid, G. Synthesis and spectroscopic properties of Mo(VI) complexes with phosphine oxide ligands and the crystal structures of [MoO2X2(OPMe3)2] (X=Cl or Br) and [MoO2Br2{o-C6H4(P(O)Ph2)2}] · 2CH2Cl2. *Polyhedron* **23,** 1915–1921 (2004).

228. Chakravarty, A. R., Cotton, F. A., Cutler, A. R. & Walton, R. A. Reactivity of the dirhenium(III) carboxylate complexes Re2(O2CCH3)2X4(H2O)2 (X = Cl or Br) toward monodentate phosphines. A novel disproportionation reaction leading to dirhenium(IV,II) alkoxide complexes of the type (RO)2X2ReReX2(PPh3)2 (X = Cl or Br; R = Me, Et, or Pr). *Inorg. Chem.* **25,** 3619–3624 (1986).

229. van Bommel, K. J. C., Verboom, W., Kooijman, H., Spek, A. L. & Reinhoudt, D. N. Rhenium(V)−Salen Complexes: Configurational Control and Ligand Exchange. *Inorg. Chem.* **37,** 4197–4203 (1998).

230. Cai, S., Hoffman, D. M., Lappas, D., Woo, H. G. & Huffman, J. C. Synthesis and structure of ReO(PMe3)(CH2SiMe3)3 and reaction with carbon monoxide. *Organometallics* **6,** 2273–2278 (1987).

231. Bakhmutov, V. I., Vorontsov, E. V. & Antonov, D. Y. NMR evidence for formation of new alcohol rhenium complexes as intermediates in ionic hydrogenations of carbonyl groups with systems composed of ReH2(NO)(CO)(PR3)2 (R = Pri, CH3, OPri) and CF3COOH. *Inorganica Chim. Acta* **278,** 122–126 (1998).

232. *MestReNova Software v10.0.2-15465*. (2015).

233. Ciani, G. F., D'Alfonso, G., Romiti, P. F., Sironi, A. & Freni, M. Rhenium(V) oxide complexes. Crystal and molecular structures of the compounds trans-ReI2O(OR)(PPh3)2 (R = Et, Me) and of their hydrolysis derivative ReIO2(PPh3)2. *Inorganica Chim. Acta* **72,** 29–37 (1983).